THE RESEARCH UNIT OF APPLIED CHEMISTRY & ENVIRONMENT
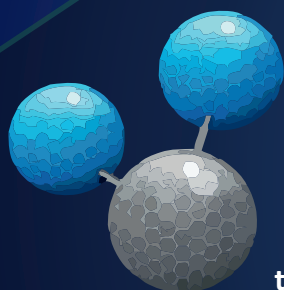
CO-ORGANIZE WITH

THE TUNISIAN ASSOCIATION OF SUSTAINABLE TECHNOLOGIES

AND THE FRENCH SOCIETY OF PROCESS ENGINEERING

ATuTeD

ASSOCIATION TUNISIENNE DES
TECHNOLOGIES DURABLES

URCAE

UNITE DE RECHERCHE CHIMIE APPLIQUEE
& ENVIRONNEMENT

2nd INTERNATIONAL CONGRESS
OF APPLIED CHEMISTRY
& ENVIRONNEMENT

ICACE 2020, Tunisia

October, 30-31, November, 01,

Proceedings

For a Sustainable Ecosystem !

1

What About Us?

The Research Unit of Applied Chemistry & Environment (URCAE) of the Faculty of Sciences of Monastir (Tunisia), formerly UR13ES63, is a research unit founded and directed since 1995 by Prof. Emer.Mohamed Farouk Mhenni. Since July 2015, the unit has been headed by Prof. Hatem Dhaouadi, Professor in the Department of Chemistry of the Faculty of Sciences of Monastir. It brings together a multidisciplinary team (Chemistry, Chemical Engineering and Textile Engineering) formed by eight professors and ten associate professors whose main research activities focus on:

Identification and valorization of natural substances

Treatment of industrial discharges and environmental impacts

Ecological textile and paratextiles

Management & valorisation of bioresources of natural substances

Sustainable process and clean technologies

Our Accomplishments

Our research quality continues to improve over the years, we have 22 theses defended: 13 in Chemistry and 09 in Textile Engineering, 22 theses in progress, 05 HU, 05 PNRI projects, 06 Projects CMCU / CMPTM / CMTE, 09 recruitments in ESRS, 06 MOBIDOC, 12 Patents, 01 startup (NatDye).

Our partnerships

We work in collaboration with several manufacturers in order to open up and exchange with the industrial world, contribute to a technology transfer between our research unit and industry, apply and promote research studies at the laboratory scale in the industrial environment in order to innovate for better competitiveness of Tunisian industry. Our partners are: CETTEX, CNCC, ONAS, SNCPA, CHIMITEX, SARTEX, SITEX, DEMCO, SCOOPTunisie, STIVEL, AgriLand.

The Second Edition of the International Congress of Applied chemistry and Environment
30th-31th October and 01st November 2020, Tunisia

ICACE
2020

THE FIRST EDITION OF "ICACE-1 (2018)"

The Applied Chemistry & Environment Research Unit (URCAE) organized its first International Congress of Applied Chemistry and Environment (ICACE-1) on May 12th and 13th, 2018 in Diar El Andalous (IBEROSTAR,5*), Sousse. This event was an excellent opportunity for researchers to present their innovative research and constituted an excellent opportunity for fruitful scientific exchanges between academics and professionals from all over the world.

We had the honor of attending very interesting plenary conferences presented by Prof. Emer. Mohamed Farouk Mhenni (Faculty of Sciences of Monastir, Tunisia), Pr. Nicolas Roche (University of Aix-Marseille, France), Pr. Orazio Taglialatela-Scafati (University of Naple Federico II, Italy) and Pr. Atef Jaouani (Faculty of Sciences of Tunis, Tunisia).

Likewise, as we want to stay connected with the industrial world, we were able to present the testimonial of several professionals, including; Mr Ramzi Zammali (Marketing and Cooperation Director, Monastir Technopark, Tunisia), Mr Mongi Nouira (General manager of S.E.A Group, Tunisia), Mr Ayatellah Hleim (General manager of Agriland, Tunisia) and Mrs. Marwa Ben Ali (General manager of the Herbeos laboratory, Tunisia).

Furthermore, several presentations of oral and written communications took place which focused on:

❖ Sustainable processes and clean technologies;

❖ Treatment of industrial waste and environmental impacts;

❖ Management and recovery of bioresources and industrial waste;

❖ Identification and valuation of natural substances;

❖ Ecological textiles and para-textiles;

❖ Circular economy.

During the first edition of International Congress of Applied Chemistry & Environment, we have recorded the participations of more than 120 researchers from 11 countries: Tunisia, Algeria, France, Morocco, Italia, Mauritania, Egypt, Senegal, Pakistan, Iran, and Australia.
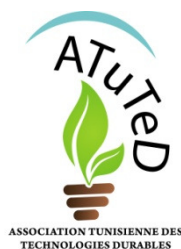
THE TUNISIAN ASSOCIATION OF SUSTAINABLE TECHNOLOGIES
(ATuTeD)

The Tunisian Association of Sustainable Technologies, ATuTeD, was born on October 24, 2018 under the leadership of a group of researchers in development of ecological processes. ATuTeD is based at the Faculty of Sciences of Monastir. This association is non-profit, scientific and cultural. It was established mainly for the purpose of promoting research, studies and the development of projects in the field of environment and sustainable technologies.

Objectives of ATuTeD

Continuing education

Provide continuous training, through the organization of scientific courses, workshops, national and international congresses in the area of expertise of the members of the association.

Scientific exchange

Establish solid and lasting scientific exchangerelationships in the field of association interests between the bodies and institutions concerned at national and international level.

Development

Participate in development of medical biology.

Promotion

Promote cultural activities in the university environment.

Expertism

Bring together all experts in the development of ecological processes(teachers, researchers, engineers, technicians, etc.) within a professional family.

New Horizons

Open new horizons concerning scientific and social activities.
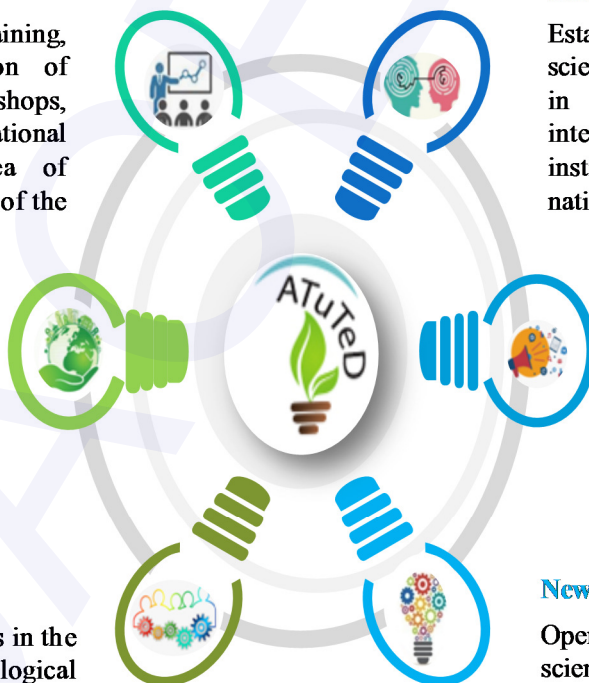
For more information about the Tunisian Association of Sustainable Technologies (ATuTeD), you can visit the web site : www.atuted.org.tn

THE SECOND EDITION OF "ICACE-2 (2020)"

The second edition of the International Congress of Applied Chemistry& Environment ICACE-2020 was co-organized by the Research Unit of the Applied Chemistry & Environment (URCAE) and the Tunisian Association of Sustainable Technologies (ATuTeD) with the French Chemical Engineering Society (SFGP).

Due to the pandemic situation caused by the covid-19 virus, the ICACE-2020 congress was held remotely from October 30th to November 01st, 2020 from Tunisia

The thematic areas of the second edition of ICACE-2020 are:

- Sustainable Processes and Clean Technologies;

- Treatment of industrial wastes and their environmental impacts;

- Management and valorization of bio-ressources and industrial waste;

- Identification and valorization of natural substances;

- Ecological textiles and para-textiles;

For this second edition of our congress, six plenary conference were scheduled and presented by international professors from France, Malaysia, Sweden and Tunisia

The Second Edition of the International Congress of Applied chemistry and Environment
30th-31th October and 01st November 2020, Tunisia

ICACE 2020

SCIENTIFIC COMMITTEE

Pr. Mohamed Farrouk Mhenni
Tunisia

Pr. Chedly Boudokhane
Tunisia

Pr. Slah Msahli
Tunisia

Pr. Néji Ladhari
Tunisia

Pr. Saber Ben abdesslem
Tunisia

Pr. Karima Horchani Ennaifar
Tunisia

Dr. Nizar Meksi
Tunisia

Dr. Marzouk Laajili
Tunisia

Dr. Saoussen Hammami
Tunisia

Dr. Ramzi Khiari
Tunisia

Dr. Sonia Dhaouadi
Tunisia

Pr. Hatem Dhaouadi
Tunisia

Pr. Noureddine Barka
Morroco

Pr. Mongi Seffen
Tunisia

Pr. Marie Odile Simonnot
France

Pr. Salah Akkal
Algeria

Pr. Mohammad Jawaid
Malaysia

Dr. Jean Fraçois Joly
France

Pr. Naceur Belgacem
France

Pr. Niklas Hedin
Sweden

Pr. Azizi Amine
Morroco

Dr. Aminoddin Haji
Iran

Dr. Sebastien Leveneur
France

The Second Edition of the International Congress of Applied chemistry and Environment
30th-31th October and 01st November 2020, Tunisia

ICACE 2020

ORGANIZING COMMITTEE

Pr. Hatem Dhaouadi
Chairman

Pr. Mohamed Farrouk Mhenni
Co-chairman

Pr. Zine Mighri
Co-chairman

Dr. Feriel Bouatay
President of organazing committee

Dr. Sonia Dhaouadi
President of scientific committee

Dr. Noureddine Baaka
Promotion & Communication

Dr. Ghazza Masmoudi
Planning & informations

Dr. Ibtissem Moussa
Planning & Informations

PhD. Marwa Souissi
Welcome & Registration

PhD. Héla Machat
Logistics

PhD.Nawres Gharrad
Logistics

Dr. Bessem Kordoghli
administrative managment

Phd. Mohamed Abdelwaheb
administrative managment

The Second Edition of the International Congress of Applied chemistry and Environment
30th-31th October and 01st November 2020, Tunisia

ICACE 2020

ICACE-2020 Program

Plenary conferences		
PC1	**"The job of a researcher"** *Pr. Emer. Mohamed Farouk Mhenni, Faculty of Sciences of Monastir*	
PC2	"Agromining, a green chain of processes to recover metals present in soils" *Pr. Marie Odile Nicolas Simonnot, University of Lorraine, France*	16
PC3	"Cellulose at the service of medecine" *Pr. Mohamed Naceur Belgacem, University of Grenoble, France*	17
PC4	"Sustainable and environmental-friendly food packaging products from oil palm biomass" *Pr. Mohamed Jawaid, University of Putra, Malaysia*	18
PC5	"Valorisation of vegetable oils: from thermal risk assessment to kinetic modelling" *Dr. Sebastien Leveneur, University of Rouen, France*	19
PC6	"CO_2 adsorbents – potential use in flue gas capture and for gas upgrading" *Pr. Niklas Hedin, University of Stockholm, Sweden*	20

Oral communications		
Oral Session 1:Treatment of industrial discharges and enviromental impacts		
C01	**"Application of Raw Sawdust, Olive Pomace and their Derived Biochars for Copper Removal from Aqueous Solution",** Ibtissem Mannai, Stéphanie Sayen, Achouak Arfaoui, Amira Touil, Emmanuel Guillon	24
C02	**"Skimmer Upgrade to Enhance De-Oiling of Petroleum Production Water: Case Study ofan Industrial Scale Skimmer",** Ines Wada, Ghazza Masmoudi, Hatem Dhaouadi	28
C03	**"Adsorption of Nitrate, Phosphate, Nickel and Lead on Soils: Risk of Groundwater Contamination",** Mohamed Abdelwaheb, Khaoula Jebali, Hatem Dhaouadi, Sonia Dridi-Dhaouadi	33
C04	**"Treatment of Rinse Water Generated in the Galvanizing Processfor Zero Liquid Discharge"** Hayet Cherif , Manel Wakkel, Refka Korbsi, Insaf Krimi, Hamza Elfil	37
C05	**"Physicochemical and Geochemical Properties of Boujaada's Mine Soils (Taza Province)"** Ikram Lahmidi, Narmine Assabar, Raouf Jabrane	40
C06	**"Physico-Chemical and Geochemical Characterization of Ain Aouda Mine's Soils"** Narmine Assabar, Ikram Lahmidi, Raouf Jabrane	43
C07	**"Thermo-chemical Calculations to Follow the Reactions of Desulfurization of Gaseous Resulting from a Coal Thermal Power Station"** Saloua Jemjami	46
C08	**"Adsorption of a Hazardous Azo Dye on Cellulose Extracted from Annual Agricultural Wastes"** Ibtissem Moussa, Manel Ben Ticha	51
C09	**"The Collection Efficiency ofan Asymmetrical Electrostatic Precipitator Model: Validation of the Experimental Results with Calculated Data Using Deutsch Model"** Kherbouche Fouad, Berdadi Bendaha Mourad	56
Oral Session 2&3:Management and valorization of bioresources and industrial wastes		
C10	**"Bio-Oil Fast Pyrolysis of Exhausted Olive Pomace: Physico-Chemical Characterization and Investigation of its Possible as Biochemical and Biofuel"** Najla Grioui, Kamel Halouania	63

The Second Edition of the International Congress of Applied chemistry and Environment
30th-31th October and 01st November 2020, Tunisia

ICACE 2020

C11	"Acoustic and Thermal Behavior of Environmental-Friendly Composite Panels Made of Various Textile Waste Sand Epoxy Resin" Wafa Baccouch, Adel Ghith, Ipek Yalcin-Enis, Hande Sezgin, Xavier Legrand, Fayala Faten	68
C12	"Removal of Thiophene by Different Adsorbents from Hot Gas" Hiba Aouled Mhemed, Sana Kordoghli, Mylène Marin Gallego, Jean-François Largeau, Fethi Zagrouba, Mohand Tazerout	73
C13	"Recycling Irons Waste as Abrasive Grains" Elaissi Arwa, Jabli Mahjoub, Alibi Hamza, Gith Adel	77
C14	"Manufacture of a Non-Woven from Natural Fibers" Elaissi Arwa, Alibi Hamza, Jabli Mahjoub, Gith Adel	81
C15	"Pyrolysis of Used Tires: Yield and Chemical Composition of Pyrolysis Oils" Marwa Ourak, Mylène Marin Gallego, Gaëtan Burnens, Sana Kordoghli, Jean François Largeau, Fethi Zagrouba, Mohand Tazerout	86
C16	"Valorization of Solid Wastes from Food Industry as Biosorbents for the Removal of Cd (II)" Nourhen Hsini, Sonia Dridi-Dhaouadi	89
C17	"Adhesion Capacity of Carboxymethyl Cellulose from Wheat Straw to Cotton Fibers" Najah Laribia, Samah Maatoug, Riadh Zouaria, Hatem Majdoub, Morched Cheikhrouhou	94
C18	"Transformation of Waste Engine Oil into Fuel by Pyrolysis" Youghourta Zerdane, Jean-François Largeau, Naim Akkouche, Hachemi Madjid, Mohand Tazerout	101
C19	"Investigation of the Effect of Olive Mill Wastewater Sludge Biochar on Seed Germination and Soil Amendment" Salma Mseddi, Wejdene Ben Chelbi, Kamel Halouani, Monem Kallel	104
C20	"Experimental and Theoretical Investigation of Drying Behavior of Sewage Sludge" Hager Hajji, Amira Touil	108
C21	"Cellulose from Tamarix Aphylla as Biosorbent for Cadmium Ions Removal" Islem M'barek, Hela Slimi, Younes Moussaoui	112

The Second Edition of the International Congress of Applied chemistry and Environment
30th-31th October and 01st November 2020, Tunisia

ICACE 2020

C29	**"Dyeing Properties and Colorfastness of Cotton Dyed with*Corchorus Olitorius* Extracted Natural Dye"**	148
	Syrine Ltaief, Nesrine Bhouri, Saber Ben Abdessalem	
C30	**"Curcumin Nanoemulsions for aTopical Application"**	153
	Mekhloufi Gozlene, Vilamosa N, Agnely Florence	
C31	**Valorization of Mycelium from PleurotusOstreatus (Jacq: Fries) Kummer and Production of Chitin and Chitosan"**	157
	Nora Benbelkacem Belabbas, Malika Mansour Benamar, Nadia Ammar Khodja, Lydia Adour	
C32	**"Effect of Geographic Variation and Extraction Method on the Chemical Composition of Borago Officnalis L. Extracts"**	161
	Imene Zribi, Ridha Ghali, Manef Abderabba	
C33	**"Design of a New Carbonic Anhydrase Inhibitors Derived from 1,5-Benzodiazepines"**	165
	Ismail Chiraz, Winum Jean Yves, Gharbi Rafik	

Oral Session 6: Ecological textile and paratextile

C34	**"Dyeing Process Using Aqueous Residue from *DittrichiaGraveolens* Hydrodistillation"**	169
	Nawres Gharred, Noureddine Baaka, Amal Dbeibia, Sonia Dridi-Dhaouadi	
C35	**"Development and Optimization of a New Process to Dye Cotton with Indigo Carmine"**	172
	Maha Abdelileh, Manel Ben Ticha, Nizar Meksi	
C36	**"Fabric's Thermal Properties Modification Through the Nanocomposite Coating"**	177
	Sawssen Ezzine, Khaled Abid, Nèji Ladhari	
C37	**"Capillary Water Absorption in a Coated Waterproof Breathable Double-Sided Knit"**	181
	Imene Ghezal, Ali Moussa, Imed Ben Marzoug, Ahmida El-Achari, Christine Campagne, Faouzi Sakli	
C38	**"Ecological and Clean Process for Dyeing Advanced Bi-component Polyesters Filaments (PET/PTT)"**	185
	Marwa Souissi, Mounir Zaag, Nizar Meksi, Hatem Dhaouadi	
C39	**"A New Natural Color Indicator Extracted from *Carissa Macrocarpa* Fruit"**	189
	Imene Ghezal, Ibtissem Moussa, Faouzi Sakli	
C40	**"Accelerated Weathering of Recycled Nonwovens Used as Sustainable Agrotextiles"**	193
	Houcine Abidi, Sohel Rana, Walid Chaouch, Bechir Azouz, Mohamed Ben Hassen, Raul Fangueiro	

E- Posters Communications

Poster session 1&2: Treatment of industrial discharges and enviromental impacts

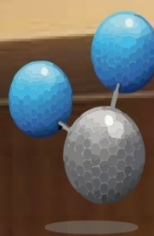| P01	**"Evaluationof Intense African Dust Events and Contribution to PM10 Concentration in Tunisia"**	200
	Houda Chtioui, Karim Bouchlaghem, Mohamed Hichem Gazzah	
P02	**"Preparation of Photo Catalyst Based on Co-ZnOand its Application in the Photo Degradation of Dye Rhodamine 6G"**	201
	Ait Ben Hammou Nabil, Khalef El Hossein, Bouchenafa-Saib Naima	
P03	**"Binary Adsorption of Nickel and Lead onto Clayey Organic Soil"**	202
	Mohamed Abdelwaheb, HatemDhaouadi, Sonia Dridi-Dhaouadi	
P04	**"Thermochemical Calculations to Follow the Reactions of Thermal Decomposition of Phosphogypsum"**	203
	Saloua Jemjami	
P05	**"Effect of Acid Treatment and Pore Size of Clay in the CO_2 Adsorption Capacity"**	204
	Nesrine Chouikhi, Sabrine Besghaier, Juan Antonio Cecilia, Mohamed Chlendi, Enrique Rodriguez Castellon, Mohamed Bagane	

The Second Edition of the International Congress of Applied chemistry and Environment
30th-31th October and 01st November 2020, Tunisia

ICACE 2020

P06	**"Improvement of Mineral Clay Properties with an Acid Treatment"**	205
	Sabrine Besghaier, Nesrine Chouikhi, Juan Antonio Cecilia, Mohamed Chlendi, Enrique Rodriguez Castellon, Mohamed Bagane	
P07	**"Effects of C/N Ratio on Carbon and Nitrogen Removalsin a Hybrid Biological Reactor"**	206
	Hela Machat, Nicolas Roche, Hatem Dhaouadi	
P08	**"Gas Hydrate Formation Process for Capture of CO_2 from Natural Gas: Experimental and Modelling Study of the Effect of New Kinetic Promotors"**	207
	Said Samer, Saheb Maghsoodloo Babakhani, Mohamed Belloum, Jean-Michel Herri	
P09	**"Experimental Investigation ofa Novel Tow Stage ESP Associated with Unipolar Charger Used for ATEX Filtration"**	208
	Kherbouche Fouad, Berdadi Bendaha Mourad	
P10	**"Characterizations and Valorization of Olive Mill Wastewater by Adsorption onto Activated Carbon"**	209
	Bekri Imene, Taleb Safia, Taleb Zoubida, Belfedal Abdelkader	
P11	**"Study of Acetone Flux Adsorbed by Activated Carbon AC35"**	210
	Noujoud Benkahla, Foued Mhiri	
P12	**"Adsorption of lead(II) Ions onto Activated Carbon Prepared from Prickly Pear Seeds (after Extraction Essential Oil)"**	211
	Rimene Dhahri, Asma Bouzidi, Younes Moussaoui	
P13	**"Comparison of the Degradability of Three Reactive Dyes by Fenton Process"**	212
	Nour El Houda Slama, Ghazza Masmoudi, Hatem Dhaouadi	
	Poster Session 3,7 & 9: Sustainable processes and clean technologies	
P14	**"New CeO_2-TiO_2, WO_3-TiO_2 and $WO3$-CeO_2-TiO_2 Meso-Structured Aerogel Catalysts for the Low Temperature NO-Scr by NH_3 in Excess O_2"**	214
	Jihene Arfaoui, Abdelhamid Ghorbel, Carolina Petitto, Gerard Delahay	
P15	**"Electrochemical Study of aMaterial on a Modified Electrode"**	215
	Rakhrour Waffa, Selloum Djamel, Benalia Mokhtar	
P16	**"Preparation of Catalysts Based on Iron Oxyhydroxides and Zirconium and their Application for the Degradation of 4-Nitrophenol by aHeterogeneous Fenton-Like Process"**	216
	Hafsa Loumi, Faiza Zermane, Benamar Cheknane, Naima Bouchenafa, Omar Bouras	
P17	**"Study of Copper Based Heteropoly Salts in the Effeciency of Synthesis of 5-Ethoxycarbonyl-4-phenyl-6-methyl-3,4-dihydropyridin-2(1H)-one"**	217
	Khiar Chahinaz, Mazari Tassadit	
P33	**"Zn Based Phosphomolybdates Salts as an Environmentally Substitutes to HNO_3 Use in the Adipic Acid Production"**	218
	Dahbia Amitouche, Tassadit Mazari, Sihem Mouanni, Catherine Roch Marchal, Chérifa Rabia	
P34	**"New Catalytic Systems foran Eco-Friendly Coumarins Production According to Pechmann Condensation Protocol"**	219
	Leila Bennini, Tassadit Mazari, Chahinez Khiar, Malika Makhloufi, Catherine Marchal Roch, Chérifa Rabia	
P35	**"Controlled Release Study ofa Water-Soluble Drug from Microspheres as Drug Carriers"**	220
	Boumediene Fatima Zohra, Faiza Debab, Meryem Mouffok, Haouaria Merine	
P36	**"Fluorescence Quantum Yield of Natural Dye Extracted from Tunisien Plant"**	221
	Nourhéne Slama, Manel Ben Ticha, Badreddine Smiri, Ritha Mghaieth, Hatem Dhaouadi	
P42	**"Green Synthesis Of A-Aminophosphonates From A-Amino Acids Esters Under Microwave Irradiations"**	222
	Sara Boughaba, Zineb Aouf, Nour-Eddine Aouf	

The Second Edition of the International Congress of Applied chemistry and Environment
30th-31th October and 01st November 2020, Tunisia

ICACE 2020

P43	"Effects Of Microorganisms On Materials And The Environment"	223
	Hannachi Mohamed Tahar, Bradji Mohamed	
P44	"Viscosity Of Imidazolium-Based Ionic Liquids At Different Temperatures: Cation And Anion Effects"	224
	Affaf Djihed Boualem, Ali Mustapha Benkouider, Ahmed Yahiaoui, Aicha Hachemaoui	
P45	"Green Sustainable Process For The Synthesis Of Daiazaphospholidine"	225
	Bouchareb Fouziaa, Diaf Ilhem, Berredjem Malika, Aouf Nour-Eddine	

Poster Session 4: Management and valorization of bioresources and industrial wastes

P18	"Co –Composting of Date Palm Wastes and Poultry Manure"	227
	Fathia Madi, RidhaHachicha, Mansour Haddad	
P19	"Optimization of Preparation Conditions of Prickly Pear Seed Cake Derived Activated Carbon Using Experimental Design Approach and Its Application for Cadmium Removal"	228
	Rimene Dhahri, Asma Bouzidi, Younes Moussaoui	
P20	"Valorization ofPrickly Pear Seed Waste as Precursor for the Production of Activated Carbons"	229
	Nourhen Hsini, Hatem Dhaouadi, Niklas Hedin, Sonia Dridi-Dhaouadi	
P21	"Functional Morphology, Physico-Chemical and Thermal Investigations of *Opuntia* (Cactaceae)"	230
	Faten Mannai, Younes Moussaoui	

Poster Session 5&6: Identification and Valorization of Natural Substances

P22	"Extraction and Analysis of Phenolic Acids Belonging to Derivatives of Hydroxybenzoic Acids and Hydroxycinnamic Acids by Pls-Irtf-Atr in Plant Extracts"	232
	Nachida Bensemmane, Naima Bouzidi, Yasmina Daghbouche, Mohamed El Hattab	
P23	"Investigation of Green Corrosion Inhibitor Based on Aloe *vera (L.) Burm*. F. for the Protection of Bronze B66 in 3% NaCl"	233
	Bouchra Benzidia, Najat Hajjaji, Abdellah Srhiri	
P24	"Effect of Extraction Technique on Phenolics Compounds and Antioxidant Propreties of Green Hull Pistacia Vera L".	234
	Manel Elakremi, Leyre Sillero, Lazher Ayed, JalelLabidi, Younes Moussaoui	
P25	"Valorization of Industrial Waste from the Lime Peel - Citrus Aurantifolia - from the Blida Region (Algeria) by Extracting Essential Oils"	235
	Boudjit Djamila, Elhadi Djamel, Announ Mohamed	
P26	"Antioxidant Power and Bioactive Effect of (*Rosmarinus Officinalis L.*)Obtained with Non-Conventional Extraction Methods"	236
	Nedra Dhouibi, Concetta Maria Messina, Rosaria Arena, Simona Manuguerra, Maria Morghese, Hatem Dhaouadi	
P27	"Chemical Composition, Antioxidant and Cytotoxic Activities of Essential Oil of Tunisian Plan: *Dittrichia Graveolens*"	237
	Nawres Gharred, Nadir Bettache, Chantal Menut, Sonia Dridi-Dhaouadi	
P28	"Chemical Composition and Antiviral Activity of Essential Oils from *Osmunda Regalis*"	238
	Sihem Bouazzi, Habib Jmii, Ridha El Mokni, Khaled Faidi, Danilo Falconieri, Alessandra Piras, Hela Jaïdane, Silvia Porcedda, Saoussen Hammami	
P29	"Green Synthesis and Characterization of Colored Clays: Cosmetic Applications"	239
	Safa Gamoudi, Amira Amraoui, Ezzeddine Srasra	
P30	Chemical Composition and Insecticidal Activityof *ClinopodiumNepeta*Subsp. *Nepeta* Essential Oil"	240
	Haïfa Debbabi, Ridha El Mokni, Ikbal Chaieb, Filippo Maggi, Giovanni Caprioli, Saoussen Hammami	

P31	**"Composition and Insecticide Potential Against *TriboliumConfusum* of the Essential Oil Extracted from Wild Carrot *(DaucusCarota Subsp. Maritimus)"*** Siwar Majdoub, Ridha El Mokni, Ikbal Chaieb, Alessandra Piras, Silvia Porcedda, Saoussen Hammami	241
P32	**"Micromorphological Investigation and Spectrophotometric Analyse of the Rosmarinic Acid Extracted from Raw Material of Rosmarin*(RosmarinusOfficinalis L.)* Growing in Tunisia and Russia"** Louati Habib, Serebryanaya Fatima, El Mokni Ridha	242
	Poster Session 8: Ecological Textiles and Para-textiles	
P37	**"Effect of Parameter of Pumice Stone Washing on the Bagging Properties of Denim Garments"** Ben Fraj Abir, Gazzah Mouna, Boubaker Jaouachi	244
P38	**"Microwave-Assisted Extraction and Dyeing of Bicomponent Polyesters Filaments with Fluorescent Natural Dye"** Marwa Souissi, Mounir Zaag, Nizar Meksi, Hatem Dhaouadi	245
P39	**"Sustainable Dyeing of Wool Fabric Using *Kermes Oak* as Source of Natural Colorant"** Noureddine Baaka, Adel Mahfoudhi	246
P40	**"Rheological study of Ecological Printing Pastes on the Quality of Printed Cotton Fabrics"** Ben Fadhel Amal, Haddar Wafa, Miled Wafa, Meksi Nizar	247
P41	**"Relation Between Mechanical Properties of PVC Synthetic Leather and Calcium Carbonate"** Mouna Stambouli, Slah Msahli , Sondes Gargoubi,Walid Chaouch, Riadh Zouari, Aweb Baccar	248

PLENARY CONFERENCES

ICACE 2020

The Second Edition of the International Congress of Applied chemistry and Environment
30th-31th October and 01st November 2020, Tunisia

ICACE 2020

Agromining, a Green Chain of Processes to Recover Metals Present in Soils

Pr. Marie Odile Nicolas Simonnot

LRGP (Laboratory Reactions and Chemical Engineering), Université de Lorraine, CNRS, 1 rue Grandville, BP 20451, 54001 Nancy, France

E-mail address : Marie-Odile.Simonnot@univ-lorraine.fr

ABSTRACT

Many soils, mine tailings and industrial waste contain metals in concentrations too low to be extracted by conventional mining processes. Nickel, for example, is naturally present in soils in many parts of the world, known as ultramafic soils. Over the course of evolution, some plants have adapted to the presence of these metals and have developed the ability to absorb them through their roots and transport them to their above-ground parts. These plants, described as hyper-accumulators or even hyper-nickelophores for nickel, contain up to several tens of grams of metal per kg of dry matter.

In the context of the scarcity of resources and the circular economy, it is important to develop processes to recover the metals extracted from the soil by plants.

At the LRGP, and with colleagues from the Laboratory Soils and Environment (LSE, Université de Lorraine, INRAE), we have been working on this topic for a little more than ten years and have been developing the "agromining" chain.

This chain is structured in two parts. The first is focused on plants and their cultivation, the aim is to understand the mechanisms that govern the hyper-accumulation of metals and to develop agronomic processes that maximize the mass of metals extracted per unit area of cultivated land, i.e. the product of the mass of plants and the target metal concentration in the plant. For nickel, for example, the cultivation of the *Odontarrhena chalcidica* plant allows the extraction of more than 100 kg of nickel per hectare.

The second part involves extracting the metals contained in the plant biomass and preparing the desired compounds with a specified purity. It implements the unit operations of process engineering and hydrometallurgy. Two main lines of work have been explored. The first consists of burning the plants and treating the ash, which contains up to 15 to 20% nickel by mass. The nickel is transferred into solution by leaching and the solution is treated to obtain the desired products. The second consists of extracting the nickel directly from the plant biomass, without combustion, and implementing the necessary separations. This situation is more complicated because the solution contains the major ions and dissolved organic matter, to which the nickel is complexed.

This approach has been applied to various metals on a small scale: nickel, zinc, cadmium, rare earths and has been transposed to the pilot scale for nickel. An environmental assessment of the chain by life cycle assessment showed that the environmental impacts were low, which justifies qualifying this chain as "green". It has also been transferred from the academic sphere to the economic sphere with the creation of the start-up Econick.

REFERENCE

Van der Ent A., Baker A.J.M., Echevarria G., Simonnot M.O., Morel J.L. (Eds) Agromining, farming for metals, 2nd edition, Springer, Cham. *In press*

The Second Edition of the International Congress of Applied chemistry and Environment
30th-31th October and 01st November 2020, Tunisia

ICACE 2020

Cellulose at the service of medecine

Pr. Mohamed Naceur Belgacem

Univ. Grenoble Alpes, CNRS, Grenoble INP*, LGP2, F-38000 Grenoble, France

E-mail address : Naceur.Belgacem@pagora.grenoble-inp.fr

ABSTRACT

The present lecture is focused on the recent advances on surface chemical modification of lignocellulosics, with a focus on biomedical applications. It will be divided into three parts:

1. The first part will be devoted to the basic consideration on surface phenomena with a special care about the difficulties associated with surface contamination, the surface energy characterization, the surface properties determinations, etc [1, 2].

2. The second part points out the interest in using polysaccharides (cellulose mainly starch) in several functional materials. These two raw materials could be subjected to several surface modification strategies, namely (i) physical treatments (ii) chemical grafting by direct condensation, "grafting from" and "grafting onto" approaches. In this context, recent works investigating green solvent-based or solvent-less systems will be reported [1, 2].

3. All these treatments aim at providing these substrates specific functions, such as hydrophobic character, anti-microbial properties, etc. [1, 2]. Typical examples of achievements in this field will be given and discussed, with a special focus on those aiming at helping medicine in specific challenges.

Finally, some relevant concluding remarks and perspectives will be given.

REFERENCES

[1] **Rol F., M. N. Belgacem M. N., Gandini A., Bras J.** Recent advances in surface- modified cellulose nanofibrils. Progress in Polymer Science, 88 (2019) 241–264

[2] **A. Gandini, Belgacem M. N.** The surface and in-depth modification of cellulose fibers. Advances in Polymer Science, 271 (2016)169-206.

* Institute of Engineering Univ. Grenoble Alpes

The Second Edition of the International Congress of Applied chemistry and Environment
30th-31th October and 01st November 2020, Tunisia

ICACE 2020

Sustainable and Environmental-Friendly Food Packaging Products from Oil Palm Biomass

Pr. Mohammad Jawaid[1,2]

[1] *Laboratory of Bio-composite Technology, Institute of Tropical Forestry and Forest Products (INTROP), University of Putra Malaysia, 43400 Serdang, Selangor, Malaysia*
[2] *Chemical Engineering Department, College of Engineering, King Saud University, Riyadh, Saudi Arabia*

E-mail id: jawaid@upm.edu.my

ABSTRACT

Governmental regulation and public awareness about plastic packaging especially single use plastics compel several European, USA and Asian Countries to introduce regulations to limit the use of plastic bags and Styrofoam products, and work towards sustainable and environmental-friendly packaging products from agricultural biomass. *Elaeisguineensis* (oil palm) is one of the most important plants in Malaysia, Indonesia and Thailand. The oil palm industry in Malaysia produced about 70 million tonnes of oil palm biomass, including trunks, fronds, and empty fruit bunches (EFB). Among the various dry fibrous biomass from oil palm tree, empty fruit bunch constituents more than 70% of fibers. EFB is one of major byproducts of oil palm mills are not efficiently utilized, and the explosive expansion of oil palm plantation has generated enormous amounts of biomass which creating environmental hazards. Oil palm Industry need to take benefits of these huge biomass and utilized it in best possible manner. Oil palm biomass can be used for making pulp and fillers, pulp can use for making paper and pulp moulding products whereas filler can be utilized to fabricate polymer composites for various application. Pulp produced from mechanical or chemical process of oil palm biomass can be utilizing to produce compostable and biodegradable pulp moulding packaging products which is light in weight, non-abrasiveness and sustainable. Oil palm based composites can be processed, compounded and extruded in the form of sheets at Industrial scale to convert this composite sheet into food packaging tray by thermo forming process.

In this talk will discuss about pulping process of oil palm biomass and how we can process oil palm pulp in different safe compostable and biodegradable products with the help of pulp moulding machine. I will also cover fabrication of composite sheet for Food packaging tray by utilizing oil palm biomass and other products.

KEYWORDS:

Oil Palm Biomass; Pulping; Pulp Moulding Process; Composite Sheet; Food packaging Tray.

The Second Edition of the International Congress of Applied chemistry and Environment
30th-31th October and 01st November 2020, Tunisia

ICACE
2020

CO₂ Adsorbents-Potential Use in Flue Gas Capture and for Gas Upgrading

Pr. Nicolas Hedin[1]

[1]*Department of Materials and Environmental Chemistry Stockholm University, SE106 9 Stockholm, Sweden*

E-mail address : niklas.hedin@mmk.su.se

ABSTRACT

Removing CO_2 from gas mixtures is today important for natural gas and biogas upgrading and also for the purification of CO_2 for various use. In such gas separation process, adsorption-driven capture of CO_2 is sometimes used as an alternative to physical absorption, chemical absorption or membrane upgrading processes. Also, in a larger context, adsorption-driven capture is and has been studied for a potential use in flue gas capture of CO_2. In this way, it could potentially offer means to reduce the cost for the capture step in the carbon capture and storage processes commonly agreed to be necessary to reduce the emissions of CO_2 to the atmosphere. I will here highlight the developments in my group when it comes to the chemistry and physics of a range of different physisorbents and chemisorbents and speculate about their potential future use in CO_2 capture and gas upgrading processes.

Valorisation of vegetable oils: from thermal risk assessment to kinetic modelling

Sébastien Leveneur[1,2]

[1]*Normandie Univ, INSA Rouen, UNIROUEN, LSPC, EA4704, 76000, Rouen, France ;*
[2]*Laboratory of Industrial Chemistry and Reaction Engineering, Johan Gadolin Process Chemistry Centre, ÅboAkadem University, Biskopsgatan 8, 20500 Turku, Finland*

E-mail address : sebastien.leveneur@insa-rouen.fr

ABSTRACT

One of the promising route for the valorisation of vegetable oil is the ones into polyurethanes (Figure 1) [1]. There are three main steps: epoxidation, carbonation and aminolysis. We investigated thermal behaviour and risk, kinetic modelling, structure-reactivity relationships, physicochemical properties and process intensification for these steps.

One of the first steps was to verify that vegetable oils and their modified form are thermally stable, thus they could be safely stored [2]. From a thermal risk viewpoint, the epoxidation by Prileschajew, i.e., in situ production of percarboxylic acid, is the most sensitive step. By using different calorimeters under adiabatic mode, we developed zero-order [3-6] and advanced kinetic models [7-8] to estimate the thermal risk parameters: Time-to-Maximum Rate under adiabatic conditions (TMRad) to measure the probability of this risk and the adiabatic temperature rise (ΔTad) to measure the risk severity. We also demonstrated that TMRad values for the epoxidation of vegetable oils and free fatty acids by using different carboxylic acids follow the Taft equation, which is based from Linear Free Energy Relationships.

From these studies, it was possible to find the safe operating conditions to perform kinetic experiments to develop advanced kinetic models for the epoxidation of vegetable oils and free fatty acids by coupling mass and energy balances [9-10]. Before the development of kinetic models for epoxidation system, we studied separately the kinetics of performic acid by perhydrolysis reaction [11]. The goal of this study was to decrease the number of parameters to estimate for the epoxidation system.

Physicochemical measurement (density, viscosity, specific heat capacity…) was carried out to find relationships between these properties and the nature of vegetable oils (fresh, epoxidized or carbonated ones) and temperature [12]. This study was fundamental for the different parameter estimation stages.

To optimize the production of epoxidized vegetable oil, we studied the factors influencing the ring-opening of epoxidized vegetable oils [13]. The developed kinetic model allows us to find the operating conditions to minimize the side reaction of ring opening, which was fundamental for the carbonation study [14-17].

The development of a kinetic model for the vegetable oil carbonation over the homogeneous catalyst TBABr required a thorough study of gas-liquid mass transfer [14-15].A mass transfer model was developed to take into account the fact that kinetics of CO2 absorption and CO2 solubility depends on the composition of vegetable oils (i.e., concentrations of double bonds, epoxide and carbonated groups). The developed intrinsic kinetic model takes into account the evolution of mass transfer kinetics, CO2 solubility and physicochemical properties (density and viscosity) during the carbonation due to the variation of epoxidized and carbonated groups concentration [15]. Several studies showed that reactivity of vegetable oil and their corresponding fatty acid methyl ester are different, but the difference of physicochemical properties was not taken into account. We compared the kinetics of carbonation of epoxidized cottonseed oil and its FAME form by using our model. A linear relationship between the ratio of $\dfrac{(k_{carbonation})_{ECSO}}{(k_{carbonation})_{EFAME}}$ and temperature was found due to similar values of kinetic constants.

The use of microwave irradiation technology for this multiphasic system can be benefit due its selective heating [18]. We applied this technology on the carbonation of epoxidized FAME from cottonseed oil [17]. A fair comparison between carbonation under microwave irradiation and under conventional heating was carried out. The kinetic modelling of these two heating systems shows that the activation energy under

The Second Edition of the International Congress of Applied chemistry and Environment
30th-31th October and 01st November 2020, Tunisia

ICACE 2020

microwave was estimated to be lowest one. We demonstrated that microwave irradiation can enhance the epoxidation kinetics by Prileschajew oxidation [19-22]. A loop reactor with an efficient mixing system was developed [20-22]. A kinetic model taking into account the microwave effect was developed [22].

For the production of polyurethane, we used the aminolysis which is the reaction between the carbonated group and amine. A reaction model was used to develop a kinetic model: aminolysis of carbonated methyl oleateby butylamine [1].The drawback of this reaction is the slow kinetics which is more pronounced with a carbonated vegetable oil for steric hindrance reason. To evaluate the steric hindrance, we are studying the aminolysis by different amines: butylamine, methyl butylamine, ethyl butylamine and dibutylamine.
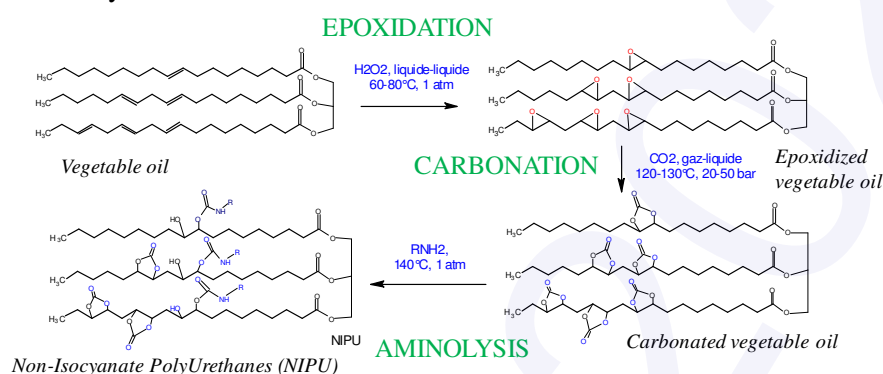
Figure 1. Reaction steps for the production of Non-Isocyanate PolyUrethanes from vegetable oils.

REFERENCES

[1] **W Pérez, X Cai, N Kebir, L Vernières, C Serra, T Salmi, SLeveneur, ChemEngJ**, 346 (2018) 271-280.

[2] **K Ait aissa, JL Zheng, L Estel, SLeveneur,** Org Proc Res Dev, 20 (2016) 948-953.

[3] **S Leveneur, F Delannoy, Y Levesqueau, JP Hébert, LEstel, B Taouk, T Salmi,** Chem Eng Trans, 36,139-144 DOI: 10.3303/CET1436024

[4] **S Leveneur, L Estel, C Crua,** JTherm AnalCalor, 122 (2015) 795–804.

[5] **W Pérez, T Salmi, LEstel, S Leveneur,** J Therm Anal Calorim, DOI: 10.1007/s10973-019-08894-2.

[6] **SLeveneur**, Org Proc Res Dev, 21(4) (2017) 543-550.

[7] **H Rakotondramaro, J Wärnå, L Estel, T Salmi, S Leveneur**, J Loss Prevent Proc, 43 (2016) 147-157.

[8] **S Leveneur, M Pinchard, A Rimbault, M S Shadloo, T Meyer**, Thermochim Act, (2018) 10–17.

[9] **S Leveneur, J Zheng, B Taouk, F Burel, J Wärnå, T Salmi**, J Taiwan InstChem E, 45 (2014) 1449–1458.

[10] **JL Zheng, J Wärnå, F Burel, T Salmi, B Taouk, S Leveneur**, AIChE J, 62 (2016) 726-741.

[11] **S Leveneur, M Thones, JP Hébert, B Taouk, TSalmi**, IndEngChem Res, 51 (2012) 13999–14007.

[12] **X Cai, K Ait Aissa, L Estel, SLeveneur**, J Chem Eng Data, 63 (2018) 1524-1533.

[13] **X Cai, JL Zheng, A Freites, LVernières, P Tolvanen, T Salmi, S Leveneur**, Int J Chem Kin, 50(2018)726-741.

[14] **JL Zheng, F Burel, T Salmi, B Taouk, SLeveneur**, IndEngChem Res, 54 (2015) 10935-10944.

[15] **X Cai, JL Zheng, J Wärnå, T Salmi, B Taouk, S Leveneur,** ChemEng J, 313 (2017) 1168-1183.

[16] **X Cai, M Matos, SLeveneur**, IndEngChem Res, 58 (2019) 1548-1560.

[17] **JL Zheng, P Tolvanen, B Taouk, K Eränen, SLeveneur, TSalmi,**ChemEng Res Des, 132 (2018) 9-18.

[18] **J Chaouki, S Farag, MAttia, JDoucet,** Can J ChemEng, DOI: 10.1002/cjce.23710

[19] **S Leveneur, A Ledoux, L Estel, B Taouk, T Salmi,** Chem EngRes Des, 92(8) (2014) 1495–1502.

[20] **AFreites, P Tolvanen, K Eränen, S Leveneur, TSalmi,** ChemEngProc, 102 (2016) 70–87.[21] **AFreites Aguilera, P Tolvanen, S Heredia, M González Muñoz, T Samson, A Oger, A Verove, KEränen, S Leveneur, JP Mikkola, TSalmi**, IndEngChem Res, 57(11) (2018) 3876-3886.

[21] **A Freites, P Tolvanen, K Eränen, J Wärnå, S Leveneur, T Marchant, TSalmi,** ChemEngSci, 199 (2019) 426-438.

ICACE
2020

ORAL

COMMUNICATIONS

Treatment of industrial discharge and environmental impacts

The Second Edition of the International Congress of Applied chemistry and Environment
30th-31th October and 01st November 2020, Tunisia

ICACE 2020

Application of raw sawdust, olive pomace and their derived biochars for copper removal from aqueous solution

Ibtissem Mannai[a,b], **Stéphanie Sayen**[b], **Achouak Arfaoui**[c], **Amira Touil**[a], **Emmanuel Guillon**[b]

(a) Laboratoire de Recherche des Sciences et Technologies de l'Environnement (LRSTE), ISSTE BorjCédriaB.P 1003, 2050, Hammam Lif, Tunisia.
(b) Institut de Chimie Moléculaire de Reims (ICMR UMR CNRS 7312), UFR Sciences Exactes et Naturelles, Moulin de la Housse, Bât. 18, BP 1039, 51687 Reims, France.
(c) Ecole Supérieure d'Ingénieurs de Medjez El Bab, Unité de recherche GDRES, Route du Kef Km 5, 9070, Medjez El Bab, Tunisia.
ibtissem.mannai@etudiant.univ-reims.fr, stephanie.sayen@univ-reims.fr, arfaoui.achouak@gmail.com, amira.touil@gmail.com, emmanuel.guillon@univ-reims.fr

ABSTRACT

In this study, the removal of Cu(II) ions from aqueous solution was investigated using four different sorbents (raw sawdust, raw olive pomace and their derived biochars). The optimum pH of copper uptake by both raw biomasses and their biochars was 7. For an introduced copper concentration equal to10^{-4}mol/L, raw olive pomace retained higher amounts of copper than raw sawdust (130.79mg/g and 44.4mg/g) of Cu initial concentration, respectively. After the artisanal pyrolysis of the two feedstocks at 300°C for two hours to prepare biochars, the adsorption capacities of both adsorbents were significantly enhanced, 95% (233.01 mg/g) for the biochar derived from sawdust and 60% (153.05 mg/g) for the one derived from olive pomace.

KEYWORDS

Adsorption, copper, biochar, sawdust, olive pomace

1. INTRODUCTION

Over the last decades, surface and ground-water and soil pollution has dramatically increased as a result of the release of several contaminants in the environment, such as pesticides and metal trace elements (MTE). In particular, the presence of MTE in water is due to the massive use of agri-chemicals in agriculture, mining activities as well as the discharge of wastewater from metallurgic industries in the natural environment [1]. The presence of these pollutants in water has adverse effects on the environment and human health. Therefore, it is urgent to remove these heavy metals from water through the use of different technologies such as precipitation, electrolysis and sorption. Sorption remains the less expensive and most effective technology for removing heavy metals from water with a wide range of sorbents used in the retention of inorganic pollutants such as activated carbons, zeolites, clays and lignocellulosic materials [2].Recently, there is a growing interest for the development of new bio-based, low-cost and sustainable adsorbents. This is the case of biochar, a highly porous, carbon-rich solid material obtained through Pyrolysis *i.e.* the thermochemical conversion of biomass in an oxygen-poor environment [3].Against this backdrop, the aim of this work is to study the performance of two raw organic wastes (sawdust and olive pomace) and their derived biochars in terms of copper removal from aqueous solution.

2. MATERIAL AND METHODS

2.1. Feedstocks

Olive pomace and sawdust were collected in an oil mill and a carpentry shop both located in the area of Mnihla (North Tunisia). The collected materials were air-dried, ground and then sieved to 200µm before undergoing an acido-basic treatment (with KOH and HNO_3) in order to obtain an insoluble solid in a wide pH-range. Finally, both biosolids were washed several times with distilled water then dried at 38°C.

2.2. Biochar preparation

Biochars used in this study were produced using an artisanal method employed by Tunisian farmers. The process, locally called "mardouma", consists in burying the raw materials (olive pomace and sawdust)

The Second Edition of the International Congress of Applied chemistry and Environment
30th-31th October and 01st November 2020, Tunisia

ICACE 2020

directly onto the soil then covering them with an impermeable layer of clay and branches to prevent air entry before setting fire to biomass. This operation lasted for two hours at a temperature of 300°C.

2.3. Adsorption experiments

The adsorption capacities of the four studied adsorbents were assessed using the batch technique. For each experiment, 25mL of copper solution (0.2 to 0.6 mmol/L) and 0.5 to 4g/L of sorbent were added into vessels. The suspensions were shaken for different durations (15 min to 8h), at pH values varying from 3 to 9, then they were filtered and the copper concentrations remaining in solution were measured by ICP-OES. In each case, the retained amount of Cu was calculated as the difference between the initially introduced and the remaining Cu concentrations.

3. RESULTS AND DISCUSSION

3.1. Characterization of the studied adsorbents

The main physico-chemical properties of the studied raw biomasses and their derived biochars are given in Table 1. The results show that the two raw biomasses have an acidic nature (pH≈ 5.5). This can be attributed to the abundance of carboxylic and phenolic acid groups in organic matter. After pyrolysis, the pH of biochars becomes alkaline (8.9 and 10.3). As for surface area and porosity, these parameters were increased after pyrolysis of sawdust while not significantly changed for olive pomace.

Table1. Selected physico-chemical properties of the studied raw biomasses and their derived biochars

Properties / Biomass	Moisture (%)	pH	Surface area (m^2/g)	Total pore volume $(10^{-3} cm^3/g)$	CEC (meq/100mg)
Raw sawdust	0.40	5.8	1.5	3.4	41.3
Sawdust-derived biochar	0.04	8.9	4.1	18.4	44.0
Raw olive pomace	0.46	5.3	1.4	5.6	25.3
Olive pomace-derived biochar	0.17	10.3	1.6	1.9	32.0

3.2. Effect of adsorbent dose

The evolution of copper removal yield as a function of adsorbent dose is given in Figure 1.
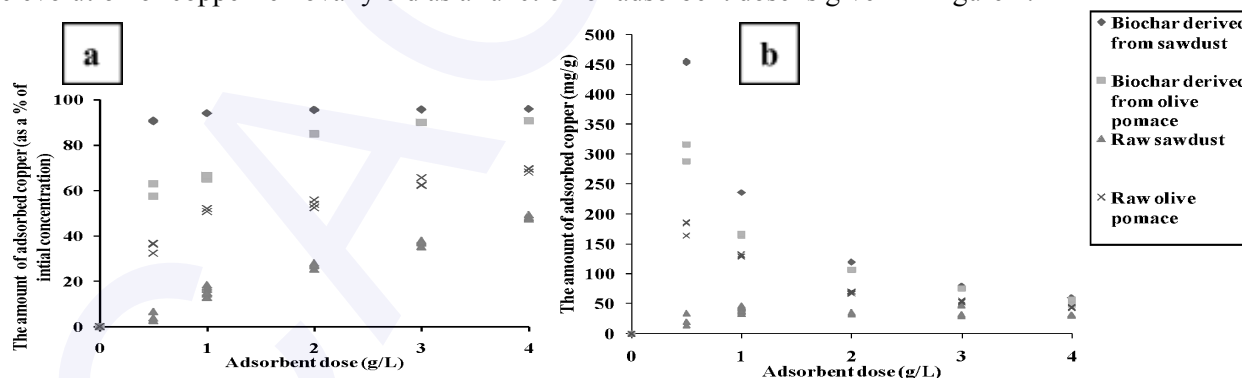

Figure 1. Biochars as a function of sorbent dose in aqueous solution ($[Cu^{2+}]_0=10^{-4}$M, time of stirring=6h and at natural sorbent pH)

Our results show that, regardless of biomass nature, the uptake of copper from solution increased with the sorbent dose (Figure 1a). In fact, the removal yields of copper obtained for the dose of 4g/L are 70% and 60%, for the raw olive pomace and the raw sawdust respectively, compared to those obtained for the dose of 0.5g/L which are 36% and 4%.After artisanal pyrolysis, the sorption capacities of both raw materials were enhanced. Indeed, at a dose of 4g/L, both studied biochars retained almost 95% of the introduced copper.

The Second Edition of the International Congress of Applied chemistry and Environment
30th-31th October and 01st November 2020, Tunisia

ICACE
2020

When expressed as mg per sorbent mass unit (Figure 1b), it is noticed that the amounts of sorbed Cu decreased with the increase of sorbent dose from 0.5 to 4 g/L. For practical and analytical reasons, the 1g/L was chosen for further experiments.

3.3. Effect of time

The kinetics of copper adsorption were performed by varying the solid/solution contact time between 15 minutes and 8 hours at an initial concentration of copper of 10^{-4}mol/L and at sorbent dose of 1g/L. The obtained kinetics are reported in figure 2.
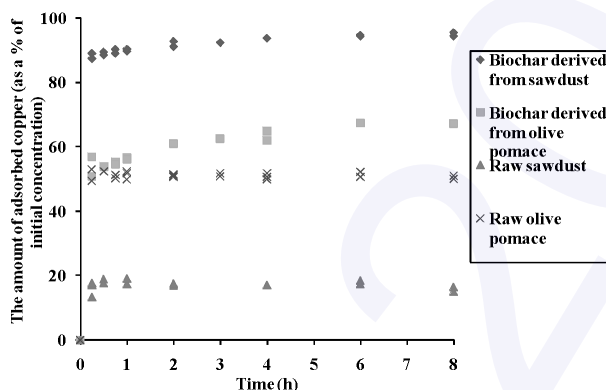

Figure 2. Evolution of removal yield of copper by sorption on raw biomasses and their derived biochars as a function of time

Figure 2 shows similar shapes of kinetic curves for the different tested biosolids: the amount of adsorbed copper increased rapidly during the first 15 minutes then ceased to evolve after two hours of stirring. The presence of a plateau indicates that the equilibrium is reached. At equilibrium, 51, 17, 61, and 93% of introduced copper were retained onto the raw olive pomace, the raw sawdust, the olive pomace-derived biochar and the sawdust-derived biochar, respectively.

3.4. Effect of pH

Figure 3 shows the effect of pH solution on the amount of adsorbedCu^{2+} by raw biomasses and their derived biochars. The contact time adsorbent/copper was taken equal to 2 hours corresponding to the equilibrium time.
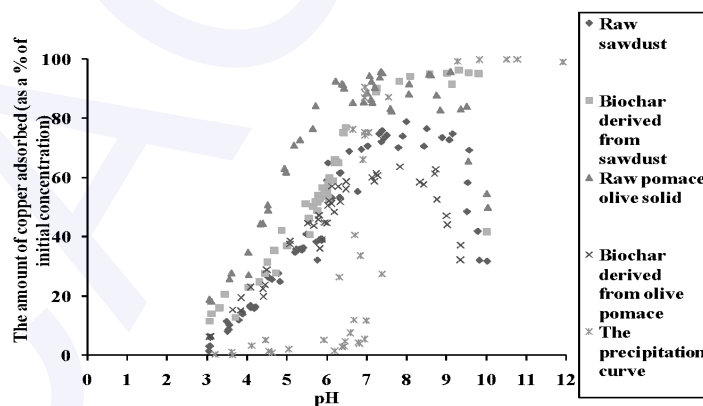

Figure 3. Effect of pH on the removal of Cu^{2+} by adsorption on raw biomasses and their biochars

The analysis of these results shows that the sorption of copper by raw materials and biochars starts at pH 3. Then, the removal yields of copper increased with the increase of pH from 3 to 7and the best copper removal efficiencies were obtained for pH 7. In fact, the higher the pH, the more the surface of studied biomasses becomes negatively charged which promotes the retention of copper cations. Thus, the optimum pH of

The Second Edition of the International Congress of Applied chemistry and Environment
30th-31th October and 01st November 2020, Tunisia

ICACE 2020

copper uptake by the raw sorbents and their biochars is 7. The decrease of copper retained above pH 7 is due to a partial dissolution of the solids in spite of the acid and base treatments.

3.5. Effect of initial concentration

As it presented the best performance in terms of Cu removal from aqueous solution, sawdust was selected to investigate the effect of initial concentration of copper on sorption.
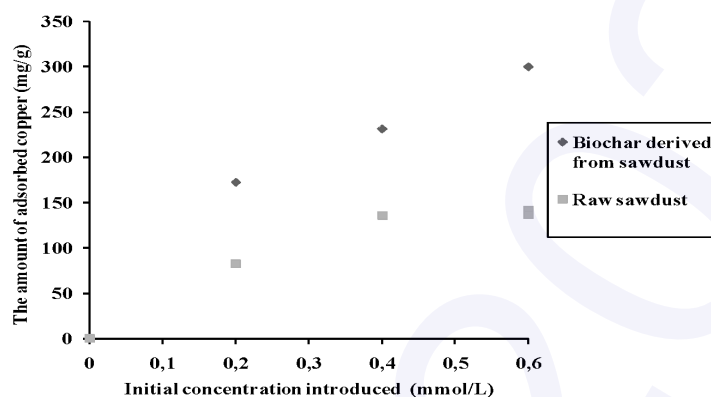

Figure 4. The amounts of adsorbed copper as a function of initial concentration C_0 ($0,2 < [Cu^{2+}]_0 < 0,6$ mmol/L, sorbent dose=1g/L, T=20°C and pH ≈5.2)

Our results show that the amount of adsorbed copper by the raw sawdust and its biochar increases with the increase of the initial concentration of copper from 0,2mmol/L to 0,6mmol/L. For an introduced copper concentration of0,6 mmol/L biochar derived from sawdust retained higher amounts of copper than raw sawdust (300mg/g and 137mg/g respectively). Thus, the sawdust-derived biochar had a copper removal efficiency more than2 fold higher than that of the raw sawdust. This is attributed to the increase of surface area and porosity of raw sawdust after pyrolysis, which favoured copper adsorption.

4. CONCLUSION

The aim of this work was to investigate the performance of two raw organic wastes (sawdust and olive pomace) and their derived biochars in terms of copper removal from aqueous solution. Our results indicate that regardless of sorbent nature, the uptake of Cu from solution increases with pH and is maximum at pH 7. Under these experimental conditions and for $[Cu^{2+}]=10^{-4}$mol/L, raw olive pomace retained higher amounts of copper than raw sawdust (50% and 20% of Cu initial concentration respectively). After the artisanal pyrolysis of the two feedstocks at 300°C for two hours, the sorption capacities of both raw sorbents were significantly enhanced. Thus, the highest removal yields of copper were obtained for the biochar derived from sawdust (about 95% of the introduced Cu) while the olive pomace-derived biochar exhibited lower affinity (60%). Our findings suggest that the valorization of the two tested biowastes through pyrolysis generates biochars that can be used as low-cost and efficient sorbents for copper removal from polluted wastewater.

REFERENCES

[1] **Dean, John G., Frank L. Bosqui, and Kenneth H. Lanouette,** Removing Heavy Metals from Waste Water, *Environmental Science & Technology*, 1972, Vol. 6, No. 6, 518–22

[2] **Kurniawan, Tonni Agustiono, Gilbert Y.S. Chan, Wai-hung Lo, and Sandhya Babel**, Comparisons of Low-Cost Adsorbents for Treating Wastewaters Laden with Heavy Metals, *Science of The Total Environment*, 2006, Vol. 366, No. 2–3, 409–26.

[3] **Kookana, R. S., A. K. Sarmah, L. Van Zwieten, E. Krull, and B. Singh**, Chapter Three - Biochar Application to Soil: Agronomic and Environmental Benefits and Unintended Consequences, *Advances in Agronomy*,2011, Vol. 112, 103-43.

The Second Edition of the International Congress of Applied chemistry and Environment
30th-31th October and 01st November 2020, Tunisia

ICACE 2020

Skimmer upgrade to enhance de-oiling of petroleum production water :

Case study of an industrial scale skimmer

Ines Wada[a], Ghazza Masmoudi[a], Hatem Dhaouadi[a]

(a)   *Unité de recherche chimie appliquée et environnement, Faculté des sciences de Monastir, Université de Monastir, Monastir, Tunisie*

ABSTRACT :

In petroleum industry huge volume of oily wastewater are produced. Volumes are continuously increasing with the oilfield age, making the applied treatment processes inefficient. In this paper, monitoring oil and grease in the inlet and outlet of existing API-skimmer showed that the existing process is not adapted to the volume of treated water. A stocks law based approach for skimmer upgrade was introduced: the upgrade solution consists on adding parallel plates coalescing chamber which can be coupled with demulsifier injection. For a given set of design targets of a specific flow rate, existing skimmer dimensions and minimum captured oil droplet diameter, the Hydro-Kinematic approach proposes a systematic way to determine the required number of plates and spacing between them. Results showed that the existing skimmer can be retrofitted by adding 84 plates spaced by 2 cm each. Demulsifier addition was proved to ameliorate the oil-water separation to attend 93.87 %.

KEYWORDS: Petroleum production water, oil-water separation, skimmer, parallel plates

1. INTRODUCTION

Oil and gas extraction needs huge volumes of water to be accomplished, especially in the case of enhanced oil recovery (EOR) with water injection [1]. Khatib and Verbeek [2] estimated that about 210 million bbl of water were consumed daily for petroleum extraction worldwide. Those huge water volumes are continuously increasing with the age of the oil field [3]. Petroleum wastewater are composed of production water contaminated essentially with hydrocarbons and having a complex composition and groundwater extracted with oil and gas.

Oil in Petroleum production water can be present under different forms; free oil as discrete oil globules with typical droplet size around 150 µm, able to rise due to flotation forces and form an oil layer on the top of the water, dispersed oil, characterized by droplet sizes ranging from 120 to 150 µm and, emulsified oil as particles with a diameter less than 20 µm which form a stable suspension in water [4].

Gravity separation is the most used separation technique for oily effluents, based on density difference between oil and water, its efficiency depends especially on the rising velocity of the oil droplets and the water flow rate. The performance of gravity separators depends on retention time, tank design, oil properties, operating conditions and the effects of chemicals if added. This treatment is ineffective with small oil droplets or emulsified oil since the oil droplet size and the retention time are inversely proportional. Indeed the American Petroleum Institute (API) research demonstrated that simple gravity separation can't be efficient for the removal of oil globules with less than 150 µm of diameter [5]. Thus, only a fraction of free oil can be removed. To improve the performances of gravity separators, it can be equipped with parallel or corrugated plates which allow the oil droplets to agglomerate and form larger particles able to float easily. Indeed, API-skimmer with parallel plates can remove oil droplets with diameter larger than 60 µm and for skimmer with corrugated plates removal can reach droplets with diameter size up to 40µm.

 In the present work, a new approach based on stocks law to evaluate the oil/water separation efficiency of an existing API-skimmer was presented. On the light of geometry evaluation results and the oil and grease monitoring at the skimmer inlet and outlet, a systematic calculation method for the upgrade of an existing separator by adding plates in order to improve oil/water separation was described. A hydro-kinematic approach is presented to calculate the number of required plates to enhance oil/water separation. A calculation example on the use of the described approach to optimize the oil/water separation was applied to an existing conventional API-skimmer. The use of a demulsifier was suggested and the optimal dose was set.

2. MATERIAL AND METHODS

2.1. Petroleum production water

Petroleum production waters object of the current study is issued from an oil industry located in El Borma field in the Tunisian south. Produced water is a mixture of formation water (55%), water injected for the EOR (40%), and industrial water used for oil desalting (5%). The volume of production water rejected daily is 14000 m^3. The nominal size for oil droplet removed is equal or higher than 150 μm. For the oil and grease monitoring sample size calculation was based upon student's t-distribution, the confidence level is 90% and the tolerated error is 2 ppm. Random sampling was performed over one week for the 24 working hour per day.

2.2. Existing API-skimmer characteristics

The studied API-skimmer used in El Borma oilfield was designed as per the API 421 monograph was and constructed on the 90's. The inlet water is coming from the three phase separation of the crude and it was treated in a water degasser before feeding the API-skimmer. The studied API-skimmer is a two channels skimmer and dimensions illustrated in figure (1) and are as follows: the skimmer depth (d) is 2.4 m, the channel length (L) and width (B) are respectively 22.8 m and 2.4 m, the vertical cross-sectional area (Ac) is 11.52 m^2 and the total separator surface area (Ah) is 109.44 m^2.

2.3. Analytical methods

2.3.1 Oil and grease monitoring

Oil and grease concentration were measured in compliance with the method EPA 1664A. Hexane with 95% purity, 99.0% saturated C6 isomers and residue less than 0.001% were used to extract oil and grease from an acidified aliquot (1 liter) of the production water sample. The hexane drained through sodium sulfate (Na$_2$SO$_4$) was then evaporated at 70 °C and the entire amount of residue left behind is weight with a precision balance type sauter 414/12 and defined as oil and grease.

2.3.2 Specific gravity

Specific gravity was measured at the design temperature (For a conservative approach the temperature of 5°C was considered as the worst case). Production water and oil both were both cooled to 5°C, clear water was cooled to 5°C. The liquid in question and an equal volume of clear water were weighed. The ratio of the liquid's weight to the weight of water is calculated and represents the specific gravity. The used balance is a precision balance type sauter 414/12.

2.3.3 Absolute viscosity

Production water absolute viscosity was measured with a Brookfield BF35 viscometer at the design temperature.

2.3.4 Basic Sediment and Water (BS &W)

To measure separation efficiency BS&W test on five 100 mL samples was performed, for each sample two centrifuge tubes were filled to the 50mLmark with the well-mixed sample directly from the sample container. Then, 50 mL of water-saturated solvent were added and tubes were vigorously shaked until the contents are thoroughly mixed. Tubes are immersed to the 100 mL mark for 10 min in a bath maintained at 60 °C before being spinned for 10 min. The tube diameter (dt) is 37.75 mm and the speed of the rotating head (r/min) was set at 5000 revolution/min, so the relative centrifugal force (rcf) was 762.52.

$$rcf = dt * [(r/min)/1335]^2 .$$

Tubes are immediately brought to a vertical position after the centrifuge stops, the volume of water and sediment at the bottom of each tube is recorded and the oil layer volume is recorded. Since the oil layer is very thin and to make sure of the accuracy of the read volume, the oil layer on the top of the tube is sucked with an electronic micropipette.

2.4. Theoretical approach

The rise rate (vertical velocity) of oil droplets (V$_t$)to the surface due to gravity difference between oil and water will be calculated on the basis of stocks law.

The Second Edition of the International Congress of Applied chemistry and Environment
30th-31th October and 01st November 2020, Tunisia

ICACE 2020

$$V_t = \left(\frac{g}{18\mu}\right) * (\rho_w - \rho_o) * D^2 \quad \text{Equation (1)}$$

According to the API 421 monograph the smaller diameter (D) of the oil droplet to be removed by parallel plates is 60 µm. So for calculation we will consider D equal to 60 µm

The vertical velocity of an oil droplet moving from the plate (n) to the plate (n+1) can be expressed as the quotient of the height between two plates (h) by the separation time (ts):

$$V_t = \frac{h}{t_s} \qquad\qquad \text{Equation (2)}$$

Assuming a laminar flow with streamlines parallel to the plate the average velocity can be defined as the fluid path length divided by the retention time.

To have an efficient separation the retention time (t_r) should be at least equal to separation time (t_s):

$$t_r = t_s \qquad\qquad \text{Equation (3)}$$

$$\frac{L_{plate}}{V_{hp}} = \frac{h}{V_{tp}} \qquad\qquad \text{Equation (4)}$$

$$\Rightarrow \quad V_{hp} = \frac{L_{plate}}{h*V_{tp}} \qquad\qquad \text{Equation (5)}$$

We have $\qquad\qquad V_{hp} = \frac{q}{h} \qquad\qquad$ Equation (6)

According to equations (5) and (6) :

$$\frac{q}{h} = \frac{L_{plate}}{h} * V_{tp} \qquad\qquad \text{Equation (7)}$$

By writing V_{tp} as defined in Equation (1) we have :

$$q = L_{plate} * \frac{g}{18\mu} * (\rho w - \rho o) * D^2 \qquad\qquad \text{Equation (8)}$$

Since we have a two channel skimmer the calculated specific flow rate (q) will be expressed by:

$$Q_{(d)} = q * B * (n' - 1) \Rightarrow \quad n' = \frac{Q_{(d)}}{B*q} + 1 \qquad\qquad \text{Equation (9)}$$

where (n') is the number of plates to be added into the API-skimmer.

The height (h) between two plates is defined as: $h = \frac{\frac{d-L_{sludge}}{\sqrt{2}}}{n}$ Equation (10)

3. RESULTS AND DISCUSSIONS

3.1. Wastewater characteristics

As recommended by the API monograph 421 and for conservative approach water specific gravity (ρw) and oil specific gravity ($\rho 0$) were measured at 5°C (the lowest temperature that can be reached at El Borma Oilfield). Values are respectfully 1072 and 822. The production water absolute (dynamic) viscosity (μ) is 0.0152 poise at 5°C.

Oil and grease monitoring covered 28 samples at the API-skimmer inlet and 28 samples at the outlet. Figure 3 illustrates the oil and grease variation during the study period. At the API-skimmer inlet the average oil and grease value is 1071 ppm and standard variation is 76.11 ppm. The fluctuation of the oil and grease value at the skimmer inlet is related to production well inconstancy and work over operations during the period of sampling. Whereas at the API-skimmer outlet, oil and grease measured values are less dispersed, the standard deviation is 7.25 ppm and the average oil and grease value is 114 ppm.
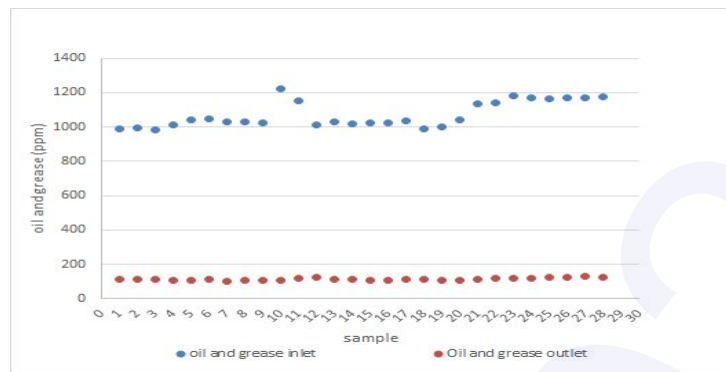
Figure 1. Oil and grease monitoring at the skimmer inlet and outlet

The skimmer average efficiency is 86%. Reject value doesn't comply with local regulation and confirms that skimmer efficiency has to be improved.

3.2. API skimmer upgrade
3.2.1 Parallel Plates Coalescing chamber design

Upgrading an undersized API-skimmer with the addition of parallel plates is a simple and cost effective option. The required plates number can be calculated by applying equation (9) and (10).

Since we have an influent with high solid content and to avoid plugging problems, angle of plate inclination from the horizontal will be equal to 45° [5] .The space (L_{sludge}) equal to 60 cm will be reserved for the sediment settling and sludge collection and removal so the height for a cubic plates pack is $[(d-L_{sludge})/\sqrt{2}]$. So for the previous water specifications and geometric considerations:

The specific flow rate between two plate is $q = 4$ cm^3.s^{-1}

The water flow in a single channel of the skimmer is $Q_{(1/2)} = 81018.5$ cm^3.s^{-1}

The required number of plates to have more efficient separation is 84

Spacing between each two plates is 2 cm

The upgraded API-skimmer configuration is shown in figure 2: The added plates will allow the treatment of more important volume of wastewater and will provide a longer path for the oil droplets to travel to the top of the separator so small droplets can coalesce and form larger droplets. An appropriate sludge removal device will allow solid evacuation and avoid clogging problems.
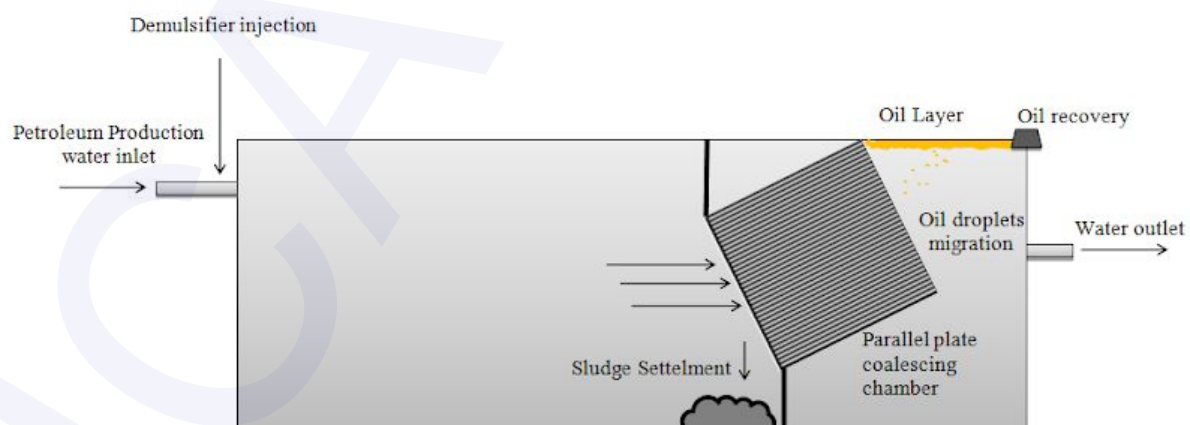

Figure 2. Oil water separation with upgraded API-skimmer

The Second Edition of the International Congress of Applied chemistry and Environment
30th-31th October and 01st November 2020, Tunisia

ICACE 2020

The developed approach can be compared to (Boraey, 2018) works [6] for the design of CPI, but the limits of Boraey's approach are that his method doesn't take into consideration constraints related to existing facilities, so it can't be applied for the upgrade of existing API-skimmer. The novel design method for conventional oil-water separators as described by Odiete and al., [7] takes into account the regulatory effluent oil limit of a country in the design and it also consider oil separation efficiency as a design parameter but the upgrade option was not investigated for the reported method.

The upgrade of existing API-skimmer reminds an interesting option on the case of mature oilfield. The approach suggested here for the upgrade is an original solution to efficiently treat increasing production water volumes.

3.2.1 Demulsifier

The initial oil and grease concentration value (C_i) is 982 ppm. The demulsifier efficiency was evaluated on the basis of the BS&W test. In figure 5 the oil layer variation with demulsifier dose was represented. Results showed that optimal oil-water separation is achieved with demulsifier dose equal to 20 ppm which corresponds to 0.12 mL of oil layer volume for 100 mL of wastewater. The recovered oil layer corresponds to (C_f) 920.14 ppm. The demulsification efficiency (C_f/C_i *100) with SSR 3510 is 93.87%.

4. CONCLUSION

In this paper, oil and grease monitoring according to the method EPA 1664A was performed for petroleum production water to evaluate skimmer separation efficiency. The API-skimmer efficiency was 86%. To enhance the performance of the separator we proposed to add parallel plates into the existing skimmer. Plates provide a longer path for the oil droplets to travel to the top of the separator so small droplets can coalesce and form larger droplets. A systematic method to determine the required number of plates to improve separation and to remove oil droplets larger than 60 µm was described. For the studied case, to fulfill the production flow rate of 14000 m3/d and remove oil droplets with smaller diameters (up to 60 microns) the existing the Api-skimmer can be retrofitted by the addition of 84 plates spaced by 2 cm each and with the addition of demulsifier. The optimal dose of a commercial demulsifier SSR 3510 is 20 ppm. The global efficiency for the API-skimmer after upgrade coupled to demulsifier injection has to be evaluated through a pilot scale unit. The used demulsifier SSR 3510 is the product already available on field and injected for the first operation of oil-water-gas separation. The nature of the demulsifier to be used for oil water demulsification needs further studies

REFERENCES

[1] **Clark, C.E., Veil, J.A.**, *Produced Water Volumes and Management Practices in the United States.* Argonne Natl. Lab. Rep. 64, 2009,
   doi.org/10.2172/1007397

[2] **Khatib, Z., Verbeek, P.**, *Water to Value – Produced Water Management for Sustainable Field Development of Mature and Green Fields,* 2002

[3] **Arnold, R., Burnett, D.B.,Elphick,J., Feeley,T.J.III , Galbrun, M., Hightower, M., Jiang, Z., Khan, M., Lavery, M.,Luffey, F. and Verbeek, P.H.J.** ,*Managing water - From waste to resource*, 2004, Vol.16, 26-41

[4] **Wang L. K., Shammas, N. K., Selke, W. A., and Aulenbach, D. B.**, *Flotation Technology*, 2010, doi:10.1007/978-1-60327-133-2

[5] Monographs on refinery environmental control, Management of water discharges.; API publication, 4211990 1st edn. American Petroleum Institute./Division of Refining / Washington, D.C., USA, 1990

[6] **Boraey, M. A.,** A Hydro-Kinematic approach for the design of compact corrugated plate interceptors for the de-oiling of produced water. *Chemical Engineering and Processing - Process Intensification*, 2018, Vol. 130, 127–133. doi:10.1016/j.cep.2018.06.006

[7] **Odiete, W. E., & Agunwamba, J. C.** , Novel design methods for conventional oil-water separators, *Heliyon,* 2019, Vol. 5, No.5,
   doi:10.1016/j.heliyon.2019.e01620

The Second Edition of the International Congress of Applied chemistry and Environment
30th-31th October and 01st November 2020, Tunisia

ICACE 2020

Adsorption of nitrate, phosphate, nickel and lead on soils: risk of groundwater contamination

Mohamed Abdelwaheb[a], Khaoula Jebali[a], Hatem Dhaouadi[a], Sonia Dridi-dhaouadi[a]

(a) *University of Monastir, Faculty of Sciences of Monastir, Research Unity of Applied Chemistry and Environment-5000 Monastir, TUNISIA*

ABSTRACT

Agricultural activities pose a significant risk of groundwater pollution. Indeed, fertilizers and treated wastewater used for irrigation are, in part, responsible for the deterioration of groundwater and surface water quality. This work presents the effect of the soil clay content on the retention of four different pollutants in order to evaluate the risk they represent for the groundwater. These contaminants are generated by two main agricultural activities: 1/ soil fertilization with phosphate and nitrate fertilizers and 2/ irrigation with treated wastewater in which heavy metals such as nickel and lead are persistent. Firstly, the characterization of the sand and clay used in this work was performed and showed a cation exchange capacity of 1.24 and 25 meq/100 g, a specific surface area of 0.12 and 67.98 m^2/g and a percentage of organic matter of 0.15 and 2 % for sand and clay, respectively. The retention isotherms on all pollutants and the Langmuir, Freundlich, Freundlich-Langmuir, Hill and Koble-Corrigan models were applied. All experimental isotherms have been successfully adjusted using the Koble-Corrigan expression. The amounts of nitrates, phosphates, nickel and lead retained by the sandy soil, for an initial pollutant concentration equal to 1 meq/L, were evaluated at 0.29, 3.89, 5.97 and 8.56 µeq/g respectively. In contact with a soil containing 30 % clay, the adsorbed amounts were estimated at 3.55, 15.00, 6.97 and 8.79 µeq/g for nitrates, phosphates, nickel and lead, respectively. These results mean that the pollutants that pose the greatest risk of groundwater contamination when carried by water through sandy soil are classified as follows lead < nickel < phosphate < nitrate while for a clayey soil, the classification becomes as follows: phosphates < lead < nickel < nitrate.

KEYWORDS: adsorption, heavy metal, clay, nitrates, phosphates, isotherm model

1. INTRODUCTION

For more than a century, agricultural activities have considerably increased their consumption of phytosanitary and fertilizers products. Unfortunately, these are often a source of groundwater pollution, especially for the more soluble ones, namely nitrates and phosphates [1], also, using treated wastewater in agricultural irrigation increases the risk of soil contamination by persistent pollutants such as heavy metals [2]. These contaminants represent a real danger to the groundwater that they can reach by the flow water infiltration.

The objective of this work is to quantify the risk of groundwater contamination by nitrates and phosphates anions and by nickel and lead cations brought to the soil surface by agricultural activities. The study was done by following the pollutant behavior onto the soil by using different isotherm adsorption models. The influence of soil clay content on groundwater contamination has been investigated in order to determine the relationship between soil composition and risk of groundwater contamination.

2. MATERIAL AND METHODS

Batch experiments were realized for the fourth ions (NO_3^-, PO_4^{3-}, Ni^{2+} and Pb^{2+}). These experiments were done by putting 2 g of soils prepared by sand and different clay contents (from 0 to 30%) in 20 mL of the ionic solution of lead, nickel, nitrate or phosphate. The solution concentrations vary from 0 to 1000mg/L (9.66 meq/L), 0 to 100mg/L (3.38 meq/L), 0 to 200mg/L (2.10 meq/L) and 0 to 500 mg/L (24.18 meq/L) for lead, nickel, nitrate and phosphate, respectively. No pH adjustment was made and all solutions showed pH

The Second Edition of the International Congress of Applied chemistry and Environment
30th-31th October and 01st November 2020, Tunisia

ICACE 2020

values between 7.0 and 7.8. Stirring was maintained for 24 hours at 200 rpm in a constant temperature (19 ± 1°C). The mixture was then centrifuged (3000rpm) for 10 minute, and the ion residual concentrations were analyzed using Atomic Absorption Spectrometer (Analytical Jena), spectrophotometer (UNICO 1200) and a specific electrode for the metallic cations, phosphates and nitrates, respectively [3]. The sand and the clay are collected from Skanes beach (Monastir, Tunisia) from Oued El Guelta (Ouardanine, Monastir, Tunisia)

In order to predict the behavior of the pollutants according to the soil composition, six models were investigated to fit the experimental isotherms: Langmuir, Freundlich, Langmuir-Freundlich, Hill, Koble-Corrigan.
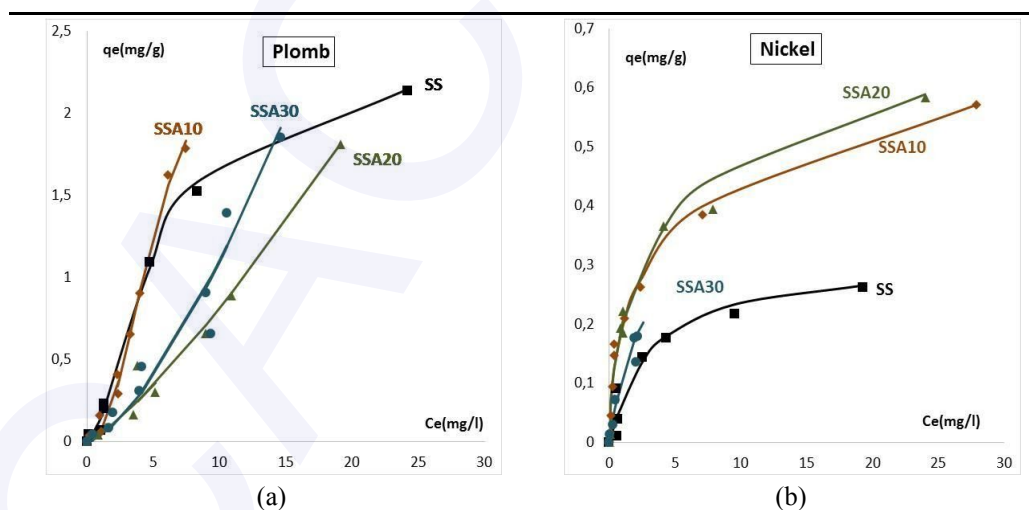
3. RESULTS AND DISCUSSIONS

The different sand and clay characterizations are presented in the table 1 which present a good properties for the sand and clay used for this study.

Table 1: Sand and clay characterization

Soil nature	Clay		Sand	
Surface area	67.97 m^2/g		0.13 m^2/g	
pH	7.25		7.78	
Humidity	4.90 %		0.06%	
Organic Matter	2.00%		0.15%	
Loss on ignition	3.36 %		0.35 %	
Cationic Exchange Capacity	25.0 meq/100g		3.5 meq/100g	
pH$_{pzc}$	**Sand**	**Sand + 10%Clay**	**Sand + 20%Clay**	**Sand + 30%Clay**
	7.10	6.60	6.60	6.70

The adsorption isotherms on the soil as a function of its clay content are illustrated in Figures 1 cationic $\left(Pb^{2+}, Ni^{2+}\right)$ and anionic (NO_3^-, PO_4^{3-}) water contaminants, respectively.

(a)   (b)

The Second Edition of the International Congress of Applied chemistry and Environment
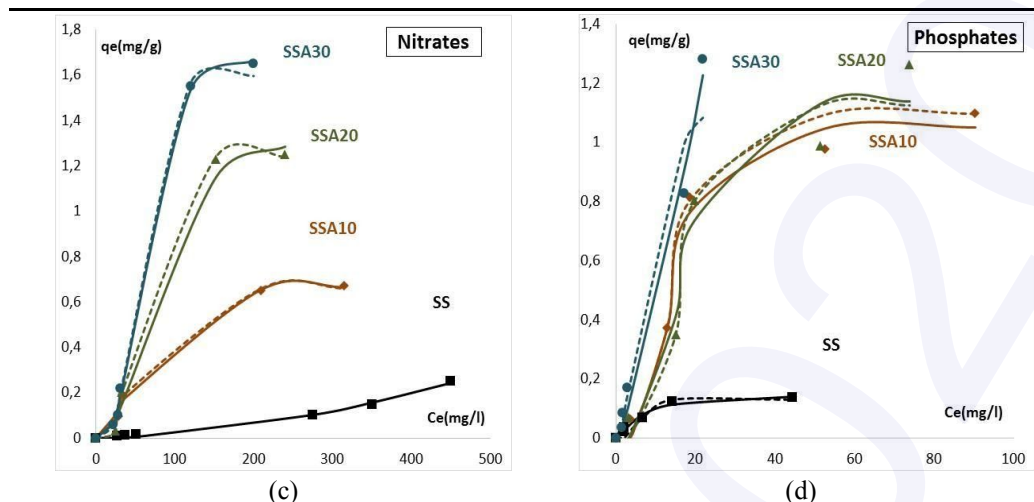30th-31th October and 01st November 2020, Tunisia

ICACE
2020

Figure 1. Adsorption isotherms of lead (a), nickel (b), nitrates (c) and phosphates (d) depending on the clay content of the soil

The points are experimental, the continuous curves are relative to the Koble-Corrigan model and the discontinuous curves are relative to the Langmuir-Freundlich model and / or to the Hill model, and SS, SSA10, SSA20 and SSA30 are the clay percent in soil from 0 to 30% respectively in the soil.

Figures 1 show that all experimental isotherms, without any exception, were successfully adjusted using Koble-Corrigan expression. This model describes an adsorption on heterogeneous surfaces and includes in its expression the Langmuir and Freundlich equations. [4]

Figure 2 compares the adsorbed amounts of the four pollutants as a function of soil clay content, the initial concentrations of the four ionic species being the same (1 meq/L).
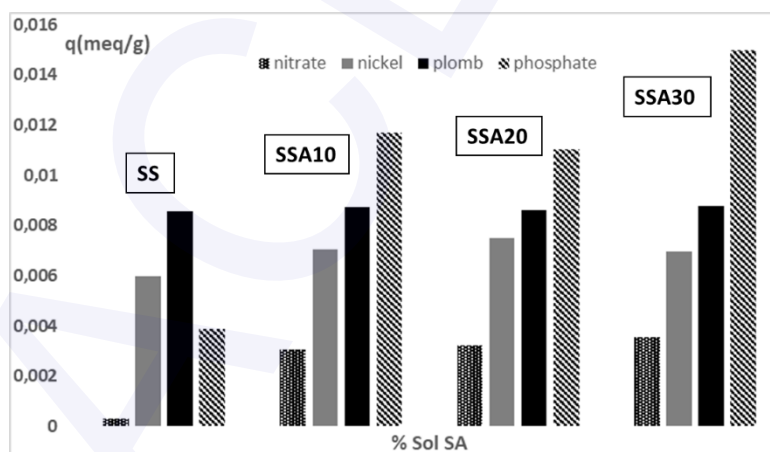

Figure 2. Effect of soil clay content on Nitrate, Phosphate, Lead and Nickel adsorption
($C_0 \approx 1$ meq/L for all pollutants))

The results show that the adsorbed quantities of anionic pollutants increase with the clay content whereas those of the cationic pollutants remain invariable. However, the classification of pollutants that pose the greatest risk of groundwater contamination depends on the nature of the soil that these pollutants cross when transported by water. For a sandy soil, this classification is given as follows:

Lead < nickel < phosphate < nitrate

While for a clayey soil, the classification is:

Phosphates < lead < nickel < nitrate

The Second Edition of the International Congress of Applied chemistry and Environment
30th-31th October and 01st November 2020, Tunisia

ICACE
2020

3. CONCLUSION

This study showed the impact of the clay nature of a soil on the risk of groundwater contamination by four ionic contaminants: nitrates, phosphates, lead and nickel. For this purpose, the retention isotherms on a sandy soil with different clay contents were made for all pollutants and the Langmuir, Freundlich, Freundlich-Langmuir, Hill and Koble-Corrigan models were applied.

All experimental isotherms, without exception, have been successfully adjusted using the Koble-Corrigan expression. This model, which includes in its expression the Langmuir and Freundlich equations, describes adsorption on heterogeneous surfaces by specifying the maximum amount of contaminant that can be retained.

Thus, we have shown that nitrates present the greatest risk of groundwater contamination due to their low retention by sandy and clayey soils.

REFERENCES

[1] Borggaard, O.K., Szilas, C., Gimsing, A.L., Rasmussen, L.H., 2004. Estimation of soil phosphate adsorption capacity by means of a pedotransfer function. Geoderma. 118, 55-61.

[2] Kumar, V., Sharma, A., Kaur, P., Sidhu, G. P. S., Bali, A. S., Bhardwaj, R., Cerda, A., 2018, Pollution assessment of heavy metals in soils of India and ecological risk assessment: A state-of-the-art, Chemosphere,216,449-462.

[3] Gupta, SS., Bhattacharyya, K.G., 2008. Immobilization of Pb (II), Cd (II) and Ni (II) ions on kaolinite and Montmorillonite surfaces from aqueous medium. J. Environmental management. 87, 46-58

[4] Ayawei, N., Ebelegi, A.N., Wankasi, D., 2017. Modelling and interpretation of adsorption isotherms. J.Chemistry.2017,

The Second Edition of the International Congress of Applied chemistry and Environment
30th-31th October and 01st November 2020, Tunisia

ICACE 2020

Treatment of rinse water generated in the galvanizing process for zero liquid discharge

Hayet Cherif [a] , **Manel Wakkel** [b], **Refka Korbsi** [b], **Insaf Krimi** [b], **Hamza Elfil** [a]

(a)Laboratory of Natural Water Treatment, Water Researches and Technologies Center, B.P. 273, Soliman 8020, Tunisia

(b)ISET Kelibia , Route Oued El Khatf Kelibia, 8090
E-mail: hayetcherif@hotmail.fr

ABSTRACT

Two processes were tested in order to treat wastewaters generated after rinsing metal steps (degreasing and pickling) in galvanizing industry located in North of Tunisia. The first one combined coagulation-flocculation process and electrodialysis to treat rinse water after degreasing and the wastewater quality was improved from 13.7 mS/cm of conductivity at 20.7°C and pH 13, 3473.7 mgO_2/L of COD, 278 mg/L Iron and 80 mg/L Lead to 1.3 mS/cm at pH 3.49, 228 mgO_2/L, 5 mg/L and 0.3 mg/L respectively. Optimum parameters used for coagulation were aluminum sulphate as coagulant, 0.9 g/L for concentration, pH 5, 150 tr/min and a time of 15 min. Flocculent used was sodium alginate with a concentration of 0.1 g/L, 40 tr/min and a time of 10 min. Electrodialysis was carried out in 10 volt and 50% of conversion rate. For the rinse water after pickling precipitation-oxidation process using $Ca(OH)_2$ and NaOH were compared and combined to membrane distillation and the results showed that pollutant levels and heavy metals of acidic solutions at pH 1.5 with a conductivity of 68.5 mS/cm containing 15 g/L of Chloride, 8.37 g/L of Iron and 483 mg/L of Zinc were reduced and the treating water conductivity was 2 mS/cm with a zero concentrations of heavy metals.

 KEYWORDS: Galvanizing process, Electrodialysis, Coagulation, Membrane distillation, Heavy metals

1. INTRODUCTION

The galvanizing industry has many negative aspects. The most obvious are a very high consumption of water, raw materials, energy and the generation of toxic wastewater [1]. It helps strengthen a piece of steel with zinc and protective coating to give the characteristics of the adhesion, the impermeability and the mechanical resistance. This technique requires a very large amount of water during its stages, which generates a large volume of wastewater loaded with heavy metals which are harmful to health and the environment [2]. To treat this industrial wastewater, several types of treatments have been used: ion exchange [3], coagulation/flocculation [2], combined photocatalytic oxidation and chemical coagulation [4], adsorption on magnetic nanoparticles [5] and complex process combined chlorine dioxide oxidation, iron filings internal electrolysis degradation and Alkalinity precipitation method [6]. The main focus of these works was to remove heavy metals especially iron, cyanide and Zn. But the electro conductivity and turbidity of generated wastewater was also high due to chloride from acid in pickling step and grease in degreasing step. In our study the feasibility of combined physic-chemical process (coagulation flocculation and oxidation precipitation) and membrane desalination process (electrodialysis and membrane distillation) were tested to treat the rinse water after degreasing and pickling bath respectively.

2. MATERIAL AND METHODS

Wastewater samples were collected from different rinsing baths in galvanization process (after degreasing and pickling at different time intervals. The properties of the collected samples including heavy metals content, pH, turbidity, electrical conductivity and major ions were measured. For the degreasing bath the coagulants used in this work processes was aluminum sulphate ($Al_2(SO4)_3.18H_2O$ and the flocculent was the alginate sodium. A Jart test was used to optimize parameters. The effluent of coagulation-floculation process was treated by electrodialysis unit. The ED cell was a PC Cell ED 64-004 (Germany) used as a conventional ED unit with dilute and concentrate compartments. ED cell was made by two polypropylene blocks supporting electrodes. One electrode was made of Pt/Ir-coated Ti stretched (anode) and the other of Ti stretched metal (cathode). The membranes and spacers were stacked between the two electrode end blocks. ED stack was made of 7 repeating sections called cell pairs. Each cell pair was made of cation and anion exchange Neosepta membranes separated by a 0.5 mm flow spacer used to generate flow paths of dilute and concentrate streams. The fluid circulation was achieved using three pumps equipped with flowmeters. The stack was equipped with three separate external plastic reservoirs, which contained 1 L of concentrate, dilute

The Second Edition of the International Congress of Applied chemistry and Environment
30th-31th October and 01st November 2020, Tunisia

ICACE 2020

and rinsing solutions. An aqueous solution of 0.1 M Na_2SO_4 was used to rinse ED electrodes in order to prevent chlorine or hypochlorite generation, which could be hazardous for the electrodes.

For the pickling bath the oxidation process was carried out using lime (Ca (OH) $_2$) and compared to sodium hydroxide. An aeration pump was used combined to diffuser for oxidation and anionic flocculent with a dose of 1.5 mg/L was added to improve sedimentation. The effluent was treated by membrane distillation. The used membrane was polyvinylidene fluoride with a pore size of 0.45 μm, a thermal conductivity of 0.041 $Wm^{-1}K^{-1}$ and an active area of $3.2* 10^{-3} m^2$.

3. RESULTS AND DISCUSSIONS

The analysis of rinse water sampled from the two rinsing bath in galvanizing manufactory was illustrated in Table 1 and 2. For the first one, after degreasing, the optimum condition for coagulation flocculation was a coagulant dose of 0.9 g/L, 0.1 g/L for flocculent dose and pH 5. After electrodialysis the treated water chemical component was near then potable water except COD and it can be reused in rinsing bath.

Table 1: Analysis of rinsing water after metal degreasing before and after treatment

Parameters	Unit	Raw water	Treated water	NT 106.02
pH		13	3.49	6.5<pH<8.5
Conductivity T= 20,1°C	mS/cm	13.71	1.3	5
COD	mg O_2/L	3473.3	228	1000
Cl$^-$	mg/L	4544	170	700
SO_4^{2-}	mg/L	3662.01	353.46	400
K^+	mg/L	16.7	1.2	-
Na^+	mg/L	2360	170	-
Al	mg/L	2.13	0.1	10
NO_3^-	mg/L	482.84	15.47	90
NTK	mg/L		11.2	100
PO_4^{3-}	mg/L	64	25.55	10
Fe	mg/L	278.5	5.683	5
Cu	mg/L	0.93	0.1	1
Mn	mg/L	29	0	1
Zn	mg/L	27	0.7765	5
Cd	mg/L	0.197	0	0.1
Total Cr	mg/L	1.8	0.3164	2
Pb	mg/L	80	0.3322	1

As described in Table 2, treated of rinsing water after pickling by combined oxidation process and membrane distillation reduced the conductivity from 68.4 to 2 mS/cm and the iron concentration from 8 g/L to 0 g/L. Suggested solution have a highly impact and the treated wastewater can be reused in the same manufactory to save a water and protect environment..

Table 2: Analysis of rinsing water after metal pickling before and after treatment

Parameters	Unit	Sample before treatment	Sample after precipitation-oxydation (with Ca(OH)$_2$	Sample after membrane distillation	NT 106.02
pH		1.5		5.98	6.5<pH<8.5
Conductivity T= 20,1°C	mS/cm	68.4	25.5	2	5
COD	mg O_2/L	1839.54	-	-	1000
Cl$^-$	mg/L	15975	15000		700

Fe	mg/L	8376	0.66	0	5
Cu	mg/L	3.86	0.22	0	1
Mn	mg/L	32	0.07	0	1
Zn	mg/L	483	2.5	0	5
Cd	mg/L	0.234	0.17	0	0.1
Total Cr	mg/L	3.233	0.37	0	2
Pb	mg/L	5.856	1.48	0	1

4. CONCLUSION

The effectiveness of two treatment process were tested for a galvanizing rinsing water, the first one was combined coagulation flocculation and electrodialysis for a rinsing water after steel degreasing and the second was oxidation combined to membrane distillation after steel pickling in concentrate HCl. Treated wastewater from the two rinsing bath quality was highly improved and it can be reintroduced in the same baths to wash metal.

REFERENCES

[1] **Johannes Fresner , Hans Schnitzer , Gernot Gwehenberger , Mikko Planasch , Christoph Brunner , Karin Taferner , Josef Mair,** Practical experiences with the implementation of the concept of zero emissions in the surface treatment industry in Austria. Journal of Cleaner Production, 2007, Vol.15 , 1228-1239.

[2]**M.Berradi, Z. Chabab1, H. Arroub1, H. Nounah2, A. El Harfi**, Optimization of the coagulation/flocculation process for the treatment of industrial wastewater from the hot dip galvanizing of steel, *J. Mater. Environ. Sci.*, 2014,Vol 5,N°.2,360-365

[3] **Elena Maranˇoˊn, Yolanda Fernaˊndez, Leonor Castrilloˊn**. Ion Exchange Treatment of Rinse Water Generated in the Galvanizing Process, *Water Environment Research*, 2005,Vol.77, N°.7,3054-3058.

[4] **R. Abdel Wahaab, A.K. Moawad, Enas Abou Taleb,1Hanan S. Ibrahim and H.A.H. El-Nazer**, Combined Photocatalytic Oxidation and Chemical Coagulation for Cyanide and Heavy Metals Removal from Electroplating Wastewater, *World Applied Sciences Journal*, 2010, Vol.8,N°. 4,462-469.

[5] **Hassan Sawalha, Maher Al-Jabari, Inaam Tamimi, Mais Shahin and Zahra Tamimi**, Characterization and Treatment of Wastewater from Galvanization Industry in Palestine, *International Journal of Environment &Water*, 2016,Vol.5, N°. 3, 37-44.

[6] **Tong Zhen-Gong**, Treating the galvanization wastewater by complex process, *BTAIJ*, 2013, Vol°8,N°.8,1108-1112.

The Second Edition of the International Congress of Applied chemistry and Environment
30th-31th October and 01st November 2020, Tunisia

ICACE
2020

PHYSICOCHEMICAL AND GEOCHEMICAL PROPERTIES OF BOUJAADA'S MINE SOILS (TAZA PROVINCE)

Ikram Lahmidi[a], Narmine Assabar[a], Raouf Jabrane[a]

(a)   *Laboratory of Intelligent System, Georesources and Renewable Energies. Faculty of Science and Technology of Fez. Morocco*

E-mail: ikram.lahmidi@usmba.ac.ma

ABSTRACT

Acid mine drainage is a form of water pollution occurring when rain, runoff, or streams come in contact with rocks rich in sulfur that are present in abandoned or currently active mines .

Boujaada's mine discharges are situated on the western slopes of Mezzaourou's watershed, and are scattered over a large superficies. It has been exploited particularly for antimony sulfides in the period between 1946 and 1953 .Thus; the mineralization present in these waste dumps indicates a pollution factor due, to its drainage by runoff. Measurements made on runoff water and wells near, the mine show an acidic pH of the water. This pollution probably generated acid mine drainage.

According to the physicochemical and geochemical analyzes, it was possible to discern a pollution of the agricultural soils of Boujaada's village, watered by the water drained from discharges, which constitute a food resource for the local population.

KEYWORDS: Acid mine drainage, Boujaada's mine, mining discharges, pollution.

1. INTRODUCTION

Acid drainage is a little-known global crisis. The UN has even labeled it the second biggest problem facing the world after global warming. In Morocco, few studies have been done in this regard of abandon mines, so we choose to study the presence of this phenomenon in Boujaada's abandoned mine.

Mezzaourou's watershed is located in the north-eastern part of Morocco, 10 km as the crow flies south of the town of Taza (mid-Atlantic region). The mineralization of Boujaada's mine is located in an area of andesitic breccias crossed by veins called Boujaada Tuffs, and is delimited on the western slopes of Mezzaourou's watershed.

In this study, we carried out Physico-chemical and geochemical analyzes to prove the presence of acid mine drainage in the study area.

2. MATERIAL AND METHODS

We proceeded to take samples from the soils and embankments around the mine. After locating their stations, they were kept and stored cool and dark, then transported to the laboratory.

Once in the laboratory, the samples were dried in ambient air (25°C), sieved to 2mm, and quartered by the cone method. Then, the following Physico-chemical analyzes were carried out: Residual humidity (CIRAD, NF ISO 11465); water pH and KCl pH (AFNOR X 31-103 et AFNOR X 31-104); electrical conductivity; determination of total organic matter by loss on ignition (NF ISO 14235) (Ball, 1964); determination of the contents of calcium carbonate ($CaCO_3$) using Bernard calcimeter method. These parameters will allow us to acquire basic knowledge, develop surveillance to detect disturbances.

As for the geochemical analyzes, the samples were well ground and preserved, then sent to the National Center for Scientific and Technical Research in Rabat, to carry out the following analyzes: Scanning electron microscope (SEM) that scans a focused electron beam over a surface to create an image, the electrons in the

The Second Edition of the International Congress of Applied chemistry and Environment
30th-31th October and 01st November 2020, Tunisia

ICACE 2020

beam interact with the sample, producing various signals that will be used to get information about the surface topography and composition. And X-ray powder diffraction (XRD) which is a rapid analytical technique primarily used for phase identification of a crystalline material and can give information on unit cell dimensions.

3. RESULTS AND DISCUSSIONS

According to the Physico-chemical analyses (Tab1), we can see that pH $_{H2O}$ in soil is equal to 7, which means it's neutral (6.5<pH<7.3).

The obtained results show that the values of soil pH in water (pH$_{H2O}$) were higher than the values obtained in pH$_{KCl}$, and knowing that the difference between the two characterizes the acidification potential of the soil, we find a difference greater than 1, this means a strong acidification potential.

As for the salinity, we found that the conductivity equals 84μs/cm (0.084 ds/m), which means absent of salinity (<4 ds/m).

Table 1: Physico-chemical parameters of the study region

Water pH	KCl pH	Conductivity (μs/cm)	PAF (%)	CaCO3 (%)	Humidity (%)
7,00	5,20	84,00	8.82	0	1.8

The results of analyzes performed by XRD (Fig1), show that the samples consist essentially of Quartz (SiO$_2$) and Saponite (Ca0.5 (Mg, Fe) 3 (Si, Al) 4 O$_{10}$ (O, H) 24 H$_2$O), with low levels of Hematite (Fe$_2$O$_3$), Magnetite (Fe$_3$O$_4$), and Plagionite (Pb5 Sb8 S17). The presence of these minerals means that soil samples contain important measure of heavy metals.
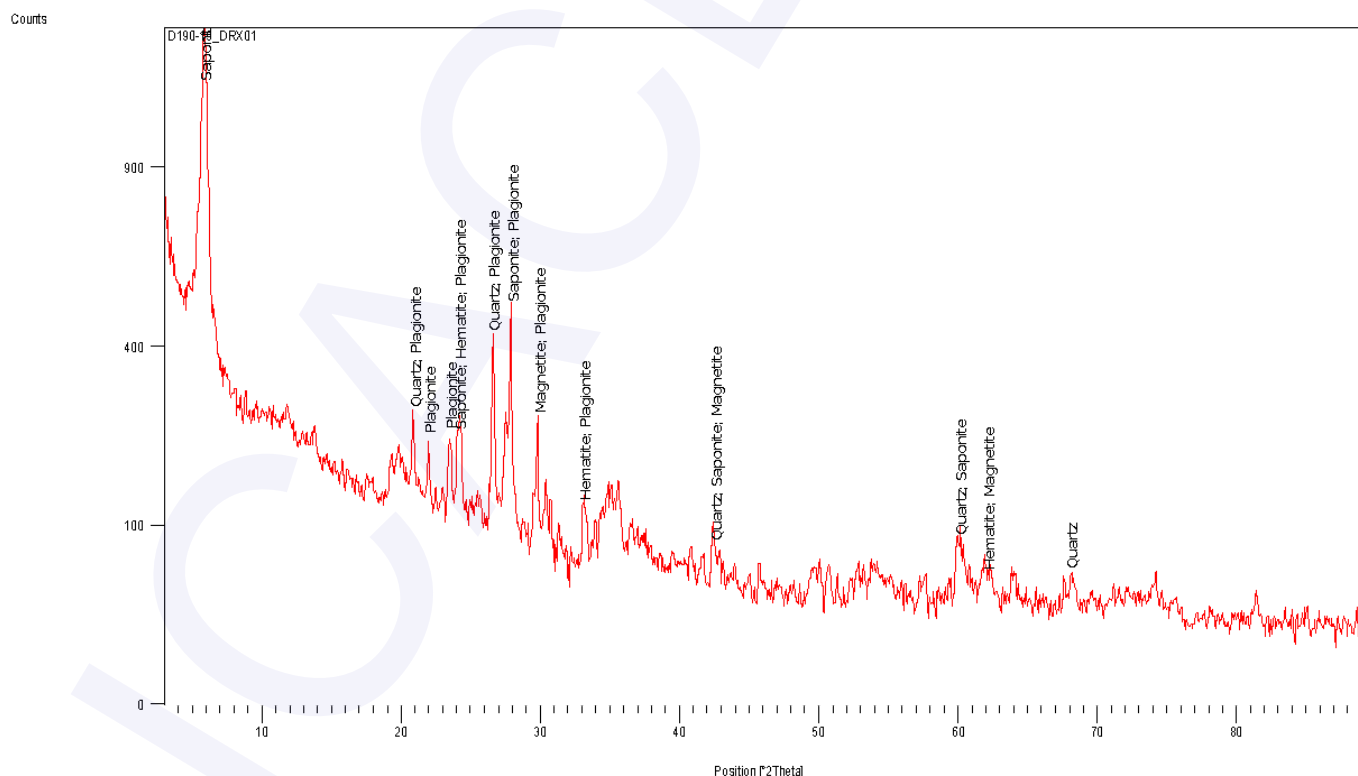
Figure 1. Main available mineral phases observed by XRD

Similarly, the observations developed by the SEM (Fig 2), confirmed the exist of the mineralogical structures mentioned above. This phase is necessary to show the contents of heavy metals in the samples, as we can see the results are higher than the norm for Si (> 1500 mg/Kg), Fe (>400 mg/Kg), and Ti (>100 mg/Kg) (AFNOR Standard NFU 44-041). With this, we can say that the study area suffers from pollution.
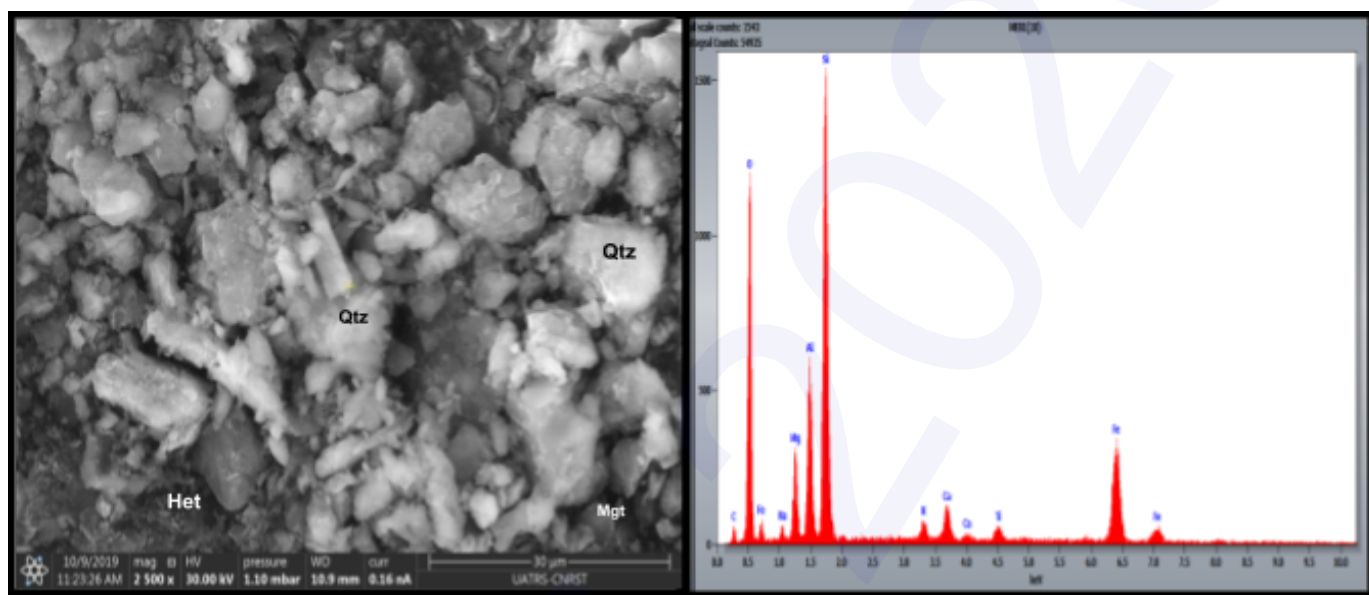

Figure 2. Images taken by SEM in separate magnification
Qtz: Quartz. Mgt: Magnetite. Het: Hematite

4. CONCLUSION

The recent situation of Boujaad's soils (Taza province Morocco) shows that they have difference between pH $_{H2O}$ and pH $_{KCl}$ greater than 1 which means a strong acidification potential, with the presence of heavy metals higher than standards (Si (> 1500 mg/Kg), Fe (>400 mg/Kg), and Ti (>100 mg/Kg)).

In conclusion, we note that this study was made to testify the presence of contamination by metallic elements in the study zone which disturb the ecosystem. This will bring us to start other in-depth studies for other environmental compartments.

REFERENCES

[1] **MOUTTAQI. A, RJIMATI. E.C, MAACHA. L, MICHARD. A, SOULAIMANI. A & IBOUH. H**, New Geological And Mining Guidebooks of MOROCCO, Volume 9, Main Mines of Morocco, Éditions du Service Géologique du Maroc –*Rabat* - N° 564, 2011,p. 337-340.

[2] **AFNOR**, French Norms, NF U 44-041, 1999.

[3] **B.R.P.M**, Archives, 1981.

[4] **LAKRIM. M,** La pollution de l'environnement par le drainage minier acide généré par les déchets miniers de la mine ferrifère de Nador. Faculté des sciences et Techniques de Fès, 2015.

Physico-chemical and geochemical characterization of Ain Aouda mine's soils (Taza Province)

Narmine Assabar[a], Ikram Lahmidi[a], Raouf Jabrane[a]

(a) Intelligent Systems, Georesources and Renewable Energies laboratory, Faculty of sciences and technologies Fez, Morocco.
E-mail : Narmine.assabar@usmba.ac.ma

ABSTRACT:

The Ain Aouda deposit presents the most important zinciferous cluster of the pleated middle atlas, which contains leaded calamine and iron oxides. Its discharges, containing metalliferous products were directly stored on a dolomitic calcareous ground, exposed to the weather conditions. This situation, would generate a real source of pollution by producing effluents loaded with metals, and will have a negative influence on the soil.

The results of ICP-AES analysis of the soil samples taken from the old mine showed Zinc and Lead contamination. Nevertheless, we note that the water pH is still basic, probably due to the important presence of carbonates. We perceive that the phenomenon of neutralization happens.

KEYWORDS: Ain Aouda Mine, Physico-chemical analyzes, geochemical Analyzes, neutral mine drainage.

1. INTRODUCTION

During mining, the rocks are fragmented, increasing the rate of acid production. In our study area, the bedrock contains large amounts of calcite and dolomite, stimulating the neutralization of the acid generated.

The Ain Aouda mine is located in the northeastern part of Morocco, in the northernmost part of the mountain range of the Middle Atlas, situated in the east of the Tazekka National Park.

The Ain Aouda mine was exploited in 1962, for a period exceeding 15 years. This exploitation has abandoned waste rock dumps stored directly on carbonated substratum, without any precaution. The heaps are exposed and reacted with water infiltration and air circulation, which would create a real source of pollution for the ecosystem. These pollutions will inevitably produce effluents that can be loaded with metals such as zinc and lead, which will have a significant negative influence on the soil, fauna and flora. Knowing that these components are among the rare sources of the population of Douar Ain Aouda who pays the high price of mining.

The aim of the work is to identify the physico-chemical and geochemical character of the soils in order to prove a discrete contamination due to the alkalinity of the substratum.

2. MATERIAL AND METHODS

We performed simple random sampling of soils. It is a known technique, which consists in taking samples at randomly selected places in the study area; we have practiced it in different areas near the zinc mine Ain Aouda.

The sampling points were previously identified in the study area in an arbitrary manner. Each sample weighed approximately 500 g. The quantity of soil obtained is spread out to remove the coarse elements. The sample of each soil underwent manual quartering, it was separated into four equal quarters of which two opposite quarters are eliminated and the other two opposite quarters are combined. This selection is homogenized and a new quartering is performed, the operation has been repeated for three times. This gives a representative sample of the initial material (PAUWELS et al, 1992 in BABA AHMED, 2012).

The soil contains a small amount of hygroscopic water, it will be essential to dry it in the open air, then, we complete the drying in the oven to remove all the water.

The Second Edition of the International Congress of Applied chemistry and Environment
30th-31th October and 01st November 2020, Tunisia

ICACE 2020

We executed various physico-chemical analyses by determining the pH (H2O), the pH (KCl) and the electrical conductivity of the soil by using a Multiparameter calibrated beforehand, according to standard ISO-NF-10390 (2005). As well as we measured the total organic matter by loss on ignition at 450 °C for 24 hours. The residual humidity was measured by loss of mass at 105 °C for 48 hours according to standard ISO 11465 / (NF X31-102). Moreover, we used Bernard Calcimeter to calculate the rate of $CaCO_3$ in our soil samples.

Geochemically, the determination of metallic elements was carried out by the ICP-AES (Atomic emission spectrometry - Source of inductive coupled plasma). This method is based on the identification and quantification of the mass percentage of metals (Pb, Zn…). Before starting this method, the samples underwent very fine grinding (> 63 μm) by mortar grinder to succeed in triacid attacks (HF, HNO3, $HClO_4$).

3. RESULTS AND DISCUSSIONS

The geochemical analyses carried out by the ICP-AES show that the lead and zinc contents are much higher, on the four samples taken in the Ain Aouda study area, than those of the norms, (Pb> 100 mg / kg, Zn> 300 mg / kg) (AFNOR Standard NFU 44-041). We are absolutely talking about existing pollution (figure1).
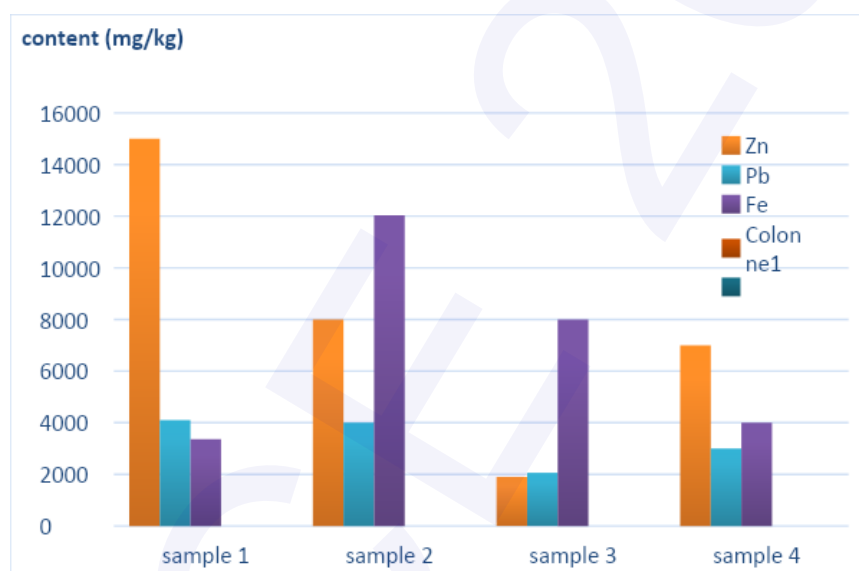
Figure 1. Zn, Pb and Fe contents (mg / kg).

Table (1) shows the results of the analyses performed, in order to determine the physico-chemical characteristics of the soils samples. The hydrogen potential (H_2O) exceeds 7.4 in all of the samples. In other words, these are slightly alkaline (7.4 <pH <7.7) to alkaline (pH> 7.7). While the pH (KCl) measured are moderately higher than the pH (H2O), with a very small difference.

The alkalinity of the hydrogen potential found in the samples can be explained by the presence of Ca CO_3 in the soils, which probably came from the carbonated bedrock present in the study area, (calcite (Ca CO_3) and dolomite (Ca Mg $(CO_3)_2$). In the end, the soils are calcareous (15% to 30%) to very calcareous (> 30 %).

The electrical conductivity varies inversely with the pH. It decreases with neutrality.

The Second Edition of the International Congress of Applied chemistry and Environment
30th-31th October and 01st November 2020, Tunisia

ICACE 2020

Table 1: Results of physico-chemical analyses of soil samples taken from different site in the study area.

Analyses Soils	pH (H_2O)	pH (KCl)	Electrical conductivity (H_2O) µs/cm	Loss on ignition (%)	Humidity (%)	$CaCO_3$ (%)
Soil 1	8,10	9,20	150,20	1,92	19,16	64,28
Soil 2	7,42	8,30	81,90	2,04	4,22	00,00
Soil 3	8,50	9,50	95,00	0,60	6,84	66,08
Soil 4	7,60	8,60	86,00	2,76	4	00,00
Soil 5	8,00	8,60	140,00	5,93	15,02	14,28
Soil 6	8,20	9,40	101,00	3,97	5,61	37,50

4. CONCLUSION

Mining harms the environment; it infers the degradation of the ecosphere.

This study concerns the identification of contamination of a single environmental compartment, which is the soil. Based on the results of analyses, this study has shown that the abandoned Ain Aouda mine, without rehabilitation in the Tazekka massif (Morocco), has the potential for pollution. This study confirm a probable contamination, which leads us to start others studies and others analyses for the others environmental compartments.

The soils surrounding the Ain Aouda mine show no acidification, it is certainly neutral mine drainage.

REFERENCES

[1] **AFNOR**, French Norms, NF U 44-041, 1999.
[2] **BABA AHMED. A,** Study of contamination and accumulation of some heavy metals in cereals, vegetables and agricultural soils irrigated by wastewater from the city of hammam boughrara, Doctoral thesis defended at the University of Abu Bekr Belkaid in Tlemcen, 2012, p. 256.
[3] **Baize. D**, Total heavy metal contents in French soils: First results of the ASPITET program, *Courrier de l'environnement de l'INRA*, 2000, n°39, p. 39-54.
[4] **B.R.P.M**, Archives, 1973.
[5] **El Hachimi. L, Bouabdli. A and Fekhaoui. M**, Mining treatment waste: characterization, polluting capacity and environmental impacts, Zeïda mine, Mibladen mine, Haute Moulouya (Morocco), *déchets sciences et techniques* – N˚63, 2013, p. 32 – 42.
[6] **Hoepffner. C**, The volcano-sedimentary complex of carboniferous age in the Tazekka massif its place in the Hercynian evolution of the Eastern Moroccan Meseta, *Sci. Géol.*, 34, 2, Strasbourg, 1981, p. 97 – 106.
[7] **ISO-10390 (2005):** Soil quality - Determination of pH. Geneva (2005). Index classification: X31-117. Edition: Compendium of standards, soil quality. Determination of pH, CH-1211, Geneva 20, Geneva, 7 p.
[8] **ISO-11465 (1994) & AFNOR (1998):** Classification index; NF X31-102: Quality of soil - Determination of the weight content of dry matter and water – Methods gravimetric., AFNOR, Standards & Reports.
[9] **LAKRIM. M,** Environmental pollution by acid mine drainage generated by mining waste from the Nador iron mine, 2015.
[10] **PAUWELS, J.M., VAN RANST, E., VERLOO, M., MVONDO, A,** Manual of soil laboratory: methods of soil and plant analysis; equipment, inventory management of glassware and chemicals, Dschang University Center, AGCD : Publications agricoles, 1992, p. 28-265.

Thermochemical calculations to follow the reactions of desulfurization of gaseous resulting from a coal thermal power station

Saloua JEMJAMI

Laboratory of Applied and Environmental Chemistry
Faculty Of Sciences and Techniques– BP 577,Km 3, Route de CASA, SETTAT - MOROCCO
Hassan 1stUniversity. BP 26000, SETTAT MOROCCO
Email : j.saloua.1@gmail.com / saloua.jemjami@uhp.ac.ma

ABSTRACT

This paper presents a theoretical study of the thermochemical calculations based on the minimization of the free enthalpy by utilization of HSC chemistry data base to follow reactions of desulphurization of gases resulting from a thermal station. The absorbent systems used are $NaHCO_3$/ Na_2CO_3 and $CaCO_3$/CaO. This desulfurization phenomenon was tested by variation of different parameters: concentration of input materials and temperature. Our theoretical results obtained confirm experimental and literature works.

KEYWORDS: Thermochemical calculations, desulfurization, limestone, sodium bicarbonate.

1. INTRODUCTION

Coal will remain an important fossil fuel at least until 2050 (BP Energy outlook 2018 Edition, Exxon Mobil 2018, EU Reference scenario 2016)[1]. Besides other impurities, various sources of coal contain from 0.1 up to 4% of sulfur which generates SO_2 during coal combustion, that transforms into acid in the atmosphere, which is a major compound of acid rain [2]. Many countries have adopted strict regulations regarding SO_2 emissions of coal boilers in power plants which represent one of the significant sources of SO_2 emissions, and that is very strongly linked to the type of coal [2].Several technologies are used in the world for reducing the sulfur emissions from thermal processes [3-7]. In order to help reduce SO_2 emissions of coal power plants, we use chemicals equilibrium by utilization of the HSC Chemistry to follow the SO_2 absorption in different absorbents such as the $NaHCO_3$/ Na_2CO_3 and $CaCO_3$/CaO systems.

It's known that the chemical equilibrium of a chemical system permits to calculate the theoretical thermodynamic properties of the system. These properties can be applied to wide variety of problems in chemistry and chemical engineering.During the last decades, the thermodynamic methods and calculations found several applications in the analysis of the various processes, and the follow-up or the creation of new technologies. Also, the development of new methods to provide for the needs of humanity in the field of energy, the choice of the optimal methods for the use of the raw material resources, measurements for the prevention of pollution and environmental protection, cannot be completed without preliminary analyses based on the known thermodynamic models. Thermochemical calculations, thus, found several applications in the analysis of the various processes and the creation of new materials and new technologies [8].

2. METHODS

The presentation of the thermodynamic tables is a problem which always keeps the scientists busy. The first thermochemical compilations of thermodynamic tables were carried out a hundred years ago, and the first data sources were then the individual publications, thereafter, these tables became collective works. It is clear that the international co-operation is the most effective means to increase the speed and the effectiveness of the preparation of a reference thermodynamic table. In the world, there are not many well known thermodynamic tables [9-13]. Among these tables, the HSC Chemistry software [9], used in this work,enables the user to simulate chemical reactions and processes on the thermochemical basis. This method does not take into account all the necessary factors, such as rates of reactions, heat and mass transfer issues, etc. However, in many cases a pure thermochemical approach may easily give useful and versatile information for developing new chemical processes and improving the old ones.

3. RESULTS AND DISCUSSION

The Second Edition of the International Congress of Applied chemistry and Environment
30th-31th October and 01st November 2020, Tunisia

ICACE 2020

3.1. First study: NaHCO₃/Na₂CO₃ system

In this system, the first reaction step of desulfurization is the thermal decomposition of $NaHCO_3$ given by the reaction (1):
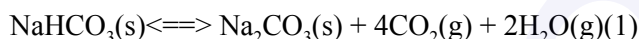
$$NaHCO_3(s) <==> Na_2CO_3(s) + 4CO_2(g) + 2H_2O(g) \quad (1)$$

Figure 1 illustrates that $NaHCO_3$ is completely decomposeddown from 200°C.
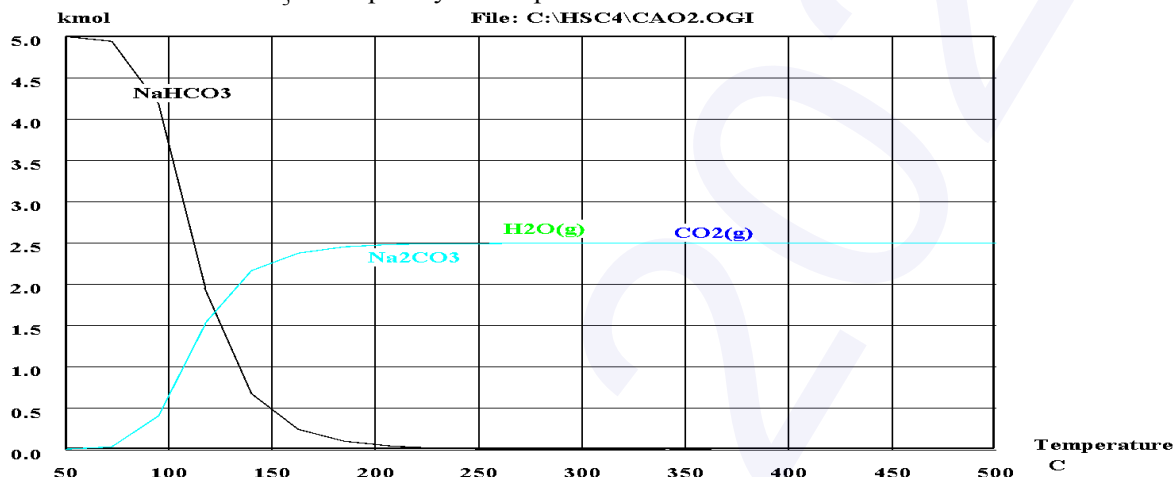
Figure 1: Thermodynamic equilibrium calculated by HSC Chemistry of $NaHCO_3$ thermal decomposition

The calculations made by HSC CHEMISTRY for the desulfurization of SO_2 (g) by the $NaHCO_3$ / Na_2CO_3 system are carried out according to reactions (2) and (3):

$$4NaHCO_3 + 2SO_2(g) + O_2(g) = 2Na_2SO_4 + 4CO_2(g) + 2H_2O(g) \quad (2)$$

$$2Na_2CO_3 + 2SO_2(g) + O_2(g) = 2Na_2SO_4 + 2CO_2(g) \quad (3)$$
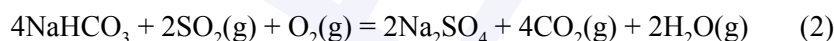
The figures 2 and 3 represent the evolution of the quantity of the various solids and gaseous according to the amount of $SO_2(g)$ (Left at 80°C, Right at 200°C. They confirm that $SO_2(g)$ reacts effectively with $NaHCO_3$ at low teperature and with Na_2CO_3 at high temperature. . For both processes, the sulfur can be captured in the form of the Na_2SO_4 compound.
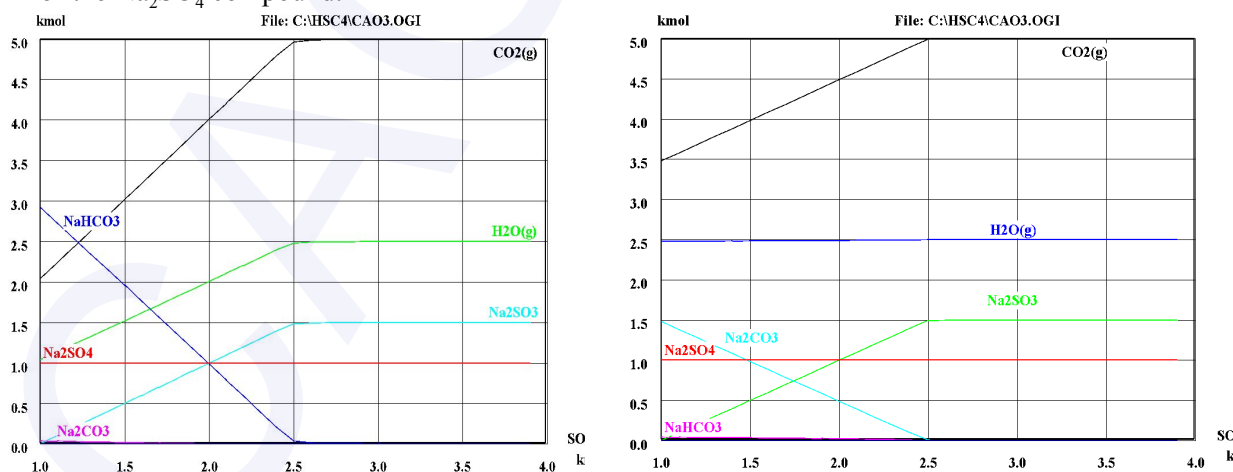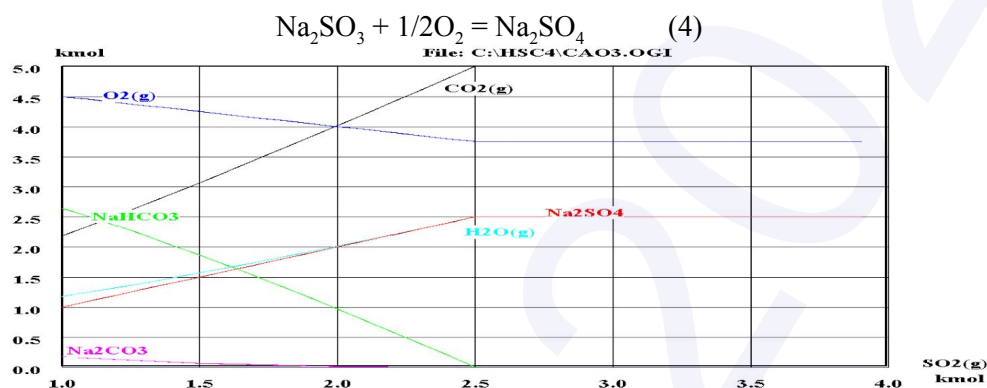
Figure 2: Quantity of the various solids and gaseous issues from desulfurization witch $NaHCO_3$ as absorbent according to the amount of $SO_2(g)$ at 80°C

Figure 3: Quantity of the various solids and gaseous issues from desulfurization witch $NaHCO_3$ as absorbent according to the amount of $SO_2(g)$ at 200°C

Regarding Figure 4, the calculations in Figure 2 have been redone by increasing the amount of oxygen. The Na_2SO_3 compound reacts with oxygen to transform into Na_2SO_4, reaction (4).

$$Na_2SO_3 + 1/2O_2 = Na_2SO_4 \qquad (4)$$

Figure 4: Quantity of the various solids and gaseous issues from desulfurization witch $NaHCO_3$ as absorbent according to the amount of $SO_2(g)$ with the increase of O_2

3.2. Second study: $CaCO_3/CaO$ system

HSC CHEMISTRY's monitoring of SO_2 desulfurization (g), by the $CaCO_3/CaO$ system, was carried out according the reactions (5) and (6):

$$2CaCO_3 + 2SO_2(g) + O_2(g) = 2CaSO_4 + 2CO_2(g) \qquad (5)$$

$$2CaO + 2SO_2(g) + O_2(g) = 2CaSO_4 \quad (6)$$
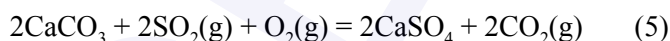
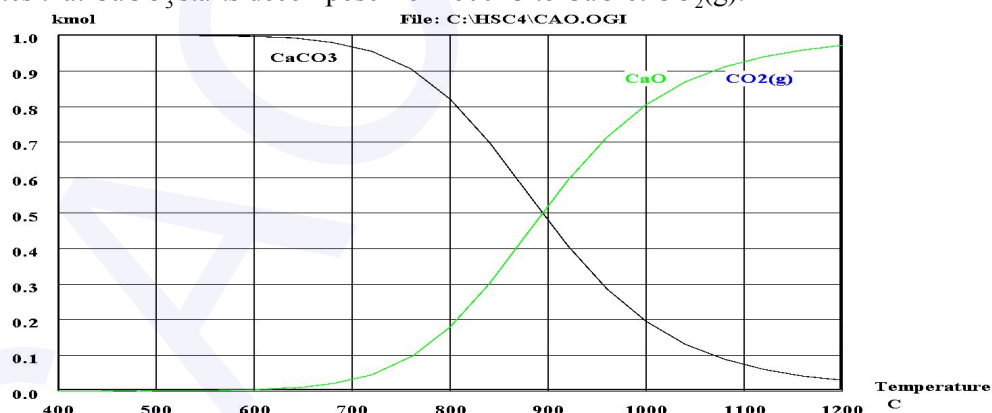Figure 5illustrates that $CaCO_3$ starts decompose from 600°C to CaO et $CO_2(g)$.

Figure 5: Thermodynamic equilibrium calculated by HSC Chemistry of $CaCO_3$ thermal decomposition

The figures 6 and 7 represent the evolution of the quantity of the various solids and gaseous according to theamount of $SO_2(g)$ (Left at 80°C, Right 1000°C). It is thus found that the SO_2 (g) reacts with $CaCO_3$ at low temperature and with CaO at high temperature. The result product in both cases is $CaSO_4$.
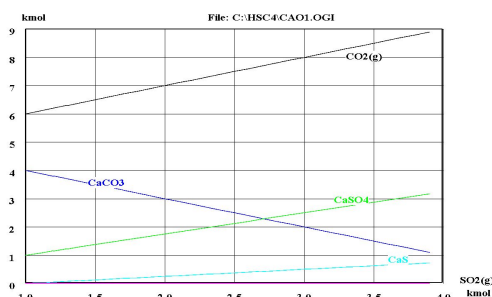
Figure 6: Quantity of the various solids and gaseous issues from desulfurization witch $CaCO_3$ as absorbent according to the amount of $SO_2(g)$ at 80°C
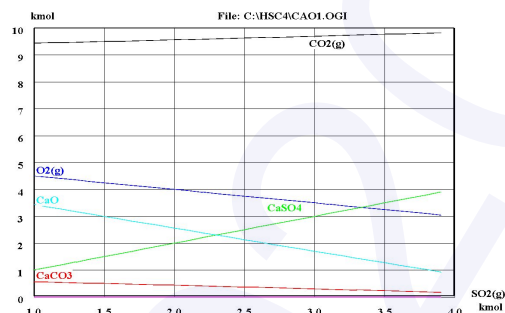
Figure 7: Quantity of the various solids and gaseous issues from desulfurization witch $CaCO_3$ as absorbent according to the amount of $SO_2(g)$ at 1000°C

4. CONCLUSION

The use of thermochemical calculations resulting at the HSC CHEMISTRY database allows us to interpret the phenomena of desulfurization of gaseous from a coal thermal station by utilization of two absorbents systems very well: $NaHCO_3$/ Na_2CO_3 and$CaCO_3$/CaO. the two studied adsorbent systems give relevant results in terms of desulfurization. In addition, the CaCO3/CaO system remains the most appropriate, given its cost and it savailability in nature. Our calculations confirm different results announced in the experimental research work [14-16].

REFERENCES

[1]**JanaJurisova, Vladimir Danielik, PavelFellner, Milan Kralik, Tomas Foltinvic**, Reactivity of calcium carbonate preparedfrom flue gas desulfurization gypsum,*ActaChimicaSlovaca*, 2019, Vol.12, N°1, 14-21.

[2] **SimionDragan, AlexandruOzunu,** Characterization of calcium carbonates used in wet flue gas desulphurization processes,*Cent. Eur. J. Chem.*,2012, Vol.10, N°5, 1556-1564.

[3] **DAM-JOHANSEN, K., HANSEN, P.F.B., OSTERGAARD, K**., High-temperature reaction between sulphur dioxide and limestone-III. A grain-micrograin model and its verification", *Chemical Engineering Science*, 1991, 46, 847-853.

[4] **Laursen, K., Grace, J.R., Lim, C.J**., Enhancement of the sulfur capture capacity of limestones by the addition of Na2CO3 and NaCl, *Environmental Science and Technology*, 2001, Vol.35,N°21, 4384-4389.

[5] **DUCARNE, E.D., DOLIGNIER, J.C., MARTY, E., MARTIN, G., DELFOSSE**, L., Modelling of gaseouspollutants emissions in circulating fluidized bed combustion of municipal refuse, *Fuel*, 1998, Vol.77, N°13, 1399-1410.

[6] **A.V. Slack , H.L. Falkenberry& R.E. Harringtonn,** Sulfur Oxide Removalfrom Waste Gases, *Journal of the Air Pollution Control Association*, 1972, Vol.22, N°3, 159-166.

[7]**M. Diaz-Somoano, M.R. Martinez-Tarazona**, Trace element evaporation during coal gasification based on a thermodynamic equilibrium calculation approach,*Fuel*, 2003, Vol.82, N°2, 137–145.

[8] **Ahmed AIT HOU**, *Etude des propriétés thermodynamiques de certains phosphates: Estimation et compilation de grandeurs thermodynamiques des Ortho-, Méta- et pyrophosphates ; Etude thermodynamique et expérimentale des phosphates du système CuO-Cu_2O-P_2O_5.* Doctorat d'Etat, Faculté des Sciences, El Jadida, Maroc, 1995.

[9] **HSC Chemistry Version 5.11, OutokumpuResearchOy**, Finland (Outokumputechnology, 2005.

[10] **The FACT database, AvailablethroughFactSage 5.2**. CRCT, Centre for Research in Computational Thermochemistry, Université de Montréal, Canada, 2005.

[11] **The GFE database**, Denmark Technical University, Denmark, 1995.

[12] **The SGTE pure substance database. Scientific Group Thermodata Europe**, available through ChemSage, GTT-Technologies and FactSage, 2005.

[13] **Ivtanthermo for Windows, GlushkoThermocenter**, Wagman, 1992.

[14] **S. Ebrahimia;b;∗, C. Picioreanua, R. Kleerebezema, J. J. Heijnena, M. C. M. van Loosdrechta**Rate-based modelling of SO_2 absorption into aqueous $NaHCO_3$=Na_2CO_3 solutions accompanied by the desorption of CO_2, *Chemical Engineering Science*, 2003, Vol.58, 3589 – 3600.

[15]**Afsin GUNGOR,**Effects of operational parameters on SO2 emission in a circulating fluidized bed combustor, *NiğdeÜniversitesiMühendislikBilimleriDergisi, Cilt, Sayı, 2012, Vol.1, 1-11*

[16] **Maria Gårding& Gunnar Svedberg**, Modeling of Dry Injection Flue Gas Desulfurization, *JAPCA*, 1988, Vol.38, N°10, 1275-1280.

The Second Edition of the International Congress of Applied chemistry and Environment
30th-31th October and 01st November 2020, Tunisia

ICACE 2020

Adsorption of a hazardous azo dye on cellulose extracted from annual agricultural wastes

Ibtissem Moussa[a, b] , **Manel Ben Ticha**[a, c]

(a) *Research Unity of Applied Chemistry & Environment, Faculty of Sciences, University of Monastir, Monastir, Tunisia.*
(b) *National Engineering School of Monastir, University of Monastir, Monastir, Tunisia.*
(c) *Fashion design and textile department, University of Taif, University college of Turabah, Saudi Arabia.*

E-mail: moussa.ibtissem@hotmail.fr

ABSTRACT:

Batch biosorption experiments were carried out for the removal of Basic Red 46 from aqueous solution by using celluloses extracted from almond shells, almond stems and fig stems as biosorbents. The adsorption investigations were carried out in various of initial pH of dye solutions, biosorbent dosage, contact time, initial dye concentration, stirring speed and salt concentration. The amount of Basic Red 46 sorbed onto the cellulose increased with the increase of dye concentration, salt concentration and stirring speed, in contrary, it decreased with increases of biosorbent dosage. The results indicate that these celluloses extracted from agricultural wastes can be employed as a low-cost alternative compared to other commercial adsorbents in the removal of a hazardous azo dye from wastewater.

KEYWORDS: Biosorption, Basic Red 46, Cellulose, Agricultural wastes.

1. INTRODUCTION

In the 21st century, environmental pollution is one of the major threats to human life. Among the different types of pollution, waste water stream is one of the major problems due to a large amount of water used in our daily life. Waste water containing dye is the major source of water pollution [1]. Dyes are extensively used as coloring agents in many industries such as textile, leather, plastic, cosmetic, food and pharmaceutical. Among these various industries, textile ranks first in usage of dyes for coloration of fiber. As a result, they generate a considerable amount of colored wastewater. These dyes are primarily of synthetic origin and have complex aromatic structures, which make them more stable to light, heat and oxidizing agents, and are usually biologically non-degradable [2]. Besides, many dyes or their metabolites have carcinogenic, teratogenic and mutagenic effects on humans and other life forms [3]. Thus, it is necessary to remove dyes from wastewater before it is discharged.

In recent years, the development of biosorption technology has represented a powerful alternative for the removal of dyes from wastewaters with the advantages of low-cost, greater profitability, ease of operation and greater efficiency [4]. Over the last few decades, there has been an increase in the use of plant waste products for dye removal by biosorption from wastewater. Some of these alternative biosorbents are neem leaf powder, loquat seed biomass, bean waste biomass, Thuja orientalis cone biomass, palm kernel fiber, durian peel and hazelnut shells [4, 5]. However, the biosorption capacities of most of the above were still limited. New economical, locally available and highly effective biosorbents are still under development.

Almond shells, almond stems, and fig stems are in high quantity, cheap and available in many regions of Tunisia. Tunisia is ranked the 8th place in producing almond by about 3.8%. Indeed, Tunisia's annual production of almond shell is about 36 000 tons such as the shell has approximately 60% of the almond fruit weight [6]. The fig tree is a very widespread tree in Tunisia and it grows in cold and humid as well as in hot and dry regions. These almond and fig by-products have no commercial usage. There are no precedent published reports on the valorization of these agricultural wastes for removing dyes from aqueous solution.

In this study, Basic Red 46 was used as a model compound. It is a synthetic azo dye which is used widely in the textile industry. Azo dyes are a class of dyes characterized by the presence of the azo group. Due to high usage of these dyes, large volumes of colored effluents are discharged into environmental water sources. The release of azo dyes into the environment is of concern due to their toxic, mutagenic and carcinogenic characteristics of the dyes and their biotransformation products [7]. Hence, removal of azo dyes from wastewater is a major environmental issue. The main object of this study was to examine the feasibility of

using celluloses extracted from almond shells, almond stems and fig stems as biosorbents for the removal of Basic Red 46 from the aqueous solution. Effects of different parameters including solution pH, biosorbent dosage and size, dye concentration, temperature, and contact time were studied to optimize the biosorption process.

2. MATERIAL AND METHODS

2.1. Preparation of biosorbent material

The preparation of extracted bleached cellulose was conducted in two steps [8, 9]. First, 10 g of almond shells, almond stems, and fig stems were impregnated in 100 mL of an aqueous soda solution (14, 9 and 15 % w/w, respectively) under stirring, for 120, 70 and 75 min, respectively at 120, 120 and 135°C, respectively. The ensuing fibers were then extensively washed with water until neutrality, before being bleached using 100 mL of sodium hypochlorite solution (30%, v/v) in alkaline pH around 13, 13 and 11, respectively, for 180 min. Finally, the bleached fibers were extensively washed with water until neutrality, purified by anti-chlorine treatment and air dried before further use.

2.2. Preparation of dye solution

Basic Red 46 was supplied by a local textile factory and used without further purification. The dye was of commercial purity (Type : Cationic, M_w: 322 g mol^{-1}, λ_{max}: 530 nm). The chemical structure is shown in Figure 1. A stock solution of 500 mg L^{-1} was prepared by dissolving accurately quantity of the dye in distilled water. The test solutions were prepared by diluting the stock solution to the desired concentrations. The pH of the working solutions was adjusted to the desired values with dilute HCl or NaOH using a pH-meter.
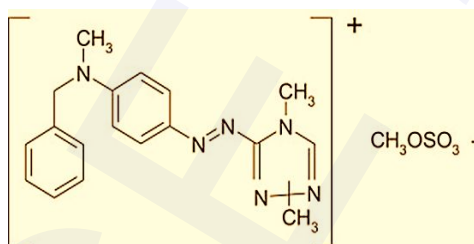

Figure 1. Chemical structure of Basic Red 46

2.3. Batch biosorption experiments

Adsorption experiments were carried out in a batch mode, using a rotary shaker using 100 mL conical flasks containing 25 mL Basic Red 46 solutions in a water bath to determine the optimum values of the experimental parameters including solution pH, biosorbent dose, dye concentration, and contact time. After each test, the samples were centrifuged for solid–liquid separation and the residual dye concentration in solution was analyzed by a UV–Vis spectrophotometer at 530 nm for Basic Red 46. The capacity of adsorption, q_e (mg.g^{-1}), was calculated by Eq. (1).

$$q_e = \frac{(C_0 - C_e)V}{m} \quad q_e = \frac{(C_0 - C_e)V}{m}$$

(1)

Where C_0 and C_e are the initial and equilibrium concentrations of dye (mg.L^{-1}), respectively; V is the volume of the solution (L) and m is the mass of dry biosorbent used (g).

The dye removal percentage can be calculated as given by Eq. (2).

$$Removal\ percentage = \frac{C_0 - C_e}{C_0}\ 100 \quad Eq. \quad Removal\ percentage = \frac{C_0 - C_e}{C_0}\ 100 \quad Eq.$$
(2)

Where C_0 and C_e (mg.L^{-1}) are the liquid-phase concentrations of dye at initial and equilibrium, respectively.

3. RESULTS AND DISCUSSIONS

3.2. Effect of solution pH

The pH of the dye solution affects not only the surface charge of the biosorbent, the degree of ionization of the materials and the dissociation of functional groups on the active sites of the biosorbent, but also the structure of the dye molecule [10]. The results of the pH studies at different pH values are shown in Figure 2. Biosorption capacity of celluloses extracted from almond shells, almond stems and fig stems for Basic Red 46 increased with increasing pH and reached a maximum level at the pH of 8. The lower biosorption of Basic Red 46 at low pH values may be explained by the competition of excess H^+ ions with the dye cation for active biosorption sites.
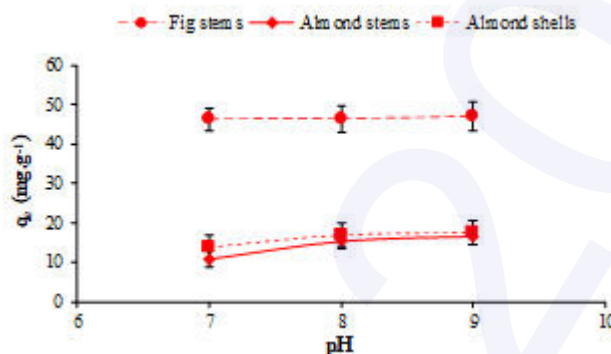

Figure 2. Effect of pH on Basic Red 46 adsorption by celluloses extracted from almond shells, almond stems, and fig stems

3.3. Effect of biosorbent dose

The concentration of biosorbent was varied in the range of 0.25-10 $g.L^{-1}$ for the removal of Basic Red 46 from aqueous solution by almond shells, almond stems and fig stems, by keeping constant all other parameters such as pH, initial dye concentration, solution volume, temperature and stirring speed. The effect of biosorbent dose on Basic Red 46 biosorption is shown in Figure 3.
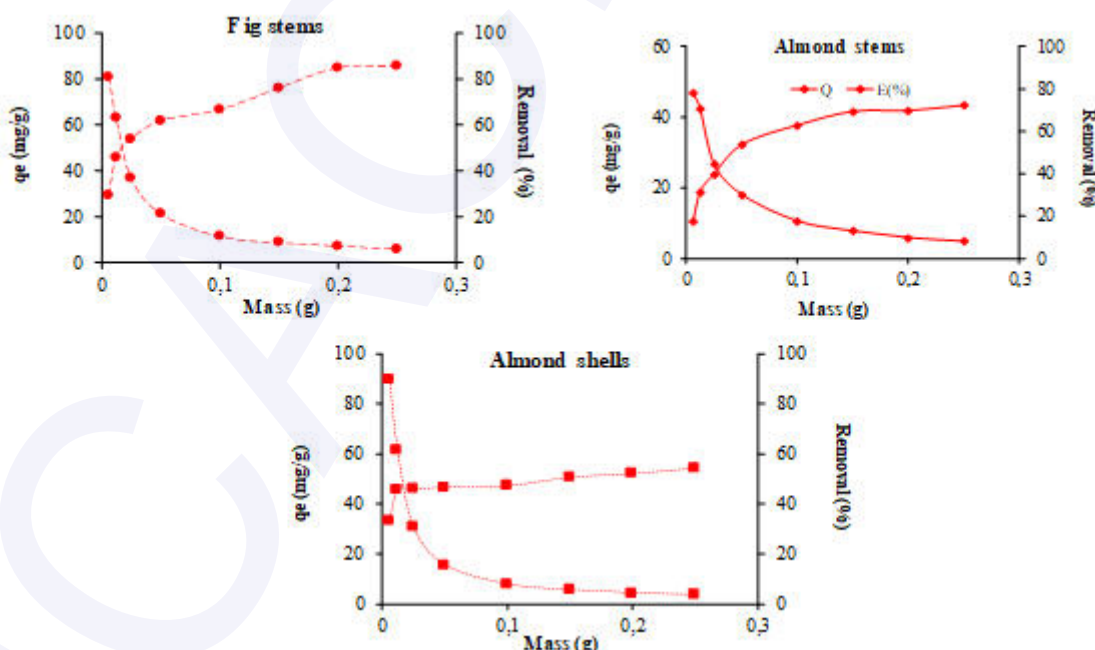

Figure 3. Effect of biosorbent dose on Basic Red 46 adsorption by celluloses extracted from almond shells, almond stems, and fig stems.

As seen from Figure 3, biosorption capacity for Basic Red 46 decreased with celluloses dosage increasing. This may be due to the decrease in the total sorption surface area available to Basic Red 46 resulting from overlapping or aggregation of sorption sites. Similar behaviour for the effect of biosorbent dosage on the dye biosorption capacity was observed and discussed in the literature for different types of biosorbents [11].

3.4. Effect of dye concentration

The initial adsorbate concentration gives a significant driving force to overcome all mass transfer resistances of dyes between the aqueous and solid phases. The effect of initial dye concentration on biosorption of the Basic Red 46 was investigated at the ranges of 10–2000 mg.L^{-1} and is shown in Figure 4. The biosorption capacity of celluloses increased with increasing of the initial dye concentration. This is probably due to the increase in the driving force of the concentration gradient, as an increase in the initial dye concentration. The initial concentration of the dye that allows for optimal adsorption is equal to 250 for Basic Red 46.
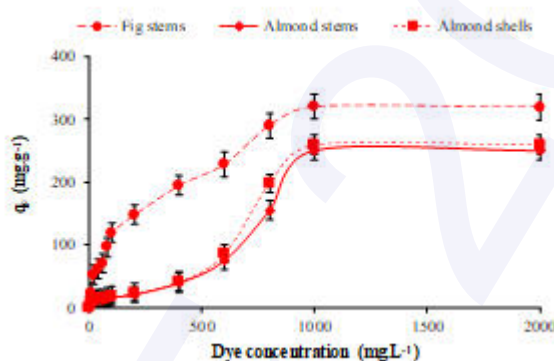

Figure 4. Effect of initial dye concentration on Basic Red 46 adsorption by celluloses extracted from almond shells, almond stems, and fig stems

4. CONCLUSION

The results reported herein indicate that celluloses extracted from almond shells, almond stems and fig stems could be successfully used to remove Basic Red 46 from aqueous solution by sorption process. The regeneration of the saturated biosorbent materials with Basic Red 46 does not required while the building reuse is possible. Thus, desorption and recovery processes could be avoided and the related costs reduced. Consequently, for environmental, economic and operational considerations, the use of celluloses extracted from almond shells, almond stems and fig stems for the removal of Basic Red 46 and other nutrients appears to be more promising.

REFERENCES

[1] **Nandi, B.K.; Goswami, A. and Purkait, M.,** Removal of cationic dyes from aqueous solutions by kaolin: Kinetic and equilibrium studies, *Applied Clay Science*, 2009, Vol.42, No.3, 583–590.

[2] **Han, R.; Ding, D.; Xu, Y.; Zou, W.; Wang, Y.; Li, Y. and Zou, L.**, Use of rice husk for the adsorption of congo red from aqueous solution in column mode, *Bioresource Technology*, 2008, Vol.99, No.8, 2938–2946.

[3] **Sun, J.-H.; Sun, S.-P.; Wang, G.-L. and Qiao, L.-P.**, Degradation of azo dye Amido black 10B in aqueous solution by Fenton oxidation process, *Dyes and Pigments*, 2007, Vol.74, No.3, 647–652.

[4] **Sarma, J.; Sarma, A. and Bhattacharyya, K.G.**, Biosorption of commercial dyes on azadirachta indica leaf powder: a case study with a basic dye rhodamine B, *Industrial & Engineering Chemistry Research*, 2008, Vol.47, No.15, 5433–5440.

[5] **Aksakal, Ö.; Ucun, H. and Kaya, Y.**, Application of Eriobotrya japonica (Thunb.) Lindley (Loquat) seed biomass as a new biosorbent for the removal of malachite green from aqueous solution, *Water Science & Technology*, 2009, Vol.59, No.8, 1631.

[6] **Moussa, I.; Baaka, N.; Khiari, R.; Moussa, A.; Mortha, G. and Mhenni, M.F.**, Application of *Prunus amygdalus* by-products in eco-friendly dyeing of textile fabrics, *Journal of Renewable*

Materials, 2018, Vol.6, No.1, 55–67.

[7] **Lin, Y.-H. and Leu, J.-Y.**, Kinetics of reactive azo-dye decolorization by *Pseudomonas luteola* in a biological activated carbon process, *Biochemical Engineering Journal*, 2008, Vol.39, No. 3, 457–467.

[8] **Moussa, I.; Khiari, R.; Moussa, A.; Abouzeid, R.E.; Mhenni, M.F. and Malek, F.**, Variation of chemical and morphological properties of different parts of *Prunus Amygdalus L.* and their effects on pulping, *Egypt. J. Chem*, 2019, Vol.62, No.2, 343–356.

[9] **Moussa, I.; Khiari, R.; Moussa, A.; Mhenni, M.F. and Naceur Belgacem, M.**, Physico-chemical characterization of polysaccharides and extraction of cellulose from annual agricultural wastes, *Cellulose Chemistry and Technology*, 2018, Vol.52, Nos.9–10, 841–851.

[10] **Crini, G.; Peindy, H.N.; Gimbert, F. and Robert, C.**, Removal of C.I. Basic Green 4 (Malachite Green) from aqueous solutions by adsorption using cyclodextrin-based adsorbent: Kinetic and equilibrium studies, *Separation and Purification Technology*, 2007, Vol.53, No.1, 97–110.

[11] **Senturk, H.B.; Ozdes, D. and Duran, C**.: Biosorption of Rhodamine 6G from aqueous solutions onto almond shell (Prunus dulcis) as a low cost biosorbent, *Desalination*, 2010, Vol.252 (2010), Nos.1–3, 81–87.

The Second Edition of the International Congress of Applied chemistry and Environment
30th-31th October and 01st November 2020, Tunisia

ICACE 2020

The collection efficiency of an asymmetrical electrostatic precipitator model -validation of the experimental results with calculated data using Deutsch model

Kherbouche Fouad[(a)], **Berdadi bendaha mourad**[(b)]

(a)   LSTE Laboratory, Université Mustapha STAMBOULI de Mascara, BP 305 mascara-29000
(b)   Université Abdelhamid Ibn BadisMostaganem, Avenue HamadouHossine, Mostaganem 27000
E-mail :kherbouche.fouad@univ-mascara.dz / kherbouche.fouad@gmail.com

ABSTRACT: In this research paper, a new electrostatic precipitator (ESP) with asymmetrical wire-to-cylinder configuration has been studied experimentally in order to evaluate the collection efficiency of high resistivity particles such as the ones released from cement manufacturing processes and validated with calculated one. The experiments are performed with cement particles ranging from 0.18 to 5 μm with a mean size of about 0.35 μm. An aerosol spectrometer is employed for characterizing the size distribution of these particles at the outlet of the ESP. The collection efficiency is estimated for various DC applied voltage magnitudes and for both positive and negative polarities. The electrical measurements show that the behavior of corona discharges is similar to that obtained in symmetrical wire-to-cylinder configuration. Results show that the particle collection efficiency of the ESP can reach 95% in the case of 1 wire-ESP. The global collection efficiency results are close to the analytical ones obtained from Deutsch model for a combined charge process.

KEYWORDS:ESP, corona discharge, asymmetrical configuration, efficiency, Deutsch model.

1. INTRODUCTION

Particle matter (PM) or called airborne particles are a mixture of solid and liquid particles suspended in the air, which have a significant impact on air quality and visibility, as well as on human health [1]. The finest particles PM_{10} (<10 μm) and $PM_{2.5}$ (<2.5 μm) can penetrate deeper into the lungs causing many diseases, such as chronic respiratory diseases and various types of cancers. Nowadays, various gas cleaning devices are applied, such as cyclones, bag filters, granular-bed filters, scrubbers, or electrostatic precipitators which is the subject of our research [2-4]. The electrostatic precipitators (ESP) are a universal apparatus for industrial gas cleaning of solid and liquid particles. High collecting efficiencies (more than 99 %) and low energy expenditures are the main benefits of ESPs [5,6]. The ESPs can be classified according to the collecting electrode geometry (cylindrical or plate type), the direction of gas flow (vertical or horizontal flow), particles recuperation system (dry ESPs using rappers or wet ESPs using water) [5, 7].

In recent research, H. Ando & al. developed an electrostatic precipitator based on moving electrodes (MEEP) and rotary brush to remove the collected dust. This device meets the need of some factories that eject high resistive dust particles in order to resolve the problem of re-entrainment due to back corona discharge [8, 9].

One of the simplest and interesting new geometries allowing the movement of the collection electrode is the use of an asymmetrical wire-to-cylinder ESP where the particles are charged due to the corona discharge generated near the wire connected to the high voltage. Then, they are collected on the whole surface of the cylindrical collection electrode. Thus, the rotation of the cylinder enables the homogenization of the dust layer and the cleaning of the surface using a static brush [2].

In this paper, the asymmetrical wire-to-cylinder ESP is studied experimentally in order to evaluate the collection efficiency in a static situation (the cylinder is immobile) for one wire-ESP and three wires-ESP. First, the current-voltage characteristics are measured with and without the presence of particles for both positive and negative polarities. Then, the collection efficiency of cement particle under various electrical conditions and flow rates is investigated by means of an aerosol spectrometer that measures the particle size distribution at the outlet of the ESP.Finally, a comparison between the simplified Deutsh model and experimental data is carried out to understand the main charging mechanism also to validate the experimental data [2, 10] (global and fractional efficiency) for this novel electrostatic precipitator configuration.

2. MATERIAL AND METHODS

The schematic representation of the asymmetrical wire-to-cylinder ESP used in this investigation for both one wire-ESP and three wires-ESP are shown in Figure 1 The high voltage electrode consists of stainless-steel wire (0.2 mm-diameter and 132 mm-length). The collecting electrode made of stainless-steel cylinder (50 mm-diameter) is connected to ground and placed at about 30 mm from the high voltage electrodes. The distance between two successive corona wires is set at 20 mm.

The origin of the coordinates corresponds to the center of the wire and the airflow is directed from the wire toward the cylinder (ox direction).
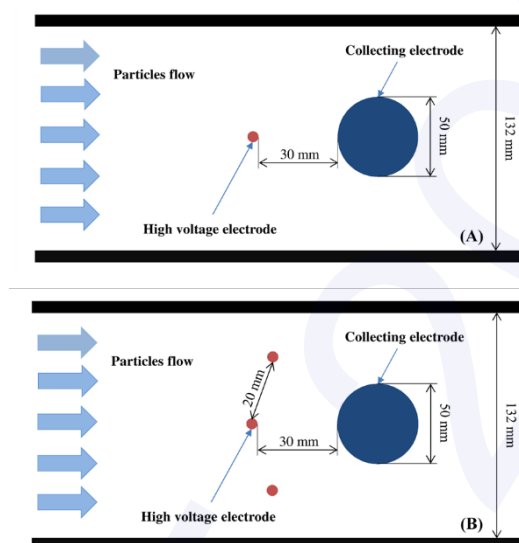

Figure 1. Schematic representation of the ESP, (A) case of 1 wire-ESP and (B) case of 3 wires-ESP.

The complete experimental bench illustrated in Figure 2 is divided into 4 parts: the power supply unit, the particle detection instrumentation, the particle supply and the wind tunnel.
- Power supply section
- Particle supply section
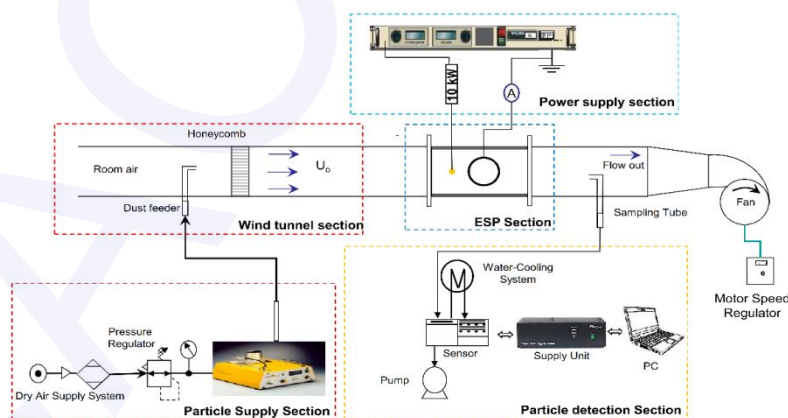- Particle detection section
- Wind tunnel section

Figure 2. Schematic of the experimental setup.

3. RESULTS AND DISCUSSIONS

3.1. Electrical characteristics

Figure 3 Shows the current-voltage characteristics of the ESP for both high voltage polarities, with and without the presence of particles in case of 1 wire-ESP and 3 wires-ESP. As expected, the discharge current increases gradually with the applied voltage when it exceeds the corona onset voltage. At a given voltage, the

discharge current is higher with the negative polarity, which is due to the difference between the apparent mobility of negative charge carriers compared to positive ones [11 - 13].

Whatever the polarity, the discharge current increases with the number of HV electrodes for a given voltage. However, the corona current generated by three wires is lower than three times the value measured with one wire (1 wire < 3 wires< 3 wire). This is due to the electric field interaction between two successive high voltage wires.

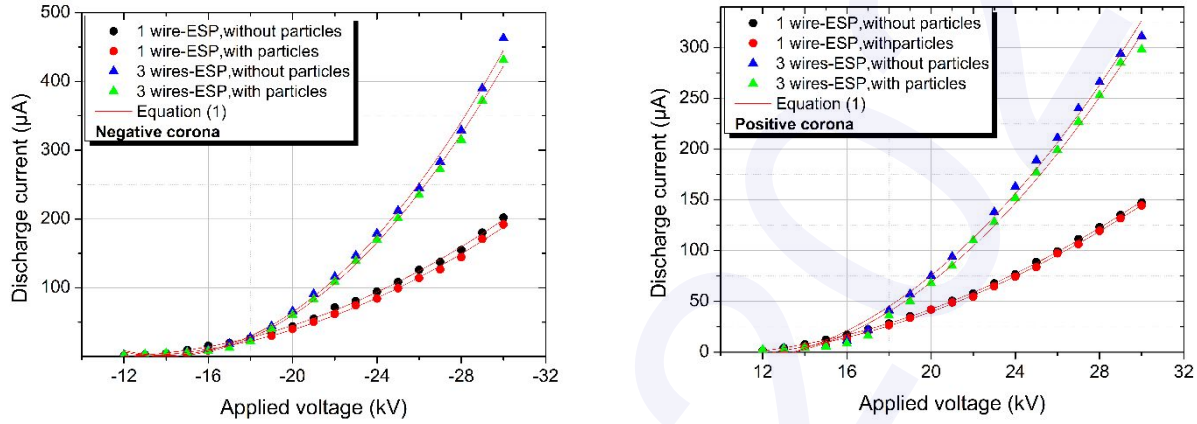**Figure 3.** Current-voltage characteristics both for negative and positive corona discharge (T = 23 °C, RH = 44 %).

The morphology of positive and negative corona discharges at applied voltages close to breakdown is shown in Figure 4 Even with asymmetrical wire-to-cylinder geometry, the negative dc corona produces discrete active spots called 'tufts' along the corona wire, while the positive dc corona induces a uniform glow around the wire [14].
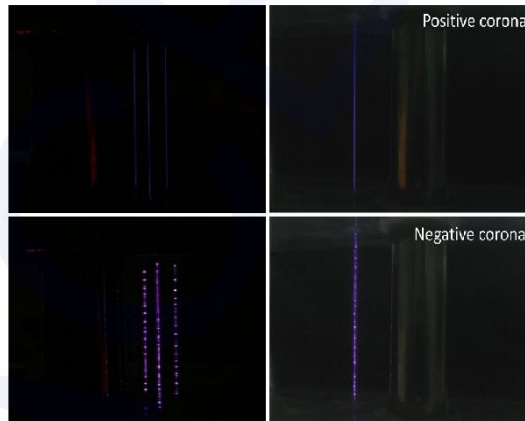

Figure 4. Morphology of positive and negative corona discharges for both 1 wire-ESP and 3 wires-ESP. Experimental conditions: voltage = ±30 kV,

3.2. Collection efficiencies

The total number collection efficiency η of the ESP in terms of number/volume is defined as follows [2]:

$$\eta = \left[1 - \frac{N_{On}}{N_{Off}} \right] \cdot 100 \% \quad (1)$$

Where N_{On} and N_{Off} are the numbers of particles per cm^3 for all particle classes with and without corona discharge, respectively.

Using the same methodology, the fractional number collection efficiency for the size class i (η_i) can be defined using the following equation:

$$\eta_i = \left[1 - \frac{N_{on,i}}{N_{Off,i}} \right] \cdot 100 \% \quad (2)$$

The Second Edition of the International Congress of Applied chemistry and Environment
30th-31th October and 01st November 2020, Tunisia

ICACE 2020

Here, $N_{on,i}$ and $N_{Off,i}$ are the numbers of particles per cubic centimeter for the size class i with and without corona discharge, respectively.

Figure 5. shows the evolution of the collection efficiency as a function of the applied voltage for both negative and positive corona discharges. With increasing the applied voltage, the collection increases and can reach 95 % in the case of one wire-ESP and 98 % in the case of three wires-ESP under -30 kV. For a given voltage, the collection efficiency is clearly higher in case of negative polarity compared to the positive one for both configurations. Due to the high mobility of negative ions, the particle charging process leads to upper values of charges in the case of negative corona [15, 16]. Furthermore, the interaction between the primary flow and the secondary flow (electric wind) seems to be relatively strong in the case of negative corona due to the difference between the spatial distributions of positive or negative corona discharges along the wire [17].
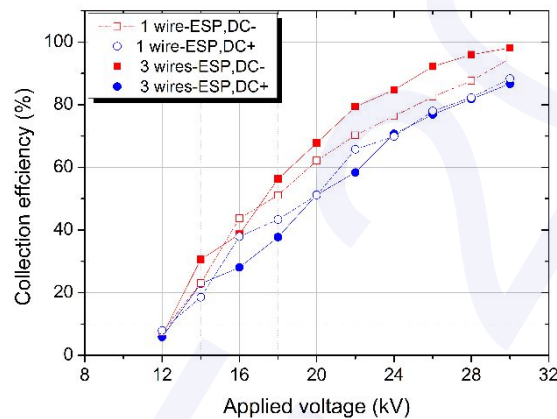

Figure 6. Collection efficiency versus applied voltage comparison for three and one wires-ESP.

3.3. Analytical estimation of the collection efficiency

In this part, an analytical model is performed to evaluate the effect of the various charging process (field and diffusion charging) on PM_{10} and $PM_{2.5}$ collection efficiency in an asymmetrical ESP configuration. The numerical models include all parameters that affect the ESP operations (particles charge, flow velocity, electric field). The collection efficiency is calculated by using the Deutsch–Anderson equation and analysed using the experimental data.The Deutsch model was developed at the beginning of the 20th century and was firstly published in 1922 by W. Deutsch still allows determining the collection efficiency of electrostatic precipitators in order to analyse their operational and designproperties. This model assumes an infinite remixing force, e.g. caused by 'turbulence', which redistributes the remaining particles at each downstream location homogeneously over the precipitator duct. Apart from the boundary layer, the particles in the downstream direction have the mean velocity of the fluid, are fully charged and migrate in a homogeneous electrical field [18,19]. According to the Deutsch theory the collection efficiency $\eta_D(d_p)$ for a particle of size d_p can be determined using the following formula [20]:

$$\eta_D(d_p) = 1 - exp^{(\frac{w_{th}A}{Q})} \qquad (3)$$

where:

w_{th} : migration velocity of the dust particle of diameter d_p,

A : area of two adjacent collecting electrodes, $A = 2 \cdot h \cdot L$,

Q: volume flow rate of the gas, calculated by the equation $Q = 2 \cdot h \cdot b \cdot u$,

h: height of the collection electrodes.

L: length of the collection electrode,

b: distance between the electrodes with different polarity,

u: velocity of the gas,

Figure 6 shows typical comparison between the analytical model and experimental data for negative applied voltage (-30 kV). analytical model can offer a good estimation of the fractional collection efficiency if we consider both field and diffusion mechanisms (combined charging) in the calculation of total particle charge.
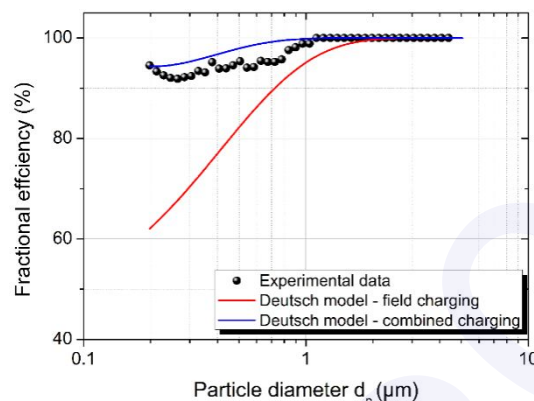
The Second Edition of the International Congress of Applied chemistry and Environment
30th-31th October and 01st November 2020, Tunisia

ICACE
2020

Figure 7. Experimental and analytical fractional collection efficiency versus particles size for -40 kV.

Figure 7 illustrates the evolution of collection efficiency as a function of the applied voltage for the particle diameter of 0.3 μm. we can observe that experimental and analytical results are very closewhich confirms the accuracy of the analytical model.especially when the corona discharge becomes stable. The combined charging mechanism governs the performance of the electrostatic precipitator for the particle with the mean diameter (0.3 μm) corresponding to the highest concentration class.
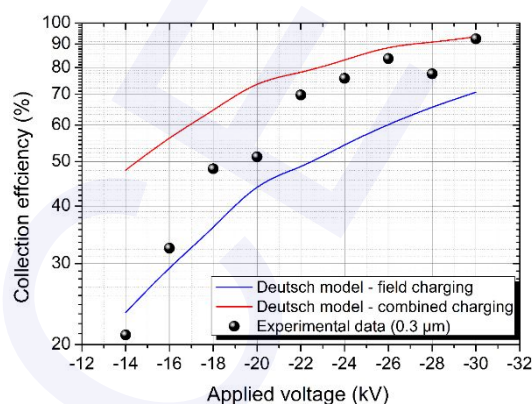

Figure 8. Experimental and analytical collection efficiency versus applied voltage for particle diameter of 0.3 μm.

4. Conclusion

In this paper, an experimental investigation is carried out on an electrostatic precipitator with asymmetrical wire-to-cylinder in one wire-ESP and three wires-ESP configurations. The main objective is to evaluate the collection efficiency of high resistivity particles such as the ones released from cement manufacturing processes.

The collection efficiency of cement particles ranging from 0.18 to 5 μm has been estimated for various dc applied voltage magnitudes for both positive and negative polarities. The effect of the flow rate and the operation time are also taken into consideration. The main results of the study are as follows.

1. The electrical measurements show that corona discharge behavior is similar to that obtained in symmetrical wire-to-cylinder configuration for both configurations.
2. Particle collection efficiency of the ESP can reach 95% in the case of one wire-ESP and 98% three wires-ESP for negative corona discharge, which confirms the potential of the asymmetrical

The Second Edition of the International Congress of Applied chemistry and Environment
30th-31th October and 01st November 2020, Tunisia

ICACE 2020

wire-to-cylinder geometry. However, the fractional collection efficiency is limited to about 90% for particles of about 0.3 μm because of breakdown voltage.

3. The collection efficiency decreases with increasing the flow rate. This result indicates the need to expand the active region for particle charging by adding more corona wires.

4. The comparison between experimental results and analytical model about the collection efficiency has revealed a good agreement. Diffusion charging mechanism can be considered as the dominant one for particle size of 0.3 μm.

REFERENCES

[1] **Li Ma**, Comparative analysis of chemical composition and sources of aerosol particles in urban Beijing during clear, hazy, and dusty days using single particle aerosol mass spectrometry, *Journal of Cleaner Production*. (2016), 112, Part 2 1319-1329.

[2] **F. Kherbouche**, Study of a new electrostatic precipitator with asymmetrical wire-to-cylinder configuration for cement particles collection, *J.Electrostat*., vol. 83, pp. 7-15, 2016.

[3] **F. Sanchez-Soberon**, Main components and human health risks assessment of PM10, PM2.5, and PM1 in two areas influenced by cement plants, *Atmosph. Environ*. (2015), 120, 109-116.

[4] **J.T. Zelikoff**, Effects of inhaled ambient particulate matter on pulmonary antimicrobial immune defense, *Inhal. Toxicol*. (2003), 15, 131–150.

[5] **H. J. White**, *Industrial electrostatic precipitation*, Addison Wesley, 1963.

[6] **A. Jaworek**, Two-stage electrostatic precipitator with dual-corona particle precharger for PM 2.5 particles removal. *Journal of Cleaner Production*, (2017) ,164, 1645-1664.

[7] **K. R. Parker**, *Applied Electrostatic Precipitation*, Chapman &Hall, 1997.

[8] **H. Ando**, Recent Technology of moving electrode electrostaticprecipitator, *Int. J. Plasma Environ*. Sci. Technol. (2011), 5, 130-134.

[9] **T. Misaka**, Improvement of reliability for moving electrode type electrostatic precipitator.10Th *International Society for Electrostatic Precipitation ICESP*, Cairns, Australia, 2006, June 25 - 29.

[10] **F Kherbouche**, Experimental study of high resistivity particles collection using an electrostatic precipitator in wire-to-cylinder configuration, *ICESP 2016*, Wrocław, Poland, 19–23 September 2016.

[11] **S. Oglesby**, *Electrostatic Precipitation*. Marcel Dekker, New York, 1978.

[12] **G.P. Reichel**,Bipolar charging of ultrafine particles in the size range below 10 nm, *J. Aerosol Sci*. (1996), 27, 931-949.

[13] **H. Nouri**, Effect of relative humidity on current–voltage characteristics of an electrostatic precipitator, *J. Electrostat*, (2012), 70 20-24.

[14] **J.S. Chang**, *Handbook of Electrostatic Processes*, Marcel Dekker Edition, NY, 1995.

[15**] J. H. Ji**, Particle charging and agglomeration in DC and AC electric fields, *J. Electrostat*. (2004), 61, 57–68.

[16**] H.-J. Schmid**, On the modeling of particle transport in electrostatic precipitators, in: Proceedings of the *7th International Conference of Electrostatic Precipitators ICESP*, September 20–25, Kyongju, Korea (1998), pp. 121–131.

[17] **W. Deutsch**, Bewegung und Ladung der ElektrizitiitstriigerimZylinderkondensator. *Ann. Phys,* (1922), 68, 335-44.

[18] **Jian-Ping Zhang**, A Numerical Simulation of Diffusion Charging Effect on Collection Efficiency in Wire-Plate Electrostatic Precipitators, *IEEE transactions on plasma science*, VOL. 39, NO. 9, 2011.

[19] **Arkadiusz Swierczok**. The collection efficiency of ESP model - Comparison of experimental results and calculations using Deutsch model", *Journal of Electrostatics* (2018), 91, 41–47.

[20] **R. Cochet**. Lois Charge des Fines Particules (Submicroniques) Etudes ThéorétiquesContrôles Récents Spectre de Particules. Coll.Int.la Physique des Forces Electrostatiques et Leurs Application, Centre National de la Recherche Scientifique, 102, 331-338., 1961

Management and valorization of bio-ressources and industrial waste

The Second Edition of the International Congress of Applied chemistry and Environment
30th-31th October and 01st November 2020, Tunisia

ICACE 2020

Bio-oil from fast pyrolysis of exhausted Olive Pomace:

Physico-chemical characterization and investigation of its

potential as biochemical and biofuel

Najla Grioui[a,b] and Kamel Halouani[a,b]

(a) University of Sfax, National Engineering School of Sfax, Micro Electro Thermal Systems (UR13ES76),
IPEIS, Road Menzel Chaker km 0.5- PO Box 1172, 3018 Sfax, Tunisia;
(b) Digital Research Center of Sfax, Technopole of Sfax, PO Box 275, Sakiet Ezzit, 3021 Sfax, Tunisia.
najla.grioui@ipeis.usf.tn; kamel.halouani@ipeis.rnu.tn

ABSTRACT

Exhausted olive pomace (EOP) agro-industrial waste was characterized and then pyrolyzed in a fluidized bed reactor at temperature around 500 °C with a nitrogen flow rate 18 min.L^{-1} during 3.27 s to produce bio-oil. A deep physic-chemical characterization of the obtained bio-oil from fast pyrolysis of EOP was performed using FTIR, ^{13}C NMR and GC-MS analyses techniques. Aliphatic and aromatic hydrocarbons, hydroxyl, carbonyl, and phenolic compounds were the major components of the EOP bio-oil, these components are useful as a resource of bio-chemicals synthetic polymers of industrial interest. EOP bio-oil can also be used as biofuel of a relatively high heat value (27.45 MJ.kg^{-1}).

KEYWORDS: Exhausted olive pomace, Fast pyrolysis, Bio-oil, Biofuel, Bio-chemicals.

1. INTRODUCTION

Tunisia ranks fourth in the world in the production of olive oil during the last ten years with an average production rate of 150.000 tons of olive oil, which is more than 8 % of the world global production. Exhausted olive pomace (EOP) is the solid residue byproduct resulting from the processes of olive oil second extraction using hexane solvent. EOP is lignocellulosic biomass that can be valorized using alternative routes of processing to be converted into an adsorbent for heavy metal removal [1] a substrate for anaerobic digestion [2], filler material for the development of novel polymer composites [3] and bioenergy [4–5]. Some studies have developed thermochemical processes in recent years to convert EOP into alternative biofuel [1, 6-7]. Among the various thermal conversion technologies, pyrolysis is a simple, more flexible and applicable technic for different biomass feedstocks to produce three main products: bio-oil, biogas, and biochar. The bio-oil can be used as a biofuel and biochemical source [6,7]. Biogas can be used as biofuel whilst, biochar can also be used as solid fuel indirect carbon fuel cell systems [8], as a soil amendment or activated carbon [9]. Besides, this process contains fundamental chemical reactions that are the originator of gasification and combustions techniques. In fact, the pyrolysis is a thermal treatment of biomass carrying out at 400-600 °C with an oxygen-free environment.   However, the implementation of this process depends on the reliable design of large-scale units, in which   the pyrolysis reactor plays an important role. The proper design of the reactor requires the knowledge and understanding of biomass pyrolysis kinetics and several operating conditions such as reactor temperature, heating rate and residence time affecting essentially the product yields and their physico chemical properties.

The main objective of this paper is to produce bio-oil from EOP via fast pyrolysis in a fluidized bed reactor, and characterize the various physical and chemical properties of the bio-oil in order to determine its potential as biofuel and bio-chemicals resource.

2. MATERIAL AND METHODS

The Second Edition of the International Congress of Applied chemistry and Environment
30th-31th October and 01st November 2020, Tunisia

ICACE 2020

The experimental methodology in this work includes the preparation and characterization of feedstock and the production and characterization of bio-oil.

The EOP sample used in this study was recuperated from an olive oil second extraction factory in the region of Agereb at Sfax city, Tunisia. This agro-industrial waste was ground and sieved to a 10-20 mesh particle size and was characterized using different analysis methods such as a Vario Micro Elementary Carbone Hydrogen Nitrogen Sulfur (CHNS) system and a Thermogravimetric Analyzer.

The pyrolysis of EOP biomass was carried out in a fluidized bed reactor at a temperature of 500 °C during 3.25 s with a nitrogen flow rate of 18 L.min^{-1} and a feed rate of 200 g.h^{-1}.

The obtained bio-oil was shipped in the laboratory where it was analyzed to determine its physico-chemical properties by following the standard test methods using various equipment such as FTIR, ^{13}C-NMR and GCMS.

3. RESULTS AND DISCUSSIONS

3.1. Properties of raw material

Obtained results from the proximate and the ultimate analysis of EOP are given in Table 1. These results show that EOP had a high content of oxygen and nearly no sulfur content which suggest that EOP can be thermal degradable with lowest SO_x emission. The values obtained from proximate analysis are in the range of the most agricultural and forest residues. The obtained HHV of EOP (14.43 MJ.kg^{-1}) is also in the range of reported HHV of other biomass essences (11-40 MJ kg^{-1}) found in literature and used as fuels [10]. The chemical analysis (Table 1) shows that the EOP has a higher lignin content (49 %) than holocellulose content (40 %) which affects the physico-chemical properties and composition of the pyrolytic bio-oil. This result means that the EOP bio-oil would be rich on phenolic compounds.

Table 1. Proximate and elemental analysis of EOP raw material.

Analysis	Sample	EOP raw material
Proximate analysis (%)	Moisture	7.31
	Ash	10.91
	Fixed carbon**	25.28
	Volatile matter	56.5
Ultimate analysis* (%)	C	39.45
	H	5.58
	N	2.68
	S	<0.8
	O**	41.2
	H/C	1.69
	O/C	0.78
Molar formula		$CH_{1.69}O_{0.78}N_{0.058}$
Lignocellulosic composition (%)	Hemicellulose	13
	Cellulose	27
	Lignin	49
Higher heating value (HHV. MJ kg^{-1})		14.43

* Dry basic. ** By difference.

3.2. Characterization of EOP bio-oil

In this section, deep characterization of physico-chemical and structural properties of EOP fast pyrolysis bio

The Second Edition of the International Congress of Applied chemistry and Environment
30th-31th October and 01st November 2020, Tunisia

ICACE 2020

oil will be developed aiming to assess its possible application as an alternative biofuel and biochemical source. The EOP bio-oil from our process is a dark brown viscous liquid. The key physical and chemical properties of the bio-oil are described in Table 2. As can be seen, bio-oil shows significantly lower amounts of oxygen and higher amounts of carbon compared to the raw biomass that is favorable for fuel applications. Moreover, EOP bio-oil is more acidic (pH=3.45) and its HHV (27.45 Mj.kg^{-1}) is higher than that bio-oils from other pyrolysis processes but significantly different from those of petroleum-derived diesel.
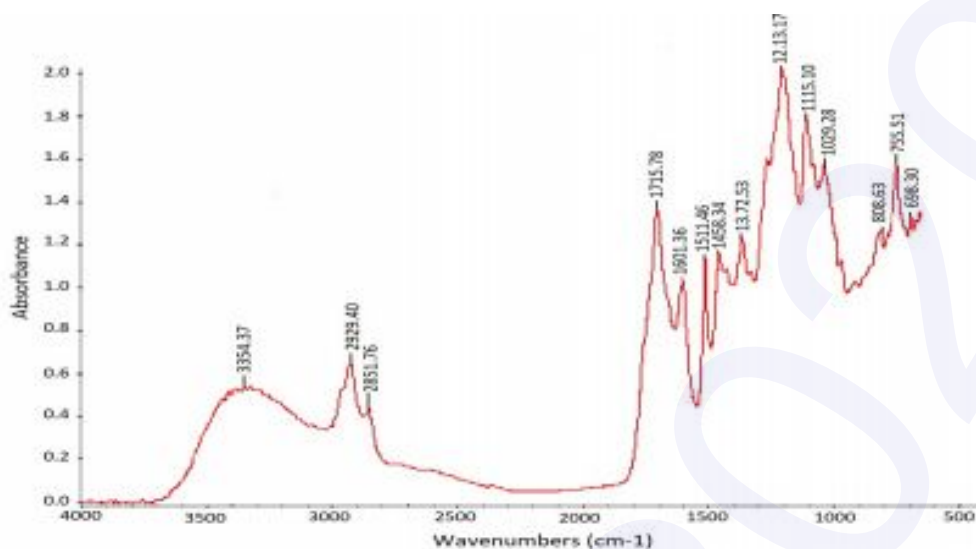
Table 2. Properties of EOP bio-oil product.

Analysis	Sample	EOP bio-oil
Ultimate analysis* (%)	C	65.09
	H	7.39
	N	1.33
	S	0.00
	O**	25.99
	H/C	1.36
	O/C	0.3
Molar formula		$CH_{1.36}O_{0.3}N_{0.01}$
Moisture (%)		3.73
Ash (%)		0.29
Higher heating value (HHV. MJ kg^{-1})		27.45
Density (g.cm^{-3})		1.17
pH		3.45

* Dry basic. ** By difference.

The FTIR spectroscopy analysis of the EOP bio-oil sample is a very useful experimental technique that can be used to show how various bonds from the raw sample are redistributed to the bio-oil products during pyrolysis. Figure 1 shows that the FTIR spectrum displays many adsorption peaks, which indicate in turn the complex nature of the examined material. Because bio-oil is a complex mixture of many organic compounds, the interpretations of the FTIR spectrum was based on data presented in the literature [11]. The EOP bio-oil presents a heterogeneous surface with different functional groups (carboxylic acid, ketone carbonyl, phenol, esters, aliphatic and aromatics hydrocarbons and etc.) available to metal absorption and would be also an excellent source of bio-chemicals if it is extracted.

The ^{13}C NMR spectrum of pyrolytic bio-oil produced from fast pyrolysis is illustrated in Figure 2. The intense peak at 77.23 ppm present in the spectrum corresponded to the solvent. ^{13}C-NMR spectrum shows that EOP bio-oil seems to be rich in long and short aliphatic chains (0 and 54 ppm), and methoxyl-phenols (54-70 ppm), the esters and carboxylic (163-180 ppm), unsaturated fatty acid (121-140 ppm), aromatic carbon (115-158 ppm) and ketones and aldehydes carbons groups (180-220 ppm). This result confirms the FTIR analysis. The presence of long aliphatic chains accounts for the energy content of the bio-oil which is expected to be used as fuel.

To confirm the FTIR and ^{13}C-NMR results of EOP bio-oil and to estimate the thermal decomposition of EOP material and the interaction of their compounds during pyrolysis, GC-MS analysis was developed. The GC MS result shows different types of compounds such as alkanes, alkenes, aromatics, phenols, saturated and unsaturated fatty acids and their derivatives esters are identified. It can be seen that the bio-oil is a very complex mixture of organic compounds of 3-19 carbons. These results confirm those of ^{13}C NMR and FTIR analysis.

The Second Edition of the International Congress of Applied chemistry and Environment
30th-31th October and 01st November 2020, Tunisia

ICACE 2020

Figure 1: FTIR spectrum of EOP bio-oil.

The major compounds of bio-oil obtained from EOP fast pyrolysis is phenol, 2-methoxy-4-(1-propenyl)- and n-Hexadecanoic acid.
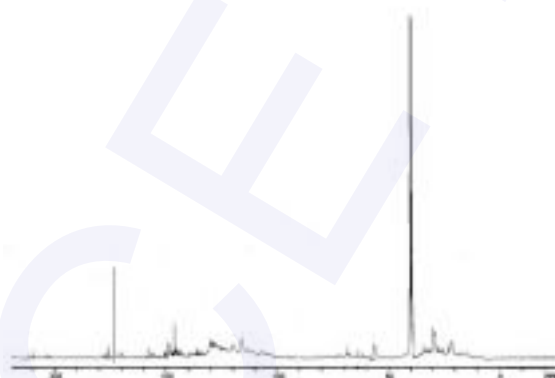

Figure 2: ^{13}C-NMR spectrum of EOP bio-oil.

4. CONCLUSION

An experimental investigation of EOP fast pyrolysis was carried out in a fluidized bed reactor under nitrogen atmosphere. The analysis of the energetic content of EOP bio-oil revealed a relatively high calorific value (27.45 MJ.kg^{-1}). The obtained bio-oil has been also characterized by FTIR, ^{13}CNMR and GC-MS techniques to identify its chemical composition. The bio-oil is showed to be a complex mixture of various components (aliphatic and aromatic hydrocarbons). The presence of Phenol 2-methoxy-4-(1-propenyl) and n Hexadecanoic acid (palmitic acid) in EOP bio-oil as a dominant group suggest their extraction from bio-oil and their separation to be fully utilized in chemical industrial applications.

Moreover, the obtained bio-oil can be utilized as synthetic fuel after upgrading. Likewise, thanks to its high content of phenol, EOP can be also used as resource of high-value chemicals and synthetic polymers.

REFERENCES

[1] Petrov N., Budinova T., Razvigorova M., Parra J., Galiatsatou P., Conversion of olive wastes to volatiles and carbon adsorbents, Biomass and Bioenergy,2008, Vol.32, 1303-1310. [2] Serrano, A, Fermoso Fernando G., et al., Performance evaluation of mesophilic semi-continuous anaerobic digestion of high-temperature thermally pre-treated olive mill solid waste, Waste

Management,2019, Vol.87, 250-257.

[3] Lammi, S., Barakat A., Mayer-Laigle C., et al., Dry fractionation of olive pomace as a sustainable process to produce fillers for biocomposites, Powder Technology, 2018, Vol.326, 44-53. [4] Sert, M., Selvi Gökkaya D., Cengiz N., et al., Hydrogen production from olive-pomace by catalytic hydrothermal gasification, Journal of the Taiwan Institute of Chemical Engineers, 2018, Vol.83, 90-98. [5] Rajaeifar, M.A., Akram A., Ghobadian B., et al., al., Environmental impact assessment of olive pomace oil biodiesel production and consumption: a comparative life cycle assessment, Energy, 2016, Vol.106, 87- 102.

[6] Ghouma, I., Jeguirim M., Guizani Ch., et al., Pyrolysis of olive pomace: degradation kinetics, gaseous analysis and char characterization. Waste and biomass valorization, 2017, Vol.8, No5, 1689-1697. [7] Martín-Lara, M., Pérez A., et al., The role of temperature on slow pyrolysis of olive cake for the production of solid fuels and adsorbents. Process Safety and Environmental Protection, 2019, Vol.121, 209- 220.

[8] Elleuch A, Halouani K, Li Y., Investigation of chemical and electrochemical reactions mechanisms in a direct carbon fuel cell using olive wood charcoal as sustainable fuel, Journal of Power Sources, 2015, Vol.281,350-361.

[9] Baccara R., Bouzida J., Fekib M., Montiel A., Preparation of activated carbon from Tunisian olive-waste cakes and its application for adsorption of heavy metal ions, Journal of Hazardous Materials, 2009, Vol.162, 1522-1529

[10] García G.B., Calero De Hoces M., Martínez García C., et al., Characterization and modeling of pyrolysis of the wo-phase olive mill solid waste, Fuel Process Technology, 2014, Vol.126,104-111.

[11] J. Coates. Interpretation of Infrared Spectra, A Practical Approach. Encyclopedia of Analytical Chemistry, R. A. Meyers, Chichester, John Wiley & Sons Ltd: 2000, 10815-10837.

Acoustic and thermal behavior of environmental-friendly composite panels made of various textile wastes and epoxy resin

Wafa Baccouch[a], Adel Ghith[b], Ipek Yalcin-Enis[c], Hande Sezgin[c], Xavier Legrand[d] and Fayala Faten[a]

(a) University of Monastir, National School of Engineering of Monastir, Laboratory of Thermal and Energetic Systems Studies, LESTE, 5000, Monastir, Tunisia
(b) University of Monastir, National School of Engineering of Monastir, Textile Materials and Process Research MPTex, 5000, Monastir, Tunisia
(c) Istanbul Technical University, Textile Technologies and Design Faculty, Textile Engineering Department, 34437, Istanbul, Turkey
(d) Lille University, National School of Arts and Textile Industries of Roubaix, Research Laboratory of Textile Materials Engineering, GEMTEX, 59000, Lille, France
E- mail: wafaabaccouch@gmail.com

ABSTRACT

In this study, four types of non-woven mats made of textile wastes were used for the manufacture of composite panels by epoxy resin infusion method. Textile non-woven wastes were afforded by Tunisian textile recycling industries. Acoustic and thermal characterization of both composite materials and their reinforcements were studied using an impedance tube, DSC and TGA analyzers. Results indicated that these environmental-friendly panels can be used to reduce the noise emission. Also, the thermal characterization showed that composites follow the same behavior of epoxy resin.

KEYWORDS: Textile waste, composite materials, environmental-friendly, epoxy resin.

1. INTRODUCTION

The textile industry is considered as the second most polluting sector in the world, accounting for 10% of the total world's carbon emissions [1]. According to the fiber year statistics of 2019, the world fiber market raised up from 74 million tons in 2005 to 106 million tons in 2018 [2]. Recycling reduces the need to landfill space, pollution and water and energy consumptions [3]. Moreover, it reduces the carbon footprint in the life cycle of textile products while the major effect of these gases is global warming [4]. For example, reusing 1 Kg of a textile product instead of producing a new one saves 6000 L of water, 3.6 Kg of carbon dioxide, 0.3 Kg of chemical fertilizer, and 0.2 Kg of insecticides [3].
The aim of this work is the valorization of different textile wastes and the production of new environmental-friendly materials with specific characteristics. For this purpose, four textile wastes offered by textile recycling companies in Tunisia were used as reinforcements to produce composite panels while epoxy resin was used as the matrix. Physical, acoustical and thermal properties of the reinforcements and their composites are explored and discussed to define their potential applications.

2. MATERIAL AND METHODS

2.1. Materials and chemicals

Four types of textile wastes supplied by textile recycling companies from Tunisia are used as reinforcement materials. The first two groups are supplied as shredded fibers and transformed into nonwovens by carding and needle-punching process. The two other groups are supplied as nonwoven form (carding, overlapping and needle-punching process) All nonwoven wastes are shown in Figure 1.

Figure 1: Reinforcement materials:(a. cotton, b. cotton/polyester, c. polyester, d. acrylic)

Epoxy resin (Sicomin, SR 8200) and its hardener (Sicomin, SD 7203) are used as a matrix material.

2.2. Composite panels manufacturing

Composite panels are manufactured using vacuum infusion method. This method uses the vacuum force to remove air from the reinforcing material and to allow the resin to infiltrate the preform. The whole process is performed at room temperature (20°C± 2°C) under 1 bar pressure and the formed panels are left for 24 h for curing. The composite materials are presented in Figure 2.
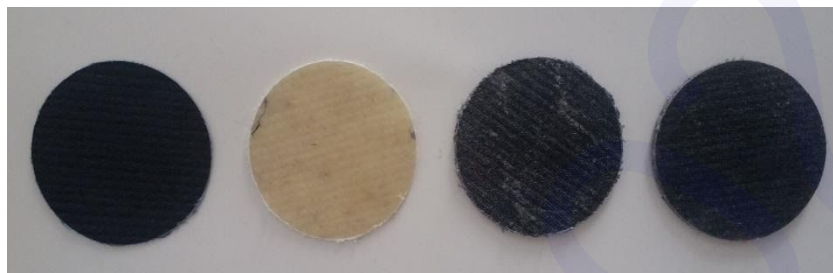

Figure 2: Composite materials reinforced by:(a. cotton, b. cotton/polyester, c. polyester, d. acrylic)

2.3. Physical analysis

The thicknesses of nonwoven fabrics are measured by the thickness gauge apparatus (James H. Heal) Wile the thicknesses of the composite panels are measured using a micrometer as indicated in ISO 527-1. The areal densities are calculated by weighting reinforcements and composite materials.

2.4. Sound absorption

The sound absorption coefficients of the manufactured non-woven and composite samples were measured using a medium type impedance tube according to ASTM E 1050-98 standard method by the mean of TestSens analyzing systems developed by BIAS. The normal incident sound absorption coefficients (α) were measured by an impedance tube for the frequency range 100 - 4000 Hz.

2.5. Thermal evaluation

TGA analyzer (Mettler Toledo) was used for the thermogravimetric analysis. The thermal stability of both reinforcement materials and composite panels were investigated by heating the samples from 30°C to 700°C with a heating rate of 10 °C/min, in a nitrogen atmosphere. The thermal behavior of reinforcement materials and composites were also analyzed by differential scanning calorimeter (Mettler Toledo). The measurements were conducted by heating the samples from 25°C to 300°C with a heating rate of 20 °C/min in a nitrogen atmosphere.

3. RESULTS AND DISCUSSIONS

3.1. Physical analysis

The technical information of reinforcement wastes and their composites are listed in Table 1.

Table 1: Technical features of reinforcements and composite materials

Materials code	Fibre content	Thickness (mm)	Areal density (g/m^2)
C	Cotton (100%)	1,7 ± 0,05	140 ± 5,4
C/P	Cotton/Polyester (60/40%)	3,0 ± 0,06	252 ± 18
P	Polyester (90%)	9,6 ± 0,07	914 ± 40
A	Acrylic (80%)	8,4 ± 0,07	800 ± 35
C-C	Cotton (100%)	0,72 ± 0,02	665 ± 21
C/P-C	Cotton/Polyester (60/40%)	1,40 ± 0,04	1300 ± 8,4
P-C	Polyester (90%)	4,00 ± 0,12	3808 ± 45
A-C	Acrylic (80%)	4,00 ± 0,1	3687 ± 40

3.2. Sound absorption

Sound absorption tests results are presented in Figure 3. Reinforcements test results show that the sound absorption coefficient generally increases with the increase of frequency. The nonwovens P and A have the best sound absorption property especially at frequencies above 1500 Hz, and they have an average sound absorption coefficient of 0.96 and 0.72 respectively between the range of 2000-4000 Hz.

The nonwoven C/P and C reach their highest absorption coefficients by around 0.45 and 0.2, respectively at 4000 Hz.

Sound tests for composite materials presented in Figure 3.b are in accordance with nonwoven test results, the composite P-C and A-C show the best sound absorption coefficients while the composite C-C shows the lowest values. The composites A-C and P-C reach a maximum of 0.65 and 0.5 respectively at 3650 Hz while composite C/P-C and C-C present an average sound absorption coefficient of 0.2 and 0.11 between the range of 3000-4000 Hz, respectively. The sound absorption coefficient all composites decreased compared to their reinforcements. In fact, the low acoustic performances are due to the elimination of the air space between fibers structure causing a change in the structure after the injection of the resin inside the structure [5, 6].
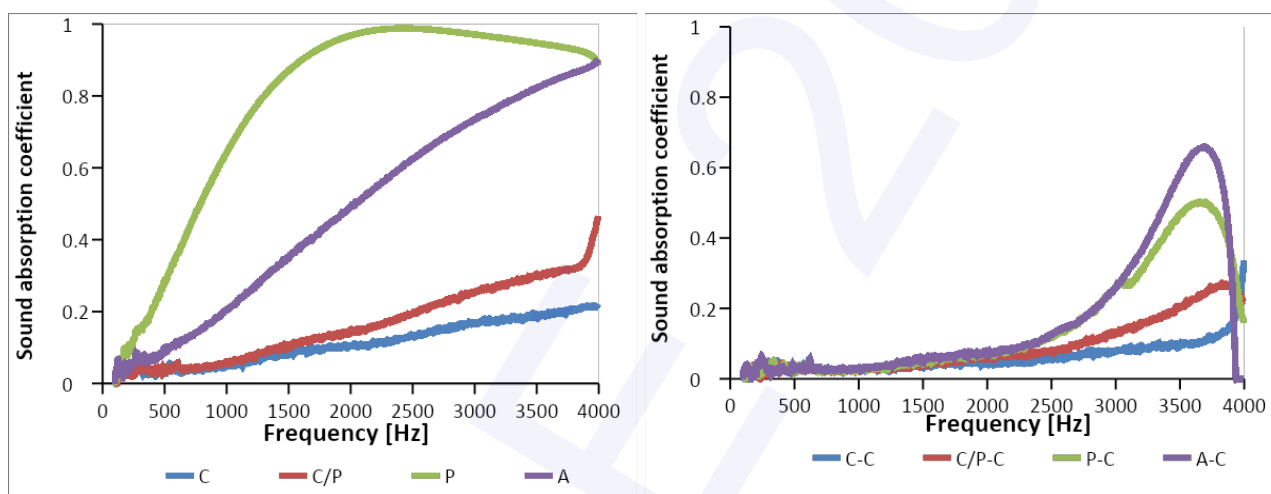

Figure 3: Sound absorption coefficient as a function of the sound frequency for a. reinforcements b. composite panels

3.3. Thermal evaluation

The thermal behavior of reinforcments and their composites are presented in Figures 4 and 5. The glass transition temperature (T_g = 80°C) and the melting temperature (T_m = 250°C) of polyester are determined from the peaks of the DSC curves of P and C/P samples. In the literature, the T_g of the polyester is 80-90°C and the T_m of the polyester is around 260°C [7]. An endothermic peak centered at around 85°C can be observed for the specimen C. This peak can be associated to the removal of adsorbed moisture from the cotton fibers. The degradation peak of cotton fibers can not be seen because they degrade above 300°C.

The sharp exotberm at about 300°C is noticed for A sample, this peak is characteristic of acrylics and may be used to differentiate them from other fibres [8]. The DSC curves of P-C and C/P-C specimens show the T_m value of the polyester at about 260°C. The T_g of epoxy resin at around 55°C, can be seen from the DSC curves of all composite samples.

The TGA curves of nonwoven fabrics show that all fabrics have an important weight loss at temperatures above 300°C. According to the literature, polyester decomposition occurs between 350°C and 450°C under nitrogen atmosphere [9]. The studied polyester waste shows two decomposition points at 365°C and 460°C. The TGA curve of C/P nonwoven fabric also shows the same characteristic with polyester fabric due to its 60% polyester content. A major weight loss of cotton fiber is visible at about 315°C, which is the degradation temperature of α-cellulose [10]. Composite panels degradation curves show that all composites decompose in one step starting with an initial temperature of 300°C and ends at approximately 500°C. This shows that composites follow the thermal behavior of the resin. In fact, the TGA curve of epoxy resin shows one step of decomposition that starts with an initial temperature of 300°C and ends with a temperature of 470°C with a final weight loss of 87%.
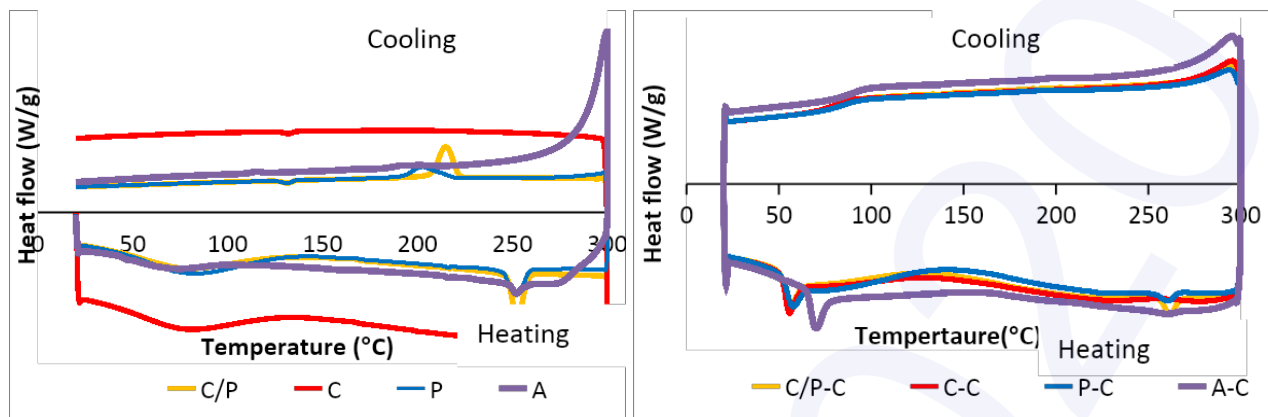
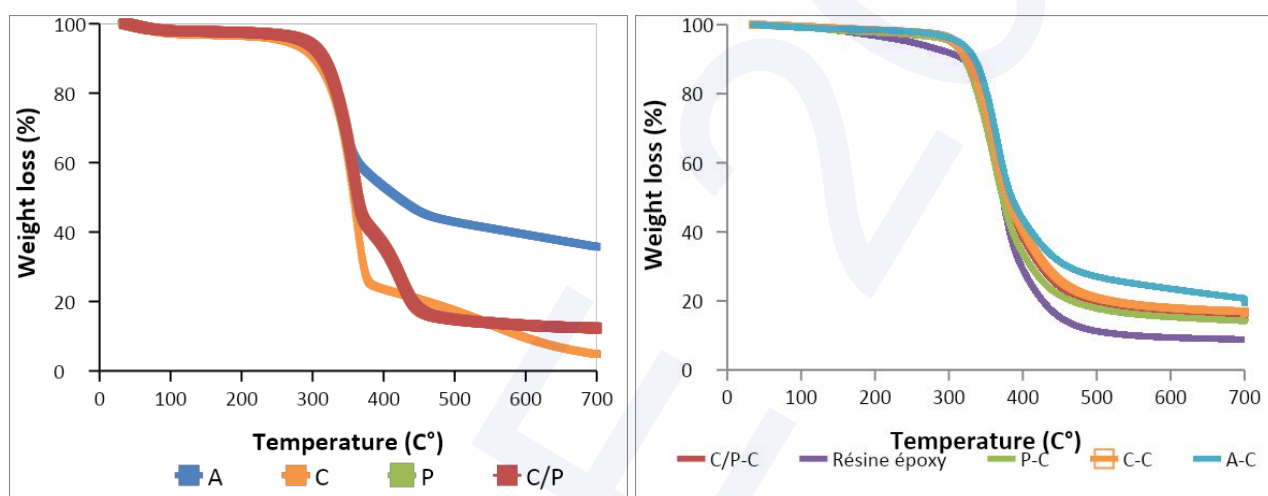Figure 4: DSC analysis for a. nonwoven fabrics b. composite materials

Figure 5: TGA analysis for a. nonwoven fabrics b. composite materials

4. CONCLUSION

In this work, cotton, polyester, cotton/polyester and acrylic nonwoven wastes were used as einforcements to develop environmental-friendly composite panels by a vacuum infusion process and epoxy resin as matrix. Acoustical and thermal tests were performed to both reinforcements and composite materials. Sound absorption tests show that the manufactured nonwovens present promising acoustic performances, however composites showed lower sound absorption coefficients compared to their reinforcements, In fact the addition of the resin to the structure reduces the voids within the structure which results in lower sound absorption performances. Thermal characterization results show that although the nonwoven fabrics present the raw material characteristics, the composite materials follow the thermal behavior of epoxy resin.

REFERENCES

[1] **Echeverria CA, Handoko W, Pahlevani F**, Cascading use of textile waste for the advancement of fibre reinforced composites for building applications, *Journal of Cleaner Production,* 2019, Vol.208, 1524 -1536.

[2] The fiber year Consulting, https://www.thefiberyear.com (accessed 28 September 2018).

[3] Bureau of International Recycling, http://www.bir.org/industry/textiles (accessed 28 September 2018).

[4] **Lou CW, Lin JH, Su KH**, Recycling Polyester and Polypropylene Nonwoven Selvages to Produce Functional Sound Absorption Composite, *Textile Research Journal,* 2005, Vol.75, 390-394.

[5] **Yang WD and Li Y,** Sound absorption performance of natural fibers and their composites, *Science China Technological Sciences,* 2012, Vol.55, 2278-2283.

[6] **Rwawiire S, Tomkova B, Gliscinska E et al.** Investigation of sound absorption properties of bark cloth nonwoven fabric and composites, *Autex Research Journal,* 2015, Vol.15, 173-180.

[7] **Demirel B, Yaras A and Elcicek H,** Crystallization Behavior of PET Materials. *BAU Fen Bilimleri Enstitusu Dergisi,* 2011, Vol.13, 26-35.

[8] **Dunn, P,Ennis, B. C.** Thermal analysis of polyacrylonitrile: Identification of acrylic fibres by differential thermal analysis, *Thermochimica Acta,* 1971, Vol.3, 81-87.

[9] **Papageorgiou GZ, Tsanaktsis V and Bikiaris DN,** Synthesis of poly(ethylene furandicarboxylate) polyester using monomers derived from renewable resources: thermal behavior comparison with PET and PEN, *Physical Chemistry Chemical Physics,* 2014, Vol.16, 7946-7958.

[10] **Shahedifar V and Rezadoust AM.** Thermal and mechanical behavior of cotton/vinyl ester composites: Effects of some flame retardants and fiber treatment. *Journal of Reinforced Plastics and Composites,* 2013, Vol.32, 681-688.

The Second Edition of the International Congress of Applied chemistry and Environment
30th-31th October and 01st November 2020, Tunisia

ICACE 2020

Removal of thiophene by different adsorbents from hot gas

Hiba Aouled Mhemed[a,b,c], Sana Kordoghli[b], Mylène Marin Gallego[a] , Jean-François Largeau[a,d], Fethi Zagrouba[b],

Mohand Tazerout[a]

(a)   GEPEA- CNRS UMR 6144, IMT Atlantique, Nantes, 44000. France
(b)   Research Laboratory for Sciences and Technologies of Environment, High Institute of Sciences and Technologies of
Environment LR16ES09, Borj Cedria, Carthage University, Tunisia
(c)   National School of Engineers of Gabes, University of Gabes, 6026 Gabes, Tunisia
(d)   Icam, 35 rue du Champ de Manœuvres, 44430 Carquefou, France
aouled_mhemed.hiba@hotmail.com

ABSTRACT

The pyrolysis of the used tires is a potentially highly efficient process for energy generation. However, the appropriate cleaning of the pyrolysis oil is a major issue, in particular for sulfur removal.

This study investigates the adsorption capacity of three adsorbents towards sulfur in hot gas. Experimental tests were carried out with thiophene as the reference sulfur compound. The selected adsorbents (char derived from spent coffee grounds, char derived from date seeds and commercial activated carbon) were tested under different temperatures and constant inlet thiophene concentration. The procedure allows evaluating the contributions of adsorption and cracking phenomena on the overall thiophene removal efficiency.

The activated carbon exhibited the highest adsorption capacity, with up to 0.66 mg/g at 700 °C.

KEYWORDS: Thiophene, waste-to-energy, hot gas, adsorption

1. INTRODUCTION

Tires have become an indispensable part of our transportation system. As a result, an increase in used tires is observed worldwide. Today, 17 million tons of used tires are produced each year in the world [1]. In order to reduce the harmful environmental impact of this waste, many works have been conducted to recover its remaining energy.

In this context, various thermochemical processes such as gasification, combustion and pyrolysis have been exanimated [2]. In this respect, the pyrolysis of the used tires has recently attracted interest. Pyrolysis is a thermochemical conversion process under inert atmosphere and high temperature. This process generates three products: a non-condensable fraction (gas), a fuel oil (liquid), and finally a carbon powder, often called a char. The obtained products could be easily handled, stored and transported, which increases the applicability of this method.

However, the presence of sulfur compounds in the by-products represent the major disadvantage of this process. The existence of sulfur compounds is explained by its presence in the vulcanization reactions during the tire production process [3]. Thiophene, benzothiophene and dibenzothiophene are the predominant sulfur compounds in the pyrolysis oil [4].

Several works have focused on the study of sulfur compounds elimination methods. Among the proposed alternatives to reduce sulfur levels, adsorptive desulfurization is considered as an attractive process.

Given the complexity of the pyrolysis oils-derived from wastes tires, we have thought to perform the adsorptive desulfurization on a synthetic liquid. This synthetic mixture aims to carry out parametric studies of the desulfurization and to identify the phenomena of competition during the adsorption.

The aim of this work was to study the dynamic adsorptive desulfurization and the cracking of thiophene in hot gas. The influence of the adsorption temperature for the removal of thiophene was examined. The adsorption performance of the produced chars, derived from agricultural wastes, as well as the commercial activated carbon was evaluated.

2. MATERIAL AND METHODS

The sulfur concentration in the model fuel was 500 ppm prepared by dissolving 37.8 g of DBT in 1 L of toluene.

The adsorbents used in this work were:
- Char derived from spent coffee grounds (SCG-C);
- Char derived from date seeds (DS-C);
- Commercial activated carbon (AC).

A pellet mill (developed in the lab) was used to obtained pellets from the spent coffee grounds. Several machine parameters were tested and optimized (water, rotation speed of the mil, material flow rate at the inlet) in order to produce pellet with high strength. Pellets of the SCG were obtained with a diameter of 6 mm and a length between 15 mm and 20 mm. The pellets were dried in an oven at 105 °C.

Date seeds (DS) were collected from Tunisia. They were crushed and washed with distilled water to remove all dirt and then oven-dried overnight at 105 °C.

 SCG-C and DS-C were obtained by pyrolysis of SCG and DS respectively in a batch reactor under an inert atmosphere, at heating rate of 5 °C.min^{-1} and a final temperature of 750 °C. Temperature was kept constant for 120 min.

Ultimate analysis of the produced char was performed with a FLASH EA 1112 Series CHNS-O analyzer.

For the adsorptive desulfurization experiments dynamic tests were performed in a cracker (developed in the lab). The Cracker consists in a tube equipped with a fine grid constituting the reactor. This reactor can be heated up to 800 °C. The gas passing through the reactor is regulated in a flow rate and can be preheated to 200 °C. A syringe pump is used to inject the solvent. The concentration of thiophene as well as toluene was measured by using a gas chromatography.

3. RESULTS AND DISCUSSIONS

3.1. Characterization of the used adsorbents

The ultimate analysis (see Table 1) shows that SCG-C and DS-C are highly carbonaceous, with a carbon content of 83.53 % and 87.12 % respectively. The high carbon content of biochar is advantageous in terms of maximizing the amount of carbon storage and could be used as an energy resource or for soil adsorption of pollutants [5]. The carbon content of biochar increased tremendously with concomitant decrease in H and O contents after carbonization. This is associated with release of volatiles in the material.

Table 1: Ultimate analysis of the different used adsorbents

	% N	% C	% H	% O	% S
SCG-C	2.86	83.53	1.75	11.86	<LD
DS-C	1.61	87.12	1.50	9.77	<LD
AC	0.27	81.41	0.75	17.57	<LD

3.2. Dynamic adsorption

The inlet concentration of adsorption column was adjusted to a constant value, and the outlet concentration was measured at a determined time interval. When the outlet concentration was equal or close to the inlet concentration, the adsorbent was considered to be saturated. The adsorption capacity was calculated as follow [6]:

$$ \tag{1} $$

Where q_m is the adsorption capacity (mg.g^{-1}); F is the total flowrate of the mixed gas (m^3.min^{-1}); C_0 and C_i are the inlet and outlet concentrations of thiophene or toluene (mg.m^{-3}), respectively; m is the mass of adsorbents (g); t is the adsorption equilibrium time (min).

3.3. Effect of adsorption temperature on thiophene removal

The experimental tests were carried out with a nitrogen flow rate of 0.2 Nm^3/h, tar concentration of 12 g/Nm^3 and 500 ppm of thiophene. The tested temperatures are 500 °C and 700 °C. All data reported in Figure 1 refer to tests of 1h at steady state condition.

According to Figure 1 (a), the char derived from spent coffee grounds is the most effective adsorbent for both toluene and thiophene adsorption at 500 °C. Under these conditions, adsorption with SCG-C reached 5.16 mg/g and 0.42 mg/g for toluene and thiophene respectively.

By increasing the temperature up to 700 °C, the adsorption of toluene by the SCG-C remained intact while the adsorption of thiophene decreased and reached 0.24 mg/g. However, the activity of the commercial activated carbon was positively influenced with the rise of the temperature (see Figure 1 (b)). Thus, the adsorption capacity reached 17 mg/g and 0.66 mg/g for toluene and thiophene respectively.

The lowest adsorption capacity for thiophene, in both temperatures, was obtained with the char derived from date seed (DS-C).

All GC analyses of the effluent gas, measured downstream of the fixed bed of the different used adsorbents detected the presence of hydrogen at 700 °C which can be explained by the tar (toluene) cracking reaction. This dependence on temperature was expected consequence of the endothermic nature of cracking reaction [7].
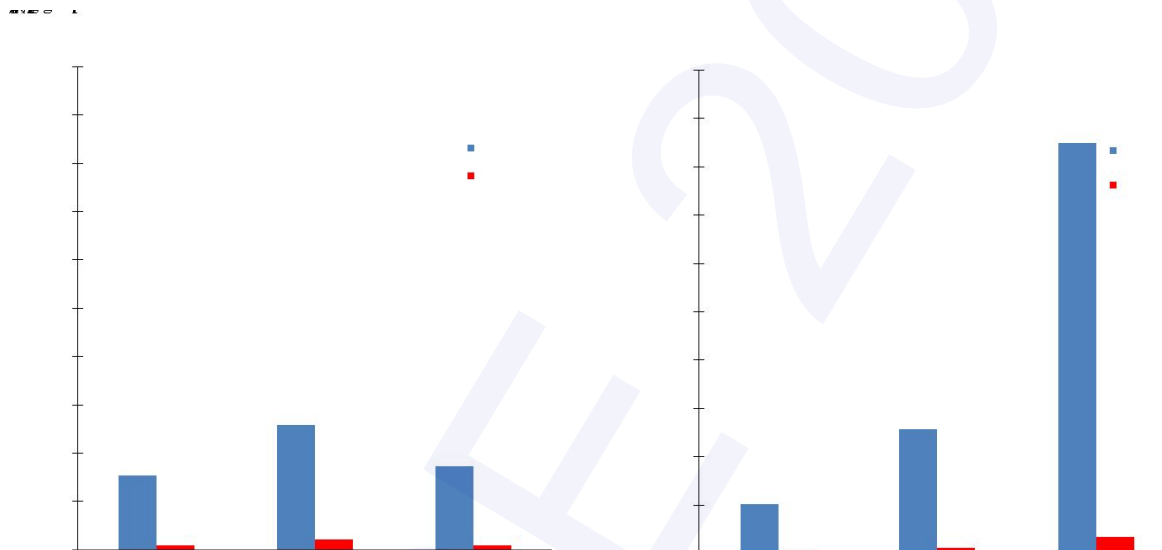

Figure 1: Adsorption capacity under 1h tests at different temperatures

4. CONCLUSION

At the current level of knowledge, the proposed hot gas adsorption system seems to be characterized by more strengths than weaknesses, which makes it an interesting approach to clean the gases resulting from the pyrolysis of wastes tires.

Char derived from spent coffee grounds is the most efficient adsorbent for thiophene removal at 500 °C. However, AC is more effective for thiophene adsorption and toluene cracking at 700 °C. Practical application of these adsorbents for thiophene adsorption might be hindered by competitive adsorption process between thiophene and toluene. For this, additional treatment of these adsorbents is necessary in order to improve their selectivity towards thiophene.

REFERENCES

[1] **Y. Zhang, C. Wu, M. A. Nahil, et P. Williams**, Pyrolysis–Catalytic Reforming/Gasification of Waste Tires for Production of Carbon Nanotubes and Hydrogen, *Energy Fuels*, 2015, Vol. 29, No. 5, 3328-3334.

[2] **I. Y. Mohammed, Y. A. Abakr, F. K. Kazi, S. Yusup, I. Alshareef, et S. A. Chin**, Comprehensive Characterization of Napier Grass as a Feedstock for Thermochemical Conversion, *Energies*, 2015, Vol. 8, No. 5, 3403-3417.

[3] **A.-M. Al-Lal, D. Bolonio, A. Llamas, M. Lapuerta, et L. Canoira**, Desulfurization of pyrolysis fuels obtained from waste: Lube oils, tires and plastics, *Fuel*, 2015, Vol. 150, 208-216.

[4] **T.-C. Chen, Y.-H. Shen, W.-J. Lee, C.-C. Lin, et M.-W. Wan**, The study of ultrasound-assisted oxidative desulfurization process applied to the utilization of pyrolysis oil from waste tires, *J. Clean. Prod.*, 2010, Vol.18, No. 18, 1850–1858.

[5] **L. E. Hernandez-Mena, A. A. Pécoraa, et A. L. Beraldob**, Slow pyrolysis of bamboo biomass: Analysis of biochar properties, *Chem. Eng.*, 2014, Vol. 37, 2283-9216.

[6] **J. Zhu, Y. Li, L. Xu, et Z. Liu**, Removal of toluene from waste gas by adsorption-desorption process using corncob-based activated carbons as adsorbents, *Ecotoxicol. Environ. Saf*, 2018, Vol. 65, 115-125.

[7] **F. Di Gregorio, F. Parrillo, E. Salzano, F. Cammarota, et U. Arena**, Removal of naphthalene by activated carbons from hot gas, *Chem. Eng. J.*, 2016, Vol. 291, 244-253.

Recycling irons waste as abrasive grains

Elaissi Arwa[a], Jabli Mahjoub[b], Alibi Hamza[c], Gith Adel[a]

(a) Textile Materials and Processes Research Unit MPTex, National Engineering School of Monastir, University of Monastir, Tunisia
(b) Department of Chemistry, College of Science Al-zulfi, Majmaah University, Al-Majmaah, 11952, Saudi Arabia.
(c) Laboratory of Study of the Thermal and Energy Systems, National School of Engineering (ENIM), University of Monastir, Tunisia.

E-mail: elaissiarwa@gmail.com

ABSTRACT

This work provides insight into the use of iron scrap as abrasive grains. The grains were characterized using FT-IR spectroscopy and SEM morphology. After abrasives manufacturing, the effect of the grains has tested by studying their effects on the abrasion test on the Martindale machine. The results showed that the composite made with irons scarp has a longer cycle of life compared to commercial abrasive.

KEYWORDS: iron, waste, abrasives, grains.

1. INTRODUCTION

Industrial waste is the waste produced by industrial activity which includes any material that is rendered useless during a manufacturing process [1]. Iron is a common, silver-colored, metal element that is magnetic and strong, is used in making steel. An abrasive is composed of a substrate as reinforcement and abrasive grains bonded together by a binder or an adhesive [2].

This research consists of developing new types of abrasives with new characteristics not available on the market, with the aim of exploiting industrial waste such as iron grains to minimize the cost price of this product.

2. MATERIAL AND METHODS

The preparation of iron is done in 3 main steps:

- Reaming of iron waste
- Grinding of this waste
- Filter the crushed quantity

The manufacturing process for abrasives is as follows:

The binder is dosed and applied by a spray gun on the support. Then, the grains are injected by the sieving process. Finally, the test pieces were dried according to the polymerization temperature.

All reagents and resins were purchased from chimitex plus Company (Chimitex plus Sarl, Sidi Abdelhamid, Monastir, Tunisie) and used without further purification.

- ● **Samples characterization**

FT-IR characterization
FT-IR spectrum was studied on composites manufactured and were recorded using a PerkinElmer FT-IR spectrometer (Tunisia). Indeed, this study makes it possible to determine the functions present in the chemical structure of the materials.

MEB characterization
The morphological characteristics of the products before and after modification were analyzed using SEM devices (FEI Ø250 Thermo-fisher, Tunisia). Samples were previously coated with gold using a vacuum sputter-coater in order to improve their conductivity and the quality of the SEM images. The acceleration voltage was 15 kV. The tests were performed with higher magnifications (× 100, × 500 and × 10000).

Granulometric assays for iron grains

According to ISO 3310-1, particle size analysis consists of determining the correspondence of the different particle size classes [3], [4]. In this study, the sieve method is applied. Indeed, a portion of 500 g of samples is dried and separated by serial vibration of superimposed sieves. Then the remaining material of each sieve is weighed to calculate the percentage of the materials of each particle size [5],[6].

3. RESULTS AND DISCUSSIONS

3.1. Granulometric test of iron grains

Figure 2 shows the cumulative particle size distribution, for each tested sample [7],[8]. The grain size distribution shows that most grains are 0.2 mm.
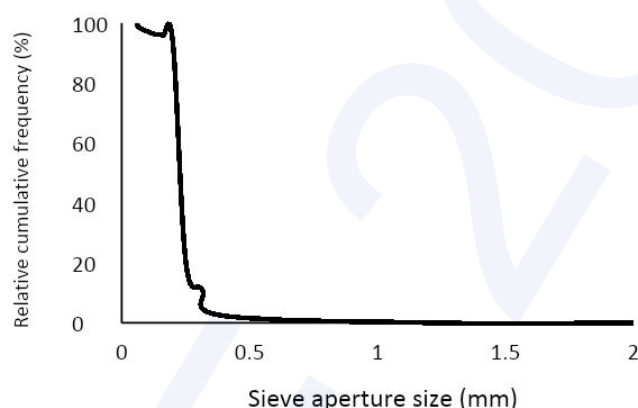
Figure 1: The particle size distribution of irons particles

3.2. FT-IR characterization

Figure 2 showed that the fibers contained broadband around 3344 cm^{-1} correspondings to the OH stretching mode [9], [10]. The Fe-O stretching may be noticed in the region 900-300 cm^{-1} [11]. The study of H.Namdouri and all [12] proves that Goethite (α- FeOOH) can consider at the pic of 1124 cm^{-1} [13]. The C=O stretch of the carboxylic acid in hemicellulose is observed at 1735 cm^{-1} [14]. Stretching groups of methyl and methylene were observed at 2920 and 2854 cm^{-1} respectively [15], [16]. The 1121 cm^{-1} band is attributed to C-O stretching.

Figure 2: FT-IR spectrum of abrasives mad using Politex resin and iron grains

3.3. MEB analysis

The apparent volume fraction and apparent void content were estimated by analyzing cross-sectional SEM images. A schematic representation of a composite made by gluing the support with iron scrap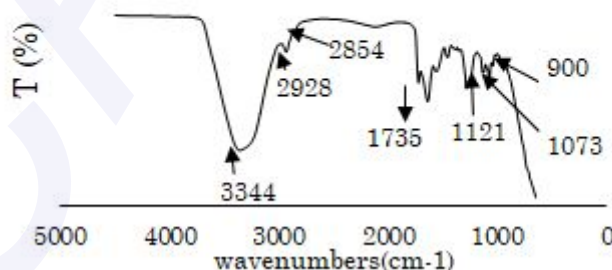 is shown in figure 3. The SEM images confirmed that the resin is distributed over the entire surface and the grains are arranged on the surface in a heterogeneous way.

Figure 4 shows the distribution of the cross-sectional area for the composite. In fact, the manufactured abrasive consists of two layers, a layer of textile support and a layer of grains bonded together by resin. SEM evaluation of the sectioned specimens revealed an adhesive resin film thickness [17]. It can be seen that the amorphous irons particles are spherical and monodisperse.
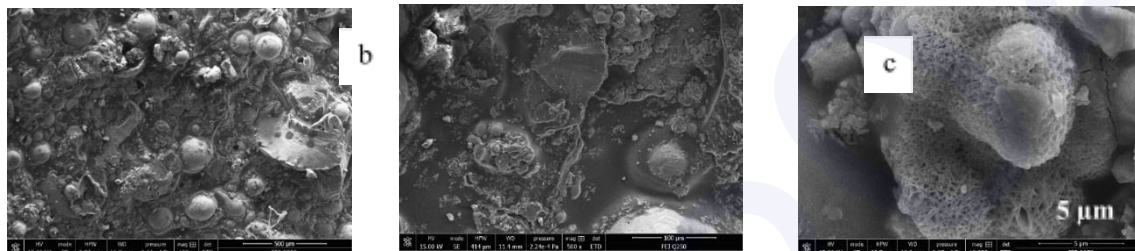

Figure 3: Abrasives manufactured with iron grains: SEM images under different magnifications (a) 100× (b) 500× and (c) 10000×
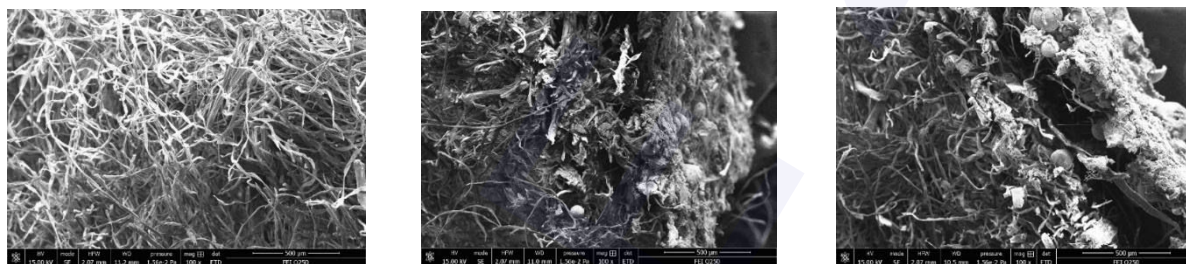
Figure 4: Side view of abrasive manufactured with iron grains 100× (a) a layer of nonwoven, (b) a layer of resin and (c) the assembly of two layers by resin

3.4. Influence of experimental conditions on the abrasion assays

In this study, we report an experimental study of the determination of the lifetime of the various composites. It involves the determination and comparison of the abrasion resistance of our abrasives by the mass loss method before and after abrasion cycles using the Martindale machine according to the ISO 12947-3 standard test method [18]. These values were then expressed as a percentage of the initial mass [19].

Table 1: The percentage of mass loss of composites and denim

Samples	Abrasive mass loss (%)	Denim mass loss (%)
Composite	59,41	42,71;10,51;13,85
abrasive paper 80	3,33	4,53
abrasive paper180	7,69	34,65
abrasive paper400	11,11	31,68

It can be seen that the application of our composites causes enormous weight losses compared to ordinary abrasive paper but the abrasion effect is better by applying fewer cycles. In fact, all composites have undergone an abrasion test of 5000 cycles until the deterioration of the denim fabric. For our composite, there are 3 cycles, the first is around 1200 turns until the deterioration of the specimen. We change the denim, the second cycle is about 1310 turns and the third is about 2490 cycles.

4. CONCLUSION

Irons waste was exploited as abrasion grains due to their features. The results of the abrasion test indicate that abrasives made with iron grains cause an imposing effect on denim compared to ordinary abrasives.

REFERENCES

[1] **Nemerow, N.L. and A. Dasgupta**, Industrial and hazardous waste treatment, 1991.

[2] **Atsugi, T, M. Shibata, and T. Koseki**, *Abrasives composition, substrate and process for producing the same, and magnetic recording medium and process for producing the same*, 1999.

[3] **Marková, I., et al.**, Granulometry of selected wood dust species of dust from orbital sanders, *Wood research*, 2016, Vol.61, No.6, 983-992.

[4] **Dubois, S. and F. Lebeau**, *Étude de la distribution granulométrique de particules de chanvre: Méthodes par tamisage et analyse d'image,* 2011.

[5] A**llen, T.**, Particle size measurement, 2013.

[6] **Bartley, P.C., B.E. Jackson, and W.C. Fonteno**, Effect of particle length to width ratio on sieving accuracy and precision, *Powder Technology*, 2019, Vol.355, 349-354.

[7] **Jensen, P.D., M. Temmerman, and S. Westborg**, Internal particle size distribution of biofuel pellets. Fuel, 2011, Vol.90, No.3, 980-986.

[8] **Di Stefano, C., V. Ferro, and S. Mirabile,** Comparison between grain-size analyses using laser diffraction and sedimentation methods, *Biosystems Engineering*, 2010, Vol.106, No.2, 205-215.

[9] **Salmén, L. and E. Bergström,** Cellulose structural arrangement in relation to spectral changes in tensile loading FTIR. Cellulose, 2009, Vol.16, No.6, 975-982.

[10] S**aleh, T.A., et al.,** Polyethylenimine modified activated carbon as novel magnetic adsorbent for the removal of uranium from aqueous solution. Chemical Engineering Research and Design, 2017, Vol.117, 218-227.

[11] **Rouchon, V., et al.**, Raman and FTIR spectroscopy applied to the conservation report of paleontological collections: identification of Raman and FTIR signatures of several iron sulfate species such as ferrinatrite and sideronatrite, *Journal of Raman Spectroscopy*, 2012, Vol.43, No.9, 1265-1274.

[12] **Namduri, H. and S. Nasrazadani,** Quantitative analysis of iron oxides using Fourier transform infrared spectrophotometry, *Corrosion Science*, 2008, Vol.50, No.9, 2493-2497.

[13] S**chwertmann, U. and R.M. Cornell**, Iron oxides in the laboratory: preparation and characterization., *John Wiley & Sons*, 2008.

[14] **Wang, X., et al.**, Characterization of KH-560-Modified Jute Fabric/Epoxy Laminated Composites: Surface Structure, and Thermal and Mechanical Properties, *Polymers (Basel)*, 2019, Vol.11, No.5.

[15] **Poletto, M., A.J. Zattera, and R.M.C. Santana**, Structural differences between wood species: Evidence from chemical composition, FTIR spectroscopy, and thermogravimetric analysis, *Journal of Applied Polymer Science*, 2012, Vol.126, No.S1, E337-E344.

[16] **Saleh, T.A., A. Sarı, and M. Tuzen**, Optimization of parameters with experimental design for the adsorption of mercury using polyethylenimine modified-activated carbon, *Journal of Environmental Chemical Engineering*, 2017, Vol.5, No.1, 1079-1088.

[17] **Patierno, J., et al.**, Push-out strength and SEM evaluation of resin composite bonded to internal cervical dentin, Dental Traumatology, 1996, Vol.12, No.5, 227-236.

[18] **Škoc, M.S. and E. Pezelj,** Abrasion resistance of high performance fabrics, *in Abrasion Resistance of Materials,* 2012, IntechOpen.

[19] **Brzeziński, S., et al.**, Applying the sol-gel method to the deposition of nanocoats on textiles to improve their abrasion resistance, *Journal of Applied Polymer Science*, 2012, Vol.125, No.4, 3058-3067.

Manufacture of a non-woven from natural fibers

Elaissi Arwa[a], Alibi Hamza[b], Jabli Mahjoub[c], Gith Adel[a]

(a) *Textile Materials and Processes Research Unit MPTex, National Engineering School of Monastir, University of Monastir, Tunisia*
(b) *Laboratory of Study of the Thermal and Energy Systems, National School of Engineering (ENIM), University of Monastir, Tunisia.*
(c) *Department of Chemistry, College of Science Al-zulfi, Majmaah University, Al-Majmaah, 11952, Saudi Arabia.*

E-mail: elaissiarwa@gmail.com

ABSTRACT

This work provides an overview of fiber recycling, which accounts for a large part of textile waste. We reported on the synthesis of a new non-woven can be used in several areas such as reinforcement of composites. It prepared from cellulosic fibers waste such as cotton and tow fibers. The effect of the chemical modification of the non-woven and the impact of the percentage of each fiber over the non-woven manufactured were investigated. The studied non-woven was characterized using FT-IR spectroscopy and SEM morphology. The results showed that the non-woven composed with 50% cotton and 50% tow and cationized has better results compared to untreated support.

KEYWORDS: waste, fibers, Non-woven, tow.

1. INTRODUCTION

In order to limit the negative impacts on the environment and to save natural resources, any waste must be treated according to its nature (recycling, recovery, incineration…). Indeed, it is not only a matter of protecting the environment from pollution, but it also results in the manufacture of a product to be used in several areas at a lower cost. Composites made from natural fibers are applied in several fields such as building construction and automotive construction. In many operations such as Polymers from carpet waste by melt processing may be used to make products in the molding process, The recycled polymers may also be used as matrices in glass fiber reinforced composites… [1]

This research consists of developing new types of non-woven with new characteristics not available on the market, with the aim of minimizing the cost price of this product and exploiting industrial waste.

2. MATERIAL AND METHODS

The non-woven is composed of tow and cotton fibers. The tow fibers composed of jute and hemp fibers and applied as plaster reinfusion. Fibers are coming from Sitex Industry.

2.1. Pre-treatment of the fibers

The fibers of tow and cotton can undergo treatments such as desizing, bleaching, cationization, mercerization, and impregnation.

- First, all fibers receive a desizing treatment to remove impurities, they were boiled for 120 minutes (liquor ratio 1:40) in a mixture of 1.5 ml / L NaOH, 3 g / L Na_2CO_3 and 4 g / L non-ionic detergent. After that, fibers were washed with hot water and then with cold water to avoid the degradation of the emulsion and the precipitation of impurities on the surface and then air-dried. Finally, they were washed with distilled water.
- The bleaching process is carried out in a solution containing 87.5 ml / l of NaOCl and 2 g / l of Na_2CO_3 (pH between 9 and 10) for 60 min at room temperature. Subsequently, they were rinsed with cold water. The fibers are then immersed in a solution containing 2 g / L of $NaHSO_3$ and H2SO4 at 30 ° C for 15 min at room temperature, washed with distilled water and air-dried at room temperature [2].
- The cationization of the fibers was studied with a [polyimethyldiallylammonium-diallylamine chloride (PDDACD) copolymer as a reagent, under alkaline conditions [3].
- The impregnation process is as follows:

First, the samples are soaked in a bath of resin solution at room temperature. Then, the samples pass between two cylinders before emerging, which allows treating all the textiles by removing the excess resin and promoting its penetration and diffusion. Finally, the drying is carried out in the drying ream at the appropriate polymerization temperature of the resin [4].

- The mercerization process consists of impregnating the non-woven into the caustic soda at 70°C for 2 hours, rinsed with distilled water and air-dried at room temperature.

2.2. Non-woven synthesis

Figure 1 summarizes the major steps for the synthesis of the non-woven. First, the fibers were mixed using the Shirley machine. The sail is obtained using the card (dry-laid carded).

A card has three parts. The first allows putting fibers through a food cylinder. While in the second part the carding operation is done essentially through the main drum and a working cylinder. And finally, a drum makes it possible to recover the sail.

The consolidation is mechanical and obtained using a needling machine. Two passages were made to obtain a more compact structure.

Figure 1: The steps for the synthesis of the non-woven abrasive: (a) opening of the fibers by Shirley machine (b) formation of the sail by the card (c) mechanical consolidation using a needling machine

The binder is dosed and applied by a spray gun into the non-woven. Then, the grains are injected by the sieving process.

Figure 2: Application of the resin

Finally, the specimens were dried at the polymerization temperature for a suitable time. For example, for the resacryl resin M, the polymerization must be carried out at 110°C for 15 minutes [5].

All reagents and resins were purchased from chimitex plus Company (Chimitex plus Sarl, Sidi Abdelhamid, Monastir, Tunisie) and used without further purification.

3. RESULTS AND DISCUSSIONS

3.1. Tensile test (Nf G 07-001)

These tests are performed on specimens in accordance with the NFG 07-003 standard in the 0 ° and 90 ° directions [6]. Figure 3 exhibits that the sample of composition 50% cotton-50% bead admits the best tensile strength.
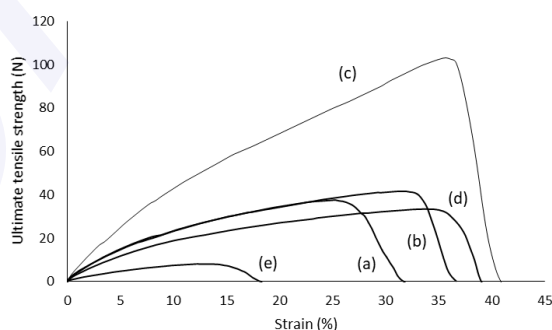

Figure 3: Ultimate tensile strength of non-woven of percentage of tow/cotton (a) 20-80, (b) 33-66, (c) 50-50,

(d) 66-33 et (e) 80-20.

3.2. FT-IR characteristics

The FT-IR spectrum of fibers, resin and composites are shown in the figures below. The characteristic region of the infrared spectrum (1700-850 cm^{-1}) of tow and cotton fibers is shown in figure 4. The figures showed that the fibers contained broadband around 3344 cm^{-1} corresponding to the OH stretching mode [7], [8].
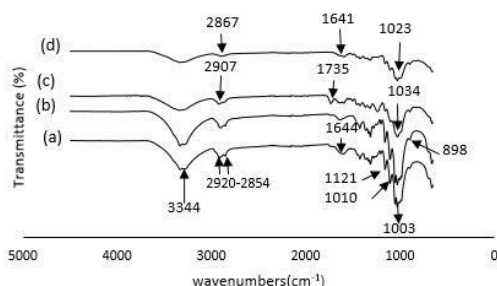

Figure SEQ Figure * ARABIC 4: The FT-IR spectrum of (a) bleached cotton fiber, (b) raw cotton fiber, (c) raw tow fiber and (d) bleached tow fiber
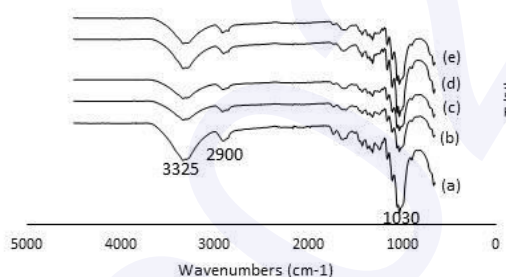
Figure SEQ Figure * ARABIC 5: FTIR spectrum of non-woven manufactured by (a) 20-80, (b) 33-66, (c) 50-50, (d) 66-33, and (e) 80-20 percent of tow-cotton

The band at 1010 cm^{-1} indicates the formation of the C-O bond which assumes the presence of cellulose [9], [10]. In fact, the 898 cm^{-1} band is attributed to β-glucosidic linkages found in the amorphous region of cellulose [11], [12]. While the crystalline structure of cellulose is observed at 1439 cm^{-1} due to the symmetrical bending of CH$_2$. The two bands at 1644 and 1121 cm^{-1} indicates the presence of crystalline cellulose II [13]. Stretching groups of methyl and methylene were observed at 2920 and 2854 cm^{-1} respectively [14], [15]. According to 4.c and 4.d, it has been observed that the bands around 2854 cm^{-1} dispected for tow fibers (methylene). The C=O stretch of the carboxylic acid in hemicellulose is observed at 1735 cm^{-1}. The peak of vibration at 1023 cm^{-1} was due to the stretching vibration C-OH in lignin [16]. Comparing with the IR spectrum of cotton fibers, in the spectrum of tow fibers the bands at 1010 cm^{-1} and 1121 cm^{-1} (stretching groups C-O) have disappeared. The variation of the percentage of fibers in the composition does not affect the composition of the final composite (figure 5).

3.3. SEM analysis

First of all, the apparent volume fraction and apparent void content were estimated by analyzing cross-sectional SEM images. Figure 6 and figure 7 are SEM images of untreated fibers applied for the manufactured nonwoven under various magnifications. Figure 6.a and figure 6.b clearly shows the shape and distribution of the macro fibrils in cotton linters. The SEM images (figure 6.c) of one individual macro fibril at larger magnification show that the surface of untreated cotton linters is almost free of trenches [17]. Figure 7 shows SEM images of bundles and single fiber of tow. Indeed, tows fibers are entangled, twisted and contain shives. The macro-fibrils are well separated and their diameters are almost the same. The beam of bundles of tow fibers was measured with a ruler and it's about 12,3 μm [18]. Figure 7.c allows that the natural tow fiber can admit cracks.
In figure 8, SEM images are obtained after the manufacture of non-woven. In this figure, significant changes on the surface are obvious as the disappearance of cracks and the roughness of the surface of cellulose fibers. There may be a relation between the surface feature and the properties of modified celluloses (figure 9 and figure 10). From the appearance of modified cellulose, we can see that fibers are stuck and more twisted [19].

Figure 6: Untreated cotton fibers: SEM images under different magnifications (a) 100× (b) 500× and (c) 10000×
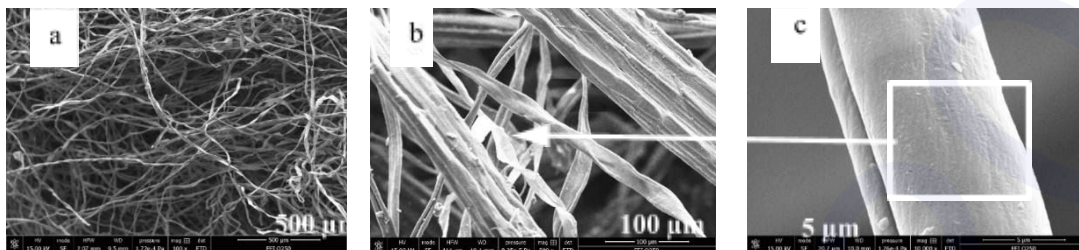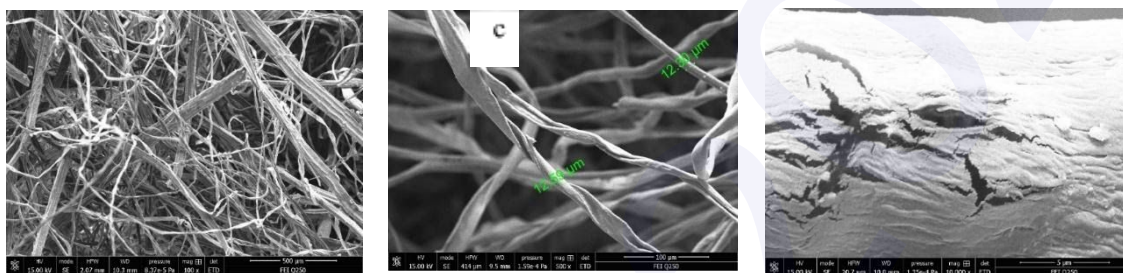

Figure 7: Untreated tow fibers: SEM images under different magnifications (a) 100× (b) 500× and (c) 10000×
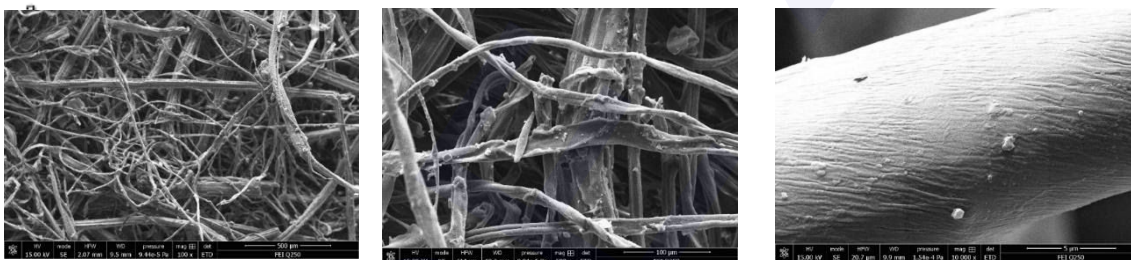

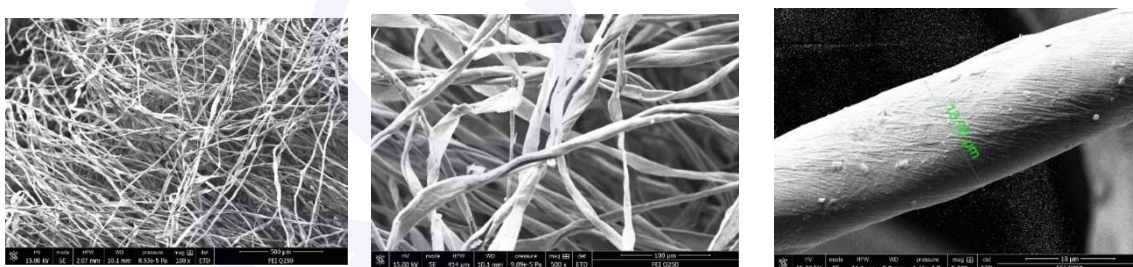Figure 8: Non-woven: SEM images under different magnifications (a) 100× (b) 500× and (c) 10000×

Figure 9: Bleached nonwoven SEM images under different magnifications (a) 100× (b) 500× and (c) 5000×
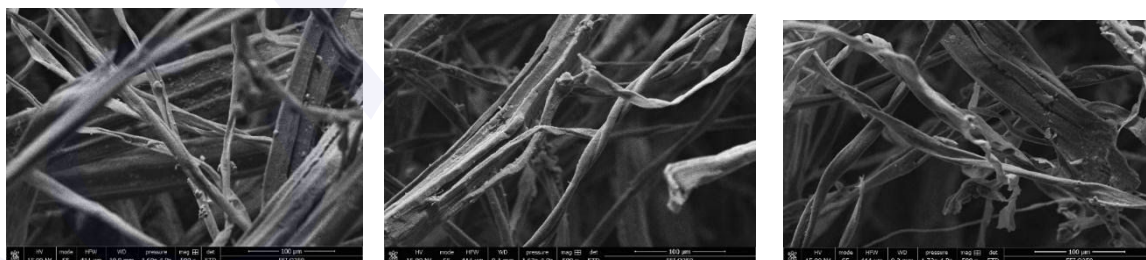

Figure 10: cationized nonwoven 500×

4. CONCLUSION

Products can be made from industrial waste. Indeed, the use of tow fibers allows us to obtain a non-woven structure that can be used in several areas. The pre-treatment such as cationization or mercerizing has effects on the fiber. It increments the amount of cellulose exposed on the surface of the fiber, thus increasing the number of possible reaction sites. In my study, I will use this support as reinforcement for the manufacture of composite, specifically abrasives.

REFERENCES

[1] **Wang Y**, Fiber and Textile Waste Utilization, *Waste and Biomass Valorization*, 2010, Vol.1, No.1, 135-43.

[2] **Jabli M, Baouab MHV, Roudesli MS, Bartegi A**, Adsorption of acid dyes from aqueous solution on a chitosan-cotton composite material prepared by a new pad-dry process, *Journal of Engineered Fibers and Fabrics*, 2011, Vol.6, No.3, 155.

[3] B**igand V, Pinel C, Da Silva Perez D, Rataboul F, Huber P, Petit-Conil M**, Cationisation of galactomannan and xylan hemicelluloses, *Carbohydrate Polymers*, 2011, Vol. 85, No.1, 138-48.

[4] **Valadez-Gonzalez A, Cervantes-Uc J, Olayo R, Herrera-Franco P**, Effect of fiber surface treatment on the fiber–matrix bond strength of natural fiber reinforced composites, *Composites Part B: Engineering*, 1999, Vol.30, No.3, 309-20.

[5] **Litim N, Baffoun A, Khoffi F, Hamdaoui M, Ben Abdessalem S, Durand B**, Effect of finishing resins on mechanical and surface properties of cotton Denim fabrics, *The Journal of The Textile Institute*, 2017, Vol.108, No.11, 1863-70.

[6] **Faure Y, Farkouh B, Delmas P, Nancey A**, Analysis of geotextile filter behaviour after 21 years in Valcros dam, *Geotextiles and Geomembranes*, 1999, Vol.17, No.5-6, 353-70.

[7] **Salmén L, Bergström E**, Cellulose structural arrangement in relation to spectral changes in tensile loading FTIR, *Cellulose*, 2009, Vol.16, No.6, 975-82.

[8] **Saleh TA, Naeemullah, Tuzen M, Sarı A**, Polyethylenimine modified activated carbon as novel magnetic adsorbent for the removal of uranium from aqueous solution, *Chemical Engineering Research and Design*, 2017, Vol.117, 218-27.

[9] **Ibrahim M, Osman O, Mahmoud AA**, Spectroscopic Analyses of Cellulose and Chitosan: FTIR and Modeling Approach, *Journal of Computational and Theoretical Nanoscience*, 2011, Vol.8, No.1, 117-23.

[10] **Kačuráková M, Smith AC, Gidley MJ, Wilson RH**, Molecular interactions in bacterial cellulose composites studied by 1D FT-IR and dynamic 2D FT-IR spectroscopy, *Carbohydrate Research*, 2002, Vol 337, No 12, 1145-53.

[11] **De Rosa IM, Kenny JM, Puglia D, Santulli C, Sarasini F,** Morphological, thermal and mechanical characterization of okra (Abelmoschus esculentus) fibres as potential reinforcement in polymer composites, *Composites Science and Technology*, 2010, Vol.70, No.1, 116-22.

[12] **Oh SY, Yoo DI, Shin Y, Seo G,** FTIR analysis of cellulose treated with sodium hydroxide and carbon dioxide, *Carbohydr Res*, 2005, Vol.28, No.340 (3), 417-28.

[13] **Carrillo F, Colom X, Suñol JJ, Saurina J**, Structural FTIR analysis and thermal characterization of lyocell and viscose-type fibres, *European Polymer Journal*, 2004, Vol.40, No.9, 2229-34.

[14] **Poletto M, Zattera AJ, Santana RMC,** Structural differences between wood species: Evidence from chemical composition, FTIR spectroscopy, and thermogravimetric analysis, *Journal of Applied Polymer Science*, 2012, Vol 126, E337-E44.

[15] **Saleh TA, Sarı A, Tuzen M**. Optimization of parameters with experimental design for the adsorption of mercury using polyethylenimine modified-activated carbon, *Journal of Environmental Chemical Engineering*, 2017, Vol.5, No.1, 1079-88.

[16] **Wang X, Wang L, Ji W, Hao Q, Zhang G, Meng Q**, Characterization of KH-560-Modified Jute Fabric/Epoxy Laminated Composites: Surface Structure, and Thermal and Mechanical Properties, *Polymers*, 2019, Vol.11, No.5.

[17] **Zhao H, Kwak J, Conradzhang Z, Brown H, Arey B, Holladay J,** Studying cellulose fiber structure by SEM, XRD, NMR and acid hydrolysis, *Carbohydrate Polymers,* 2007, Vol 68, No.2, 235-41.

[18] **Martin N, Davies P, Baley C.** Comparison of the properties of scutched flax and flax tow for composite material reinforcement, *Industrial Crops and Products*, 2014, Vol 61, 284-92.

[19] **Yin C, Li J, Xu Q, Peng Q, Liu Y, Shen X**, Chemical modification of cotton cellulose in supercritical carbon dioxide: Synthesis and characterization of cellulose carbamate, *Carbohydrate Polymers*, 2007, Vol 67, No.2,147-54.

The Second Edition of the International Congress of Applied chemistry and Environment
30th-31th October and 01st November 2020, Tunisia

ICACE 2020

Pyrolysis of used tires: yield and chemical composition of pyrolysis oils

Marwa Ourak[a,b,c], Mylène Marin Gallego[a], Gaëtan Burnens[a], Sana Kordoghli[b], Jean François Largeau[d], Fethi Zagrouba[b], Mohand Tazerout[a]

(a) GEPEA- CNRS UMR 6144, IMT Atlantique, Nantes, 44000. France
(b) Research Laboratory for Sciences and Technologies of Environment, High Institute of Sciences and Technologies of Environment, Borj Cedria, Carthage University, Tunisia
(c) National School of Engineers of Gabes, University of Gabes, 6026 Gabes, Tunisia
(d) ICAM
marwa.ourak@imt-atlantique.fr

ABSTRACT
Used tires are a detrimental waste to the environment whose treatment has become a major issue. Tires thermal valorization via pyrolysis leads to the production of three products of interest: char, gas, and pyrolysis oil. These two last have a high-energy potential and can be used as alternative fuels [1]. The oil also has the advantage of containing valuables molecules such as toluene, benzene, xylene but also d-limonene whose chemical valorization is strongly studied in the literature [2]. The evolution of the composition of the pyrolysis oils as a function of the semi batch reactor temperature is an original result and has shown that they are mainly composed of volatile organic molecules. The existence of competition in production between d-limonene and p-cymene, as well as the reduction of the C7 content in favor of heavier molecules of the C10 lumps, are also proved.

KEYWORDS Pyrolysis, waste tire, chemicals recovery, d-limonene.

1. INTRODUCTION

The tires have an excellent heating value estimated at 34 MJ / Kg since they are mainly composed of synthetic rubber, a derivative of oil, and natural rubber. They are therefore excellent candidates for producing innovative fuels and chemicals with high economic value. This thesis is part of a PHC Utique project whose objective is to propose a process of valorization of the volatile materials resulting from the pyrolysis of the tire for industrialization. The interest of this thesis is to develop and defend pyrolysis as a heat treatment process with great economic interest. The products from tire pyrolysis are oils (liquid fuels) with high energy value (40-42 MJ/kg), combustible gases (20-65 MJ/m³), and char [3]. In addition to their use as fuels, pyrolysis oils are a potential source of light aromatic components such as benzene, toluene, xylene (BTX), d-limonene, etc., which have a higher market value than crude oils. In this study, the powder of trucks tires scrap was pyrolyzed in a semi batch reactor. The liquid samples are recovered separately then analyzed by GC-MS-FID analysis in order to identify its compositions. Furthermore, a particular attention was paid to the majority composition of different carbon number lumps. The most abundant product was d-limonene, which had been competing with the p-cymene. Both molecules with BTX are chemicals with high value that can improve the economic feasibility of this process.

2. MATERIAL AND METHODS

The powder of heavy vehicle scrap tires (HVT) was used in these experiments. The powder has been characterized and. The C:H ratio was around 11 which show that this raw material is favorable to pyrolysis. The pyrolysis of scrap tires was carried out in a cylindrical semi batch reactor (1L) with a total power of 1260 watts. The pyrolysis plant used in this study is shown in Figure 1. All experiments were carried out at a maximum temperature of 500 °C. The liquid samples were recovered separately over time then analyzed by gas chromatography coupled to a flame ionization detector and a mass spectrometer (GC-MS-FID) in order to identify its compositions.
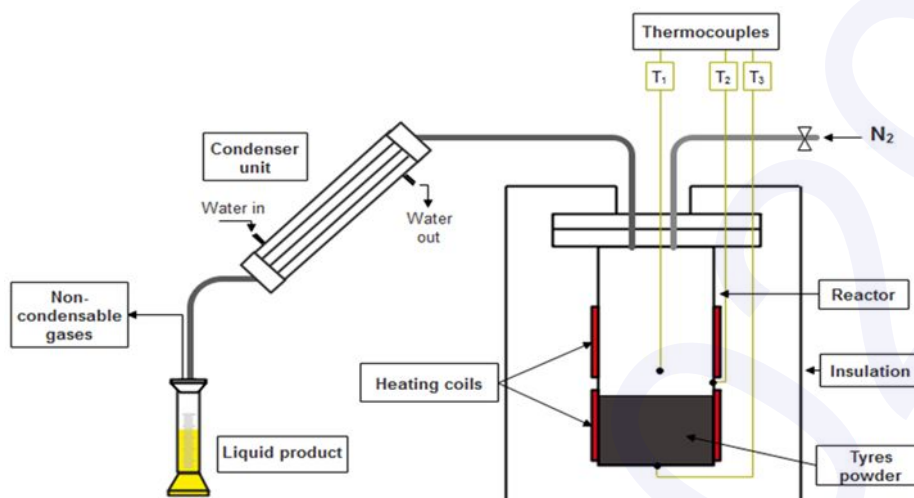
Figure 1 : Schematic diagram of pyrolysis reactor

3. RESULTS AND DISCUSSIONS

The pyrolysis product yields in char, oil, and gas are shown in Table 1. The amount of gas shown is obtained by difference. Pyrolysis oils are complex mixtures containing different families of hydrocarbon compounds ranging from C4 to C25. More than a hundred compounds have been identified.

Table 1: Product yields and reaction time

Yields (wt%)	Without N_2	With N_2
Liquid	18.4 - 38.5	28.1
Char	35.7 - 47.7	41.1
Gas	17.6 - 43.7	30.8
Reaction time (min)	110	80

Table 2 presents an extract from the representative families of these oils. BTX (benzene, toluene, p,o-xylene), d-limonene and p-cymene are the most abundant compounds in this plethora of chemicals and they have higher market value than crude oils. They are widely used as solvents and raw material in chemistry (dyes, pharmaceuticals pesticides polymers, perfumes, etc.)

Table 2: Composition by chemical family of pyrolysis oils

Aliphatic compounds	Single ring aromatic compounds	Polyaromatic hydrocarbons	Others
Heptene	P-cymene	Dimethyl naphthalene	Ethyl-methyl cylohexane
Hexadecane	Dimethyl indene	Naphthalene	D-limonene
Hexene	Ethyl benzene		Propenyl cyclohexene
Nonene	Ethyl indene		
Octane			
Pentadecane	Ethyl-methyl benzene		
	Styrene		
	Toluene		
	Trimethyl benzene		
	P,o-xylene		

The Second Edition of the International Congress of Applied chemistry and Environment
30th-31th October and 01st November 2020, Tunisia

ICACE 2020

3.1. Crude tire oil analysis

The evolution of the oils composition as a function of the temperature of the reactor is an original result and asserts that the pyrolytic liquid composition is no longer the same throughout the pyrolysis. A depletion of the liquid carbon chain molecules from 4C to 7C from the start of pyrolysis towards the end of the pyrolysis in favor of heavier organic molecules of 9C lumps and more was noted too. In the starting condensates sample C7 fraction yield was around 20.4 wt% of the liquid product. Reaching the end of pyrolysis, the reactor temperature was already 500°C, the products shifted into upper molecular weights and the C10 fraction was the most (about 19.6 wt%).

3.2. D-limonene and p-Cymene competition

Another original result of this study was the existence of a competition between the production of d-limonene and p-cymene: the yield of d-Limonene decreases with temperature while the p-cymene yield increases. This competitive trend is presented in Figure 2, which shows a gradual growth on p-cymene yield with a swift drop on d-limonene yield.
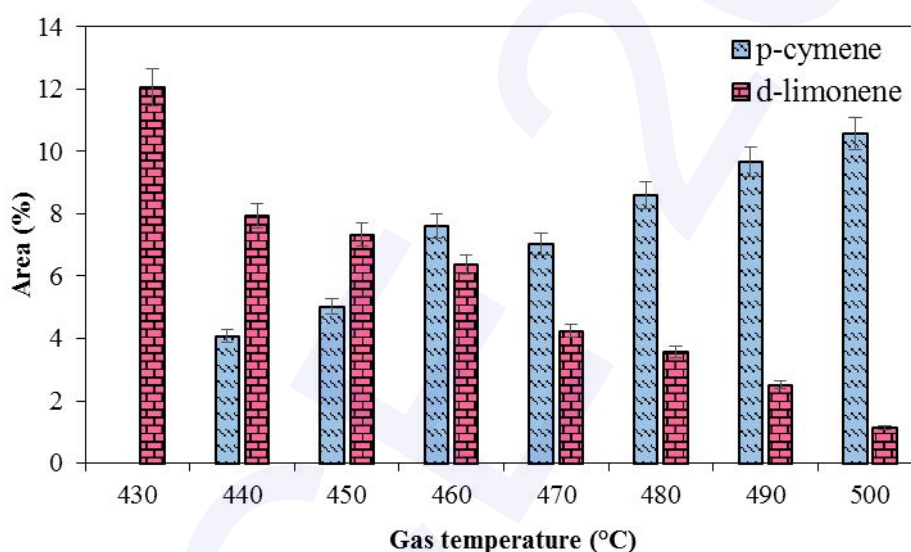
Figure 2 : D-limonene and p-cymene content of the pyrolysis oil

D-limonene has already been declared in different studies as a major chemical with a maximum content of about 18% by weight in our pyrolysis oil. The formation of d-limonene can be explained by the condensation of 2 isoprene molecules via a classical Diels-Alder reaction [3,4]. The passage of a molecule of d-limonene towards the p-cymene can be explained by a migration of two protons: it is an isomerization of d-limonene (a diene) thus giving a terpene which evolves itself towards a more stable state which is that of p-cymene by aromatization [4].

3.3. Gas career effect on oil composition

It was concluded that this passage from d-limonene to p-cymene is due to the secondary reactions, which took place following the long residence time of the volatile molecules in the reactor. To see the effect of this parameter on this competition, we introduced a carrier gas flow. The first result is that the recovery of the liquids started very early compared to manipulations without nitrogen advancing from 430 °C to 360 °C. The d-limonene content has been improved: there is very little p-cymene produced (does not exceed 4 % of the surface area) while the d-limonene area has not decreased of 23 % from 450 °C and after.

4. CONCLUSION

The study presented the results of the characterization of pyrolytic oil samples from pyrolysis of scrap tires on a batch reactor. They were composed mainly of volatile organic components. The

original results to this work was the depletion of the of liquid molecules with a carbon chain below 7C in favor of larger carbon chain in addition to the competition of d-limonene and p-cymene.

REFERENCES

[1] **Alkhatib, R., Loubar, K., Awad, S., Mounif, E., et Tazerout, M.** Effect of heating power on the scrap tires pyrolysis derived oil, *Journal of analytical and applied pyrolysis*, 2015, Vol.116, 10-17.

[2] **Quek A., Balasubramanian R.** Liquefaction of waste tires by pyrolysis for oil and chemicals-a review, *Journal of analytical and applied pyrolysis*, 2013, Vol.101, 1–16.

Williams P.T., Pyrolysis of waste tyres: a review, *Waste Management*, 2013, vol.33, 1714–1728

[3] **Danon, B., van der Gryp, P., Schwarz, C.E., Görgens, J.F.** A review of dipentene (dl-limonene) production from waste tire pyrolysis, *Journal of analytical and applied pyrolysis*, 2015, Vol.112,1-13.

The Second Edition of the International Congress of Applied chemistry and Environment
30th-31th October and 01st November 2020, Tunisia

ICACE 2020

Valorization of solid wastes from food industry as biosorbents for the removal of Cd (II)

Nourhen HSINI[a], Sonia DRIDI-DHAOUADI[a,b]

(a)   Research Unity of Applied Chemistry and Environment, University of Monastir, Faculty of Sciences of Monastir, -5000 Monastir, TUNISIA.

(b)   University of Monastir, Preparatory Institute for Engineering Studies, -5000 Monastir, TUNISIA.

E-mail: hcini.nourhen2016@gmail.com

ABSTRACT

This work is part of the valorization of three solid wastes such are prickly pear seeds PPS, prickly pear peels PP and pomegranate peels GP, collected from Tunisian food industry and used as adsorbent materials for the elimination of cadmium ions. The adsorption experiments were carried out in batch mode. The solid surfaces were firstly characterized using physicochemical techniques (Chemical composition, pHpzc, Boehm titration, FT-IR and SEM). The results of these characterizations showed that PPS has the higher quantities of the lignocellulosic components: 31-45 %. For all materials, the carboxylic and phenolic functions are preponderant: 1.8-1.5 meq.g^{-1}, 1.6-2.4 meq.g^{-1} and 1.4-1.3 meq.g^{-1} for PPS, PP and GP, respectively. Cd (II) adsorption by the solids showed that the maximum retention capacities of Cd (II) were 20.4 mg.g^{-1}, 16.4 mg.g^{-1} and 16.6 mg.g^{-1} for PPS, PP and GP, respectively.
This work showed that the used solid wastes can be successfully valorized as adsorbents for the cadmium elimination from wastewater.

KEYWORDS: solid waste, adsorption, cadmium elimination

1. INTRODUCTION

This work is part of the reduction of the environmental impact of the solid wastes generated from agri-food industries such as those of fruit transformation. These wastes such are prickly pear seeds and its peels and pomegranate peels are actually valued as cosmetic products (mask for the skin). However, this recovery is insufficient to overcome the huge volumes of waste generated every year. On the other hand, the quality of cosmetics is subject to increasingly stringent regulations. The use of these solids as adsorbents for the removal of pollutants (cadmium ions) present in aqueous industrial effluents is the objective of this work.

2. MATERIAL AND METHODS

2.1. Biosorbent collection and physicochemical characterizations

Three novel materials were collected from Tunisian agri-food industries, prickly pear seeds (PPS) from oil extraction industry, prickly pear peels (PP) and pomegranate peels (GP) from fruit juice canning industry. The raw materials were dried, powdered and used as biosorbents for Cd(II) elimination.

Fourier Transform Infra Red spectroscopy (FT-IR) was carried out for all biomaterials using a Perkin Elmer Spectrum FTIR.

The morphologies of the solids were studied by using a scanning electron microscope JEOL JSM-7000F. The chemical compositions was carried out by different standards methods such are T 210 cm-03, T211 om-02, T211 om-02, T204 cm-07 and T 222 om-06.

The pH of zero charge values were evaluated for all material surfaces following the protocol described by Lopez *et al* 1999 [1]. The Boehm method was applied to evaluate the amounts of acidic and basic functions present on biomaterial surfaces

2.2. Cadmium retention experiments

Adsorption experiments were performed in batch mode for the three materials. 0.2 g of biosorbent was mixed for 24 h at 20 °C with a volume of 20 mL of cadmium solution whose concentration varied from 10 to 1000 mg.L^{-1}. The residual Cd (II) (non adsorbed) was analyzed using atomic absorption spectroscopy (contrAA HR-CS AAS - Analytic Jena), which allowed the calculation of the amount of metal ion retained per gram of biosorbent as shown in equation (1):

$$Qe = \frac{(C0-Ce)V}{m} \qquad (1)$$

Where C_0 (mg.L^{-1}) is the initial cadmium concentration, Ce (mg.L^{-1}) the cadmium concentration at equilibrium, V (mL): the solution volume, and m (g): the mass of adsorbent.

Three isotherm models, namely Langmuir, Freundlich and Sips models, were used in order to express the equilibrium relationship between the adsorbed quantity of cadmium per unit mass of adsorbent and the concentration of the metal cation in solution [2].

3. RESULTS AND DISCUSSIONS

3.1. Physicochemical characterizations

The chemical composition, the amounts of surface functions and the pH of zero charge (pH$_{pzc}$) are given, for the three biomaterials, in Table 1.

Table 1: Chemical composition, surface acid functions and pHpzc of the of prickly pear seed waste PPS, prickly pear peel waste PP and grenade peel waste GP.

Biomaterials	PPS	PP	GP
Chemical composition (%)			
Moisture	1.13	7.03	3.91
Ash	2.41	20.0	5.31
Extractives	0.69	2.59	0.79
Klason lignin	45.0	4.12	19.0
Hollocellulose	40.2	11.1	0.34
α-Cellulose	31.4	4.46	2.78
Acid functions (meq.g^{-1})			
Phenols	1.48	2.41	1.60
Lactones	0.12	-	-
Carboxyls	1.79	1.60	1.42
Total	3.39	4.01	3.02
pH$_{pzc}$	5.75	3.70	3.20

The results show that PPS has small amounts of moisture, ash and extractives but a significantly higher lignin, hollocellulose and α-cellulose contents comparing to PP and GP materials. The pH$_{pzc}$ values, estimated between 3 and 6 for the used biomaterials, indicate that important amounts of acid functions are present on the solid surface and more particularly on the surface of PPS. This observation is confirmed by the results of the Boehm titration. Indeed, the amount of carboxylic functions on PPS surfaces is higher than that on PP and GP surfaces. Moreover, the lactonic functions are in small quantity on PPS and completely absent on PP and GP.
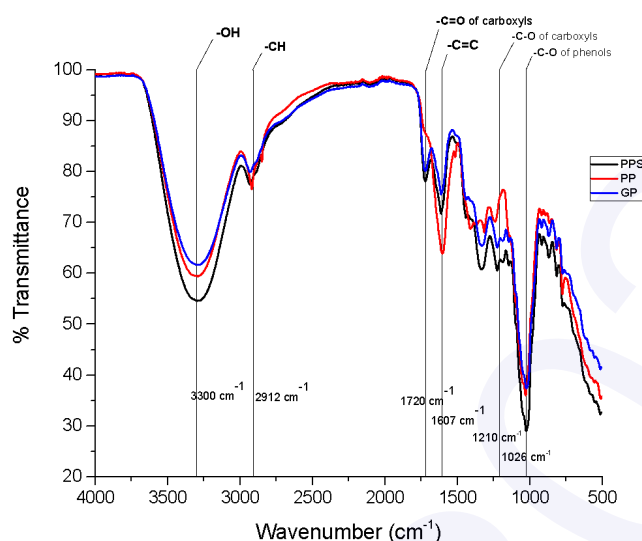
Figure 1: Spectra FT-IR of prickly pear seed waste PPS, prickly pear peels PP and pomegranate peels GP.

As shown in Figure 1, the FT-IR spectra of the PPS, PP and GP materials show that all the biosorbents exhibit the same surface functions. Thus, the most significant bands reveal the existence of carboxylic and phenolic sites: a broad absorption band around 3300 cm^{-1} corresponding to the -OH bound function, a fine band 1720 cm^{-1} corresponding to –C=O of the carboxylic acid, a band 1607 cm^{-1} corresponding to the aromatic doublet -C=C, a fine absorption band at 1210 cm^{-1} attributed to the –C-O bond of the carboxylic acid and an intense band around 1026 cm^{-1} corresponding to –C-O bond of the phenols.

As shown in Figure 1, the FT-IR spectra of the PPS, PP and GP materials show that all the biosorbents exhibit the same surface functions. Thus, the most significant bands reveal the existence of carboxylic and phenolic sites: a broad absorption band around 3300 cm^{-1} corresponding to the -OH function, a band 1631 cm^{-1} corresponding to the aromatic doublet -C=C, a fine absorption band at 1238 cm^{-1} attributed to the –C-O bond of the carboxylic acid and an intense band around 1023-1031 cm^{-1} corresponding to –C-O bond of the phenols.

3.2. Cadmium adsorption studies

Figure 2 illustrates the experimental and modeled isotherms of cadmium adsorbed on the three materials. Table 2 shows the parameters and regression coefficients of the Langmuir, Freundlich and Sips models used to correlate the experimental results.

(a) (b) (c)
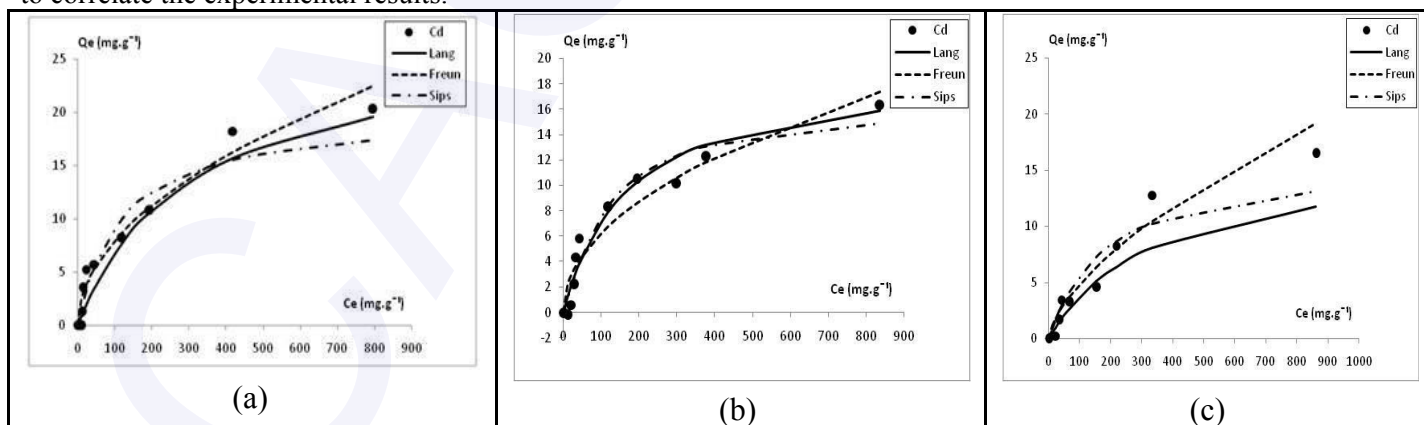
Figure 2: Experimental and modeled adsorption isotherms of Cd (II) on (a) PPS (b) PP and (c) GP.

Table 2: Isotherm modeling parameters

Biomaterials	Langmuir		Freundlich		Sips	

	K_L L.mg^{-1}	Q_{max} mg.g^{-1}	R²	K_F L.mg^{-1}	n_F	R²	K_S L.mg^{-1}	n_s	R²
PPS	0.003	27.0	0.94	0.79	0.50	0.96	0.008	1.01	0.93
PP	0.006	19.1	0.95	0.68	0.48	0.98	0.004	1.17	0.95
GP	0.003	16.6	0.71	0.25	0.64	0.92	0.005	1.00	0.83

Figure 2 shows that the experimental isotherms are correctly fitted with the Freundlich model for all the three materials, with higher regression coefficients varying between (R²) 0.96 and 0.98. This result is not surprising since Freundlich model represents an adsorption on heterogeneous sites. On the other hand, Figure 2 indicates that the maximum adsorption capacity of cadmium, deduced from the experimental isotherms, is higher for PPS followed by PG and finally PP. These results can be explained by the important amount of carboxylic functions on PPS. Thus, the adsorption mechanism is very probably a complexation of cadmium with the oxygen ligand of the carboxylic groups [3].

4. CONCLUSION

This work highlights the environmental interest of using solid wastes, which are prickly pear seed ~~waste~~ PPS and its peels PP and pomegranate peels GP, generated in large amounts from food industries. It has been shown that the use of these materials as biosorbents for the elimination of Cd (II) metal is possible. The obtained isotherms showed that the adsorption of cadmium is satisfactorily described by the Freundlich model. The physicochemical characterizations showed that the retention mechanism that occurs is probably a complexation of the metal ion with the oxygen ligand of the acid functions. The production of activated carbons from this waste constitutes the major perspective to this work.

REFERENCES

[1] **Lopez-Ramona, M.V., Stoeckli, F., Moreno-Castilla, C., Carrasco-Marin, F**, On the characterization of acidic and basic surface sites on carbons by various techniques, *Carbon*, 1999, Vol.37, 1215–1221.

[2] **Syafiuddin, A., Salmiati, S., Jonbi, J., Fulazzaky, M.A**, Application of the kinetic and isotherm models for better understanding of the behaviors of silver nanoparticles adsorption onto different adsorbents, *J Environmental Managmente*, 2018, Vol.218, 59-70.

[3] **Richards, S., Dawson, J., Stutter, M**, The potential use of natural vs commercial biosorbent material to remediate stream waters by removing heavy metal contaminants, *J Environironmental Management*, 2019, Vol.231, 275–281.

The Second Edition of the International Congress of Applied chemistry and Environment
30th-31th October and 01st November 2020, Tunisia

ICACE 2020

Adhesion Capacity of Carboxymethyl Cellulose from Wheat Straw to Cotton Fibers

Najah Laribi[a], Samah Maatoug[a], Riadh Zouari[a], Hatem Majdoub[b]and Morched Cheikhrouhou[a]

(a) University of Monastir, ISET Ksar Hellal, Laboratory of Textile Engineering, B.P 68 Ksar Hellal, 5070, Monastir, Tunisia

(b) University of Monastir, Faculty of Sciences of Monastir, Laboratory of Interfaces and Advanced Materials, Bd of the environment, 5019, Monastir, Tunisia

ABSTRACT

Wheat Straw (WS) is a low-cost agricultural by-product considered as cellulose rich waste biomass resource; this makes it a good potential for production of cellulose derivatives such as carboxymethyl cellulose. The proposal of this study was to extract cellulose from this biomass, to synthesize carboxymethyl cellulose (CMC) and to study the potential of application of CMC synthesized as a textile sizing agent to cotton fibers. The carboxymethylation reaction, was carried out with NaOH and monochloroacetic acid (MCA) as the reagent, giving result to a CMC with a degree of substitution of 0.86. Adhesive properties of the so-synthesized product, as a low-cost sizing agent, were evaluated by studying breaking force and elongation at break of 100% cotton rovings impregnated with CMC synthesized in different sizing conditions. The results provided that CMC from wheat straw had good adhesion to cotton rovings rendering him qualified for warp yarns sizing applications.

KEYWORDS: Wheat straw, carboxymethyl cellulose, cotton roving, adhesion.

1. INTRODUCTION

During the process of weaving, the warp yarns can break because of the complex mechanical actions including cyclic extension, abrasion and bending. Breaking of warp yarns during weaving causes loom stoppages, decreases productivity and creates fabric defects. Therefore, prior to weaving, warp yarns, are generally given a protective coating of a polymeric film forming agent (sizing agent) to enable them to withstand better the additive forces during weaving.

CMC is a hydrophilic type size that has good adhesion to polar fibers, e.g. cotton fibers [1]. Carboxymethyl cellulose (CMC) is water soluble cellulose based binder. Chemically, it is made by reacting monochloroacetic acid or its sodium salt with alkaline cellulose and reagent properties, temperature, and concentration are major process parameters. CMC is soluble in hot and cold water.

Wood or cotton have been considered as the most important sources of cellulosic fibers, however, concerns on the environment and diminishing of forest caused by the increased demand for wood resources led to the increased interest in the exploitation of non-wooden cellulosic materials [2]. Billions of metric tons of biomass are generated every year from the agricultural industry worldwide including liquid, solid and gaseous residues that may be considered one of the most abundant, cheap and renewable resources on earth [3]. Low-cost agricultural by-products can be an attractive source of cellulose extraction. Wheat straw is a typical agricultural by-product that is annually produced in abundance world-wide (529 Million tons/year) [4]. It contains 15-25% lignin, 35-45% cellulose, and 20-30% hemicelluloses and needs proper disposal. One possible avenue could be as inexpensive warp yarns sizing.

In this context, the present study deals primarily with synthesis of low-cost carboxymethyl cellulose from an agricultural by-product; the wheat straw, and secondly studies the adhesion of carboxymethyl cellulose synthesized, as a size base material, for cotton fibers. Effects of plasticizer concentration and temperature of sizing solution on adhesion properties to cotton fibers were also investigated.

2. MATERIAL AND METHODS

2.1 Materials

Wheat straw (Triticum aestivum L.) was collected from local farms in Beja, located in northwestern Tunisia.

The Second Edition of the International Congress of Applied chemistry and Environment
30th-31th October and 01st November 2020, Tunisia

ICACE 2020

It was cut into small pieces and dried in an oven at 50°C for 24 h. The obtained material was milled and sieved to a granulometry having a size range between 100 μm and 1 mm.

Combed cotton rovings (with linear density of 1.5 ktex), glycerol (as a plasticizer) and commercial CMC (CARBO 150 RH) were provided by a textile industry. Rovings were made from 100% cotton fibers and they were used for sizing adhesion strength and breaking elongation tests without any chemical pretreatment.

2.2 Methods

Extraction of cellulose and synthesis of carboxymethyl cellulose from wheat straw

The synthesis of CMC from Tunisian wheat straw has already been reported in our previous study [5] were CMC was synthesized with different degrees of substitution (0.43, 0.91 and 1.37) by varying the concentration of the etherification agent (MCA).

Since most warp size grades of CMC have a DS in the 0.65–0.85 range[1], we have synthesized in the present study a CMC with a degree of substitution belonging to this interval. For this, 5 g of the washed and dried cellulose was immersed in 30 mL of 1-butanol while stirring mechanically for 1h at 60°C, and then 30 mL of 40% aqueous sodium hydroxide solution was added and the mixture was stirred for 12h at 60°C in order to convert cellulose into alkali-cellulose. The carboxymethylation reaction is done after the addition of the selected quantity of monochloroacetic acid (7.5 g) and the etherification reaction was allowed to occur during 8 h at 60°C (figure 1).
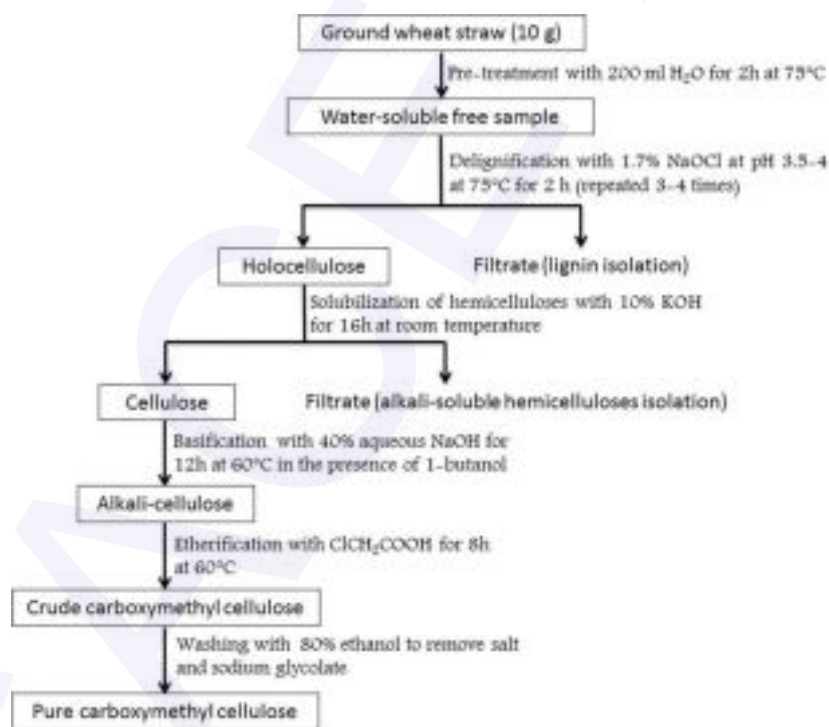
Figure 1: Flow diagram for the preparation of CMC from wheat straw

Characterization of CMC synthesized

・Degree of substitution (DS) of CMC

The degree of substitution defined as the average number of sodium carboxymethyl groups substituted per anhydroglucose unit was determined by the standard titration method (ASTM, 1961). Briefly, five grams of dried CMC was added to 200 mL of HNO_3-methanol mixture and kept for 3 h, and then the surplus was washed with 70% methanol. 2 g of dried material was dissolved in a mixture of 200 mL of distilled water and 30 ml of NaOH (1N). The obtained solution was titrated using HCl (1N) and the DS of CMC synthesized was determined using the following equations [6]:

The Second Edition of the International Congress of Applied chemistry and Environment
30th-31th October and 01st November 2020, Tunisia

ICACE 2020

$$DS = 0.162A/(1 - 0.058A) \ (1)$$

$$A = (bc - de)/f \ (2)$$

Where f (g) is the weight of sample of CMC; A is the equivalent weight of NaOH required per gram of sample; b (mL) is the NaOH solution quantity; c is the normality of solution of NaOH; d (mL) is the amount of HCl solution and e is the normality of solution of HCl.

・CMC molecular weight

CMC was dissolved in 0.78 M NaOH solution and the intrinsic viscosity [η] of carboxymethyl cellulose synthesized was determined using an Ostwald viscometer. The molecular weight M_w of CMC was calculated from the "Mark–Houwink–Sakurada" relationship (equation (3)) [7]:

$$[\eta] = K(M_w)^\alpha \qquad (3)$$

・Purity of CMC

5 g of CMC synthesized was washed several times with 80% ethanol and absolute methanol for removing by-products containing sodium chloride (NaCl) and sodium glycolate ($HOCH_2COONa$) produced during the etherification reaction. Then, 2 g of it was dissolved in 50 mL of bi-distilled water at 80°C and stirred for 15 min until completely dissolved. Then, the solution was centrifuged for 1 min at 4000 rpm and precipitated solids were collected. Then, 50 mL of pure acetone was used for the re-precipitation of the dissolved CMC. Finally, the recovered CMC was filtered and dried in an oven at 50°C to constant weight. The purity of the CMC was given by the following equation [8]:

$$Purity\ (\%) = \frac{Weight\ of\ dried\ residue}{Weight\ of\ specimen\ used} \times 100 \qquad (4)$$

Adhesion of CMC from wheat straw to cotton fibers

Since rovings are a loose assembly of fibers that have almost no strength, increase in roving strength impregnated in the sizing solution would be a good indicator of the adhesion efficiency between size and fibers. For this, the rovings wound on a specially designed metal support were immersed in the sizing solution for 5 min, and then the metal support was removed from the solution and placed vertically in the atmosphere to allow the drying of the rovings. Finally, the sized and dried samples were conditioned before testing at 20°C and 65% relative humidity. Tensile properties of rovings, namely peak load and peak elongation, were tested using LS5 Lloyd testing machine (AMETEK Sensors, Test and Calibration, Germany) using a load cell of 100 N in a traverse speed of 50 mm/min and the gauge length is 100 mm. 20 samples for each experimental condition were tested and each condition was made in triplicate. Average and ± one standard deviation between the three experiments were determined and reported.

Microscopic observation of sized rovings before and after breaking

In order to evaluate the extent of permeation of the size into the roving according to the conditions of impregnation, a microscopic observation of the sized rovings before and after breaking was performed using a Leica M50 stereo microscope.

3. RESULTS AND DISCUSSIONS

3.1. Carboxymethyl cellulose from wheat straw properties

A CMC with DS of 0.86 was synthesized, characterizing it as water soluble and the DS value obtained in the present study is in the required range for warp yarns sizing. According to DS result, the CMC synthesized is classified as mono-substituted; just one of the three free hydroxyl groups (OH) in the molecule of glucose

The Second Edition of the International Congress of Applied chemistry and Environment
30th-31th October and 01st November 2020, Tunisia

ICACE 2020

was substituted by a carboxymethyl group (OCH$_2$COONa).

Table 1 summarizes the physical characteristics of CMC prepared from wheat straw. The CMC produced was an odorless white powder. It is totally soluble in water and insoluble in ethanol. The product thus obtained is classified as semi-refined because its purity is about 92.3% which can be used successfully for textile warp sizing [1].

Table1: Physical characteristics of CMC prepared

Parameters	CMC characteristics
Color	White
Form	Powder
Odor	Odorless
Degree of substitution	0.86
Solubility	Totally soluble in water
Purity (%)	92.3

The parameters evaluated to calculate the degree of polymerization and molecular weight of carboxymethyl cellulose synthesized were presented in table 2. From the data, the molecular weight of carboxymethyl cellulose obtained is about that may be categorized as medium viscosity average molecular weight of CMC [9].

Table 2: Determination of intrinsic viscosity, degree of polymerization and molecular weight of CMC prepared (in the case of CMC K = 37×10−5 dl/g and α = 0.61 at 35 ◦C)

	Intrinsic viscosity [η]	Degree of polymerization [DP]	Molecular weight (g.mol^{-1})
CMC prepared	0.80	1278	295,000

3.2. Effect of size preparatory conditions on adhesion performance

The tensile strength of the unsized roving is presumed to be zero. Accordingly, the increase in strength of the sized roving is considered as a direct quantitative measure of the adhesive power of the sizing material. As the present study deals with the potential of use of CMC synthesized as warp yarn sizing agent, we have studied its ability to temporarily improve the physico-mechanical properties of cotton rovings.

The effect of size temperature

The effect of temperature of sizing paste on the adhesion behavior of sized roving is evident from the data presented in Figure 2. It is obvious from the data that increasing size temperature from 40°C to 90°C, the peak load increases evidently from 35.51 N to 72.14 N and consequently the adhesion between cotton roving and size has improved. This can be explained by the fact that the temperature is related to fluidity so by increasing the temperature the sizing paste is of good fluidity which in turn affects both the level of size pick up and extent of penetration and therefore the size can be distributed homogeneously between the fibers in the cotton roving.

The Second Edition of the International Congress of Applied chemistry and Environment
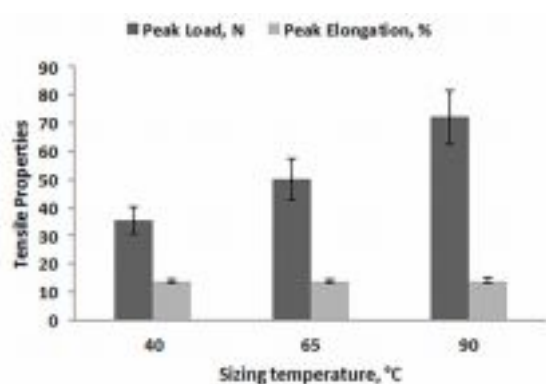30th-31th October and 01st November 2020, Tunisia

ICACE 2020

Figure 2: Influence of temperature of sizing solution on tensile properties of 100% cotton rovings. Sizing was done with a CMC concentration of 6% (w/v) and glycerol concentration of 30 wt. %
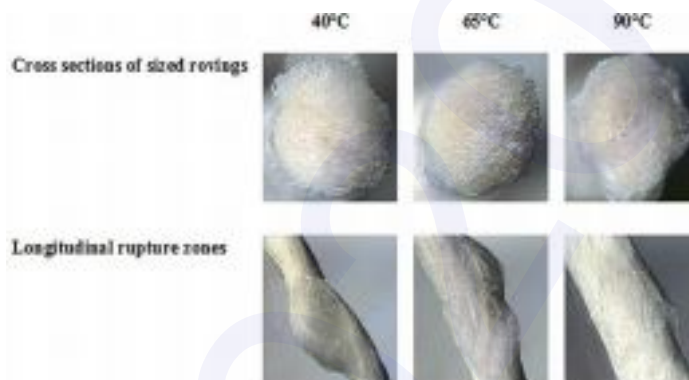
Figure 3: Photographs of cross sections and longitudinal rupture zones of 100% cotton rovings sized at different temperatures of sizing solutions (40, 65 and 90°C).

Figure 3 shows the microscopic observation of cross sections and longitudinal observations of rupture zones of cotton rovings sized at different temperatures. During the sizing process, the size solution gradually permeates from the outside into the roving. From the cross sections, it can be observed that the area of size attached to the surface of roving grows with an increase of temperature treatment, which implies that the absorption ability of the roving for the CMC size from wheat straw has been greatly promoted by the temperature.

The effect of plasticizer concentration

Adding glycerol, CMC molecules became liberating and stretching, increasing contact area among CMC and cotton fibers contributed to high adhesion. Figure 4 reveals that adhesion properties of glycerol-plasticized CMC synthesized sizes were higher than additive free CMC sizes at the same add-on and that increasing the concentration of glycerol (from 20 to 40 wt.% based on the weight of CMC) mainly affects the elongation at break of the rovings coated with the sizing agent.
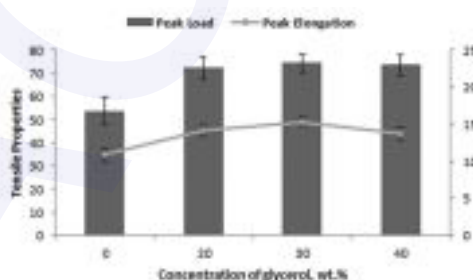
Figure 4: Influence of percent glycerol on tensile properties of 100% cotton rovings. 0-40 wt. % glycerol were added for preparation of sizing solutions. Sizing was done with a CMC concentration of 6% (w/v) and at 90°C for 5 min.

Elongation at break, also known as fracture strain, is the ratio between changed length and initial length after breakage of the test specimen. It expresses the capability of specimen to resist changes of shape without crack formation. And having the highest elongation at break shows that cotton roving coated by the glycerol plasticized CMC film provides a good extensibility which is required during the weaving process.

From figure 4, it is observed that the peak elongation of cotton roving coated with glycerol-plasticized CMC increased from 14.1% to 15.32% when plasticizer content increased from 20% to 30% and decreased from 15.32% to 13.76% when plasticizer content increased from 30% to 40%. However, there was no significant change in roving strength when increasing glycerol concentration from 20 wt.% to 40 wt.% although the

The Second Edition of the International Congress of Applied chemistry and Environment
30th-31th October and 01st November 2020, Tunisia

ICACE 2020

concentration of 30 wt.% shows a slight increase in roving strength. As a result, adding glycerol as a plasticizer agent to CMC synthesized size at a concentration of 30 wt.% provides the highest adhesion to cotton fibers by supplying the better strength and elongation of sized cotton rovings.

4. CONCLUSION

In this study, utilization of the newly tailored polymeric carboxymethyl cellulose from wheat straw product in sizing of cotton yarns was tested to assess their suitability as sizing agent. 100% cotton rovings samples were used to improve the adhesion of the polymer to cotton fibers. Influence of the size preparation conditions on the cohesiveness of rovings has been studied and results demonstrate that CMC synthesized is able to improve the tensile properties and abrasion resistance of their coated (sized) cotton materials.

Use of CMC from wheat straw for warp yarn sizing will result in value addition to wheat straw agricultural by-product and thus benefit agriculture, textiles and the environment.

REFERENCES

[1] **Goswami B.C., Anandjiwala R.D., Hall D**., Textile sizing: CRC press, 2004.

[2] **Oun A.A., Rhim J.W.**, Isolation of cellulose nanocrystals from grain straws and their use for the preparation of carboxymethyl cellulose-based nanocomposite films, *Carbohydrate polymers,* 2016, Vol.150, 187-200.

[3] **Santana-Méridas O., González-Coloma A., Sánchez-Vioque R**., Agricultural residues as a source of bioactive natural products, *Phytochemistry reviews,* 2012, Vol.11, 447-66.

[4] **Kapoor M., Panwar D., Kaira G.**, Bioprocesses for Enzyme Production Using Agro-Industrial Wastes: Technical Challenges and Commercialization Potential, *Agro-Industrial Wastes as Feedstock for Enzyme Production: Elsevier*, 2016, 61-93.

[5] **El Aribi N., Maatoug S., Zouari R., Majdoub, H., Cheikhrouhou M.**, Carboxymethylcellulose preparation from wheat straw; effect of degree of substitution on rheological properties, *International journal of applied research on textile*, 2019, 51-57.

[6] **Toğrul H., Arslan N.**, Production of carboxymethyl cellulose from sugar beet pulp cellulose and rheological behaviour of carboxymethyl cellulose, *Carbohydrate Polymers*, 2003, Vol 54, 73-82. [7] **Yeasmin M.S., Mondal M.I.H.**, Synthesis of highly substituted carboxymethyl cellulose depending on cellulose particle size, *International journal of biological macromolecules,* 2015, Vol 80, 725-731. [8] **Golbaghi L., Khamforoush M., Hatami T.**, Carboxymethyl cellulose production from sugarcane bagasse with steam explosion pulping: Experimental, modeling, and optimization, *Carbohydrate polymers*, 2017, Vol 174, 780-788.

[9] **Wüstenberg T**., Cellulose and cellulose derivatives in the food industry: fundamentals and applications, *John Wiley & Sons*, 2014.

Transformation of waste engine oil into fuel by pyrolysis

Youghourta Zerdane[a,b,c]**, Jean-François Largeau**[a,b]**, Naim Akkouche**[b]**, Hachemi Madjid**[c]**,**

MohandTazerout[b]

(a)   Icam, 35 rue du Champ de Manœuvres, 44430 Carquefou, France
(b)   GEPEA- CNRS UMR 6144, IMT Atlantique, Nantes, 44000. France
(c) LEMI Laboratory, University of Boumerdes, Independence Avenue, 35000 Boumerdes.Algeria
youghourta.zerdane@icam.fr

ABSTRACT

The conversion of waste engine oil into products similar to conventional fuel was studied in this work. The oil pyrolysis experiment was carried out at atmospheric pressure in a discontinuous cylindrical reactor, ranging from room temperature to 650 °C, with a heating rate of 10 °C /min. The products obtained consist mainly of liquid (86.77 %), gas (10.44 %) and solid (3.52 %). The analysis of these fractions was studied by Fourier transform infrared spectroscopy (FTIR) for the liquid and by micro-gas chromatography (Micro GC) for non-condensable gases. Liquid analysis results have indicated the presence of naphthenic and aromatic hydrocarbons which confirm and justify its potential application as an alternative fuel. The gases produced are essentially composed of ethylene, propylene, butenes, methane, H2 and CO; represent chemical raw materials and energy sources of great value.

KEYWORDS: Waste oil, Conversion, Pyrolysis, Alternative fuel, Energy

1. INTRODUCTION

The waste engine oils generated mainly by the automotive sector whose annual production was estimated at 24 million tones worldwide [1], represent a great danger for the environment. After its use, the oil becomes contaminated by the remaining products of the additives added for the new oil and by the products resulting from degradation during its use. The presence of heavy metals, phenols, polycyclic aromatic hydrocarbons and other contaminants threatens human health and represents a great ecological danger [2]. According to experts « one liter of waste oil can pollute a million liters of water ». The elimination of this waste becomes a challenge for modern society. The strategies adopted to manage this effluent different from one country to another, conventionally the techniques used are, incineration to produce heat, vacuum distillation and hydro-treatment for re-refining However, these pathways become increasingly less important because of their environmental impact and the poor quality of the products obtained [3]. Therefore, several studies have been made to develop other techniques such as transformation of these oils in alternative fuel through a thermally by removal process called pyrolysis. This technique is very promising with major environmental and economic interests [4].

Pyrolysis is a thermochemical process that involves the decomposition of organic matter using heat in an inert atmosphere, it allows to obtain three fractions: gaseous, liquids, solids, can be used as fuels or for other applications [5]. The yield of the products depends on the operating conditions such as the temperature, the residence time, the heating rates, the humidity and the composition of the load.

In this study, used engine oil is pyrolysed in order to produce a fuel. The yield and composition of the liquid and gaseous fractions obtained are studied.

2. MATERIAL AND METHODS

The Second Edition of the International Congress of Applied chemistry and Environment
30th-31th October and 01st November 2020, Tunisia

ICACE
2020

The waste oil used in this experiment is a mixture of the lubricating oils of automobile engines. Before the pyrolysis reaction, the oil sample undergoes a pretreatment by filtration using a vacuum filtration device using a WHTMAN brand filter to remove metallic particles, soot and other impurities.

The pyrolysis experiment was carried out at atmospheric pressure in a discontinuous stainless steel reactor with the following dimensions (06 cm in height and 4.8 cm in diameter). The reactor was heated by an electrical system. The temperature was controlled and monitored by a thermocouple placed in the center of the reactor and connected to a PID temperature regulator of STATOP 48-49 brand. At the start of the experiment, the system was purged of air using nitrogen N2 with a flow rate of 20 ml / min. The gas vapors produced was condensed on passage through a condenser cooled with a refrigerating fluid at 15 °C. The non-condensable gases are collected in a gas sampling bag. The reaction was carried out with a heating rate of 10 °C /min and the set temperature was set at 650 °C, at this temperature the reaction was maintained for 30 min. The liquid products obtained are analyzed by Fourier transform infrared spectroscopy (FTIR) of the Perkin Elmer Spectrum-two brand and the characterization of the non-condensable gases was carried out by micro-gas chromatography (Micro-GC) of the Agilent 3000-A brand.

3. RESULTS AND DISCUSSIONS

3.1. Yield of products obtained:

The pyrolysis products obtained consist of three fractions: liquid, solid and gaseous as shown in figure 1. The liquid product represents the large quantity produced with a yield of (86.77 %) compared to the gas with (10.44 %) and the solid (3.52 %). These results are in agreement with the yields of liquids from pyrolysis observed in previous work [6]. The high yield of this liquid fraction is very important for future use as an alternative liquid fuel.
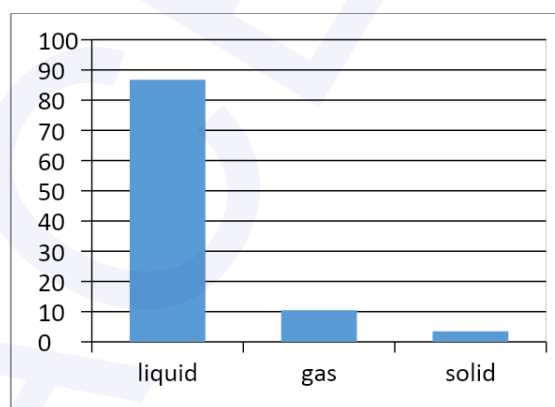
Figure 1: The fractions produced from the pyrolysis of the waste oil

3.2. Composition of non-condensable gases:

The composition of the non-condensable gases from pyrolysis is given in Table 1. The main compounds are hydrocarbons consisting mainly of alkane, ethylene, propylene, butenes. In addition, the presence of hydrogen with a significant amount (12.50 %), presents a valuable potential source of synthesis gas [5]. This is in agreement with the work of S.S Lam and all [5]. given the probable use of this gas in the future, the presence of CO_2 in considerable quantities will be very harmful [5]. These results show the very high chemical value of these pyrolysis gas compounds.

Table 1: Composition of non-condensable gases

Elements	Composition in %
H2	12,50
CH4	14,66
CO	2,87
CO2	15,14
C2H4	10,65
C2H6-C2H2	13,30
C3H6-C3H8	12,85
C4H8	16,71
C4H10	1,31
total	100%

3.3. Results of the FTIR:

FTIR analysis is a technique used for the characterization of pyrolysis products [7]. The spectra obtained are represented in Figure 2.

In the wavelength range 2922.9, 2854.3 and 1458.4 cm^{-1} we observe high intensity peaks which corresponds to methyl hydrogen in aromatic configuration [3]. On the other hand, the medium intensity peaks centered on 2955.1 and 1639.9 cm^{-1} showed a naphthenic configuration as well as the stretching vibration of the methylene chain CH. In the range 1458 and 720.1 cm^{-1} we observe centered peaks which presented acids, ketones and aldehydes [3].

Figure 2: FTIR spectrum of pyrolysis liquid

The Second Edition of the International Congress of Applied chemistry and Environment
30th-31th October and 01st November 2020, Tunisia

ICACE 2020

4. CONCLUSION

In this study, waste engine oils were converted to liquid pyrolysis products, gas and solid residue. In terms of yield, a considerable fraction of pyrolytic liquid was recovered (86.77%) compared to the gaseous fraction (10.44 %) and the solid residues (3.52 %).The presence of aromatics and naphthenic hydrocarbon compounds in the pyrolysis liquid was highlighted by the FTIR analysis. The characterization of non-condensable gases was carried out by a gas-phase micro-chromatograph which showed the presence of very interesting compounds such as ethylene, propylene.

In the end, this process allowed us to transform this hazardous waste that is not respectful of the environment into a potential resource of energy from hydrocarbons and hydrogen and which also has economic advantages.

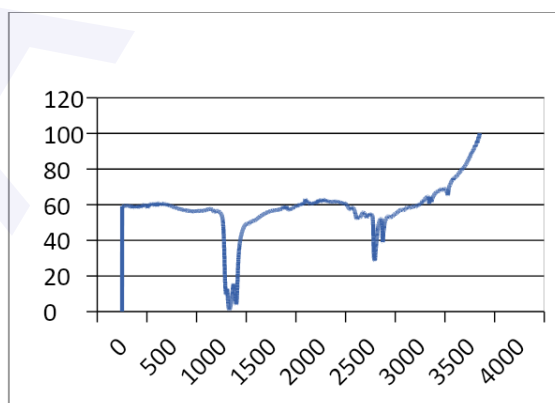The presence of CO_2 in the pyrolysis gases considered as a harmful element can be eliminated by gas treatment processes such as amine washing.

As perspectives, A GC-MS gas chromatographic characterization accompanied by an analysis of the physico-chemical parameters (viscosity, density) and of the calorific power as well as the flash point of the pyrolysis liquid obtained is planned in our next research work.

New pyrolysis tests with new catalysts are planned in order to optimize the yield and improve the quality of the products obtained.

REFERENCES

[1] **M. F. Gómez-Rico, I. Martín-Gullón, A. Fullana, J. A. Conesa, and R. Font**, Pyrolysis and combustion kinetics and emissions of waste lube oils , *Journal of Analytical and Applied Pyrolysis*, 2003, vol. 68-69,527-546.

[2] **R. Maceiras, V. Alfonsín, and F. J. Morales**, Recycling of waste engine oil for diesel production, *Waste Management*, 2017, vol. 60, 351-356.

[3] **I. Ahmad and al.**, Valorization of spent lubricant engine oil via catalytic pyrolysis: Influence of barium-strontium ferrite on product distribution and composition, *Journal of Analytical and Applied Pyrolysis*, 2016, vol.122, 131-141.

[4] **Geum-Ju Song, Yong-Chil Seo, Deepak Pudasainee and In-Tae Kim**, Characteristics of gas and residues produced from electric arc pyrolysis of waste lubricating oil, *Waste Management,* 2010, vol.30, No.7, 1230-123.

[5] **S. S. Lam, A. D. Russell, C. L. Lee, S. K. Lam, and H. A. Chase**, Production of hydrogen and light hydrocarbons as a potential gaseous fuel from microwave-heated pyrolysis of waste automotive engine oil, *International Journal of Hydrogen Energy*, 2012, vol. 37, No.6,5011-5021.

[6] **Y. Zouad, L. Tarabet, K. Khiari and R. Mahmou**, Effect of heating rate and additives (MgO and Al2O3) on a diesel like-fuel issued from waste engine oil pyrolysis, *Petroleum Science and Technology*, 2019, Vol.37, No.10, 1184-1193.

[7] **V. Tihayet P and Gillard**, Pyrolysis gases released during the thermal decomposition of three Mediterranean species , *Journal of Analytical and Applied Pyrolysis*, 2010,vol. 88, No.2,168-174.

Investigation of the effect of olive mill wastewater sludge biochar on seed germination and soil amendment

Salma MSEDDI [a,b], Wejdene Ben Chelbi [a], Kamel HALOUANI [b,c], Monem KALLEL[a]

(a) Laboratory of Environmental Engineering and EcoTechnology (GEET), ENIS, University of Sfax, Tunisia
(b) UR13ES76: Micro Electro Thermal Systems (METS), ENIS, University of Sfax, Tunisia
(c) Digital Research Center of Sfax, Technopole of Sfax, PO Box 275, Sakiet Ezzit, 3021 Sfax – Tunisia
E-mail: mseddi.salma@gmail.com

ABSTRACT

Olive mill wastewater (OMW) management is currently considered as an imperative challenge for the olive oil industry due to its high pollution potential. In this context, thermal treatment by pyrolysis seems to be a promising technique to valorize the olive mill wastewater sludge (OMWS).The fast pyrolysis of this organic biomass leads to the production of biochar with interesting physic-chemical characteristics for soil amendment. Indeed, biochar is recently advocated in agricultural applications for improving soil quality; therefore, its agronomic add-value was investigated. In this work, the assessment of the effects of biochar, from OMWS pyrolysis, on seeds germination was investigated before its application on soil. The germination test for different materials used, showed interesting results (one day for the mean germination time) but the use of biochar only, inhibits the germination of seeds. These results correlated with the application of biochar on soil which improve the soil amendment and germination of seeds.

KEYWORDS: Olive mill wastewater Sludge (OMWS), Biochar, Germination, Soil amendment

1. INTRODUCTION

The investigation has been established to find an environmentally friendly strategy for the valorization of olive mill wastewater (OMW). In fact, due to their serious impact on the environment, different technologies and treatments methods (physical, chemical and biological processes) of OMW have been developed and tested. The thermal treatment seems to be a promising technique to benefit from the energy content of the OMW [1]. In particular, pyrolysis has the advantage to produce gaseous, liquid and solid products that could be recovered in different manners. The solid product called "biochar" can be used for energy production, activated to be an efficient adsorbent or it can be used for soil amendment [2]. The practice of soil amendment with biochar has received increased attention thanks to its potential to sequester carbon, improve the biological activities of the soil, improve the chemical properties such as retention capacity of nutrients and also improve the holding capacity of water retention [3]. However, Igalavithana et al., [4] showed that the capacity of a biochar to enhance soil is determined by the biomass feedstock and the pyrolysis operating conditions during the production of the biochar; therefore, different steps were used and experimentally proved during this research. First of all, the monitoring of the fast pyrolysis of olive mill wastewater sludge (OMWS), and then a preliminary evaluation of biochar (physicochemical properties).After that, the evaluation of the effects of biochar on seeds germination and plant growth were investigated.

2. MATERIAL AND METHODS

The biochar was produced by slow pyrolysis in a fixed bed reactor at 600°C. The biomass feedstock was converted to biochar via a Tunisian carbonization process using the pilot plant. The apparatus includes two metallic carbonization chambers connected to a combustor of the recycled carbonization fumes by two insulated gas channels. The combustor was connected to a heat exchanger permitting to heat the two carbonization chambers by the combustion gases. The temperature of the carbonization chambers was controlled by a thermocouple connected to an air blower in the combustor inlet. The main properties of

biochar (pH, porosity, elemental composition) were determined. Mercury porosimetry analysis were carried out using an Autopore IV 9500 mercury porosimeter (Micromeritics, USA) for porosity characterization of the biochar sample. Elemental analysis of biochar was performed using a Vario Micro Elementar Carbon-Hydrogen-Nitrogen- Sulfur (CHNS) system.

To evaluate the application of biochar for soil amendment, two tests (germination test, pot growth) were performed to investigate the phytotoxicity of the different materials (soil/ biochar/OMWS) on seeds of sunflowers. The germination tests were performed according to Zucconi's test [5]. Later, these seeds were planted in pots filled with agricultural soil of CHAAL. The experimental protocol is at short time for two months. It consists of two treatments (control/soil with 1% biochar) with three replications of each treatment. Sunflower seedlings were chosen to be irrigated and evaluate the impact of amendment soil with biochar on these plants growth.

3. RESULTS AND DISCUSSIONS

3.1. Characterization of biochar

The characterization of biochar showed a basic pH, large porosity, high water retention capacity and low presence of heavy metal (table 1)

Table 1: Main properties of OMWS biochar

Parameters	value
Physical characteristics	
HCC (%)	37±0.02
Porosity (%)	58.54
Permeability (mdarcy)	6432±2.5
Chemical characteristics	
pH	7.8 ±0.03
EC (mS/cm)	2.03 ±0.02
OM (%)	0.3 ±0.05
Elemental analysis (%)	
MgO	1.13
AlO$_3$	1.11
SiO	5.01
PO	3.39
SO	5.04
KO	49.17
CaO	15.32
Fe O	2.20
Cl	17.01

3.2. Germination test

Table 2 shows the germination index (GI) of sunflower and phytotoxicity of soil, OMWS and biochar. GI value lower than 50% implies significant phytotoxicity, values ranging from 50% to 80% are related to moderate phytotoxicity. GI values over 80% suggest no phytotoxicity and values >100% demonstrate phytostimulation (Emino and Warman, 2004).

Table 2: Germination Index and phytotoxicity of different materials used

Materials	GI (%)	Phytotoxicity
Soil Chaal	148	Phytostimulant
OMWS	104	Phytostimulant
OMWS Biochar	55	Moderate phytotoxicity

These results of germination test correlated with the results showed in figure 1 and 2 showing the effect of the use of different materials respectively on the mean germination time of seeds and on the level mortality of seeds. As showed in figures 1 and 2, the biochar has an inhibitory effect on seeds germination due to the presence of organic and toxic compounds that they not be reduced under the permitted limits. Therefore, we should use a low dose of biochar in soil.

Figure 1.Effect of different materials on MGT of seeds   Figure 2.Effect of different materials on LMS of seeds
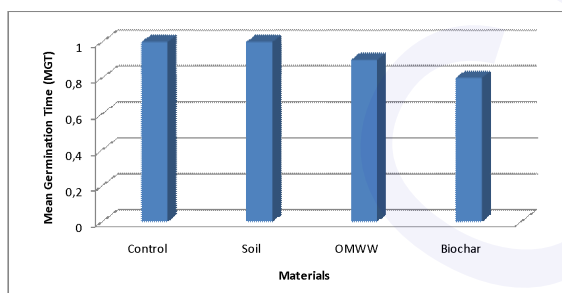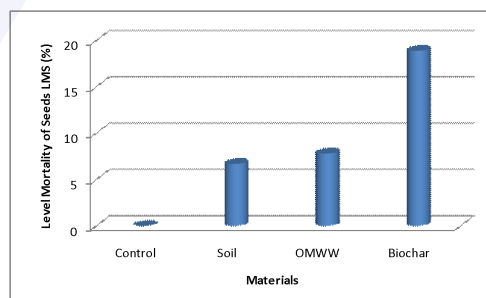
3.3. Pot growth

The application of biochar, as a bio-fertilizer, with the 1% dose, under controlled conditions, showed promising results, for the growth of sunflower seeds in terms of growth of stems of sunflowers and number of leaves (Figure 3)

Figure 3.Effect of the application of 1% biochar in soil on the number of leaves of sunflowers
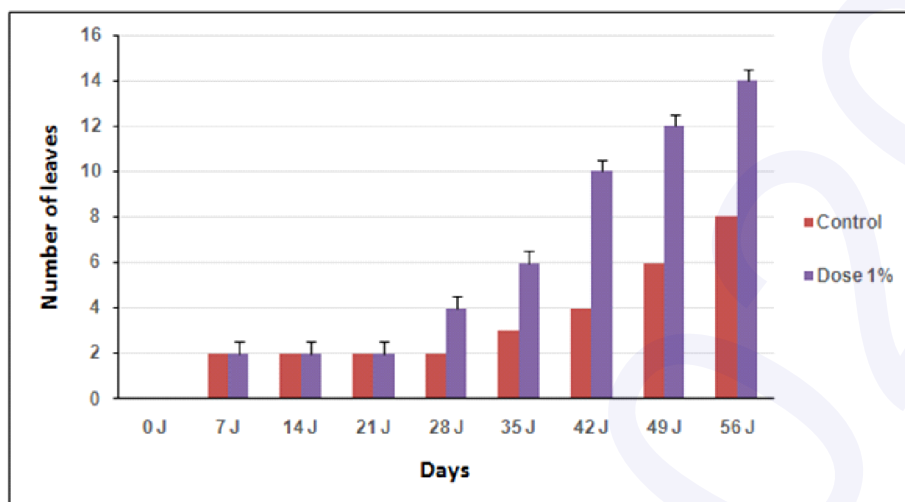
4. CONCLUSION

These preliminary results indicated the benefit application of biochar as soil amendment with low dose of 1%. The application of higher doses needs more investigation of the characterization of biochar and soil properties.

As perspectives, we need to realize a pilot studies for a better investigation of the parameters of the pyrolysis as well as the monitoring of the properties of the soil and the biochar as well as the parameters of the plants at long term.

REFERENCES

[1] Haddad K, Jeguirim M, Jerbi B, Chouchene A, Dutournié P, Olive Mill wastewater: from a pollutant to green fuels, agricultural water source and biofertilizer, *ACS Sustainable Chem.Eng.,* 2017,Vol.5,No.10, 8988-8996

[2] Guo M, He Z, Uchimiya SM, *Agricultural and Environmental Applications of Biochar: Advances and Barriers,* Soil Science Society of America, Inc., Madison, WI 53711, USA, 2016, 1-14

[3] Abel S, Peters A, Trinks S, Schonsky H, Facklam M, Wessolek G, Impact of biochar and hydrochar addition on water retention and water repellency of sandy soil, *Geoderma,* 2013, Vol.202-203,183-191

[4] Igalavithana AD, Ok YS, Usman ARA, Al-Wabel MI, Oleszczuk P, Lee SS, *Agricultural and Environmental Applications of Biochar: Advances and Barriers,* Soil Science Society of America, Inc., Madison, WI 53711, USA, 2016, 123-144

[5] Zucconi F, Monaco A, Forte M, Bertoldi, M. De., Phytotoxins during the stabilization of organic matter. *Composting of agricultural and other wastes,* 1985, 73–86

Experimental and Theoretical Investigation of Drying Behavior of Sewage Sludge

Hager HAJJI [a], Amira TOUIL [a]

(a)Université de Carthage, Institut Supérieur des Sciences et Technologies de l'Environnement de Borj Cédria, LR16ES09 Laboratoire de

Recherche des Sciences et Technologies de l'Environnement LRSTE; Tunisia

E-mail: amira.touil@gmail.com

ABSTRACT

The main objective of this paper is to formulate an accurate transport model analyzing the simultaneous transfers of heat and mass within sewage sludge slices. The volume shrinkage of the product is calculated and a linear relation was established to describe the experimental variation of shrinkage of the product versus its moisture content. Effective diffusion coefficient of moisture transfer was determined using the Fick law at three drying temperatures (60, 70, and 80∘ C). Equilibrium moisture contents decreased as the temperature increased. The GAB model fitted well the desorption isotherm data for sewage sludge slices with the monolayer moisture content depending on the temperature. The thin-layer convective and infrared drying behavior of sewage sludge was experimentally investigated in the temperature range from 50°C to 80°C. The drying rate was found to increase with temperature, thus reducing the total drying time. Based on the simultaneous heat and mass transfer, a mathematical model was proposed for predicting the temperature and moisture distribution in the drying sample, applying Fick diffusion equation. A numerical solution was developed for the proposed model using an implicit finite difference method in bi-dimensional system. The suggested model considers sludge deformation and determines the time and space evolutions of moisture, temperature and solid displacement within sewage sludge slices.

KEYWORDS : Sewage sludge, Drying, Heat and mass transfer, Modeling

1. INTRODUCTION

Tunisia, located in a more or less arid bioclimatic floor, has been working for several years to rationalize the exploitation of the country's natural resources (water, energy ...), in addition to the establishment of various mechanisms capable of solving the various problems in this area, including purification and wastewater treatment, tools that have proven their performance and their great utility in the agricultural sector. Currently more than 106 treatment plants have been set up in Tunisia and treat 238 million m3 annually of waste water. In 2013, the treatment plants in operation produced about 200 thousand m3 of dried sludge including 95 thousand m3 from treatment plants of Greater Tunis. [1-2]**.** Consequently, who says water purification also says sludge production. Yet in a firstly, the objective of these stations was essentially to guarantee the discharge of quality water defined with little concern for the sludge generated by the purification processes. Consequently, the management of the sludge produced will become a crucial question in the short term.

In this context, sludge drying is one of the possible solutions downstream of the stations, before the agricultural and/or thermal recovery. The drying of the sludge allows stabilization, increase the dryness by reducing the water content, also reduces their volume to consider recovery and disposal sectors. Several water treatment stations have different drying terms. Therefore, launch of projects by looking for the most economical, reliable and acceptable drying technologies. Before everything, the characterization study of the product behaviors is a more sensitive point to know to better achieve their renewal objectives.

We are interested in this work in the recovery by drying of water treatment sludge used such as a solar drier is a device for drying the sludge by air circulation heated, the energy supply is provided by the

solar. Drying is characterized by several parameters: the drying temperature, the drying speed, the exposure time, the size of the drying device, dryness rate (humidity rate), material characteristics absorbent, transparent and insulating

The main objective of this paper is to study the behavior of sewage sludge slices during drying and to formulate an accurate transport model analyzing the simultaneous transfers of heat and mass within sewage the product.

2. MATERIAL AND METHODS

Shrinkage of sewage sludge slices during drying is unavoidable because heating and removal of water from the product matrix may cause stresses in the structure, hence leading to structural collapse, changes in volume, shape deformation, and capillaries contraction. Ideally, it can be considered that the shrinkage of the material is equal to the volume of the removed water. Therefore, a parametric relationship can be obtained which relates the volume shrinkage to the moisture content of the material. The equilibrium relation between the apparent density of the product and its moisture content was investigated by means of an apparatus based on Archimedes's law. The volume of the sample is determined by measuring the difference in weight of that sample above and under water.

Desorption isotherms were determined using a static gravimetric method at four temperatures: 40∘C, 50∘C, 60∘C and 70∘C over a relative humidity range of 5–90%.

The Clausius–Clapeyron equation was used to evaluate the net isosteric heat of water desorption by using the GAB theoretical model in the studied temperature range.

The convection drying was carried out using a convective dryer while the infrared drying was carried out using an IR moisture analyzer (MB35). Effective diffusion coefficient of moisture transfer was determined using the Fick law at three drying temperatures (60, 70, and 80∘ C).

3. RESULTS AND DISCUSSIONS

3.1. Physico-chemical and Thermodynamic characterization

Fig. 1 shows the experimental variation of the specific volume versus the average moisture content of sewage sludge slices. The specific volume varies linearly versus product moisture content. This linear evolution corresponds to a total shrinkage, which means that the volume loss is equal to the volume of removed moisture (Fig.2). Similar results are found for other products [3-5].
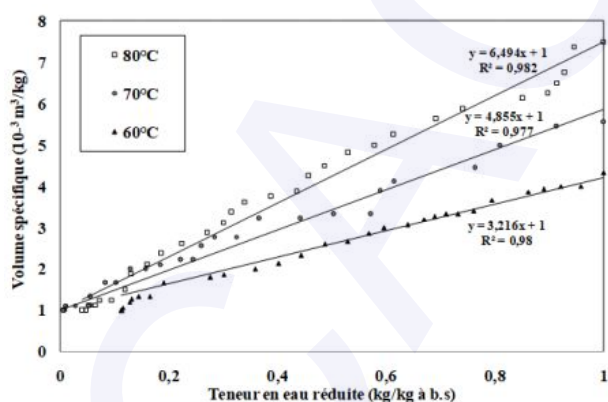
Figure 1: Specific volume versus product moisture content
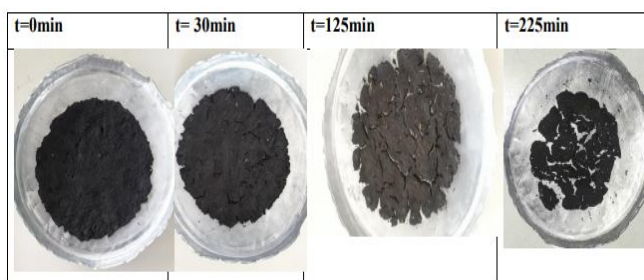
Figure 2: Shrinkage of sewage sludge slices

The desorption isotherms curves (Fig. 3) exhibited type II behavior, according to Brunauer's classification. Equilibrium moisture contents decreased as the temperature increased. The GAB model (Fig. 3) fitted well the desorption isotherm data for sewage sludge slices with the monolayer moisture content depending on the temperature.
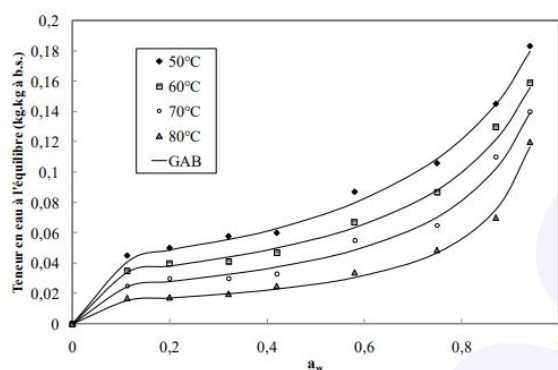
Figure 3: Desorption isotherms fitted by GAB Model

The net isosteric heat and the differential entropy decreased strongly as the moisture content increased respectively.

3.2. Drying curves

The thin-layer convective and infrared drying behavior of sewage sludge was experimentally investigated in the temperature range from 50°C to 80°C. The drying rate (Figs. 4 and 5) was found to increase with temperature, thus reducing the total drying time.
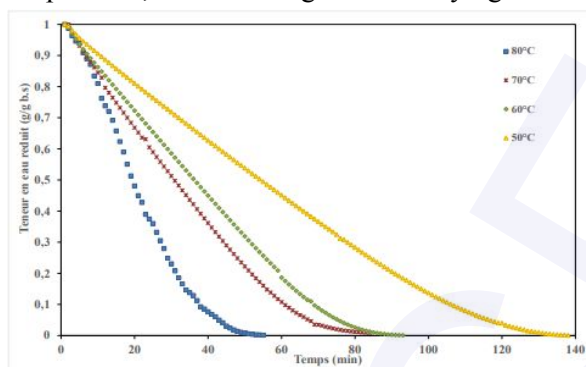
Figure 4: Water content versus time drying
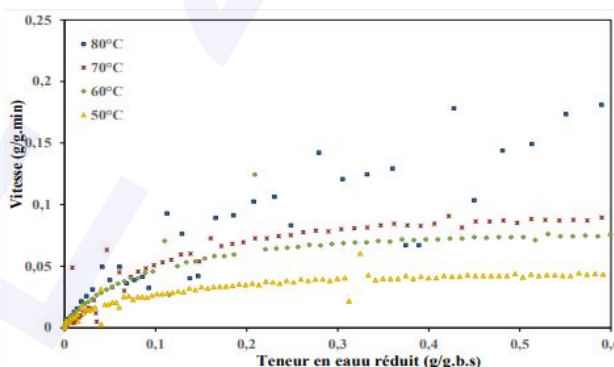
Figure 5: Drying kinetics

3.3. Effective Moisture Diffusivity

Using experimental drying data, the logarithm of moisture content is plotted against time for different air temperatures and in each case the moisture diffusivity is estimated by using the slopes derived from the linear regression of the ln(w) against time. Analysis of the experimental data revealed the existence of linear relationships between these parameters. Results of Effective Diffusivities and Activation Energies are shown in table 1.

Table 1. Effective Diffusivities and Activation Energies of sludge during convective and infrared drying

	T (°C)	Infra-red drying	Convective drying
Dffective Diffusivity x 10^{-9} (m²/s)	50	5,025	3,36
	60	7,65	3,77
	70	9,3	3,8
	80	13,9	6,24
Activation Energy (kJ.mol^{-1})		27	1,55

3.4. Mathematical modeling

Based on the simultaneous heat and mass transfer, a mathematical model was proposed for predicting the temperature and moisture distribution in the drying sample, applying Fick diffusion equation.

A numerical solution was developed for the proposed model using an implicit finite difference method in bi-dimensional system.

The macroscopic equations governing heat and mass transfers in the cubic porous slab are summarized as follows:

Mass balance equation: $\rho_s \left(\frac{\partial w}{\partial t} + V_s \vec{grad}(w) \right) = Div(\frac{\rho}{1+w} D\vec{grad}(w))$ (1)

Energy balance equation: $\rho c_p \frac{\partial T}{\partial t} + V_s \vec{grad}(\rho c_p T) - \frac{D}{1+w} \vec{grad}(w).\vec{grad}(\rho c_p T) = div(\lambda_s.\vec{grad}T)$ (2)

To solve the set of equations, we have used the commercial finite element solver COMSOL 5.

The suggested model considers sludge deformation and determines the time and space evolutions of moisture, temperature and solid displacement within sewage sludge slices. (Figs 6 and 7).
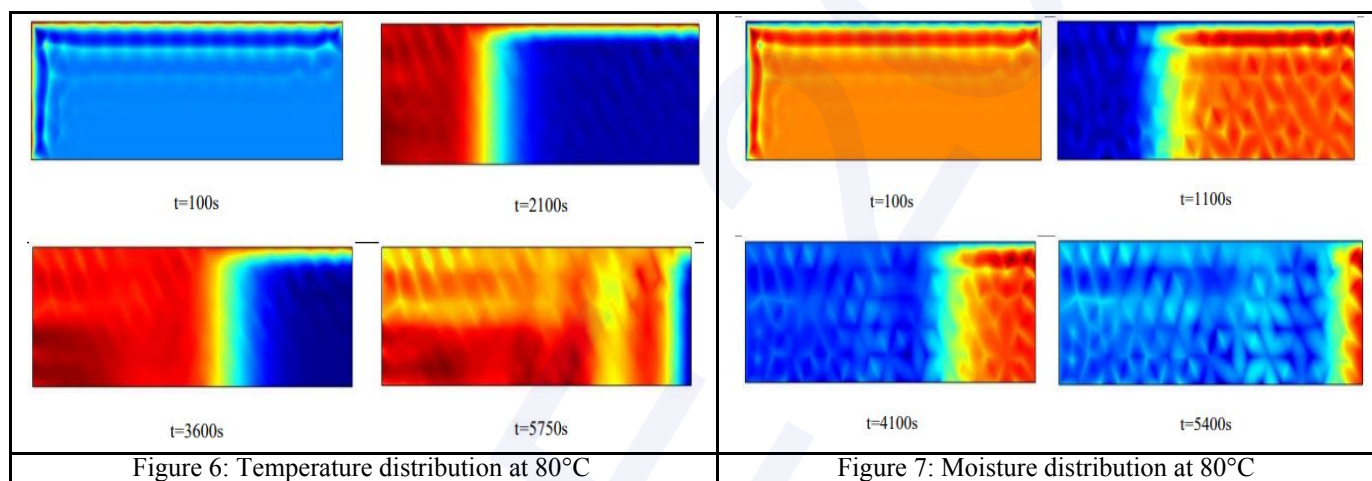
t=100s	t=2100s	t=100s	t=1100s
t=3600s	t=5750s	t=4100s	t=5400s
Figure 6: Temperature distribution at 80°C		Figure 7: Moisture distribution at 80°C	

4. CONCLUSION

At the end of this study, we have been study of the physico-chemical and thermal behavior of sludge under the effect operating conditions for a drying process were carried out via: The establishment of sorption isotherms and dehydration kinetics during the drying process of the sludge applied in different operating conditions to be able to analyze the different phases. Fine modeling of coupled mass and heat transfers during drying assuming the mud is a saturated porous medium. It's a simulation approach and overall digital optimization of the process based on a physical drying model.

REFERENCES

[1] ONAS ; rapport annuel 2013.

[2] **Rayen Slim**, *Etude et conception d'un procédé de séchage combiné de boues de stations d'épuration par énergie solaire et pompe à chaleur*, thèse de doctorat, Ecole des Mines de Paris.

[3] **D. Mihoubi, S. Timoumi, and F. Zagrouba**, Modelling of convective drying of carrot slices with IR heat source, *Chemical Engineering and Processing*, vol. 2009, Vol.48, No. 3, 808–815.

[4] **A. Talla, J.-R. Puiggali, W. Jomaa, and Y. Jannot**, Shrinkage and density evolution during drying of tropical fruits: application to banana, *Journal of Food Engineering*, 2004, Vol. 64, No. 1, 103–109.

[5] **M. E. Katekawa and M. A. Silva**, A review of drying models including shrinkage effects, *Drying Technology*, 2006, Vol. 24, No. 1, 5–20.

Cellulose from Tamarix Aphylla as biosorbent for cadmium ions removal

Islem M'barek[a,c] , **Hela Slimi**[a], **Younes Moussaoui**[b,c]

(a) Material, Environment and Energy Laboratory (UR14ES26), Faculty of Sciences of Gafsa, University of Gafsa, Tunisia.
(b) Organic Chemistry Laboratory (LR17ES08), Faculty of Sciences of Sfax, University of Sfax, Tunisia.
(c) Faculty of Sciences of Gafsa, University of Gafsa, Tunisia.
E-mail: y.moussaoui2@gmx.fr.

ABSTRACT

Cadmium ions were retention from an aqueous solution onto biosorbent which is cellulose isolated from Tamarix aphylla's stem. The structural proprieties of the used biopolymer was determined by SEM and FTIR. Then the adsorption process was done with optimization of pH and time contact, concentration of cadmium on aqueous solution, the amount of cellulose. After optimization an isotherms modelizations were carried out by Langmuir, Freundlich, Temkin and Dubinin-Radushkevichhe models. The freundlich was described as the most suitable for cadmium ions adsorption. Physi-chemical sorption of cadmium ions may be taken place and it could explain by the pseudo-second order model was carried out to control and evaluate the adsorption process.

KEYWORDS : biosorbent, cellulose, cadmium, adsorption.

1. INTRODUCTION

For this work, we interested to isolate cellulose fiber from the stem of Tamarix aphylla. This plant available worldwide [1] and it belongs to the family of Tamaricaceae, adapt simultaneously in desert, sand and also alluvial saline soil [2]. We success to get rid of the cellulose and its properties were determined subsequently by FTIR, MEB. Afterward, this cellulose was used as biosorbent to eliminate the cadmium ions from the contaminated water. Different parameters which influence on the adsorption process efficiency were examined. Because the cadmium metal is categorized as non-biodegradable waste rejected over and over again by the industry, so its elimination is obligation for the environment safety. For decades, many sorbent were used for this purpose, indeed there are a huge number of studies on the potential of biosorbents for removal of cadmium ions [3]. The best of our knowledge, there is no research pursues the cadmium ions adsorption using as a sorbent the cellulose isolated from Tamarix aphylla's stem. So that this is the main lines of our research work.

MATERIAL AND METHODS

The Tamarix aphylla were used as a raw material. The removing of cadmium ions from an aqueous solution was carried out by mixing this solution with the biosorbent (cellulose). The cadmium ions concentration in the solution was measured by flame atomic absorption spectroscopy (Varian 220 AA) .After adsorption experiments, the equilibrium adsorption capacity Q_{ads} (mg g^{-1}) was calculated according to Eq. (1)

$$Qe = \frac{(c0-ct)*v}{m}$$

where C_0 and C_t (mg L^{-1}) are concentrations of cadmium ions in aqueous solution at the initial and equilibrium respectively, V (L) is the volume of the solution, and m (g) shows the biosorbent weight

All chemicals reagents (Acetic acid glacial, Sodium chlorite and Sodium hydroxide) were purchased from System Chem AR and Sigma–Aldrich and used without further purification.

2. RESULTS AND DISCUSSIONS

2.1. Cellulose proprieties

The visual observation as shown below in the figure1 improve the pure white colour of cellulose which confirmed the homogeneity texture by SEM micrographs (Figure2), in addition the SEM showed an important porous surface of cellulose. The infrared spectra below (Figure3) identified the specifics groups of cellulose mainly the hydroxide one in 3400 cm $^{-1}$ and the C-O-C link on bond around 890 cm $^{-1}$

2.2. Adsorption parameters optimization

The adsorption sorption capacity Q_{ads} had the highest value 140 mg/g in an acidic medium along a large period of time (1200min) , also an important cadmium ions concentrations 40mg/l and a modest cellulose amount 0.04g enhance the cellulose's efficiency to remove the cadmium ions Cd^{2+}

2.3. Adsorption isotherms and kinetic studies

The Freundlich model seems as the best model which describes the adsorption process according to the value of R^2 (0.97) which is the higher value comparing of that of the other three isotherms Langmuir, Dubinin–Radushkevich and Temkin as shown below in the table1. Comparing to the value of R^2 (0.999) for the pseudo-second-order and that of pseudo-first order (0.927). We may conclude that the adsorption of cadmium follows the pseudo-second order model

Figure 1: Visual observation of Cellulose

Figure 2: SEM micrograph of cellulose

W avenumber(cm^{-1})
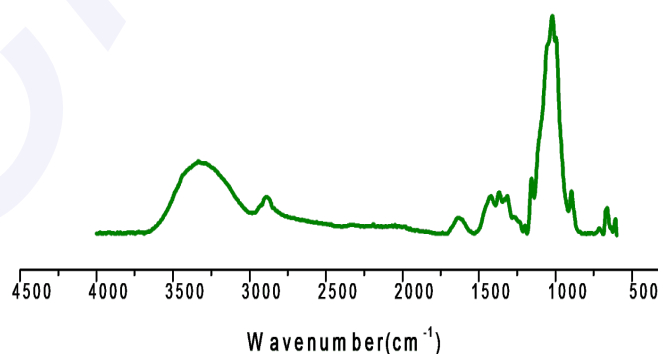
Figure3: FTIR Spectra of cellulose

Table 1: Adsorption isotherms models

	Freundlich	Langmuir	Temkin	Dubinin–Radushkevich
R^2	0.977	0.91	0.926	0.719

2.4. Equations and unit

Equilibrium adsorption capacity Q_{ads} where C_0 and C_t (mg L^{-1}) are concentrations of cadmium ions in aqueous solution at the initial and equilibrium respectively, V (L) is the volume of the solution, and m (g) shows the biosorbent weight

$Qe= \frac{(c0-ct)*v}{m}$ Eq. (1)

Pseudo first order and Second order are respectively Eq2 and Eq3

$. Ln(Q_e - Q_t) = Ln(Q_e) - k_1 t$ Eq. (2)

$t/q_t = 1/k_2 q^2_{ads} + 1/q_{ads}$ Eq. (3)

3. CONCLUSION

Visual observation and SEM microscope were followed to describe the morphology of cellulose, its structural chemical groups were determined by infrared spectroscopy. Then it was used for cadmium ions removal from contaminated water without any chemical modification or surface activation. The equilibrium adsorption capacity was Q_{ads} 120 mg g^{-1} with moderation various operatories conditions. The best parameters were an acidic medium pH around 4, with0.04g of cellulose amount and a cadmium ion concentration 40mg/L along 1200 min. The freundlich isotherm and second-pseudo order are the more followed suitable models for cadmium ions retention. To put it briefly, cellulose has an important potential as biosorbent for cadmium ions removal and the obtained absorption results were very encouragement.

REFERENCES

[1] **M.K. Saad, R. Khiari, E. Elaloui, Y. Moussaoui**, Adsorption of anthracene usingactivated carbon and Posidonia oceanica, *Arab. J. Chem*, 2014,7, 109–113.

[2] **Mohamed A.A. Orabi, Shoko Taniguchi, Susumu Terabayashi, Tsutomu Hatano,** Hydrolyzable tannins of tamaricaceous plants. IV: micropropagation and ellagitannin production in shoot cultures of Tamarix tetrandra, *Phytochemistry*, 2011,72, 1978-1989.

[3] **Hayes, W.E., Walker, L.R. Powell**, Competitive abilities of *Tamarix aphylla* in southern Nevada E.A. *Plant Ecol,* 2009, 202, 159-167.

Sustainable processes and clean technologies

The Second Edition of the International Congress of Applied chemistry and Environment
30th-31th October and 01st November 2020, Tunisia

ICACE 2020

Ecological dyeing of atmospheric pressure plasma-treated polyester fabric using Logwood dye

Najla Krifa[a], **Wafa Miled**[a], **Riadh Zouari**[a], **Behary Nemeshwaree**[b], **Christine Campagne**[b], **Morshed Cheikhrouhou**[c]

(a)   Textile engineering laboratory, Ksar Hellal, B.P 68 Ksar Hellal 5070, Tunisia
(b)   ENSAIT, GEMTEX, F-59100 Roubaix, France
(c)   Higher Institute of Arts and Crafts of Sfax, Sfax, Tunisia
E-mail: krifa_najla@hotmail.com

ABSTRACT:

A plasma-treated polyester fabric was padded without and with an ecofriendly formaldehyde-free acrylate binder using Logwood as a natural dye. The effect of plasma treatment was characterized using zeta potential measurements and chemical quantification assessment using TBO dye. The resulting dyeing performances were compared in terms of color strength and fastness properties according to standard methods. Experimental results revealed that plasma pretreatment enhance the color strength of the dyed polyester fabric due to the incorporation of new oxygen containing polar functional groups on its surface under plasma discharge. In addition, significant color strengths were noted while combining plasma treatment and acrylate binder ensuring the best improvement in color strength values and offering remarkable fastness properties (4/5).

KEYWORDS: Polyester, Logwood, plasma treatment, ecofriendly, dyeing performance.

1. INTRODUCTION

Shifting toward natural bio-based dyes for coloration in textile manufacturing and finishing processes is becoming a straightforward step to overcome synthetic dyes defects. Indeed, synthetic dyes are harmful for the environment since they contain several heavy metals, chromium substances, and some auxiliary chemicals, which are very polluting causing health problems and contaminating ecosystems and water sources [1].

Thus, reviving interest once again on natural colorants is being needed as natural dyes are usually renewable, bio-degradable and eco-friendly [2].

Recently extensive research works are being carried out on application of natural dyes to textile substrates. A new approach is being investigated to reduce duration, chemical composition and to improve the dyeability performance of natural dyes on several fabrics. To achieve this purpose, implementation of plasma technology is gaining a strike interest as being a competitive solution to conventional wet-chemical treatments. Plasma technology is a suitable surface modification technique that does not require the use of water and chemicals, used to enhance functionality and attributes of polymers such as polyester [3]. A plasma is a partially ionized gas where positive and negative ions, electrons, and radicals react and collide. All these excited species can interact with the uppermost atomic layers of the material surface leading to new reactive species formation [4]. Thereby, new functional sites needed for the attachment of natural dyes molecules to the surface of the fibers are produced.

Thus, the aim of this study is to investigate the dyeing performances of polyester fabric without and with different ecofriendly treatments based on PET surface modification using plasma and/or formaldehyde-free acrylate binder, using pad-dyeing technique in order to reduce excessive water, time and chemicals consumption used under exhaust dyeing processes [5].

2. MATERIAL AND METHODS

2.1. Materials and Chemicals

A 100% polyester woven fabric (PET) of a density of 208 g/m² and a thickness of 0.415 mm was used throughout this study.

The Second Edition of the International Congress of Applied chemistry and Environment
30th-31th October and 01st November 2020, Tunisia

ICACE 2020

Bio-based materials Logwood (Haematoxylum campechianum L.) was received from Couleurs de plantes (France). Acrylic binder free of formaldehyde (Dicrylian AC-01) was purchased from Huntsman Corporation and Ortho Toluidine Blue (TBO) was obtained from sigma Aldirich. The cited chemicals were of analytical grade and they were used as received.

2.2. Plasma treatment

The plasma treatment was carried out using air atmospheric plasma machine Coating Star (Ahlbrandt System, Germany). The following machine parameters were kept constant: electrical power of 1 kW, frequency of 30 kHz, ceramic electrode length of 0.5 m and inter-electrode distance of 1.5 mm. The speed was set to 2 m/min and the power to 1000 W corresponding to a treatment power of 60 kJ/m². Each side of the fabric was treated twice.

2.3. Surface characterization of fabrics

For the assessment of the effectiveness of surface activation process, zeta potential was measured by streaming potential measurements using Zetacad equipment. Furthermore, the cationic dye Ortho Toluidine Blue TBO was used to estimate by a staining method the amount of new active groups incorporated on the fabric surface following plasma treatment [6].

2.4. Pad-dyeing procedure

PET fabrics were padded with a dye solution (50 mL, pH5) combining logwood dye (20 g/L) and acrylate binder at different concentrations (0, 20, 50 g/L). The dyed samples were then dried and cured at 160°C for 3 min. Subsequently, the dried samples were washed using a commercially nonionic detergent at 40°C for 20 min and then rinsed in soft water and left to air dry under ambient conditions.

2.5. Color measurements of dyed samples

Spectral reflectance factors were measured using a Datacolor Spectraflash SF600 reflectance spectrophotometer (Datacolor International). K/S values were automatically calculated using the Kubelka-Munk equation [7]:

$$\frac{K}{S} = \frac{(1-R)^2}{2R}$$ (1)

Where R is the reflectance of the dyed fabric at the maximum absorption wavelength, S is the scattering coefficient, and K is the absorption coefficient of the dyed fabrics.

2.6. Fastness properties: Wash and rub fastness

The wash fastness test was assessed using the standard ISO 105:C10 wash fastness test protocol. The change in shade and the degree of cross staining were assessed visually using grey scales. The rub fastness test was assessed using the standard ISO 105:X12 where samples were placed on the base of a crockmeter. The staining on the cotton sample was assessed using grey scale. In addition to dry rub fastness, wet rub fastness was tested.

3. RESULTS AND DISCUSSIONS

3.1. Zeta potential and carboxylic groups evaluation of plasma treated polyester fabric

Zeta potential results presented in Table 1 proved that the global charge of the polymer material have entirely decreased after the surface activation process. This behavior is mainly due to incorporation of new polar groups such as hydroxyl, carbonyl and carboxyl as a result of PET polymer chain scissions under plasma discharge, which was confirmed by chemical quantification analysis using TBO dye as the amount of -COOH functions increased from 0.313 µmol/g for untreated sample to 1.308 µmol/g for plasma treated one.

Table 1. Streaming zeta potential values (mV) and density of carboxylic groups of PET surface fabric at different PH values

	Zeta potential values (mV)				Density of carboxylic groups (µmol/g)
pH	3	5	7	9	< 2
Untreated PET	6	-10	-55	-58	0.313
Plasma treated PET	-7	-46	-78	-80	1.308

3.2. Color measurement results

Color strength expressed as K/S for the untreated and plasma treated colored polyester fabrics padded without and with an ecofriendly acrylate binder (free of formaldehyde) is given in Figure 1. Results demonstrate clearly that pretreatment based on plasma surface activation process enhanced the color strength of the dyed polyester fabrics due to the newly added functional chemical groups. The improvement in color strength is arisen additionally as the binder concentration increases. The maximum values of K/S, 3.04 at a wavelength of 460nm was noted for a plasma treated PET fabric with an acrylate binder concentration of 50 g/L. Literally, acrylate binder established a robust network structure [8]. Under this film dye, particles remained fixed, which ensured a high stability to outside forces that would try to remove the dye from the textile substrate, such as washing or rubbing. Thus, the higher the concentration of binder is, the greater amount of locked dye particles.
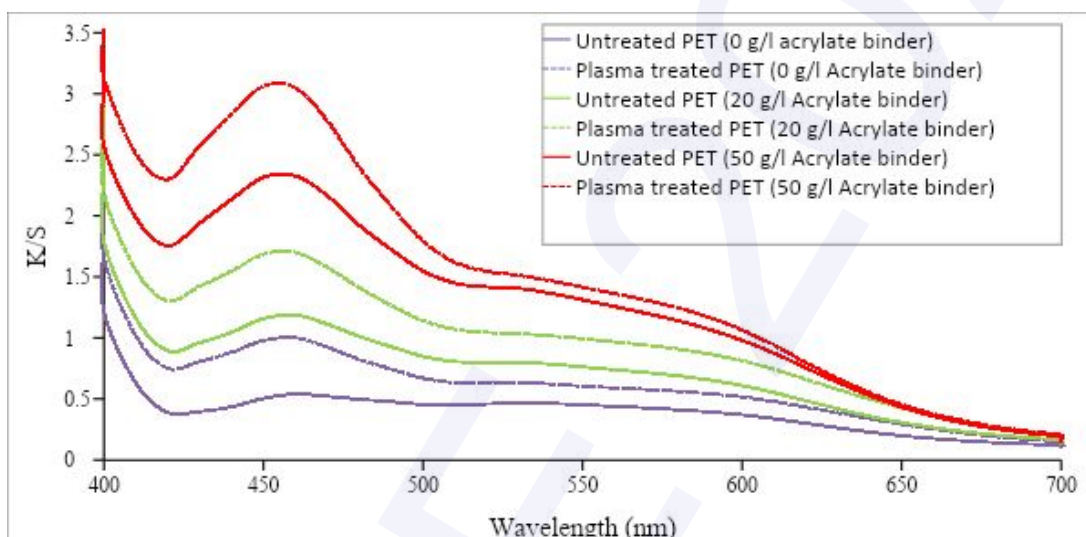
Figure 1. Color Yield results according to M2 under different acrylate binder concentrations

3.3. Color fastness properties

The results given in Table 2 indicates that the effect of binder concentration is statistically significant on the washing and rubbing fastness of the dyed samples. In fact, the binder plays a key role in preparing high-performance of dyed samples as it provides strong chemical interactions in covalently crosslinked networks forming stable film entrapping logwood dye inside. So, better mechanical stability is obtained while increasing binder concentration.

The lower ratings of color fastness properties (2-3) observed in table 2 can be explained by the dye accumulation on the fabric surface as the padding process relies only on surface deposition and affinity between the colorant and textile surface remain weak.

Table 2. Washing (ISO 105:C10) and rubbing (ISO 105:X12) fastness properties

Acrylate Binder Concentartion	Wash fastness		Rubbing fastness			
			Dry		Wet	
	U*	P.T*	U*	P.T*	U*	P.T*
0 g/L	2-3	3	2	2-3	2	2-3
20 g/L	3-4	4	4-5	5	3-4	4
50 g/L	4	4-5	5	5	3-4	4

U*: untreated sample
P.T*: Plasma treated sample

Above all, samples dyed after plasma treatment showed slightly better washing fastness properties, which may be due to the more ionic attraction between newly made ionic sites on the plasma-treated fibers and the dye. Rubbing fastness was also quietly greater in the case of the plasma-treated samples. This is mainly due to the modification of the surface morphology of polyester fabric after plasma treatment [9].

4. CONCLUSION

In this study, a polyester fabric with a prior surface activation based on dielectric barrier discharge (DBD) treatment was dyed with natural Logwood dye using padding technique without and with formaldehyde-free acrylate binder.

Results demonstrate that plasma treatment enhanced the color strength of the dyed polyester fabric as new functional groups were embedded in polyester surface making fibres more hydrophilic. These findings were confirmed by both surface chemical composition and zeta potential assessments. The improvement in color strength was arisen additionally while increasing formaldehyde-free acrylate binder concentration ensuring as a result the best fastness properties (4/5).

Accordingly, the application of Logwood dye on polyester fabric while combining atmospheric pressure plasma treatment and padding techniques can be considered as an effective approach as an environmentally friendly dyeing process.

REFERENCES

[1] **M. Abdul, G. Elisabeth, A. Rais**, Environmental Deterioration and Human Health: Natural and anthropogenic determinants, *Springer Netherlands*, 2014, 55-71.

[2] **S. Verma, G. Gupta,** Natural dyes and its applications: a brief review, *International Journal of Research and Analytical Reviews*, Vol.4, No.4, 2017, 57-60.

[3] **R. Morent, N. De. Geyter, J. Verschuren**, Non-thermal plasma treatment of textiles, *Surface and Coatings Technology*, Vol.202, No.14, 2008, 3427-3449.

[4] **M. J. Shenton, G. C. Stevens**, Surface modification of polymer surfaces: atmospheric plasma versus vacuum plasma treatments, *Journal of Physics D Applied Physics* , Vol.34, No.18, 2001, 2761-2768.

[5] **R. Mongkholrattanasit, J. Kryštůfek, J. Wiener**, Dyeing and fastness properties of natural dyes extracted from eucalyptus leaves using padding techniques, *Fibers and Polymers*, Vol.11, No.3, 2010, 346–350.

[6] **S. Sano, K. Kato, Y. Ikada**, Introduction of functional groups onto the surface of polyethylene for protein immobilization, *Biomaterials*, Vol.14, No.11,1993, 817-22.

[7] **S. Shahidi, M. Ghoranneviss, J. Wiener**, Improving synthetic and natural dyeability of polyester fabrics by dielectric barrier discharge, *Journal of Plastic Film & Sheeting*, Vol.31, No.3, 2015,1-23.

[8] **M. Iqbal, J.Mughal, M. Sohail, A. Moiz, K. Ahmed, K.Ahmed**, Comparison between Pigment Printing Systems with Acrylate and Butadiene Based Binders, *Journal of Analytical Sciences*, *Methods and Instrumentation*, Vol.2, No.2, 2012, 87-91

[9] **S. Abou Rich, T. Dufour, P. Leroy , L.Nittler , J. J. Pireaux, F. Reniers**, Low-density polyethylene films treated by an atmospheric Ar-O$_2$ postdischarge: functionalization, etching, degradation and partial recovery of the native wettability state, *Journal of Physics D Applied Physics*, Vol.47, No.6, 2014, 1-12.

The Second Edition of the International Congress of Applied chemistry and Environment
30th-31th October and 01st November 2020, Tunisia

ICACE 2020

Cotton fibers dewaxing effect on adhesion capacity of polyvinyl alcohol cold size

Asma Rahmouni, Sameh Maatoug, Neji Ladhari

University of Monastir, Textile Engineering Laboratory. B. P. 68 Ksar Hellal 5070, Tunisia
E-mail : okasmus@hotmail.com

ABSTRACT

The objective of this research was to survey the effects of de-waxing of cotton roving on the adhesion of cold polyvinyl alcohol (PVA) size to raw cotton fibers for cotton warp sizing at room temperature. The adhesion of two type of PVA cold size to raw and de-waxed cotton fiber substrates was studied by using an impregnated roving method. The adhesion was evaluated in terms of the tensile strength, breaking extension and work of break of a slightly sized roving. It was founded that de-waxing and cleaning of cotton fibers enhance significantly the adhesion capacity of the PVA cold size to cotton fibers substrate. Moreover, the adverse influence of cotton wax on the adhesion power will be eliminated after pre-wetting process of raw cotton warps with hot water.

KEYWORDS: Cold sizing, Adhesion, Cotton roving, De-waxing.

1. INTRODUCTION

Sizing of cotton warp yarns is usually carried at high temperature, more than 95°C because cotton fiber is hydrophobic due to the existence of its surface cuticle layer, which is mainly composed of pectin and waxes [1]. The non-cellulosic wax, which is distributed on the surface of raw cotton fibers, impedes wetting of the cooked aqueous size and retards the impregnation of the size into cotton warp yarns. In high-temperature sizing, the wax can melt and be cleaned off from the fiber surface. Therefore, a large amount of steam energy is consumed for maintaining high temperature throughout the sizing process [2].

It is evident that the energy consumed in warp sizing will be saved if paste temperature can be decreased. However, the wax becomes a serious problem in low temperature and cannot melt in cold size. Thus, there is an urgent need to clean the cotton fiber surface and remove the wax. There are different chemical methods for non-cellulosic components removal including de-waxing, scouring, bleaching, extraction etc. [3]. Concerning processing of cotton, a de-waxing pretreatment could be used for improvement of wettability and adhesion of a sizing agent on cotton yarn [4].

Strong adhesion of the size to fibers is recognized as an extremely important behavior [5]. The adhesion is capable of enhancing the strength of sized yarns by bonding the fibers in warps together. It is also able to diminish yarn hairiness by pasting yarn hairs back onto yarn body [6]. Consequently, the behavior is closely related to the quality of sized warps [7]. There was no investigation to provide an efficient way for improving the adhesion of cold polyvinyl alcohol (PVA) sizes to raw cotton fibers by de-waxing pretreatment. Accordingly, the main objective of this study is to investigate the wet de-waxing method to improve adhesion of PVA to cotton fibers. In this work, a raw and de-waxed cotton roving samples were treated with two different cold PVA size formulation. After the treatment, mechanical properties of samples were tested, the cross-section of the sized roving was observed, and then the morphology of the cotton surface was performed.

2. MATERIAL AND METHODS

Raw cotton roving with a linear density of 1100 tex used as substrate for adhesion measurement was offered by SITEX industry (Sousse, Tunisia). Average length and fineness of cotton fibers in the roving were 29.1 mm and 1.59 dtex, respectively. Polyvinyl alcohol (PVA2488) with a degree of hydrolysis of 87%-89% and molecular weight average of 24,000 g/mol. An aqueous formulation of Polyvinyl alcohol (AVIROL AEK Cold sizing agent) purchased by Pulcra Chemicals, Germany. Distilled water was used in all experiments.

Viscosity measurements (mPa.s) of each sizing solution were done at 25°C according to ISO 6388 by a rheometer (Rheotec RC 30-CPS). The roving samples were used to determine the adhesiveness of the size to the fibers using the impregnated roving method. The sized roving samples were tested to determine their tensile strength and elongation as a measure of the adhesion of the sizing agent to the fibers. Testing was performed on a MTS tensile tester (Model: Lloyd LR5K) using a gauge length of 10 cm and crosshead speed

The Second Edition of the International Congress of Applied chemistry and Environment
30th-31th October and 01st November 2020, Tunisia

ICACE 2020

of 50 mm/min. Surface morphology of raw and de-waxed cotton fibers was observed under Thermo Scientific Q250 scanning electronic microscope (SEM). In order to assess the extent of permeation of the size into the roving, a 0.1 mol/L iodine solution was utilized to stain the cross sections of the sized roving, which were then observed under a Leica optic microscope.

3. RESULTS AND DISCUSSIONS

3.1. Influence of cotton wax on adhesion of PVA size/cotton fibers

The influence of cotton wax on the adhesion of two type of PVA sizes, a 6% cooked PVA aqueous paste (PVA2488) and a cold sizing agent (AVIROL AEK) composed of aqueous formulation of polyvinyl alcohol with additives, to cotton fibers was examined. The adhesion was evaluated by the comparison on tensile strengths of sized raw cotton roving and de-waxed ones at 25°C of two sizes applied to roving substrate. The results was presented in Figure 1.
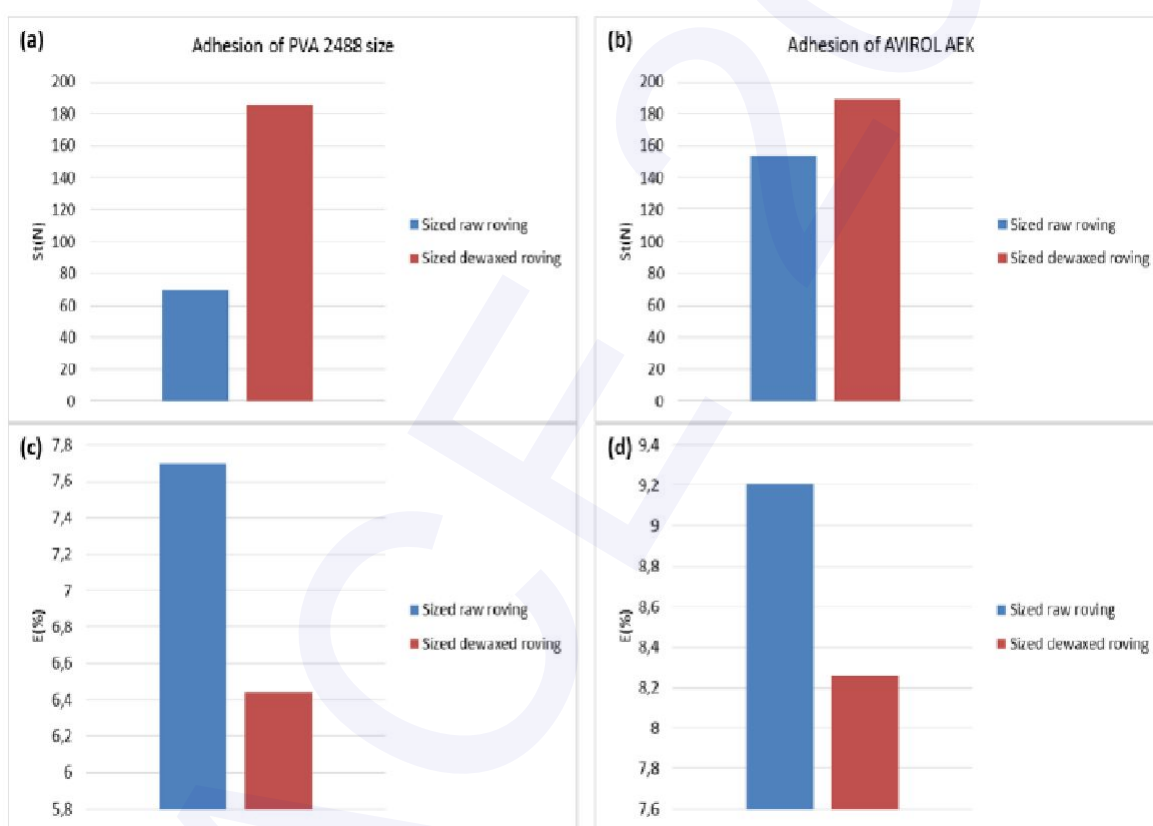
Figure 1: Strength (a)/(b) and elongation (c)/(d) of sized raw and de-waxed roving with PVA2488 and AVIROL AEK

As seen from Figure 1, tensile strengths of PVA2488 sized roving are low then those of AVIROL AEK sized roving. This is due to the different viscosity values of PVA sizes, which are 150cP for PVA2488 and 200cP for AVIROL AEK. It was observed from Figure 1 that the strengths related to the adhesion of cooked PVA2488 and cold PVA size Avirol to raw cotton fibers are significantly lower than those of de-waxed cotton fibers at room temperature (25°C) when the wax does not melt and not cleaned of by the cold PVA sizes. This implies that the adhesion to raw cotton was weaker than that of de-waxed cotton at low temperature. The wax distributed on the surface of row cotton fibers is a hydrophobic substance and imparts hydrophobic character, which disfavors the wetting of the aqueous size onto the surface of cotton fibers and adversely affect the adsorption of cotton fibers to the paste. For this reason, de-waxing is required for enhancing the adhesion of cold PVA to cotton fibers in cold sizing process. Therefore, the wax on cotton fibers must be removed if cotton warp yarns will be sized at low temperature. However, it is impossible to remove fiber waxes in aqueous cold sizing solution. Accordingly, a pre-wetting process with hot water

The Second Edition of the International Congress of Applied chemistry and Environment
30th-31th October and 01st November 2020, Tunisia

ICACE 2020

before impregnation of the yarn in cold size solution can be employed to remove wax and improve wetting of the cold size in the fiber, which will improve significantly the quality of the cold sizing process. It can be observed from figure 1 that strength of roving is increasing after de-waxing process whereas the elongation is decreased. This is because size material more penetrates into the roving body and makes the fibers bound inside roving increasing its strength and decreasing its elongation.

3.2. Cross-section of raw and de-waxed sized roving samples

Figure 2 illustrates the cross sections of the cotton roving after being stained by iodine. During the sizing process, the size solution gradually permeates from the outside into the roving. The circular dark black area positively correlates with the absorption ability of the roving for the size after de-waxing treatment.
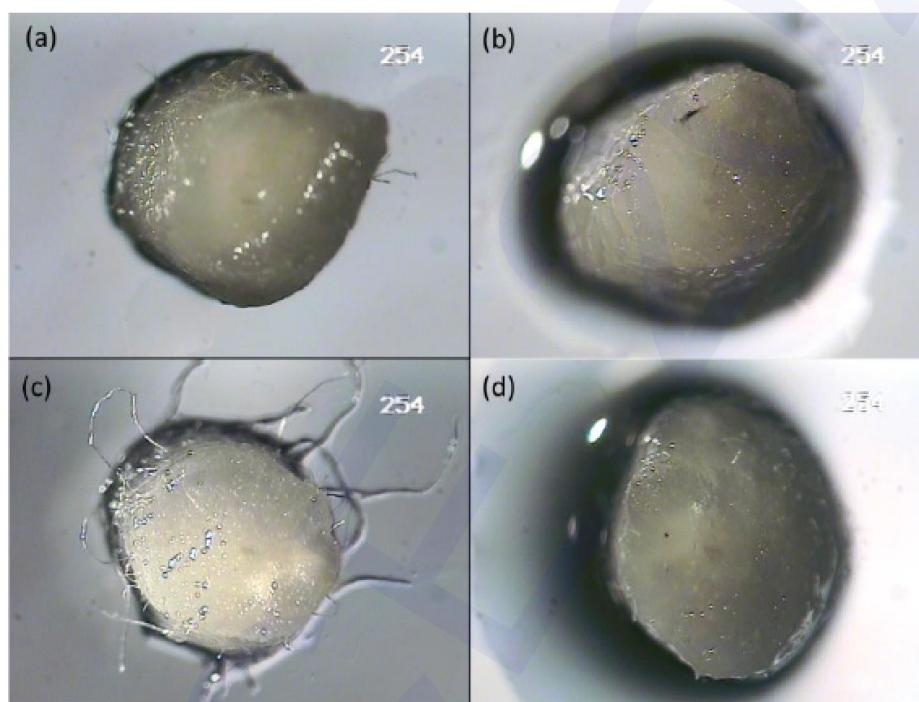
Figure 2: Photographs of roving cross-sections: (a, c) raw samples sized and (b, d) de-waxed samples sized with PVA2488 and AVIROL AEK, respectively.

It can be observed that the color darkens and its area grows with the sized de-waxed roving, which implies that the absorption ability of the roving for the cold PVA sizes has been greatly promoted by the de-waxing process. When the temperature of de-waxing process is greater than the melting point of cotton wax, the wax distributed on the surface of cotton fibers can melt and be removed from the fiber surface. The normally hydrophobic surface of raw cotton becomes hydrophilic, leading to direct contact between cellulose fibers and PVA sizes. Therefore, strong adsorption of size is achievable. In addition, Figure 2b-d shows good adhesion of size to fibers leading to a more homogenous size layer, due to a better adsorption of the fiber for the cold size in this condition.

3.3. Morphology of raw ant de-waxed cotton fibers

The surface morphology analysis of cotton fibers before and after de-waxing was carried out employing a scanning electronic microscopy. The result was depicted in figure 3 (A) and (B).
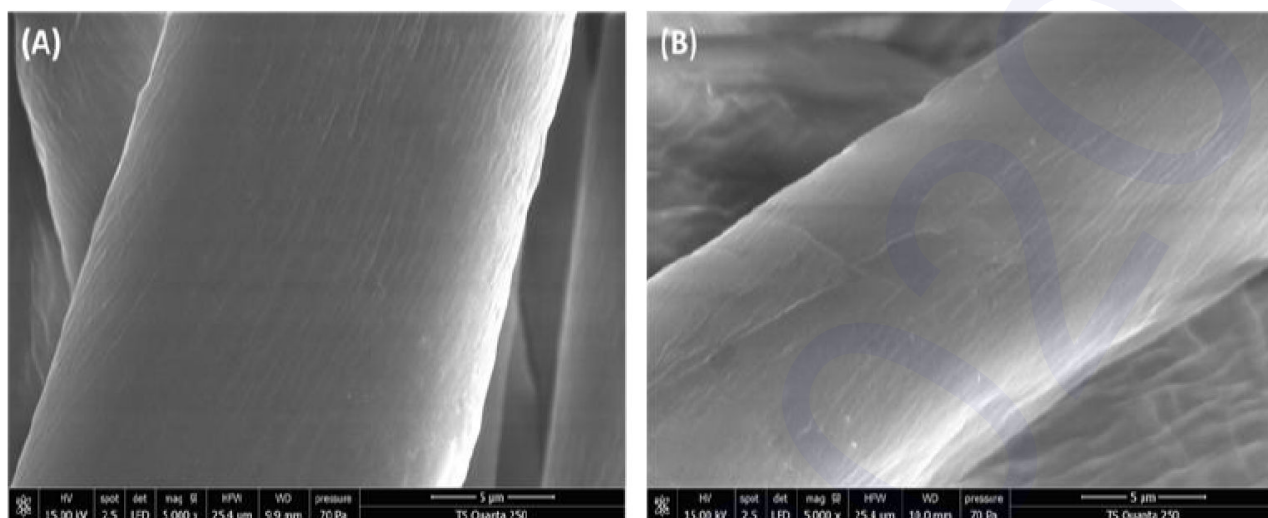
Figure 3: SEM images of raw cotton fibers (A) and de-waxed cotton fibers (B)

Cotton as a natural fiber has a complex morphology with twisted structure. Therefore, it was very difficult to observe eventual changes in surface morphology. By comparing the images (A) and (B), changes in the morphology of fiber surface were observed. It was observed that raw cotton fiber had a smooth surface, while de-waxed fiber had slight increase of surface roughness. The differences in fibers morphology between raw and de-waxed samples indicating that the waxes covering the surface has been removed.

4. CONCLUSION

The results obtained in this work prove that the non-cellulosic wax distributed in the surface of cotton fibers was able to diminish the adhesion of cold PVA size to cotton yarns when the sizing process was carried at room temperature. The hydrophobic character of the wax disfavors the wetting and spreading of the aqueous cold size solution onto the surface of fiber, which adversely affected the adhesion power of the size. Furthermore, the wax on raw cotton fibers must be cleaned off before the impregnation of raw cotton warps with cold PVA sizes at room temperature.

On the other hand, chemical methods for removing non-cellulosic components in cotton fibers include de-waxing, scouring, bleaching, extraction etc. comprise an important amount of chemical and energy waste. This lead to establish other procedures for textile materials modifications, which are fast, economic, and ecological. Consequently, employing low temperature plasma as a cleaner treatment for textiles becomes more useful.

REFERENCES

[1] **Wakelyn PJ, Bertoniere NR, French AD, Thibodeaux DP, Triplett BA, Rousselle MA, Goynes WR, Edwards JV, Hunter L, McAlister DD, Gamble GR**, Cotton Fibers. In: Lewin M (ed) Handbook of fiber chemistry, 3rd edn., Taylor & Francis Group, London, 2007, 521-666.

[2] **Y. Tong,** Research and Application of Energy Saving Technology in Textile Warp Slashing Process, *Applied Mechanics and Materials*, Vol.508, No.1, 2014, 223-226.

[3] **Stana-Kleinschek K, Ribitsch V,** Electrokinetic properties of processed cellulose fibers, *Colloid Surface A* , Vol.140, 1998, 127-138.

[4] **Zhifeng Zhu, Wei Li, and Yuanyuan Liu**, Electroneutral Cornstarch by Quaternization and Sulfosuccinylation to Improve the Adhesion of Cold Starch Paste to Raw Cotton for Low-Temperature Sizing, *Fibers and Polymers*, Vol.18, No.6, 2017, 1106-1114.

[5] **Zhifeng Zhu, Peihua Chen**, Carbamoyl ethylation of starch for enhancing the adhesion capacity to fibers, *Journal of Applied Polymer Science,* Vol.106, No.4, 2007, 2763-2768.

[6] **Zhu, Z. F., Cheng, Z. Q**, Effect of inorganic phosphates on the adhesion of mono-phosphorylated cornstarch to fibers, *Starch/Stärke*, Vol.60, 2008,315-320.

[7] **Trauter, J., Vialon, R., Stegmeier, T,** Correlation between the adhesive strength of sizes and clinging tendency, *Melliand Engineering,* Vol.72, 1991,251-254.

The Second Edition of the International Congress of Applied chemistry and Environment
30th-31th October and 01st November 2020, Tunisia

ICACE 2020

Monoacylglycerol and diacylglycerol production by hydrolysis of refined vegetable oil by-products using an immobilized lipase from *Serratia* sp. W3

Zarai Zied[a], Ahlem Edahech[a], Francesco Cacciola[b]

(a)   *Laboratory of Biochemistry and Enzymatic Engineering of Lipases, National School of Engineers of Sfax, University of Sfax, PB 1173, Km 4 Road Soukra, Sfax, Tunisia*

(b)   *Dipartimento di Scienze Biomediche, Odontoiatriche e delle Immagini Morfologiche e Funzionali, University of Messina, Via Consolare Valeria, 98125 Messina, Italy*

E-mail : zaraizied@hotmail.fr/zied.zarai@isbs.usf.tn

ABSTRACT

In the present work, the hydrolysis of lipid fraction by-products of refined vegetable oils was performed by *Serratia sp.* W_3 lipase immobilized on $CaCO_3$. This support was selected out of 4 carriers as it exhibited the finest activity support (950 U/g) and the most satisfactory behavior at use. The immobilized lipase $_{was}$ stable and active in the whole range of pH and temperature, yielding a 75% degree of hydrolysis at optimal environmental conditions of pH 8.5 and temperature 55°C. TLC, GC and LC methods were evaluated to determine the analytical characterization of hydrolysis products. For monoacylglycerols, diacylglycerol fractions identified in the samples, a novel approach by LC method was employed. The adopted approach allowed the use of basic instrumentation set-ups, without the need of sophisticated detectors, such as mass spectrometers. Thus, it could be an effective alternative to produce emulsifiers from cheap vegetable oils.

KEYWORDS: by-products; refined vegetable oils, monoacylglycerols, diacylglycerols, immobilized microbial lipase.

1. INTRODUCTION

Oils and fats are mainly composed of triacylglycerols (TAGs). Their hydrolysis is accomplished with a high-pressure steam (70 bar) and an elevated temperature (250°C) [1] and might produce valuable free fatty acids (FFAs), monoacylglycerols (MAGs) and diacylglycerols (DAGs) and glycerols [2]. The major drawbacks of this process include high energy consumption, low yields, and poor product quality [3]. Compared to the chemical technique, the enzymatic catalyzed hydrolysis of fats and oils, under mild temperature and pressure, is a very promising method for production of FFAs, MAGs and DAGs [4].

The aim of the present study was to develop an eco-friendly method for the enrichment of DAGs and MAGs in by-products of refined vegetable oils by hydrolysis and esterification with glycerol using a new microbial immobilized lipase from *Serratia sp.* W_3 (LSm) and *Candida Antarctica* lipase (Novozyme 435), as biocatalysts. The by-products of refined oils mostly serve as additives in animal nutrition or in soap industry. Using biotechnology, these low value materials may have the potential of being processed into value-added products. Based on these considerations, once this operation was achieved, the characterization of eventually produced MAGs and DAGs was carried out by TLC, GC, and LC methods. Interestingly, MAGs, DAGs and TAGs were identified *via* a novel approach based on the use of a home-made LRI database and dedicated software. Such an approach allowed the use of basic instrumentation set-ups, without the need of sophisticated detectors, such as mass spectrometers.

2. MATERIAL AND METHODS

2.1. Synthesis of monoacylglycerols and diacylglycerols

The hydrolysis reaction was performed in screw-capped flasks placed in a constant temperature at 55°C and mixed by agitation at 200 rpm. Different ratios of buffer/oil were mixed with different amounts of LSm. The commercial lipase used in this study is the Novozyme 435.

The Second Edition of the International Congress of Applied chemistry and Environment
30th-31th October and 01st November 2020, Tunisia

ICACE 2020

2.2. Qualitative analysis of reaction products

The composition of the hydrolysis product was investigated by thin layer chromatography (TLC) on silica 60 F254 previously activated at 60°C for 30 min. The lipids were extracted with *n*-hexane and separated on TLC using hexane/diethyl ether/acetic acid (90:10:0.5, *v/v/v*) as a mobile phase. After drying the plate, spots were visualized by placing the plate in a chamber saturated with iodine. TAGs, MAGs, DAGs and FFAs were detected as brown spots and identified.

3. RESULTS AND DISCUSSIONS

3.1. Optimal Reaction Conditions

The optimal hydrolysis conditions were an enzyme amount of 1425 IU and substrate molar ratio oil: hexane was of 1:4 each and an incubation time of 30 h and 24 h for the Novozyme 435 and *Serratia sp. W3* lipase, respectively. Under these conditions, the maximal hydrolysis was about 75 %. Linder [5] studied the hydrolysis of salmon oil by Novozyme SP 398 and obtained a hydrolysis rate of 40% after 24 h of reaction. Wanasundra [6] reported that hydrolysis of seal blubber oil and menhaden oil using microbial lipases reached 80 and 70%, respectively after 70 h of reaction time.

3.2. Characterization of hydrolysis products by TLC analysis

The TLC profiles showed that under the action of the LSm, the content of TAGs undergwent a rapid decrease to the same sample hydrolyzed by Novozyme 435 after longer time. Consequently, the content of MAGs and DAGs undergo a major increase by the action of the LSm. Hence, the hydrolysis of triacylglycerols using lipase of *Serratia sp. W3* immobilized onto $CaCO_3$ can be an attractive method to produce MAGs and DAGs that can be used as food emulsifier. Therefore, the LSm was an attractive biocatalyst to carry out the synthesis in a solvent-free system and the hydrolysis reactions.

3.3. Characterization of hydrolysis products by GC and LC methods

Vegetable oils were analyzed by means of GC-MS/FID and UHPLC-ELSD [7]. An innovative chromatographic approach was applied to demonstrate their suitability to such a complete case-study, which required both qualitative and quantitative analyses. A novel approach for the identification of TAGs by the LC methods was employed, based on the use of a home-made LRI database and dedicated software. This approach allowed the use of basic instrumentation set-ups, without the need of sophisticated detectors, such as mass spectrometers. Table 1 lists MAGs, DAGs and TAGs identified in the samples, along with their calculated LRI values, directly compared with those reported in the database. The identification of MAGs generated by hydrolysis was instead performed by HPLC-ESI-MS analyses, since they are not included in the database due to the non-availability of quite expensive standard materials. Within this context, the present work represented the first application of the novel LRI-based identification system in LC and the investigated samples gave the possibility to insert MAG species in the database.

The chromatograms of olive oil (time 0) and hydrolyzed olive oils by Novozyme 435 and LSm (time 30 h and 6 h, respectively), are reported in Figure 1 to show the separation of all acylglycerols. The chromatographic profiles showed that, under the action of the LSm, the content of TAGs undergo a more rapid decrease with respect to the same sample hydrolyzed by Novozyme 435 under the effect of time. Consequently, the content of MAGs and DAGs undergo a major increase by the action of the LSm. Monolinolein (L) and monoolein (O) were the main MAGs produced by hydrolysis of olive oil and refined olive oil, a significant content of monostearin (S) was also obtained by hydrolysis of pomace oil, and monopalmitin (P) was identified only in samples of hydrolyzed soybean in co-elution with monoolein.

To compare the reaction kinetics of both lipases, a kinetics plot was built for the most abundant TAG (triolein) in all the oils, reporting its normalized area against hydrolytic times (Figure 2). It appears evident that the novel LSm was in all cases more efficient since it was able to reduce TAG concentration at a very low level already after 4 or 6 h.
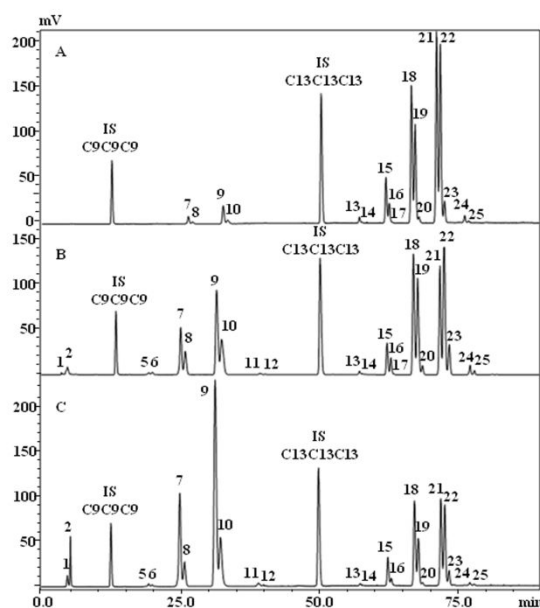
Figure 1: UHPLC-ELSD chromatograms of (A) olive oil, (B) olive oil hydrolyzed by commercial lipase after 30 h, (C) olive oil hydrolyzed by *Serratia sp. W3* lipase (LSm) after 6h.
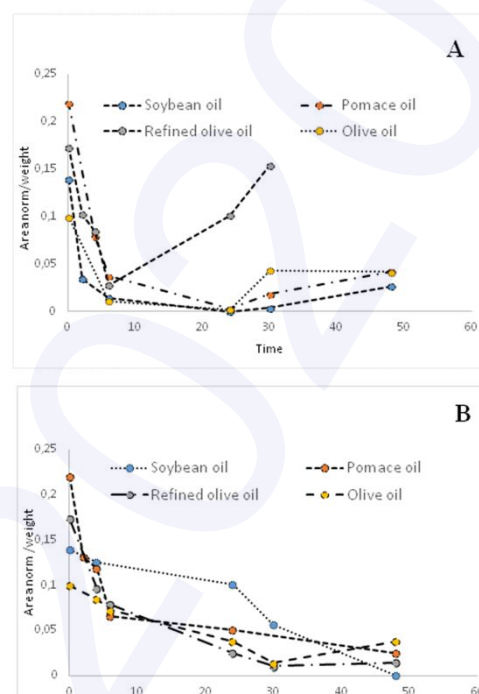
Figure 2: Kinetic plots of triolein hydrolysis by LSm (A) and Novozyme 435 (B).

Table 1: Identified MAGs, DAGs and TAGs in the analyzed samples.

N.	Compound	Trivial name	LRI_{sp}*	LRI_{lib}	Δ
1	L	Monolinolein	2451[#]	-	-
2	O	Monoolein	2459[#]	-	-
3	P	Monopalmitin	2519[#]	-	-
4	S	Monostearin	2552[#]	-	-
5	LL	Dilinolein	2932	2922	+10
6	LnO	Linolenoyl-oleyl-glycerol	2953	2942	+11
7	LO	Linoleoyl-oleyl-glycerol	3123	3117	+6
8	PL	Palmitoyl-linoleoyl-glycerol	3153	3147	+4
9	OO	Diolein	3336	3340	+4
10	PO	Palmitoyl-oleoyl-glycerol	3362	3363	+1
11	SO	Stearoyl-oleoyl-glycerol	3568	-	-
12	SP	Stearoyl-palmitoyl-glycerol	3599	-	-
13	LLL	Trilinolein	4168	4160	+8
14	LnLO	Linolenoyl-linoleoyl-oleoyl-glycerol	4186	4192	+6
15	LLO	Dilinoleoyl-oleoyl-glycerol	4343	4342	+1
16	LnOO	Dioleoyl- linolenoyl-glycerol	4364	4360	+4
17	LnOP	Linolenoyl-oleoyl-palmitoyl-glycerol	4386	4383	+3
18	LOO	Dioleoyl- linoleoyl-glycerol	4509	4516	-7
19	PLO	Palmitoyl-linoleoyl-oleoyl-glycerol	4537	4539	-2
20	PPL	Dipalmitoyl-linoleoyl-glycerol	4573	4571	+2
21	OOO	Triolein	4721	4729	-8
22	POO	Dioleoyl-palmitoyl-glycerol	4749	4756	-7
23	PPO	Dipalmitoyl-oleoyl-glycerol	4780	4776	+4
24	SOO	Dioleoyl-stearoyl-glycerol	4938	4948	-10
25	SOP	Stearoyl-oleyl-palmitoyl-glycerol	4969	4961	+8

4. CONCLUSION

Serratia sp. W3 lipase has been investigated as a hydrolysis pre-treatment catalyst to produce MAGs and DAGs. Reached results indicated that alternative uses of LSm during MAG and DAG production might be more appropriate. Enzyme catalysts are less sensitive to FFAs compared to their chemical complements. Consequently, enzymatic hydrolysis could be done first followed by an esterification reaction using LSm. This process could be used to ensure that all FFAs as well as unreacted MAGs and DAGs were removed from the stream product. The use of LSm was proved to be beneficial for the production of emulsifiers from cheap vegetable oil by-products.

REFERENCES

[1] **Noor I.M., Hasan M., Ramachandran K.B.**, Effect of operating variables on the hydrolysis rate of palm oil by lipase. *Process Biochemistry*, Vol.39, 2003, 13-20.

[2] **Weber N., Mukherjee K.D.**, Solvent-free lipase-catalyzed preparation of diacylglycerols. *Journal of Agricultural and Food Chemistry* 2004, Vol.52, 2004, 5347-5353.

[3] **Berger M., Schneider M.P.,** Enzymatic esterification of Glycerol II. Lipase catalyzed synthesis of regioisomerically pure 1(3)-rac- Monoacylglycerols. *Journal of the American Oil Chemists' Society,* Vol. 69, 1992, 961-965.

[4] **Yang B., Zhao G., Lin H.,** Hydrolysis of olive oil with immobilized lipase in a tapered column reactor. *Chinese Journal of Process Engineering*, Vol. *3*, 2003, 206-211.

[5] **Linder M., Fanni J.**, **Parmentier M**., Proteolytic extraction of salmon oil and PUFA concentration by lipases. *Journal of Marine Biotechnology*, Vol. *7*, 2005, 70-76.

[6] **Wanasundra U.N., Shahidi F.,** Lipase assisted concentration of ω-3 polyinsaturated fatty acids in acylglycerol forms from marine oils, *Journal of the American Oil Chemists' Society,* Vol. *75*, 1998, 945-951.

[7] **Mondello L., Beccaria M., Donato P., Cacciola F., Dugo G., Dugo P.,** Comprehensive two-dimensional liquid chromatography with evaporative light-scattering detection for the analysis of triacylglycerols in *Borago officinalis*. *Journal of Separation Science*, Vol.34, 2011, 688-692.

The Second Edition of the International Congress of Applied chemistry and Environment
30th-31th October and 01st November 2020, Tunisia

ICACE 2020

Ozone finishing of textiles: Waste management, sustainability and toxicity study

Sarra Ben Hamida[a], Wafa Miled[a], Neji Ladhari[b] Mika Sillanpaa[c]

(a)   Laboratory of Textile Engineering, Higher Institute of Technological Studies of Ksar Hellal, Monastir University, 68, Avenue Hadj Ali Soua, Ksar Hellal 5070, Monastir, Tunisia
(b)   Higher Institute of the Fashion Trades, Stah Jabeur Golf Avenue 5000, University of Monastir, Tunisia
(c)   Department of Civil and Environmental Engineering, Florida International University, Miami, FL 33174, USA
E-mail: benhmida.sarra87@gmail.com

ABSTRACT

An abstract not exceeding the laundering of dyed garments by ozone is an effective and innovative alternative that gives a rich range of washed shades with a considerable reduction of water, energy and chemicals consumption. A further study on the denim ozonation wastes was done and rinse baths were analyzed. The by-products in different operating conditions were identified and their chemical toxicity via the inhibitory effect of bioluminescent bacteria, *Vibrio fischeri* was investigated. Isatin (1H-indole-2,3-dione) detected by GC-MS analysis is the main compound formed on the surface of ozonated jeans. It exhibited a considerable antibacterial activity which makes it hazardous to aquatic environment. However, Ozonation wastes remain less toxic compared to the rest of the bleaching wastes.

KEYWORDS: Toxicity, Garments, Environment, Ozone, Waste.

1. INTRODUCTION

Protecting our environment involves controlling the reduction of pollutants generated by anthropogenic and in particular industrial activity. Today, global awareness made industrial discharges tightly controlled, limited and subject to increasingly stringent regulations. Industrial decision-makers are led to select suitable manufacturing processes in order to manage water resources well and minimize toxic discharges that threaten the environment. In fact, huge amounts of water are spent in denim wash since it is the most worn garment in the world. It is well known that this process is very dependent on the use of water, chemicals and stones to achieve the desired discoloration effects. This calls into question the sustainability of the whole process [1]. In this context, the denim laundry industry is seeking to develop eco-friendly technologies that can guarantee the reduction of textile effluents. Certified denim brands have become more aware of this issue and are committed to encouraging the production of ecological denim. "Waterless" treatments have today become a lasting trend for the substitution of traditional wet denim washing treatments [2]. Therefore, Ozone washing technology is an innovative process that can be a green alternative for the use of stone and enzymes. The use of ozone in the textile field has imposed itself in recent years due to the advantages that this oxidant has offered [3]. The present research aims to the optimization of the ozonation treatment of wet denim garment. To carry out this study, the response surface methodology (Box-Behnken design) was used to establish mathematical models involving different parameters (ozone concentration, treatment time, moisture content of the fabric) which affect the chosen response ΔL^* (lightness degree of the treated garment). The bioluminescence method which is an efficient and reliable way to investigate the ecotoxicity level of the water samples was used as well in this work to evaluate chemical toxicity of ozonation wastewater.

2. MATERIAL AND METHODS

The desized fabric (Composition 98.8 % Cotton+ 1.2 % Lycra, Dye indigo) was treated with ozone using Jeanologia G2Plus industrial ozone machine. In the present study, the three-level, three-factorial Box–Behnken experimental design was applied to investigate and validate process parameters affecting the degradation of the indigo dye from the surface of the denim garment. Ozone concentration 12-108 g/Nm^3, treatment time 3-23 minutes and moisture content of the fabric 20-40 % were input variables, the factor levels were coded as −1 (low), 0 (central point) and 1 (high). **Tab.1** shows the experimental parameters and

The Second Edition of the International Congress of Applied chemistry and Environment
30th-31th October and 01st November 2020, Tunisia

ICACE 2020

the experimental Box–Behnken design levels used. MINITAB 18 was data used as the statistical software to analyze the data.

Table1. Independent factors and their coded levels used for optimization

Factors	Units	Symbols	High coded level	Low coded level
Ozone concentration	g/Nm^3	A	1	-1
Treatment time	min	B	1	-1
Moisture content	%	C	1	-1

The yellowish product on the surface of the fabric was extracted with methanol and dichloromethane for gas chromatography analysis and in water for toxicity assay in 50 ml falcon tube at room temperature for 30 minutes with 200 rpm shaking. The total organic carbon content during the treatment was monitored by measuring their non-purgeable organic carbon (NPOC) abatement. The NPOC in samples was quantified by a TOC analyzer (Model: TOC-VCPH Shimadzu, Japan). Organic carbon compounds were combusted and converted to CO2, which was detected and measured by a non-dispersive infrared detector (NDIR). For the NPOC analysis, potassium hydrogen phthalate solutions were used as standards. The COD, BOD and TN tests were performed by using LCK500, LCK555 and LCK338 standard HACH cuvette tests, respectively. For COD, 2 mL of sample was added in cuvette and digested for 2 h at 148 0C. The samples were then cooled to room temperature and COD was analyzed by LANGE reader. The aqueous extract of ozonated jeans samples that were frequently used at the textile industry was tested using the Titertek Berthold Sirius L single tube Luminometer to determine the dose from which the aqueous extract becomes toxic. The device includes a toxicity test kit based on bioluminescence of *vibrio fischeri* microorganisms. The tests were conducted according to the BioTox ^{TM} test kit instructions for use. Light emission of bacteria was measured at 2 different times 5s and 15 min and results were executed by the FB12/Sirus PC software in order to determine the EC_{20} end EC_{50} inhibition values of the tested samples. Toxicity of wet ozonation rinse bath was also tested and compared to regular bleaching waste bath.

3. RESULTS AND DISCUSSIONS

3.1. Optimization of wet ozonation process

The statistical significance of the BBD model was assessed by analysis of variance (ANOVA). The P values were calculated, and the results showed that the following variables are not significant (P> 0.05): Ozone concentration (g / Nm^3) x Ozone concentration (g / Nm^3); Treatment time (min) x Treatment time (min). Moisture content (%) x Moisture content (%). On the other hand, the P value = 0.9 associated related to the lack of fit, is higher than the significance level α = 0.05. The model is therefore significant and well-adjusted to the data. In particular, the correlation coefficient R^2 = 98.62% proves that the model is perfectly predictable. The equation describing the model after elimination of non-significant terms is given as an uncoded variable as follows
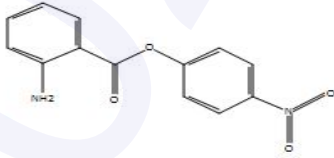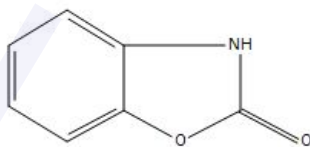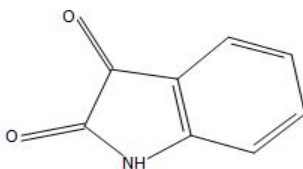
ΔL* = 5,54 -0,0128× Ozone concentration (g/Nm^3) - 0,1551 × Treatment time (min) + 0,296 × Moisture content (%) + 0,001302 × Ozone concentration (g/Nm^3) × Treatment time (min) + 0,001089 × Ozone concentration (g/Nm^3) × Moisture content (%) + 0,00713 Treatment time (min) × Moisture content (%)

3.2. Identification of ozonation by-products

Results of wet denim ozonation presented in **Tab.2** show that the peak eluting at 27.949 minutes is of prime importance and it was identified as 1H-indole-2,3-dione (isatin) according to its mass spectrum (m/z 147). Moreover, the treatment can lead to the decomposition of indigo and the formation of different products that contain more ozone. A smaller peak was identified as 4-Nitrophenylanthranilate (m/z 179) that was eluted at 25.259 min. The degradation of this compound may lead to the formation of anthranilic acid which has been reported in many research studies as one of the ozone/indigo degradation by-products. An extended ozonation of the jeans produced another compound with a smaller peak yield 2(3H)-Benzoxazolone (m/z

136) eluted at 23.829 min. Indole is was the main oxidation by-product detected in the ozonation rinse bath. This can be attributed to the selective oxidation of ozone which targeted the indigo -C=C- double bond. The cleavage of the chromophore group occurred more rapidly which explains the abundance of isatin compared to other degradation by-products resulting from the indigo ring opening [4].

Table 2. Oxidation by-products resulting from ozonation of wet jean fabric detected by GC-MS

Identification number	Compound	Main mass fragmentation values (m/z)	Retention time (min)	Structure
W1	4-nitrophenyl 2-aminobenzoate	120, 92, 65	25.259	
W2	3H-1,3-benzoxazol-2-one	135, 79, 52	23.829	
W3	1H-Indole-2,3-dione	147, 119, 92, 64	27.794	

The ozonation by-products are easily degradable than the indigo dye in the denim laundry wastewater. In fact, isatin is a less complex compound than indigo and its degradation in the environment can occur more rapidly.

3.3. Physico-chemical analysis of ozonation wastewater

TOC of wet and dry jeans ozonation rinse bath shown in **Tab.3** increased with the increase of ozone concentration. Higher values of TOC confirm the important degradation of the dye.

Table 3 : COD and TOC values of different wastes

	O_3 (g/N.m³)	COD (mg/L)	TOC (mg/L)
Wet ozonation rinse bath	20	87.2	211.5
	40	193	219.4
	60	261	287.4
	80	177	295.2
Dry ozonation rinse bath	20	173	57.03
	40	174	72.31
	60	170	93.01
	80	175	116.4
Denim laundry waste	-	271	258.6

3.4. Evaluation of chemical toxicity

Ecotoxicity evaluation of wet, dry jeans and Denim laundry waste revealed that all of three treatments exhibited an antibacterial activity against *vibrio fisheri* in dose dependent manner. The effective concentrations caused 20% and 50 % (EC_{20} and EC_{50}) of growth inhibition were calculated for each treatment (**Tab.4**). The best treatment with an ecological relevance is that with a highest EC_{20} and EC_{50}.

Table 4 : EC_{20} and EC_{50} values of tested samples

Treatment	EC_{20} (%)	EC_{50} (%)
Dry ozone	7.70	24.43
Wet ozone	5.55	13.47
Denim laundry waste	3.38	7.62

Hence, we concluded that dry ozone is the best treatment which exhibited higher EC_{20} and EC_{50} followed by wet ozone treatment and finally the denim laundry waste. The nitrogenous heterocyclic compounds should be responsible for the enhanced toxicity of the wet ozonation rinse bath [5]. However, ozonation waste is less toxic than the regular denim finishing waste. As a matter of fact, the degradation of ozonation by-products by microorganisms in the environment have been the subject of many studies which revealed that they are more relevant to biodegradation process than the initial form of the dye [7].

4. CONCLUSION

Our study has shown that the model studied is perfectly predictable. In addition, ozonation becomes more effective in the presence of moisture and gives a wide range of faded fabrics. In fact, ozone degrades cellulose and releases the indigo due to the breakdown of glyosidic bonds, hence the increase in discoloration of the fabric. For industrial applications, low ozone concentrations are recommended, which are non-toxic according to the results obtained. The ozonation of wet denim leads to the formation of a significant amount of 1H-indole-2,3-dione. Additionally, the toxicity evaluation of the rinse bath showed that ozonation waste exhibited almost similar inhibition levels to regular finishing waste.

REFERENCES

[1] **S. S. Muthu**, Sustainability in Denim*, Woodhead publishing in textile,* 2017, 372

[2] **R. Paul**, Denim Manufactures, Finishing and Applications, *Woodhead publishing in textile*, 2015.

[3] **B. Garcia**, Reduced water washing of denim garments*, Woodhead publishing in textile*, 2015, 405–423.

[4] **L. Dsikowitzky, J. Schwarzbauer,** *Industrial organic contaminants: identification, toxicity and fate in the environment, Environmental chemistry letters,* Vol. 12, 2014, 371-386.

[5] **W.H. Glaze**, Reaction products of ozone: a review, *Environmental Health Perspectives,* Vol. 69, 1986 151.

[6] **K. Witkoś, K. Lech, M. Jarosz,** Identification of degradation products of indigoids by tandem mass spectrometry, *Journal of mass spectrometry*, Vol. 50, 2015, 1245-1251.

[7] **E. Khelifi, H. Gannoun, O. Thabet, H. Bouallagui, M.-L. Fardeau, Y. Touhami, B. Ollivier, M. Hamdi**, Exploring by-products generated by the anaerobic degradation process of synthetic wastewater containing indigo dye, *Desalination and Water Treatment*, Vol. 53, 2015, 1977-1985.

The Second Edition of the International Congress of Applied chemistry and Environment
30th-31th October and 01st November 2020, Tunisia

ICACE 2020

Water minimization in food industries by applying water-pinch analysis

Keivan Nemati-Amirkolaii[a], Hedi Romdhana[a], Marie-Laure Lameloise[a]

(a)   *Université Paris-Saclay, INRAE, AgroParisTech, UMR SayFood, 91300, Massy, France*
E-mail: keivan.nemati-amirkolaii@agroparistech.fr
hedi.romdhana@agroparistech.fr
marie-laure.lameloise@agroparistech.fr

ABSTRACT

Optimizing the reuse and recycling of water is a major challenge for the food industry. Using the right strategy to minimize environmental impact and production costs become essential. Application of this method needs R&D development, for the food industry, where there is a lack of knowledge on process integration, pollutant indicators data and volumes of water and discharge at specific steps of the food processing line. Firstly, the energy pinch method has been developed to optimize the heat networks, afterward, different variations emerged (like water pinch). Water pinch can be used to optimize the water consumption and discharges in industries, so it can be a perfect choice for energy-intensive and water-consuming sectors. Food industries are complex, multi-contaminant and multi-source systems, so, the mathematical formulation of these systems is challenging. Current work is an overview of the water pinch method applied to the food-industries. The challenges, advantages and future of applying this method in food industries are addressed.

KEYWORDS: Water, Water Pinch, Food Industry, Mathematical Modeling

1. INTRODUCTION

Energy efficiency would increasingly become a preference for improving environmental and economic performance in the food industry. By the environmental and economic regulations, a variety of measures are imposed in this industry. Due to climatic hazards originated from human activities and the denaturation of freshwater sources, there is a need to save water resources, particularly in the areas where these resources are declining. Additionally, the current regulations such as the new EU rules that aim to minimize pollution from water (2455/2001/EC and 2000/60/EC) demand some restrictions on which the discharges that are loaded with organics like carbon, nitrogen, phosphorus, acid, etc. are reduced and/or optimized. In the face of such a situation, the food industry needs to replace existing simple measures and operate new efficient methods. However, the annual cost of the techniques such as the integration of high-performance equipment for water purification recommended by the European IPPC Directive (96/61/EC) amounts to 2.5–3.5 million euros [1]. Therefore, it is necessary to investigate the possibility of reducing water consumption and polluting load before integrating the purification equipment by utilizing mass integration means. In this regard, setting energy targets based on the optimization of resources is one of the most fundamental concepts of pinch analysis [2] that seeks to allocate limited resources to demand in the best possible way. This method is provided for several applications, that minimizing water consumption is only one of them. Finally, further research has led to methods that show how water consumption and various industrial utilities like hydrogen, oxygen, etc. can be minimized.

2. MATERIAL AND METHODS

There are many developments of the pinch method, which optimizes primary resources such as energy, water, raw materials etc. and includes efforts on various applications. The research literature shows that pinch analysis was initially extended to heat integration [2]. Compared to the thermal pinch, more applications of this method cover different fields, especially mass integration [3], design and management of hydrogen networks [4], minimization of oxygen consumption of the microorganisms used for waste degradation [5], emergy analysis [6,7], CO2 emission targeting [8,9], and supply chain management [10].

The Second Edition of the International Congress of Applied chemistry and Environment
30th-31th October and 01st November 2020, Tunisia

ICACE 2020

2.1. Water pinch method

Water pinch is a well-organized way to reduce freshwater and wastewater, particularly for the most water-consuming and energy-intensive **sectors**. Wang and Smith [3] in their research explained that mass pinch analysis is a special type of mass integration, especially to decrease the consumption of water or other fluids. Later, by applying analogy with thermal pinch analysis, a systematic method was introduced to optimize the water networks of industrial sectors [11,12]. The results of this new method were as attractive as energy analysis as a traditional method for water consumption optimization. In their studies, Almato et al. [13] showed that it is possible to save 63-72% of the water used in a fruit juice industry. Thevendiraraj et al. [14] and Tokos and Novak Pintaric [15] report**ed** that 30% of water consumption in a brewery workshop and citrus juice production workshop can be reduced. Recently, a combination of the water pinch method and mathematical optimization has been proposed that can save up to 30% of water consumption in a corn refinery [16]. The pinch method was first proposed by Linnhoff [17] as energy pinch and then different types of this method were developed and evolved one after another. One of the variations that changed this method was the mass integration pinch, which aimed to design a systematic way to reduce water consumption and discharges, especially for the most water and energy consuming factories. At first, it was Wang and Smith [3] who used this method and called it water pinch analysis, and then other researchers such as El-Halwagi, Gabriel, and Harell [11] and Prakash and Shenoy [12] tried to improve its efficiency by making new variations or suggesting more effective methods. Many other works have used a similar perspective but focus only on the food industry (juice, brewery, and corn refinery) [13–15]. Given the energy pinch definitions and its flexibility, which includes a range of different items such as water, oxygen, etc., it seems necessary to find the similarities of each component in new variations of pinch to use this method. Some similarities between the energy and water pinch methods can be seen, which helps us to apply this method for water recourse as well. [18]

2.2. Water pinch and food industries

To implement the water pinch method in the agro-food industry, we have to deal with each operation separately; such information is effective in obtaining more accurate results. To examine this classification and the various type of operations in different cases, we will deal with three kinds of the food industry (brewery, citrus, and sugar industries). Generally, two types of water-using operations can be distinguished from each other: mass transfer-based operations and non-mass transfer-based operations. In the first case, direct contact between the water, the equipment walls, and/or the processed material leads to the bulk pick-up of contaminants. In the second case, water flow is an energy utility, reactant, or product of a chemical reaction. According to the usual brewery routine [15], 18% of operations are non-mass transfer-based ones and 82% are mass transfer-based operations. The results obtained from the citrus plant show that most of the operations (64%) are mass transfer-based ones and non-mass transfer-based operations are far less [14]. Also, findings from the sugar factory indicate that more than half of the operations (up to 55%) are mass transfer-based ones and the rest are non-mass transfer-based operations [19]. In addition to saving freshwater, employing water pinch analysis has some economic aspects. Given the above findings from the four types of food industries (citrus, sugar, fruit juice, and brewery), as shown in **Table 1**, we can see a range of economic savings in investments that fluctuates from 23% to 69%, and payback period varies between 5 days to 4 months, which indicates the economic benefits of using this method along with environmental and other benefits.

Table 1:Obtained water savings by applying water pinch method in food industries [18]

	Operation	Indicator	Fresh water	Savings
Citrus plant	continues	COD	2500 à 4000 m3/month/2500 à 4000 + water from pressing	30%
Beet sugar factory	continues	pH, COD, Brix	240/246 t/h	69%
Fruit juice	Batch	PINCH monocontaminant	96 m3/35 m3	64%
Brewery	Batch	PINCH monocontaminant	653 300 m3/year	23%

The research literature shows that the use of the water pinch in food sectors such as dairy and beverage (including the citrus and food juice industry) has a significant effect on minimizing the consumption of freshwater and wastewater production. The average decrease rate in different sectors is between 27 (for the

The Second Edition of the International Congress of Applied chemistry and Environment
30th-31th October and 01st November 2020, Tunisia

ICACE 2020

beverage sector) and more than 65% (for palm oil mill industries); These ratios are rated for wastewater production between 28 (in the beverage sector) and over 75 (in the dairy industries). **Figure 1** shows information about the average wastewater production in different sections.
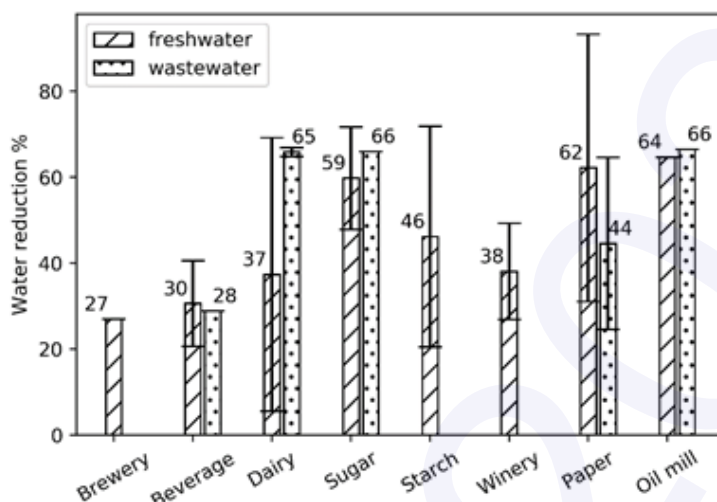

Figure 1: The reduction rate in freshwater (wastewater) consummation (production) in food industries [18]

2.3. Challenges and R&D toward pinch

To use any particular method, it is necessary to extract the required data through measurements or simulation, part of which is the result of the evaluation of industrial sectors and another part is data that has been standardized in the research literature. Also, this data may be derived from the numerical simulation. Normally, the required information about the type and number of pollutant indicators, limiting water data like limiting concentration, the minimum and maximum water flow rate in input and output and threshold values of pollutant indicators for each operation, etc. should be extracted, and at the same time, the problem of the process type, which can include different processes such as batch, continuous, or semi-continuous, is also important. Implementing the pinch method in food sector processes is critical; Because a large part of these industries has continuous process operations and this method is usually dedicated to such processes in the research literature, but the batch or semi-continuous type processes in these industries must be considered. One of the challenges we face in this method is to provide an adapted model for a variety of processes that can even be considered in further research.

The data from the article databases mentioned below are significant. The Food sector different pollutant indicators and their frequency of use presented in **Table 2**, which can be a good guide for the utilization of indicators in each industry; for example, in the dairy industry, the most used indicator is microbial count (five times), followed by Electrical Conductivity (EC) (three times), and also Chemical Oxygen Demand (COD) and turbidity, each used two times. According to this figure, it is not difficult to find that indicator could be far more effective in developing a water pinch method by considering the pollutant indicators [18].

Given the diversity of processes in the food industry, another important challenge is choosing one or more pollution indicators. In most cases, a combination of various constraints is used, including food safety, too strict regulations, and environmental issues. Although water and the potential of water reuse are available in factories, process management is not as flexible as regulatory constraints, which often prevents the reuse of lower quality water. Extending the application of the pinch method should take into account recent considerations by defining the minimum expected water quality and by screening solutions that integrate risk assessment. It is also necessary to consider Pinch analysis as a tool to increase the advantageous solutions and the possibility to discuss changes in food industry standards which until now limited and not flexible. Another important point is how to provide effective food security and sustainable solutions at the same time. There is another fundamental challenge that is specific to sustainable development and addresses the feasibility of a water network without unacceptable levels of environmental degradation; for instance, inputs that are required (e.g., chemical solvents, energy resources, etc.) if there are regeneration steps proposed by

the pinch in the water network. Therefore, it's recommended that the environmental efficiency of any solution obtained by the pinch analyze and carefully examined by integrating Life Cycle Assessment or water footprint analysis.

Table 2: Food sector different pollutant indicators and their frequency of use

	Dairy	Brewery	Citrus plant	Sugar plant	Ethanol plant	Starch plant	Meat	Winery	Paper
COD	2	1	1	3	1		1	1	1
pH	1	1	1	2	1		1		1
EC	3	1					1		
TSS	1		1			1		1	1
TDS				1		1			2
TOC	1					1	1		
BOD				2	1				
Microbial Count	5			2			3		
TURBIDITY	2			2					
OG					1				
brix				1					

3. CONCLUSION

The application of pinch analysis can reduce water use in the food industry by 20-40%. In particular, the development and applying this method in the food industry could lead other factories to use it and save more water. The central idea of this method is to minimize water consumption by recognizing water streams that can be reused in an operation where water quality is important. The water minimum demand can be targeted by using graphical tools or automated design methods. What can be a significant challenge in turn is the data extraction problem, which is a very important step in the implementation of an optimal analysis.

It can be said that it is almost impossible to identify all the factors that affect water chemistry, the microbiological aspect, and the quality of the food product in this industry. It is not uncommon to select representative pollutant indicators in some food sectors. This is why the development of numerical tools is of particular importance for the development of pinch analysis and its application in the food industry. As can be seen, the predominant tendency is to use methods such as mathematical programming to solve complex problems; But this mathematical method, like nonlinear problems, which are often non-convex, is simply not applicable, which means that the global optima are not usually obtained. This is a point that has recently attracted the attention of numerous studies. By considering the nature of multi-contaminant mathematical models and to solve these models, development of multi-criteria optimization methods is inevitable. As mentioned earlier, solving complex system models requires evolutionary methods, and testing new methods against traditional approaches (GA, PSO, etc.) could be interesting in further research.

REFERENCES

[1] **Klemes, J.; Friedler, F.; Bulatov, I.; Varbanov, P**, Sustainability in the Process Industry: Integration and Optimization, *Green Manufacturing & Systems Engineering; McGraw-Hill Professional: New York, NY, USA*, 2010.

[2] **Linnhoff, B.; Flower, J.R,** Synthesis of Heat Exchanger Networks: I. Systematic Generation of Energy Optimal Networks. *AICHE Journal*, Vol. 24, 1978, 633–642.

[3] **Wang, Y.P.; Smith, R**, Wastewater Minimization. *Chemical Engineering Sciences, Vol.* 49, 1994, 981–1006.

[4]**Alves,J**, Analysis and Design of Refinery Hydrogen Distribution Systems 1999, *Available online:http://ethos.bl.uk/OrderDetails.do?uin=uk.bl.ethos.563097*, accessed on 19 August 2018.

[5] **Zhelev, T.; Ntlhakana, J**, Energy-environment closed-loop through Oxygen Pinch,*Computer. Chemical Engineering*, Vol. 23, 1999, 79–S83.

[6] **Odum, H.T,** Systems Ecology: An Introduction, *John Wiley and Sons: New York, NY, USA*, 1983.

[7] **Zhelev, T.K.; Ridolfi, R,** Energy Recovery and Environmental Concerns Addressed through Emergy –Pinch Analysis, *Energy,* Vol. 31, 2006, 2486–2498.

The Second Edition of the International Congress of Applied chemistry and Environment
30th-31th October and 01st November 2020, Tunisia

ICACE 2020

[8] **Linnhoff, B.; Dhole, V.R,** Targeting for CO_2 emissions for Total Sites,*Chemical Engineering Technologies*, Vol. 16, 1993, 252–259.

[9] **Tan, R.R.; Foo, D.C,** Pinch analysis approach to carbon-constrained energy sector planning, *Energy*, Vol. 32, 2007, 1422–1429.

[10] **Zhelev, T.K,** On the Integrated Management of Industrial Resources Incorporating Finances, *Journal of Cleaner Production,* Vol. 13, 2005, 469–474.

[11] **El-Halwagi, M.M.; Gabriel, F.; Harell, D,** Rigorous Graphical Targeting for Resource Conservation via Material Recycle/Reuse Networks*, Industrial & Engineering Chemistry Research*, 2003, 42, 2003, 4319–4328.

[12] **Prakash, R.; Shenoy, U.V,** Targeting and design of water networks for fixed flowrate and fixed contaminant load operations, *Chemical Engineering Sciences*, 2005, 60, 2005, 255–268.

[13] **Almató, M.; Sanmartí, E.; Espun, A.; Puigjaner, L**, Rationalizing the Water Use in the Batch Process Industry, *Computers & Chemical Engineering*, Vol. 21, 1997, 971–976.

[14] **Thevendiraraj, S.; Klemeš, J.; Paz, D.; Aso, G.; Cardenas, G.J**, Water and wastewater minimization study of a citrus plant*, Resources, Conservation & Recycling,* Vol. 37, 2003, 227–250.

[15] **Tokos, H.; Pintariˇc, Z.N**, Synthesis of batch water network for a brewery plant, *Journal of Cleaner Production*, Vol. 17,2009, 1465–1479.

[16] **Bavar, M.; Sarrafzadeh, M.H.; Asgharnejad, H.; Norouzi-Firouz, H,** Water management methods in food industry: Corn refinery as a case study,*Journal of Food Engineering*, Vol. 238, 2018,78–84.

[17] **Linnhoff, B.; Flower, J.R**, Synthesis of Heat Exchanger Networks: II. Evolutionary Generation of Networks with Various Criteria of Optimality, *AIChE Journal*, Vol. 24, 1978, 642–654.

[18] **NEMATI-AMIRKOLAII, K.; ROMDHANA, H.; LAMELOISE, M.,**Pinch Methods for Efficient Use of Water in Food Industry: A Survey Review, *Sustainability*, Vol. 11, N. 16, 2019, 4492.

[19] **Ensinas, A.V.; Nebra, S.A.; Lozano, M.A.; Serra, L.M,** Analysis of process steam demand reduction and electricity generation in sugar and ethanol production from sugarcane, *Energy Conversion and Management,* Vol. 48, 2007, 2978–2987.

Identification and valorization of natural substances

The Second Edition of the International Congress of Applied chemistry and Environment
30th-31th October and 01st November 2020, Tunisia

ICACE 2020

Chemical composition and antioxidant activity of tannins extract from green rind of *Aloe vera* (L.) Burm. F.

Bouchra Benzidia[a], Mohammed Barbouchi[b], Malak Rehioui[a], Hind Hammouch[a], Nadia Belahbib[c], Najat Hajjaji[a], Abdellah Srhiri[d]

(a) Laboratory of Materials, electrochemistry and Environment (LMEE), Department of Chemistry,Faculty of Science, Ibn Tofail University, BP 133, 14000, Kenitra, Morocco.
(b) Laboratory of Molecular Chemistry and Natural Substances, Moulay Ismail University, Faculty of Science, B.P 11201 Zitoune, Meknes, Morocco.
(c) Laboratory of botany, biotechnology and plant protection, Faculty of Science, University ibn Tofail, BP 133, 14000, Kenitra, Morocco.
(d) Servichim Sarl, 101 Rue Maamoura, n. 10 Kenitra, Morocco.

E-mail: benzidia1511@gmail.com

ABSTRACT

In the present study, we are interested in one of the most valuable medical plants, *Aloe vera*. This succulent plant possesses exceptional therapeutic virtues. This study aims to characterize tannins extract of *Aloe vera* by gas chromatography coupled with mass spectrometry. Phytochemical screening, morphological and histological identification of the species and extraction from its green rind. The antioxidant activity of the tannins extract was tested using the DPPH method. The main identified constituents are palmitic acid (11.91%), (E)-phytol (14.40%), linolenic acid (16.59%), diisooctylphtalate (11.84%). The tannins extract was also fractionated over a silica gel dry column. Three main fractions were isolated. The phytochemical screening showed the presence of alkaloid, tannins, flavonoids, sterols, triterpenes, mucilages, oses, holosides and other reducing compounds metabolites, as for the coumarines and saponins, they were absent. The tannins extract showed moderate antiradical activity.

KEYWORDS: *Aloe vera*, phytochemical screening, tannins, antioxidant activity, histological identification.

1. INTRODUCTION

Many new antioxidant molecules have been selected and determined from herbs and spices. The daily intake of these foods might be one of the major and promising sources against major diseases leading to a healthier life. To consider a natural composite as an antioxidant substance, it is important to investigate its antioxidant activities in vitro. Our study adopts this approach and aims to demonstrate the efficiency of the tannin extracts from the green rind of *Aloe vera*.

Since a long time, Aloe has been used throughout history to treat some illnesses. *Aloe vera* (L.) Burm. F. (Syn: *Aloe barbadensis* Mill.) is widely known as a medicinal plant that belongs to the Xanthorrhoeaceae family. The Aloe comprises more than 180 species and hybrids native to sunny, arid areas in Southern and Eastern of Africa, which was subsequently introduced into Northern Africa, Spain (Valencia and Granada), Gibraltar, China, and the West India. In Morocco, it was introduced at the beginning as an ornamental plant, but currently as a medicinal one.

The leaves of *Aloe vera* includes great vitamins, minerals, amino acids, natural sugars, enzymes and other benefits for health care due to bioactive compounds with emollient, purgative, antimicrobial, antinflammatory, aphrodisiac, antioxidant, antifungal and cosmetic values. *Aloe vera* principally proceeds as skin healer and prevents injury of epithelial tissues. Also proceeds as extremely powerful laxative, cures acne and gives a youthful glow to skin on the external use [1].

This study aims to investigate for the first time the chemical composition of the tannins extract obtained from the green rind of *Aloe vera* and its fractions. The tannins extract and its fractions were also used to evaluate the antioxidant potential of the plant.

2. MATERIAL AND METHODS

The Second Edition of the International Congress of Applied chemistry and Environment
30th-31th October and 01st November 2020, Tunisia

ICACE 2020

2.1. Identification of the plant

After its morphological description, *Aloe vera* is identified on the basis of the histological aspect of the leaf using the double-stained: carmine-iodine green [2]. More precisely, this technique consists in staining the cell wall with iodine carmine-green: the pecto-cellulosic wall is pink colored and the lignified wall is colored in blue-green. The anatomical sections are then mounted between the two slides in a drop of water and then they were observed under an optical microscope at different magnifications to determine the plant tissues that constitute those leaves. The observed cuts were subsequently photographed using a digital camera.

2.2. Phytochemical screening of plant material

Phytochemical constituents of *Aloe Vera* leaves were determined by different qualitative tests such as alkaloid (Dragendorff's), tannins (Ferric chloride test and stiasny reaction), anthraquinones, flavonoids (Magnesium and hydrochloric acid reduction), saponins (Foam index), triterpenes and sterols (Liebermann-burchard's test), oses and holosides (Alcohol saturated with thymol), mucilages (Alcohol 95% test), coumarins (UV-Lamp at 366 nm) and reducing compounds metabolites (Fehling's test) was performed by the following standard methods [3].

2.3. Fractionation and analysis

The Fractionation was performed using a classic chromatographic technique. The separation of tannins extract constituents was achieved via elution over a silica gel column.
The analyses process of the studied samples was carried out using (Gas Chromatograph/Mass Spectrometer).

2.4. DPPH Free radical scavenging activity

The power of plant extracts to scavenge DPPH free radicals was specified on the basis of method [4]. An aliquot of 0.1 ml of the TAV was mixed with 3.9 ml freshly prepared DPPH solution (concentration of 25 mg in 100 mL ethanol). After 30 minutes of samples incubation in darkness, the absorbance was measured at 515 nm. Ascorbic acid was used as positive control.

3. RESULTS AND DISCUSSIONS

3.1. Histological study of *Aloe vera* leaves

The microscopic structure of the *Aloe vera* leaf allowed us to distinguish:
- A superior epidermis and an inferior epidermis with a thick cuticle on the two external faces of the limbus and stomata.
- Towards the inside of the epidermis, an assimilative parenchyma formed of about 7 to 8 layers of chlorophyll cells, some of which contain crystals of calcium oxalate (site 1).
- An aquiferous parenchyma with hypertrophied cells, rich in mucilage (hydrated gel) allowing the retention of the water, thus giving a succulence to the leaf which reduces the loss of water. This parenchyma occupies the central zone of the limbus and is devoid of crystals.
- In the contact zone between the two parenchyms, the ribs (crib-vascular bundles) are located. Each conducting beam consists of xylem vessels, a few tubes of the phloem above which are found large cells with very thin wall corresponding to the vascular parenchyma and a cellulosic sheath surrounding the conductive beam.

The Second Edition of the International Congress of Applied chemistry and Environment
30th-31th October and 01st November 2020, Tunisia

ICACE 2020
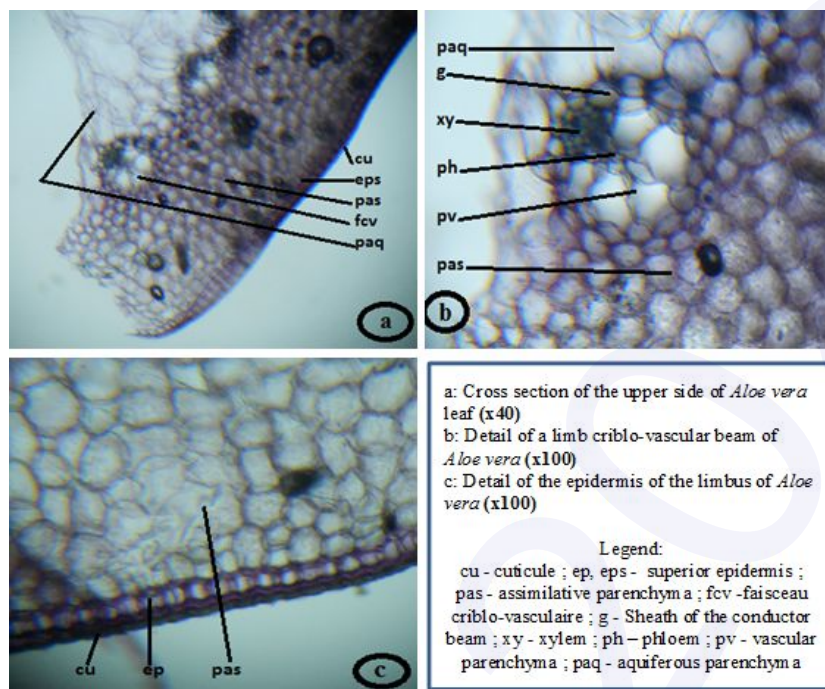
Figure 1: Cross section of the upper side of the *Aloe Vera* Leaf.

3.2. Phytochemical screening

The phytochemical screening of *Aloe vera* leaves, showed the presence of alkaloids, tannins, flavonoids, sterols, triterpenes, oses, holosides, mucilages and reducing compounds metabolites and the absence of saponins and coumarines.

3.3. Chemical composition of the tannins extract

The GC/MS analysis of the extract was done: Nine compounds, accounting for 72.81% of the TAV, as well as 14 compounds representing 93.55% of F_1, 8 compounds representing 79.82% of F_2 and 7 compounds 89.63% of fraction F_3.

The TAV showed that the major constituents were linolenic acid (16.59%), phytol (14.40%), palmitic acid (11.91%), and diisooctyl phtalate (11.84%) whereas the major constituents of the first fraction contained palmitic acid (25.99%), dibutyl phthalate (17.97%), and linoleic acid (11.71%). In addition, the second fraction consisted respectively of dibutyl phthalate (30.93%), butyl cyclobutyl phthalate (11.61%), phthalic acid, and butyl 2-pentyl ester (11.10%). The principal common constituents of the third fraction were diisooctylphtalate (54.13%) and 9-heptadecanone (11.35%). The results show that F_1 is rich in fatty acids, especially in: (9-oxononanoic acid (2.27%), palmitic acid (25.99%), 17-octadecynoic acid (3.80%) and linoleic acid (11.71%). The TAV extract contained palmitic acid (11.91%), 17-octadecynoic acid (6.20%), linolenic acid (16.59%) and chrysophanic Acid (3.82%).

3.4. Antioxidant activity of the tannins extract of *Aloe vera*

The antioxidant capacity has been given from the IC_{50} (Table 1). It is the concentration of the antioxidant giving 50% inhibition of DPPH in the test solution. The evaluation of the antioxidant capacity of the TAV and its fractions (F_1, F_2 and F_3), show that the IC_{50} values are 1.85, 3.70, 5.51 and 11.04 mg/ml, respectively. This activity is lower than that of ascorbic acid showing an IC_{50} of 0.05 mg/ml. TAV and F_1 which are richer in fatty acids show the most important antioxidant power. The high antioxidant activity detected in TAV may be due to some major compounds as phytol and palmitic acid that are known for their various biological activities [5].

Table 1 IC_{50} concentration of DPPH scavenging capacity from bioactive compounds.

Bioactive compounds	IC_{50} (mg/mL)
TAV	1.85
F_1	3.70
F_2	5.51
F_3	11.04
Ascorbic acid	0.05

4. CONCLUSION

In this work, we have focused on the study of the antioxidant activity of the tannins extract obtained from the green rind of *Aloe vera*. On the basis of the plant identification, we have been able to deduct that the transverse cut made for *Aloe vera* is compatible with the one described in the literature. According to the phytochemical tests, we have found that *Aloe vera* is rich in alkaloids, tannins, flavonoids, sterols, triterpenes, oses, holosides, mucilages and reducing compounds metabolites. The main constituents of the TAV were: palmitic acid (11.91%), phytol (14.40%), linolenic acid (16.59%) and diisooctylphtalate (11.84%). The in vitro antioxidant activity showed that the tannins extract of *Aloe vera* has a moderate antiradical activity.

REFERENCES

[1] **Sahu, P.K., Giri, D.D., Singh, R., Pandey, P., Gupta, S., Shrivastava, A.K., Kumar, A., Pandey, K.D.**, Therapeutic and medicinal uses of Aloe vera: a review, *Pharmacology & Pharmacy,* Vol.4, N°8, 2013, 599-610.

[2] **Prat, R.,** Expérimentation en biologie et physiologie végétales. *Editions Quae & Hermann, Paris*, 2007, 56-57.

[3] **Raaman, N.,** *Phytochemical Techniques,* New India Publishing Agency, New Delhi, 2006, 19-24

[4] **Brand-Williams, W., Cuvelier, M.E., Berset, C.**, Use of a free radical method to evaluate antioxidant activity, *Food Science Technology,* Vol.28, 1995, 25-30.

[5] **Benzidia B., Barbouchi, M., Hammouch, H., Belahbib, N., Zouarhi, M., Erramli, H., Ait Daoud, N., Badrane, N., Hajjaji, N**., Chemical composition and antioxidant activity of tannins extract from green rind of *Aloe vera (L.) Burm. F*. *Journal of King Saud University*, Vol.31, 2019, 1175–1181.

The Second Edition of the International Congress of Applied chemistry and Environment
30th-31th October and 01st November 2020, Tunisia

ICACE 2020

In vitro antileishmanial activity of *Artemisia herba-alba* Essential oil from Tunisia

Zeineb Maaroufi[a,b], Sandrine Cojean[c], Philippe M. Loiseau[c], Florence Agnely[a], Manef Abderraba[b], Ghozlene Mekhloufi[a]

(a)   *Université Paris-Saclay, CNRS, Institut Galien Paris Sud, Châtenay-Malabry, France*
(b)   *Laboratoire Matériaux Molécules et applications, Institut préparatoire des études scientifiques et techniques, Univ. De Carthage, La Marsa, Tunisie*
(c)   *Université Paris-Saclay, UMR CNRS 8076, BioCIS, Chimiothérapie Antiparasitaire, Châtenay-Malabry, France*
E-mail: zeineb.maaroufi@u-psud.fr

ABSTRACT

The antileishmanial potential of essential oil (EssOil) extracted from aerial part of *Artemisia herba-alba* harvested in two different areas in Tunisia (area 1 and area 2) was studied. GC-MS analysis showed that EssOil from area 1 was characterized by high camphor content (32.26 %), while, the area 2 EssOil chemotype was α-thujone (67.56 %). EssOil from area 1 exhibited the best antileishmanial activity with IC_{50} values of 2.8 and 6.2 µg/mL against intramacrophage amastigotes and axenic amastigotes of *Leishmania major*, respectively, these values being in the same range as those obtained with miltefosine, the reference drug. Besides, this EssOil is safe for macrophages (Selective Index > 10). In contrast, EssOil from area 2 exhibited a lower activity. The harvest site seemed to influence EssOil compositions as well as their antiparasitic activity and cytotoxicity. EssOil from area 1 appeared as a promising source for the antileishmanial molecules. Further investigations are needed to identify molecules responsible for its antileishmanial activity.

KEYWORDS: *Artemisia herba-alba*, Essential oil, Antileishmanial activity, Cytotoxicity

1. INTRODUCTION

Leishmaniases are a complex of tropical parasitic diseases causing 12 million cases worldwide [1]. Cutaneous leishmaniasis (CL), the most common form of Leishmaniasis, causes a skin ulcerative lesion at the site of the infective sandfly bite and leaves indelible scars causing serious social prejudice [2]. Currently, in the absence of a vaccine for human use, chemotherapy based on antimony derivatives represents the first line treatments. Nonetheless, many limitations have been reported due to their toxicity, high cost, and parasite resistance [3]. Therefore, the development of new drugs, less or nontoxic, more efficient and which would be accessible especially for low-income people who are the most affected by this disease, is becoming a priority [4]. In this context, medicinal plants and extracts represent a source of a wide range of bioactive molecules and have always been used for many centuries as natural remedies especially for parasitic diseases [5]. Essential oils (EssOils), extracted from different plant parts, have been largely reported for their antileishmanial properties [6]. One of the best antileishmanial effects was reported for *Artemisia* species, belonging to the family of the *Asteraceae*. Indeed, sesquiterpenes lactone extracted from this plant aqueous extract including artemisinin are highly effective drugs against many *Leishmania* species [7].

This work dealt with the investigation of antileishmanial potentialities against two forms of *Leishmania major* of EssOil from *Artemisia herba-alba*, a medicinal and strongly aromatic shrub, extracted from two different geographical areas in Tunisia. The aim was to check if the variation in the harvest site climatic and ecological parameters could affect EssOil composition and its antiparasitic activity and cytotoxicity.

2. MATERIAL AND METHODS

2.1. Selection and collection of plant materials

Artemisia herba-alba was collected from two different sampling sites in Tunisia. Harvested part, geographical and ecological sampling sites are gathered in Table 1. The Voucher specimen number of this plant is P.1.01. The harvesting period extended from September to October 2016.

The freshly cut plants were dried at ambient temperature with active ventilation. Then, they were stored at ambient temperature.

Table 1: Harvesting conditions of *Artemisia herba-alba*

Harvested part	Harvesting area (notation)	Geographical coordinates	Mean pluviometry	Bioclimate
Aerial part	*Krib* (Area 1)	Long 9°08' ; Lat 36°18' Altitude 900 m [8]	542 mm/year [9]	Semi-arid sub-level higher [10]
	Sidi Bouzid (Area 2)	Long 9°30'; Lat 35°02' Altitude 327 m [11]	377 mm/year [9]	Arid bioclimatic stage [11]

2.2. Essential oils extraction by hydrodistillation

Dried plants were subjected to hydrodistillation for 2 hours using a modified Clevenger-type apparatus. The essential oil obtained was dried over anhydrous sodium sulfate and stored in amber vials at 4°C until further analysis. The extraction yields were calculated.

2.3. Essential oils characterization by GC-MS

10 µL of diluted EssOil (1:10 ratio with ethyl acetate, HPLC Grade) was injected into the GC (7890A) -MS (5975C inert MSD with Triple-Axis Detector) Agilent unit under the following conditions: capillary column HP-5MS (5% phenyl)–methylpolysiloxane (60 m $\Box$ 0.25 mm, 0.25 µm film thickness) interfaced with an Agilent mass selective detector 5975 C inert MSD. The carrier gas was N_2 at 1 mL/min. Molecules under an amount of 0.2 % were not considered.

2.4. Antileishmanial activity and cytotoxicity

The differentiation of *Leishmania major* (MHOM/PT/92/CRE26) promastigotes into axenic amastigotes was achieved by dilution of 10^6 promastigotes in stationary phase of growth in 5 mL of amastigote medium (M199 1x supplemented with 40 mM HEPES, 100 mM adenosine, 0.5 mg/l hemin, 10% fetal bovine serum (FBS), 2 mM $CaCl_2$ and 2 mM $MgCl_2$), then by an overnight incubation at 37°C in 5% CO_2.

2.4.1. *In vitro* activity on axenic amastigotes

A suspension of 10^6 parasites/mL of *L. major* axenic amastigotes was prepared. EssOils were added to this suspension at concentrations ranging from 100 to10^{-4} µg/mL obtained by serial dilution. Miltefosine (HePC) was used as a positive control with final concentration from 100 µM to 97.6 nM. Cultures were incubated 72 h at 37 °C in the dark under 5 % CO_2 atmosphere. Finally, amastigotes viability was assessed using the SYBR® green I incorporation method. Activity was expressed as 50 % inhibitory concentration of growth (IC_{50}) calculated using ICEestimator [http://www.antimalarial-icestimator.net/MethodIntro.htm]. Experiments were carried out in triplicates.

2.4.2. *In vitro* activity on intramacrophage amastigotes and cytotoxicity

Macrophages (cell line Raw 264.7) were seeded at 2×10^5 cells/well containing DMEM (Applied Biosystems) supplemented with 10% FBS, 2 mM $CaCl_2$ and 2 mM $MgCl_2$. Then, promastigotes were added with a density of 16 parasite-to-cell ratio. EssOils and miltefosine dilution in DMEM was processed in the same way as for the axenic test. Both infected and non-infected macrophages without treatment were used as negative controls. Plates were left 72 h at 37°C with 5 % CO_2. In parallel, EssOils cytotoxicity was evaluated using the same procedure in the absence of parasites during an incubation time of 48 h. Parasites/cells viability was achieved using SYBR® Green I incorporation method. Experiments were carried out thrice at least.

Antileishmanial activity and cytotoxicity were expressed as 50 % inhibitory concentration (IC_{50} and CC_{50}, respectively). Moreover, selectivity index (SI) was calculated by the ratio CC_{50} to IC_{50} in order to assess the selectivity of the treatment towards parasites.

3. RESULTS AND DISCUSSIONS

3.1. Extraction yield

Extraction yield did not vary significantly ($p > 0.05$) from a harvest area to another with a mean value of 1.2 wt%. Similar extraction yield results (~ 1 wt%) were obtained for Algerian *Artemisia herba-alba* EssOil extracted from the plant aerial part [12].

3.2. Essential oils chemical composition

Chemical compositions of *Artemisia herba-alba* EssOils from area 1 and area 2 are shown in Table 2. EssOils from area 1 and area 2 showed respectively eighteen and seven identified components that represent around 98% by weight (wt/wt) of the total EssOils composition.

Table 2: Composition of *Artemisia herba-alba* EssOils from areas 1 and 2 analyzed by GC-MS.

Compound	Relative composition (wt%)	
	Area 1	*Area 2*
α –pinene	1.92	-
camphene	3.62	-
β-phellandrene	0.59	4.43
o-cymene	0.88	-
eucalyptol	8.59	4.43
α-thujone	13.97	**67.56**
trans-p-menth-2-en-1-ol	0.76	-
1.6-dimethylhepta-1.3.5-triene	16.00	1.62
isopinocarveol	1.78	2.43
(-)-camphor	**32.26**	3.86
isocyclocitral	1.61	-
α-pinocarvone	2.69	-
borneol	4.24	-
(-)-terpinen-4-ol	1.24	-
cis-verbenone	0.57	-
verbanyl acetate	2.06	-
bornyl acetate	0.93	-
β-thujene	-	13.86
3.5-heptadienal	4.55	-
Total (%)	98.28	98.19

In **bold**: major compound (chemotype)

EssOil from area 1 was characterized by high camphor content (32.26 %), followed by 1.6-dimethylhepta-1.3.5-triene (16 %), and α-thujone (13.97 %). However, the area 2 EssOil was mainly

composed of α-thujone (67.56 %). Both EssOils were characterized by an abundance of oxygenated monoterpenes that represented between 71% (area 1) and 92% (area 2) of compositions.

It is important to notice that the chemotype of *Artemisia* EssOil from area 1 was described for the first time in our study. In fact,1,6-dimethylhepta-1,3,5-triene had never been described as one of major compounds in an *Artemisia* EssOil but only in trace (~ 0.05 %) [13].

3.3. Antileishmanial activity against *Leishmania major* axenic and intramacrophage amastigotes, and cytotoxicity

An EssOil was considered highly effective against the parasite when IC_{50} value was lower than 10 µg/mL, and moderately effective when IC_{50} was between 10 and 20 µg/mL. Moreover, an EssOil was considered as selective to parasite and safe to macrophage when the SI was higher than 10 [14].

The best growth inhibitory effect on axenic amastigote form was shown by EssOil from area 1 that exhibited a comparable ($p > 0.05$) activity as those of miltefosine, the reference drug (Table 3). In contrast, no interesting activity against axenic amastigote form was shown by EssOil from area 2 ($IC_{50} > 20$ µg/mL).

Concerning the activity against intramacrophage amastigote form, EssOil from area 1 exhibited the best inhibitory effect, close to activity obtained with miltefosine ($p > 0.05$). Moreover, this EssOil had presented the highest SI value revealing its safety to host cells and high selectivity to parasites. On the other hand, as for the axenic form, a poor activity was proved by EssOil from area 2.

The intramacrophage activity of EssOil from area 1 was significantly ($p < 0.05$) enhanced compared to that observed against the axenic amastigote form. Interestingly, this may be due to easier targeting of host factors by one or several components of this EssOil, hindering the parasite development. Active compounds acting indirectly on pathogens *via* macrophage activation are assumed to be less likely to induce drug resistant pathogens [15].

Table 3: Antileishmanial activity and cytotoxicity of *Artemisia herba-alba* essential oils from area 1 and area 2

Sample	IC_{50} Axenic amastigote	IC_{50} Intramacrophage amastigote	CC_{50}	Selectivity index
EssOil, area 1	6.2 ± 0.6 [a,A]	2.8 ± 0.4 [a,B]	44.6 ± 1.3 [a,C]	16
EssOil, area 2	> 100 [d,A]	45.2 ± 3.5 [d,B]	64.1 ±1.5 [b,C]	1.4
HePC	2.7 ± 0.4 [a,A]	2.0 ± 0.6 [a,A]	62.1 ± 4.4 [b,B]	31.4

IC_{50} and CC_{50} are expressed in µg/mL; HePC: Hexadecylphosphocholine (miltefosine), the positive control.
a−c and A-C: Means within respectively, a column and a line with different letters were significantly different ($p < 0.05$).

As camphor (the major compound of EssOil from area 1) did not show any antileishmanial efficacy [16], EssOil of *Artemisia herba-alba* harvested in area 1 is potentially a promising source of active molecules against *Leishmania major* parasite. Therefore, deeper investigations are required to identify compounds responsible for the observed activity.

4. CONCLUSION

This study demonstrated that antileishmanial activity and cytotoxicity of *Artemisia herba-alba* EssOils depended significantly on harvest area and *Leishmania major* form. EssOil from area 1 krib showed the best antileishmanial potential against both free-living and intracellular amastigotes without having any cytotoxic effect on host cells. This study demonstrated the high potential of EssOils extracted from *Artemisia herba-alba* aerial part harvested from different areas in Tunisia to inhibit *Leishmania major in vitro* development. Further investigations are needed to identify active molecules by bio-guided fractionation. This research could contribute to the discovery of effective drugs against cutaneous leishmaniasis.

The Second Edition of the International Congress of Applied chemistry and Environment
30th-31th October and 01st November 2020, Tunisia

ICACE
2020

REFERENCES

[1] **WHO**, WHO | Leishmaniasis, Fact sheet, 2017.

[2] **K. Aoun** *et al.***,** Cutaneous Leishmaniasis in North Africa: a review, *Parasite*. 2014, 21, 215-223

[3] **M. Akbari** *et al.,* Application of nanotechnology in treatment of leishmaniasis: A Review, *Acta Trop.*, 2017, 172, 86–90.

[4] **A. Oryan***,* Plant-derived compounds in treatment of leishmaniasis., *Iran. J. Vet. Res.*, 2015, 16, 1–19.

[5] **J.P. Anthony** *et al.,* Plant active components - A resource for antiparasitic agents?, *Trends Parasitol.*, 2005, 21, 462–468.

[6] **A. El Asbahani** *et al.***,** Essential oils: From extraction to encapsulation, *Int. J. Pharm.*, 2015, 483, 220–243.

[7] **L.G. Rocha** *et al.,* A review of natural products with antileishmanial activity, *Phytomedicine,* 2005, 12, 514–535.

[8] Official municipality website: *commune-elkrib.gov.tn*

[9] OpenStreetMap, Les données climatiques pour les villes du monde entier, 2019.

[10] **M. Mizouri** *et al., Des Ressources En sols de la Tunisie*, Feuille de Maktar Nouvelle approche méthodologique, 1984.

[11] Official municipality website: *commune-sidibouzid.gov.tn*

[12] **T. Dob** *et al.***,** Chemical composition of the essential oil of *Artemisia herba-alba Asso* grown in Algeria., *J. Essent. Oil Res,* 2006, 18, 685–690.

[13] **A. Sardashti**, Chemical composition of essential oils from two *Artemisia* species and their antimicrobial effect in drinking water, *Med. Plants*., 2012, 4, 514-519.

[14] **T.B. Le** *et al.*, *In vitro* anti-leishmanial activity of essential oils extracted from Vietnamese plants, *Molecules.,* 2017, 22, 1–12.

[15] **G. De Muylder** *et al.***,** A Screen against *Leishmania* Intracellular Amastigotes: Comparison to a Promastigote Screen and Identification of a Host Cell-Specific Hit, *PLoS Negl. Trop. Dis.,* 2011, 5, e1253.

[16] **V. Zheljazkov** *et al.***,** Content, composition, and bioactivity of the essential oils of three basil genotypes as a function of harvesting, *Planta Med*, 2008, 74, 380-385.

The Second Edition of the International Congress of Applied chemistry and Environment
30th-31th October and 01st November 2020, Tunisia

ICACE 2020

Dyeing properties and colorfastness of cotton dyed with *Corchorus olitorius* extracted natural dye

Syrine Ltaief[a], Nesrine Bhouri[a], Saber Ben Abdessalem[a]

(a)   University of Monastir, ENIM, MPTEX UR17ES33, Ave Ibn Jazzar Monastir, 5000, Tunisia
syrineltaief3@gmail.com
bhourinesrine@yahoo.fr
saber_ba@yahoo.fr

ABSTRACT

The main purpose of this paper is to study the dyeing properties of cotton fabric dyed with *Corchorus olitorius* as natural dyes. The extraction of dyes from the leaves of *Corchorus olitorius* was conferred by an ultrasonic process. The extracted dye was used for dyeing cotton fabric using different mordants such as copper sulfate, ferrous sulfate, and aluminum sulfate and by varying the mordanting process. The effect of treatment variables on the color strength of dyed fabric was also examined. It was found that pH, temperature and the dyeing time influences considerably the results. Results show an increase in color strength values when using mordants. The fastness properties of dyed cotton against washing, light, dry and wet rubbing were assessed and noticeable to good fastness grades were obtained.

KEYWORDS: *Corchorus olitorius*, Natural Dye, Cotton, Color Strength.

1.   INTRODUCTION

Nature provides a wealth of plants that yield color for the purpose of dying; many have been used since antiquity. Natural dyes extracted from plants, animals or minerals without chemical processing show better biodegradability and higher compatibility with the environment [1, 2].They are also non-toxic and have renewability potential. The production of synthetic dyes depends on the petrochemical source, and some of these dyes contain carcinogenic amines. The application of these dyes poses serious health risks and negatively influences the ecological balance of nature [3-5]. In addition, many countries have already imposed strict environmental standards on these dyes, noting Germany's prohibition of azo dyes [6]. In this situation, a higher demand is oriented towards greener alternatives. Therefore, natural dyes are among the promising options for the development of a more environmentally friendly textile dyeing process.*Corchorus olitorius* is among the most popular edible plants in northern Africa and the Mediterranean region [7]. It is an Afro Arabian annual herb(known as Molkhyia or Jew's Mallow) rich in kaempferol glycosides, rutin, and isoquercitrin flavonoids. It is considered a source of carotenoids, vitamin C, vitamin E, fatty acids and minerals and having demulcent, diuretic, lactagogue, purgative and tonic properties [8]. It is considered as a folk remedy for aches and pains, managing diabetes, hypertension[9] and swellings, becoming an ingredient of facial creams, lotions, hair tonics and hand creams. *Corchorus olitorius* leaves are used for cystitis, dysuria, fever and gonorrhea, while its cold infusion is said to restore the appetite and strength [10].

The present study describes an ecological process for dyeing the cotton fabric with a natural dye extracted from *Corchorus olitorius*. Efforts have also been done to optimize the best mordanting method using various mordants.

2. MATERIALS AND METHODS

Corchorus olitorius used during this work were purchased from Gabes region in the southeast of Tunisia in February 2018 (Figure 1). To ensure the homogeneity of the material, all the quantity used was purchased from the same supplier.

The Second Edition of the International Congress of Applied chemistry and Environment
30th-31th October and 01st November 2020, Tunisia

ICACE 2020

Figure 1: (a) *Corchorus olitorius* leaves; (b) Leaf powder of Corchorus olitorius

In this study, cotton plain weave fabric was used for dyeing. The cotton fabric was scoured and bleached fabric of 107 g/m^2, 29 ends per cm and 22 picks per cm.

The metallic salts used were ferrous sulfate ($FeSO_4$), cobalt sulfate ($CuSO_4$) and Alum ($KAl (SO_4)_2$) purchased from Sigma Aldrich Tunisia and used without further purification.

The extraction was carried out using an unconventional ultrasonic process using ethanol as a solvent under 70°C temperature conditions, 25 min duration and 1/10 bath ratio. The extracted dye was analyzed using a UV-Visible spectrophotometer (HACH DR 3900) in the visible range of 380 - 780 nm.

1.1 Dyeing procedure

To investigate the potential use of the extracted colorant, cotton fabrics were dyed at a liquor ratio of 40:1 by exhaust dyeing method. The dyeing process was done in a laboratory dyeing machine (AHIBA Datacolour International USA). Then the dyed fabrics were rinsed with water and dried at room temperature. Dye bath pH, temperature, and the dyeing time were the three dyeing conditions studied. The pH of the dyebath was adjusted by adding acetic acid and sodium carbonate solution.

The color strength (K/S) of the dyed fabrics was measured using a Datacolor SF 650 X Spectrophotometer using D65 illuminant.

1.2 Mordanting methods

In the case of mordanting, pre mordanting, metamordanting and post-mordanting were used. Three mordants including aluminum sulfate hydrate (alum), ferrous sulfate and copper sulfate were used with a concentration of 1% (w/w with respect to the fabric).

1.3 Fastness properties

The dyed samples were tested according to ISO standard methods. The specific tests were ISO105-X12, colorfastness to rubbing; ISO 105-C02, colorfastness to washing and ISO 105-B02, colorfastness to light.

3. RESULTS AND DISCUSSION

3.1 Effect of the dye bath pH

Figure 2 shows the effect of pH on the color strength obtained by *Corchorus olitorius* phenolic extract. As can be observed, the pH of the dyes solution is an important parameter for the adsorption process. In fact, the effect of dye bath pH can be attributed to the correlation between dye structures, the fiber used and the dye stability [11]. The color strength increases considerably from pH 4 to pH 8, these results can be attributed to the highest thermal stability of the extracted dyestuffs in this range. At pH > 8, an important decrease in the K/S values is observed indicating that the electrostatic interactions between the cotton fiber and the phenolic extract play an important role in the adsorption of the dyestuff onto cotton. The pH value was fixed at 8 in all subsequent experiments and adjusted with dilute solutions of sodium carbonate.
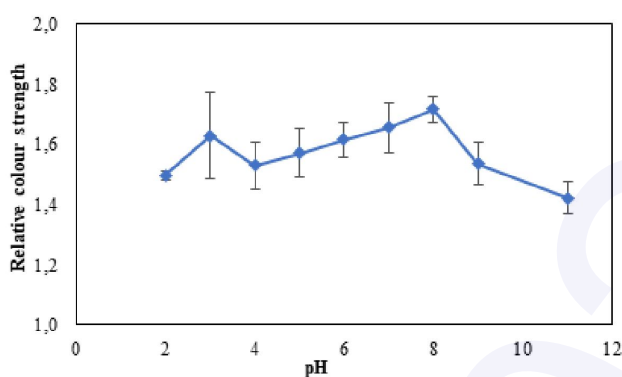
Figure 2: Effect of the dye bath pH on the color strength of the dyed fabric

3.2. Effect of the dyeing temperature

As shown in Figure 3 the color strength increases with the increase of dyeing temperature to reach a maximum value of K/S at 110°C. Indeed, heating increases the cotton fiber swelling, and the solubility of the extracted dyestuff became higher, thus the diffusion of the dye molecules to the fiber became easier and thus the color strength value increases.
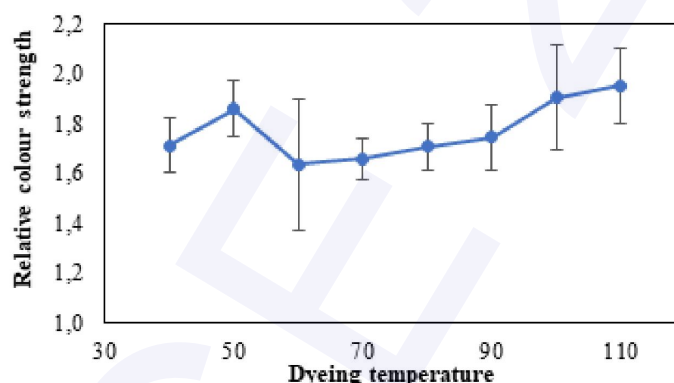
Figure 3: Effect of the dyeing temperature on the color strength of the dyed fabric

3.3. Effect of the dyeing duration

The effect of dyeing time on color strength is shown in Figure 4. From this figure, It can be noticed that the color strength was improved when the dyeing time increased until a maximum of 60 min. Above this value, a decrease in the K/S was observed. Indeed, this can be explained by the high exhaustion of the dye bath at 60 min. For longer periods of time and at high temperatures, the dyestuff is degraded and transformed into colorless substances. The results indicate that 60 min is a suitable time for dyeing with a *Corchorus olitorius* extracted dyes.
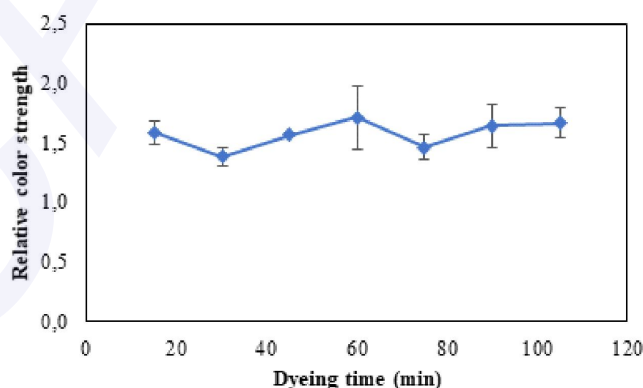

Figure 4: Effect of the dyeing time on the color strength of the dyed fabric

3.4. Effect of mordanting

The effect of mordanting methods on dyeing of cotton with different mordants is shown in Figure 5. It was observed that the K/S value of the dyed cotton fabrics increases considerably by using a pre-mordanting process. It can be seen also that the best results of the color strength were reached with copper sulfate mordant. Indeed, the use of a mordant in a pre-mordanting dyeing process allows the formation of an insoluble complex including the dyes molecules, the mordant and the functional groups of the fiber.
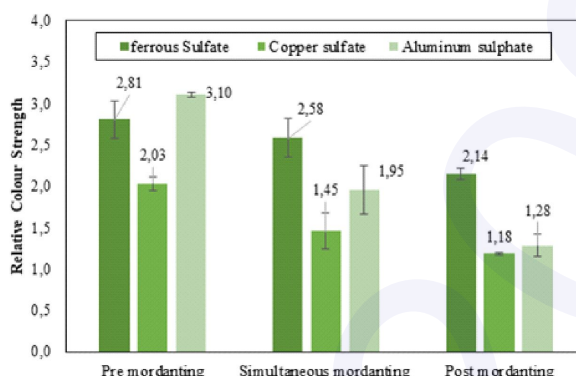
Figure 5: Effect of mordanting on the color strength of the dyed fabric

3.5. Fastness properties of dyed cotton

The color fastness of dyed fabric with and without mordant was given inTable 1. The samples of colorfastness to washing were assessed on the basis of change in color and staining on the adjacent fabrics with the help of grayscale. It is indicated that sample mordanted with ferrous sulfate gave the best washing fastness in comparison to the sample dyed with the extract and the other samples treated with copper sulfate and aluminum sulfate.The washing fastness of dyed fabric showed that mordanting improved the rating from poor to good.This was attributed to metal dye complex formation onto irradiated fabric through covalent bond formation when these mordanted fabrics were exposed to detergents did not detach.

Table 1: Effect of Pre mordanting on the fastness properties of the dyed cotton

Mordant	Wash ISO 105-B01	Light ISO 105-B01	Rubbing ISO 105-X12	
			Dry	Wet
No Mordant	3	2	3/4	3
$FeSO_4$	4/5	4	4	3
$CuSO_4$	4	4	3/4	3
$Al_2(SO_4)_3$	4	3	3/4	3

Colorfastness to light is a very important factor that gives information that whether the color applied on the fabric is stable to light or not. Table 1, indicates that samples dyed with ferrous sulfate and copper sulfate mordant gave the best fastness grade. This improvement is due to the formation of coordination bonds

The Second Edition of the International Congress of Applied chemistry and Environment
30th-31th October and 01st November 2020, Tunisia

ICACE
2020

between the cotton fiber and the mordant on the one hand and between the mordant and the natural dye on the other.

Colorfastness to rubbing used to determine the stability of the dyed color on the fabrics. Table 1 shows that the sample dyed and mordanted with ferrous sulfate showed the best behavior towards color fastness to rubbing. In the case of wet rubbing, a noticeable staining range was obtained with all three mordants. This observation is correlated to the fact that the use of mordant ameliorates the penetration of the dye into the cotton fabric.

4. CONCLUSION

The current work has developed an efficient method for dyeing cotton using an ecological extract of *Corchorus olitorius*. The influence of different experimental conditions on dyeing properties was examined. Natural dye applied with different mordanting methods enhances the fastness properties of dyed cotton fabric. The experimental results showed also that the best dyeing performance was achieved using aluminum sulfate as a mordant.

References

[1] **Goodarzian, H. and E. Ekrami**, Wool dyeing with extracted dye from pomegranate (Punica granatum L.) peel. *World Applied Sciences Journal,* Vol. 8, N°11, 2010, 1387-1389.

[2] **Angelini, L.G., et al**., Rubia tinctorum a source of natural dyes: agronomic evaluation, quantitative analysis of alizarin and industrial assays. *Industrial Crops and Products,* Vol.6, N°3-4, 1997, 303-311.

[3] **ade Campos Ventura-Cmargo, B. and M.A. Marin-Morales**, Azo dyes: Characterization and toxicity-A review. *Textiles and Light Industrial Science and Technology,* Vol.2, N°2, 2013, 85-103.

[4] **Goodarzian, H. and E. Ekrami**, Extraction of dye from madder plant (Rubia tictorium L.) and dyeing of wool. *World Applied Sciences Journal*, Vol.9, N°4, 2010, 434-436.

[5] **Jothi, D**., Extraction of natural dyes from African marigold flower (Tagetes erecta L.) for textile coloration. *Autex Research Journal,* Vol.8, N°8, 2008, 49-53.

[6] **Almahy, H., M. Ali, and A. Band**, Extraction of Carotenoids as natural dyes from the Daucus carota Linn (carrot) using ulturasound in Kingdoum of Saudi Arabia. *Research Journal of Chemical Sciences,* Vol.3, N°1, 2013, 63-66.

[7] **Najjaa, H., et al.**, Antioxidant and antimicrobial activities of Allium roseum L."Lazoul," a wild edible endemic species in North Africa. *International journal of food properties*, Vol.14, N°2, 2011, 371-380.

[8] **Handoussa, H., et al.**, Anti-inflammatory and cytotoxic activities of dietary phenolics isolated from Corchorus olitorius and Vitis vinifera. *Journal of Functional Foods*, Vol.5, N°3, 2013, 1204-1216.

[9] **Oboh, G., et al.**, Inhibitory effect of polyphenol-rich extracts of jute leaf (Corchorus olitorius) on key enzyme linked to type 2 diabetes (α-amylase and α-glucosidase) and hypertension (angiotensin I converting) in vitro. *Journal of Functional Foods*, Vol.4, N°2, 2012, 450-458.

[10] **Adegoke, A. and B. Adebayo-Tayo**, Phytochemical composition and antimicrobial effects of Corchorous olitorius leaf extracts on four bacterial isolates. *Journal of Medicinal Plants Research*, Vol.3, N°3, 2009, 155-159.

[11] **Guesmi, A., et al.**, First application of chlorophyll-a as biomordant: sonicator dyeing of wool with betanin dye. *Journal of Cleaner Production*, Vol.39, 2013, 97-104.

The Second Edition of the International Congress of Applied chemistry and Environment
30th-31th October and 01st November 2020, Tunisia

ICACE 2020

Curcumin nanoemulsions for a topical application.

Mekhloufi Gozlene[a] ; Villamosa Nicolas[a] ; Agnely Florence[a]

(a) Université Paris-Saclay, CNRS, Institut Galien Paris Sud, 92296, Châtenay-Malabry, France.

E-mail: ghozlene.mekhloufi@u-psud.fr

ABSTRACT

Curcumin has many interesting biological properties. However, it is poorly soluble and stable in aqueous media. Thus, its formulation is complex. Nanoemulsions (NEs) are proposed as encapsulating systems to increase curcumin solubility while protecting it from degradations. Results showed that the incorporation of curcumin within the oily phase of NEs did not modify the size and the zeta potential of nanodroplets as well as NE stability over time. Nevertheless, a creaming phenomenon was observed in NEs over an 80-day storage period. An *in vitro* study with Franz cells showed that curcumin diffused slowly through a synthetic membrane mimicking the skin. Thus, curcumin encapsulation in the dispersed phase of NE seemed to be a promising strategy to increase its solubility and diffusion through a synthetic skin model with a view of a topical application.

KEYWORDS: Curcumin, Encapsulation, Nanoemulsions, Franz cell, synthetic membrane.

1. INTRODUCTION

Many studies have established that curcumin has many possible applications in the pharmaceutical field through its anti-inflammatory, anti-oxidant, antimicrobial or anti-cancer properties [1]. Despite its proven usefulness in the therapeutic field, curcumin is a molecule difficult to formulate. Indeed, the major disadvantages of curcumin are its low solubility and its degradation in aqueous media. To solve these major issues, the choice of innovative formulations seems to be essential. Potentially nanoemulsions could overcome these hurdles and this kind of system has been little explored with curcumin. Nanoemulsions (NEs) are colloidal dispersions characterized by very fine droplets with a mean diameter ≤ 200 nm and a narrow size distribution [2]. As for conventional emulsions, NEs are thermodynamically unstable systems. However, they have a higher kinetic stability to gravitational separation, flocculation, and coalescence because of their nanosized droplets [3]. To ensure droplet formation and to maintain NEs stability, synthetic surfactants are often used. However, these emulsifiers directly or indirectly raise toxicity and environment issues [4]. Hence, there is an increasing demand for natural and biodegradable products. Proteins are good candidates as emulsifiers. In fact, they are known to stabilize emulsions by forming a viscoelastic, adsorbed layer onto the oil droplets [5]. They are able to generate repulsive steric and electrostatic interactions between these oil droplets [6]. The stabilization of NEs by β-lactoglobulin (βlg), the major protein of whey, is an alternative approach to replace synthetic surfactants by biocompatible polymers. Emulsion stabilization by proteins is already widespread in the food industry. However, this approach is not yet applied in the pharmaceutical and cosmetic industries.

The aim of this study was to encapsulate curcumin within a βlg-stabilized NEs for a topical application and to determine its diffusion through a synthetic membrane. The effectiveness of this formulation as a delivery system of curcumin was thus determined.

2. MATERIAL AND METHODS

2.1 Determination of curcumin solubility in different oils

Curcumin solubility in three different oils, namely Miglyol 812, sweet almond oil, and wheat germ oil, was determined by UV/vis spectrophotometer at 419 nm (wavelength of maximum of absorbance determined experimentally).

The Second Edition of the International Congress of Applied chemistry and Environment
30th-31th October and 01st November 2020, Tunisia

ICACE 2020

2.2. Preparation of nanoemulsions

The aqueous phase was prepared by dissolving βlg powder in potassium phosphate buffer solution (PBS at pH 7.0). The concentration of βlg solutions (1 wt%) was checked by UV/vis spectrophotometer at 278 nm, using the specific extinction coefficient of 9.6 dL.cm^{-1}.g^{-1} [7]. NEs were then prepared by first mixing 5 wt% of oily phase (Miglyol 812) with 95 wt% of βlg solution with high shear mixer. The pre-emulsion was then passed through a high pressure homogenizer [8]. For curcumin-loaded NEs, curcumin was solubilized at 0.25 wt% concentration in the oily phase prior emulsification.

2.3. Characterization of nanoemulsions

The mean droplet size, size distribution, polydispersity index (PDI), and zeta potential (ζ) of NEs with and without curcumin were measured using a dynamic light scattering instrument (Zetasizer Nano ZS90, Malvern). NEs stability was evaluated over 80 days by visual observations and by using a Turbiscan Classic MA 2000 (Formulaction) that measured transmitted and backscattered light intensities versus the height of the sample. Interfacial properties of βlg and curcumin at Miglyol 812/water interface was studied with a pendant drop tensiometer (Teclis-IT concept).

2.4. *In vitro* diffusion experiments

In vitro diffusion studies were carried out in a Franz Cell system (at 37°C) over 48 hours. A Strat-M® membrane (Merck Millipore) was used to mimic human skin in this study. Curcumin-loaded NEs and curcumin solubilized in Miglyol 812 were placed in the donor compartment. Aliquots were collected in the receptor compartment (composed of 90/10 (v/v) PBS/ethanol, 0.1 wt% Tween 20, and 0.04 wt% ascorbic acid) at different times to follow the curcumin diffusion through the membrane. Curcumin concentration in the receptor compartment was determined by UV/vis spectrophotometer at 425 nm.

3. RESULTS AND DISCUSSIONS

3.1. Curcumin solubility in oils

The solubility of curcumin in the three chosen oils was determined. The difference in curcumin concentration solubilized in these oils can be related to the difference of oils' composition. Indeed, the chosen oils differ by the length of triglycerides chains, which is an important parameter in the solubility of hydrophobic molecules in oils [9]. Curcumin showed the highest solubility in Miglyol 812. This latter is composed of medium chain triglycerides (caprylic and capric acids [10]) whereas sweet almond oil and wheat germ oil contain long chain triglycerides (palmitic, oleic, and linoleic acids [11]). The shorter the triglyceride chains, the better the solubility of curcumin since there are more polar groups per mass unit. Thus, Miglyol 812 was selected to constitute the oily phase of the NE encapsulating curcumin (at 0.25 wt % concentration).

3.2. Nanoemulsions' stability

NEs (with or without curcumin) were formulated, characterized, and their stability over time determined. The droplet size of NEs (with or without curcumin) was about 200 nm with a narrow size distribution (PDI < 0.2) indicating a monomodal size distribution. In addition, the ζ value was similar for both NEs (around − 63 mV). Note that the global negative charge of droplets was due to the adsorption of negatively charged protein (as pH > pI of βlg = 5.1) at the oil/water interface [5]. The presence of curcumin in the oily phase did not affect the size and surface charge of droplets.

80 days after their formulation, NEs with and without curcumin seemed visually stable as no creaming or clarification was observed with the naked eye. Nevertheless, Turbiscan analysis highlighted a decrease and an increase of the backscattered intensity at the bottom and the top of the tube, respectively (Figure 1). The creaming phenomenon was thus present for both NEs. Moreover, droplet mean diameter did not evolve over 80 days showing that there was no coalescence of droplets. Thereby, the instability due to creaming can be reversible by simple manual shaking of the NEs. The βlg adsorption at the oil/water interface conferred elastic properties to the interface, which is likely to prevent droplet coalescence. Curcumin also adsorbed at the oil/water interface and lowered the interfacial tension. The elastic behavior to the interface was obtained much more progressively than with the protein alone.
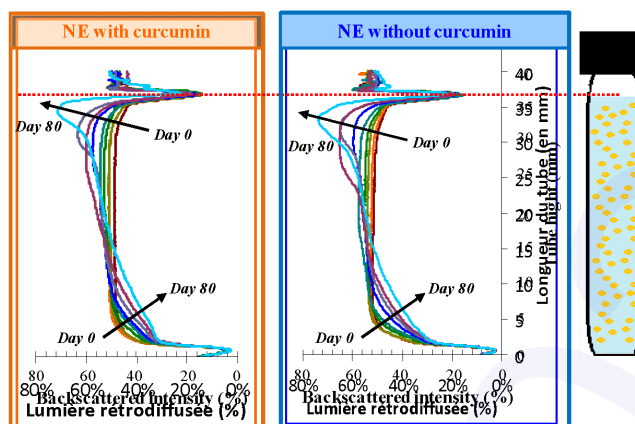
Figure 1. Time evolution of backscattered intensity for NEs with and without curcumin (yellow frame and bleu frame, respectively). Arrows indicate the evolution over 80 days.

3.3. *In vitro* diffusion of curcumin

The diffusion study showed that curcumin could be released gradually from the dispersed phase of NEs and even from Miglyol 812 alone and diffuse through a synthetic membrane mimicking human skin. This result was also visible by simple observation of the receptor compartment of Franz cell at 48 hours (Figure 2). This study showed that there is a constant flow of diffusion over 7 hours which indicates a slow diffusion of curcumin through the membrane.
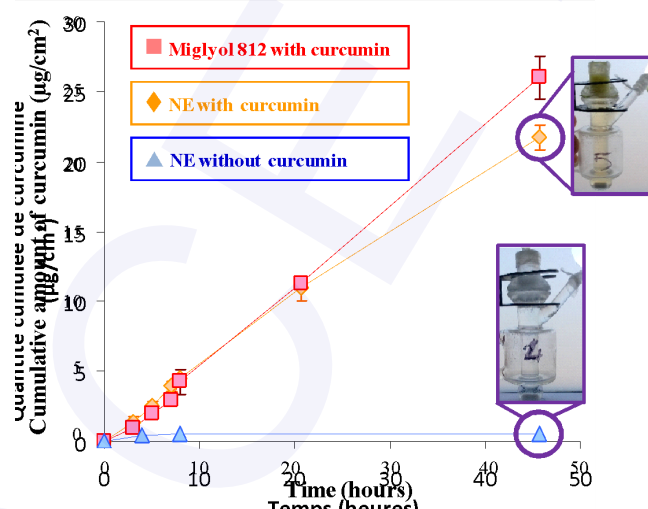
Figure 2. Time diffusion of curcumin through Strat-M® membrane from different formulations: curcumin solubilized in Miglyol 812 (—) and curcumin encapsulated in NE (—). NE without curcumin was the negative control (—).

4. CONCLUSION

The incorporation of curcumin within the oily dispersed phase did not modify the characteristics of NE as well as its stability over time. Nevertheless, the stability study revealed a creaming phenomenon within NEs which is reversible by hand agitation and will not be a limitation for the use of NEs. The diffusion study in Franz cells showed that curcumin diffused slowly through the synthetic membrane and could potentially have a local effect. Thus, the encapsulation of curcumin in the dispersed phase of NE seemed to be a promising strategy to increase its solubility and control its delivery through skin.

REFERENCES

[1] **Aggarwal B.B., Bhatt I.D., Ichikawa H., Ahn K.S., Sethi G.,Sandur S.K..Shishodia C.S.** Curcumin - Biological and medicinal properties. In: *Turmeric: The genus Curcuma*. Ravindran P.N. and Collectif. Boca Raton (Eds), London, New York: CRC Press, 2007, 297-368.

[2] **Mason T.G., Wilking J.N., Meleson K., Chang C.B., Graves S.M**. Nanoemulsions: Formation, Structure, and Physical Properties. *Journal of Physics: Condensed Matter*, Vol.18, N°41, 2006, 635–666.

[3] **Tadros T., Izquierdo P., Esquena J., Solans C.** Formation and stability of nano-emulsions, *Advances in Colloid and Interface Science*, 108-109, 2004, 303-318.

[4] **Cserháti T., Forgács E., Oros G.** Biological activity and environmental impact of anionic surfactants, *Environment International,* Vol.28, 2002, 337–348.

[5] **Bouyer E., Mekhloufi G., Le Potier I., Du Fou de Kerdaniel T., Grossiord J.L., Rosilio V., Agnely F.** Stabilization mechanism of oil-in-water emulsions by β-lactoglobulin and gum arabic*, Journal of Colloid and Interface Science,* Vol. 354, 2011, 467–477.

[6] **McClements D.J.** Protein-stabilized emulsions, *Current Opinion in Colloid & Interface Science*, Vol. 9, 2004, 305-313.

[7] **Townend, R., Winterbottom, R.J., Timasheff, S.N**. Molecular Interaction in β-lactoglobulin. II. Ultracentrifugal and Electrophoretic Studies of the Association of β-lactoglobulin below its Isoelectric Point. *Journal of the American Chemical Society*, Vol. 82, 1960, 3161-3168.

[8] **Ali A., Mekhloufi G, Huang N, Agnely F.** β-lactoglobulin stabilized nanemulsions - Formulation and process factors affecting droplet size and nanoemulsion stability, *International Journal of Pharmaceutics*, Vol. 500, N°1-2, 2016, 291-304.

[9] **Ahmed K., Li Y., McClements D.J., Xiao H.** Nanoemulsion- and Emulsion-Based Delivery Systems for Curcumin: Encapsulation and Release Properties. *Food Chemistry*, Vol. 132, N°2, 2012, 799–807

[10] Supplier data.

[11] **Rowe R.C., Sheskey P.J., Quinn M.E.** *Handbook of Pharmaceutical Excipients*, 6th ed. London, Chicago: Pharmaceutical Press, 2009, 888.

The Second Edition of the International Congress of Applied chemistry and Environment
30th-31th October and 01st November 2020, Tunisia

ICACE 2020

Valorization of Mycelium from *Pleurotus ostreatus* (Jacq: Fries) Kummer and production of chitin and chitosan

Nora Benbelkacem Belabbas[a], Malika Mansour Benamar[b], Nadia Ammar Khodja[c], Lydia Adour[d]

(a) Department of Chemistry, Faculty of Sciences, Mouloud Mammeri University, Tizi-Ouzou (Algeria)
(b, c) Plant Production, Improvement and Protection Laboratory, Faculty of Biological and Agronomic Sciences, Mouloud Mammeri University, Tizi-Ouzou (Algeria)
(d) University of Algiers 1, Ben Youcef Ben khedda (Algeria)
norapg13@gmail.com

ABSTRACT:
Chitin and chitosan, polysaccharides similar to cellulose, have proven their interests in the fields of biology, medicine, environment, pharmacy, food industry, etc. The work published for the past 5 years has proposed to develop fungal biomass as an alternative source to marine biomass. The objective of this study is to enhance the mycelium of a local strain, *Pleurotus ostreatus* (Jacq: Fries) Kummer and to extract chitin and chitosan. Chemical treatments with 1M NaOH then 0.35M CH_3COOH made it possible to extract 19.5% of the chitin and 0.51% of the chitosan. The chitin and the chitosan obtained were characterized by FTIR and SEM.

KEYWORDS: Biomass, Chitin, Chitosan, Mycelium condensed, *Pleurotus ostreatus*

1. INTRODUCTION

Chitin and chitosan are the two biopolymers which continue to arouse more and more the interest of researchers and scientists because of their numerous applications in agriculture [1], environment [2], medicine [3, 4], in food industry [5], paper and textile industries [6]. Chitin is a polymer formed from N-acetyl-D-glucosamine molecules linked by β (1-4) glycosidic bonds [7]. It is the second most abundant polysaccharide after cellulose [8]. It is found mainly in marine litter, shrimp and crab, in the backbone of squid and in the cuticle of insects. It is also present in the cell walls of many fungi, in particular Basidiomycetes, Ascomycetes and Phycomycetes [9]. Chitosan, a cationic polysaccharide formed from β-(1-4) D-glucosamines [10] is naturally present in Mucorales (Zygomycetes) [11]. Commercially, it is obtained effectively from the deacetylation of chitin in shellfish [12]. The condensed mycelium of a local strain of Basidiomycete, *Pleurotus ostreatus* (Jacq: Fries) Kummer is used in this study for the chemical extraction of chitin and chitosan. It is cultivated in the laboratory on a mixture of agricultural and agro-industrial residues (olive pomace, coffee grounds and wheat straw). The chitinous chitin and chitosan biopolymers extracted are characterized by infrared IR and SEM scanning electron microscopy.

2. MATERIAL AND METHODS

2.1- Material

2.1.1- Fungal Material

A local strain of *Pleurotus ostreatus* (Jacq: Fries) Kummer (POL) isolated in Oued-Aissi by Mansour -Benamar in 1993 (Mansour Benamar et al., 2007) [13]. It has since been maintained by successive subcultures and new re-isolations, using freshly formed carpophore, at the Plant Production, Improvement and Protection Laboratory of the Faculty of Biological and Agronomic Sciences of Mouloud Mammeri University in Tizi- Ouzou (Algeria).

2.1.2- Cultivation substrate

Pleurotus strain used was grown on a mixture of agricultural and agro-industrial residues: olive pomace (OP) - coffee grounds (CG) - wheat straw (WS), come from Tizi-Ouzou prefecture, Algeria

2.2- Methods

2.2.1- Culture of POL

The Second Edition of the International Congress of Applied chemistry and Environment
30th-31th October and 01st November 2020, Tunisia

ICACE 2020

The POL culture was carried out on the GO (44%) / MC (44%) / PB (10%) mixture humidified, supplemented with 2% $CaCO_3$ and inoculated with 7% of POL white.

2.2.1- Recovery and preparation of the condensed mycelium

We have called condensed mycelium; the carpophore drafts whose growth has stopped the feet and the small mushrooms whose weight does not exceed 2g.

2.2.2- Extraction of chitin and free chitosan

The protocol used for the extraction of chitin and free chitosan from the condensed mycelium powder of local *Pleurotus ostreatus* is based on the work of Rane and Hoover (1993) and Crestini et al (1996) [14, 15] : a mass of condensed mycelium powder was treated with 1M NaOH at 121 °C for 15min followed by an acid treatment with CH_3COOH (0.35M) at a rate of 1g/100mL at 95 °C for 5h. The solid fraction was centrifuged, it represents chitin. As for the liquid phase which represents chitosan, we performed precipitation by adding small volumes of 2M NaOH up to pH 9 to 10. The chitin and chitosan obtained were washed with distilled water to pH neutral, dried at 60 °C and then weighed.

3. RESULTS AND DISCUSSION

3.1- Extraction of chitin and chitosan

The yield of chitin isolated from POL condensed mycelium is approximately 195 mg/g of dry biomass, which is equivalent to a yield of 19.5%. Shiitake's feet contain a yield of 25.08 to 36.72% [16] in chitin; it is close to our result. *P. ostreatus* [17] and *Lactarius vellereus* [18] contain 15.3 and 11.4% respectively. On the other hand, *Agaricus bisporus* and *Lentinula edodes* produces lower yields; they are respectively 6.67% and 8.07% for the hat and 7.31% and 6.55% for the feet [19]. As for chitosan, its content was low, 0.51%. It is compared with that produced by the Zygomycete *Rhizopus oryzae* on rice straw 0.56% [20] and the basidiomycete *Lentinula edodes* on wheat straw 0.62% [21] for 12 days. *R. oryzae* grown on potato peelings from a potato chip factory, after 5 days of fermentation [22] and *Aspergillus niger* [21] produce a high content, 1.08% and 1.71% respectively. On mango bean residues, *R. oryzae* produces a low content, 0.16% of the weight of the growing medium [23].

3.2- Characterization of chitin and chitosan

3.2.1- Infrared spectroscopy (IR)

The infra-red spectra of chitin and chitosan (figure 01 and 03) isolated from the mycelium of POL resembles the infra-red spectrum of standard chitin and chitosan (figure 02 and 04) of crustaceans but with an intensity of peaks very weak features. The spectrum of the isolated chitosan is characterized by the disappearance of the Amide II band of chitin.
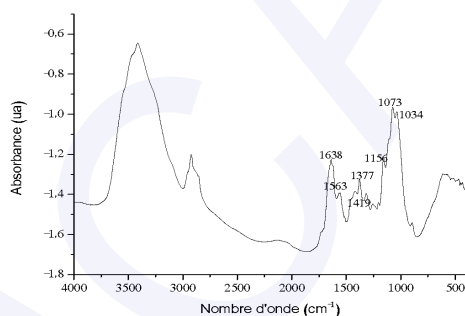

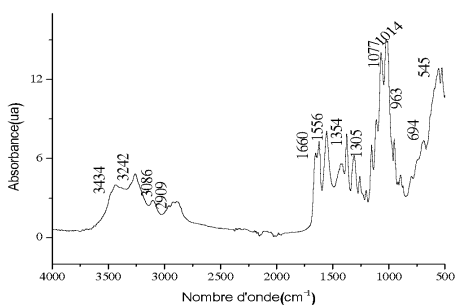
Figure 1: Chitin FTIR spectrum of POL   **Figure 2:** Commercial chitin FTIR spectrum
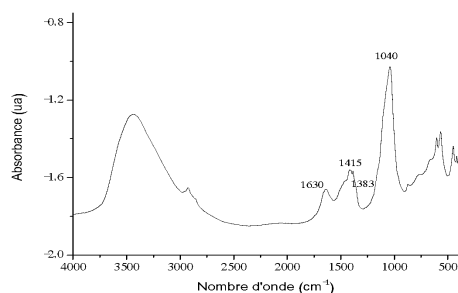
The Second Edition of the International Congress of Applied chemistry and Environment
30th-31th October and 01st November 2020, Tunisia

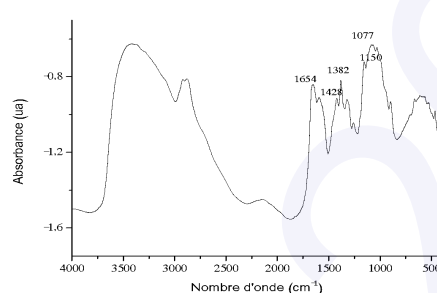ICACE 2020

Figure 3: Chitosan FTIR spectrum of POL   **Figure 4:** Commercial Chitosan FTIR spectrum

3.2.2- Electronic scanning microscopy (SEM)

Analysis by electronic scanning microscopy (SEM) of chitin and chitosan isolated from POL (photo A and B) shows that their surface is respectively of nanofibrous [24] and heterogeneous nanoproous [17] crystalline structures.
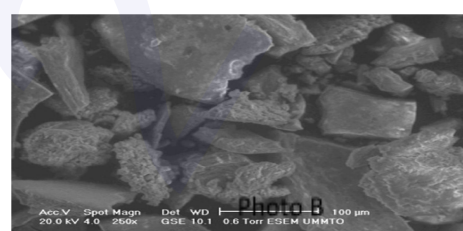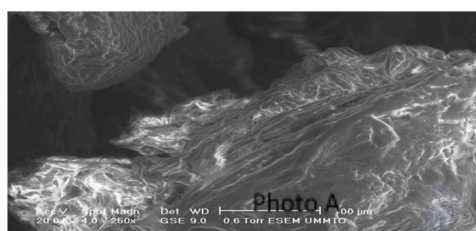
Figure 5: Micrograph of POL chitin (A) and chitosan (B)

4. CONCLUSION

The basic and acidic chemical treatment of the condensed mycelium of local *Pleurotus ostreatus* leads to isolation of chitin and chitosan, the respective amounts are estimated as 195 mg and 5.1 mg per gram of dry fungal biomass. Compared to the values obtained by other authors, it appears that these fractions exist in variable quantities according to the physicochemical and nutritional parameters, the fungal species and according to the mode of extraction. FTIR and SEM analyzes show that the chitin and chitosan obtained from the condensed mycelium resemble standard chitin and chitosan respectively.

3. REFERENCES

[1] **Nwea N, Stevens WF, Montet D, Tokura S**, Decomposition of myceliar matrix and extraction of chitosan from *Gongronella butleri* USDB 0201 and *Absidia coerulea*reak ATCC 14076, *International Journal of Biological Macromolecules*, Vol. 43, 2008, 2-7

[2] **Kanmani P., Aravind J., Kamaraj M., Sureshbabu P., Karthikeyan S.**, Environmental applications of chitosan and cellulosic biopolymers, *Bioresource Technology*, Vol. 242, 2017, 295-303

[3] **Ikeda I, Sugano M, Yoshida K, Sasaki E, Iwamoto Y, Hatano K**, Effects of chitosan hydrolysates on lipid absorption and on serum and liver lipid concentration in rats, *Journal of Agricultural and Food Chemistry*, 1993, 41:431–5.

[4] **New N, Maeda Y, Stevens WF, Furuike T, Tamura H**, Growth of fibroblast cell NIH/3T3 on chitosan and chitosan–glucan complex scaffolds. *Polymer*, Vol. 56, 2007, 2181

[5] **Aranaz I, et al**, Functional Characterization of Chitin and Chitosan, *Current Chemical Biology*, Vol. 3, 2009, 203-230

[6] **KLeekayai T, Suntornsuk W**, Production and characterization of chitosan obtained from *Rhizopus oryzae* grown on potato chip processing waste, *World Journal of Microbiology and Biotechnology*, Vol. 2, 2011, 1145–1154

[7] **Muzzarelli R. A. A.**, Chitin. 1st edition. *Pergamon Press, New York*, 1977, 326.

[8] **Wan ACA, Tai BCU**, Chitin-A promising biomaterial for tissue engineering and stem cell technologies, *Biotechnology Advances*, Vol. 31, N°8, 2013, 1776–85.

[9] **Roberts G A F**, Chitin Chemistry, 1992 MacMillan Press, London, 350.

[10] **Dutta PK et al**., Chitin and chitosan for versatile applications. *Polymer Reviews*, Vol. 42, N°3, 2002, 307–54.

[11] **Felse, A. P.; Panda, T**., Studies on applications of chitin and its derivatives. *Bioprocess Engineering,* Vol. 20, 1999, 505-515.

[12] **WU T. et al.**, Chitin and Chitosans Value-Added Products from Mushroom Waste, Journal of *Agricultural and Food Chemistry*, Vol. 52, 2004, 7905-7910

[13] **Amrane T. & Belkacemi T**., valorisation de résidus agricoles par la culture d'une souche locale d'un champignon comestible. Mémoire de master 2 en Sciences Biologiques, spécialité Protection de l'Environnement, Faculté des Sciences Biologiques et des Sciences Agronomiques, Université Mouloud Mammeri de Tizi-Ouzou, 2017, 42

[14] **Rane KD, Hoover GD**, An evaluation of alkali and acid treatments for chitosan extraction from fungi, *Process Biochemistry*, Vol. 28, 1993, 115–118

[15] **Crestini C, Kovac B, Kovac B, Givannozzi-Seramanni G**, Production and isolation of chitosan by submerged and solid state fermentation from *Lentinus edodes*, *Biotechnology and Bioengineering, Vol.50* 1996, 207–210

[16] **Ming-Tsung Yen and Jeng-Leun Mau**, Preparation of fungal chitin and chitosan from shiitake stipes, *Fung. Sci*, 2006, 21, 1–11

[17] **Di Mario, F. et al**, Chitin and chitosan from Basidiomycetes, *International Journal of Biological Macromolecules*, 2008, 43 8–12

[18] **Erdogan, S., Kaya, M., Akata, I**, Chitin Extraction and Chitosan Production from Cell Wall of Two Mushroom Species (*Lactarius vellereus* and *Phyllophora ribis*). *AIP Conference Proceedings*, 2017, 1809, 020012

[19] **Vetter, J,** Chitin content of cultivated mushrooms *Agaricus bisporus*, *Pleurotus ostreatus* and *Lentinula edodes*. *Food Chemistry*, 2007, 102(1), 6-9.

[20] **Khalaf SA**, Production and characterization of fungal chitosan under solid-state fermentation conditions, *International Journal of Agriculture and Biology,* Vol. 6, 2004, 1033–1036

[21] **Ospina Álvarez, S. P., Ramírez Cadavid, D. A**., **Escobar Sierra, D. M., Ossa Orozco, C. P., Rojas Vahos, D. F., Zapata Ocampo, P. et Atehortúa, L**, Comparison of Extraction Methods of Chitin from *Ganoderma lucidum* Mushroom Obtained in Submerged Culture. *BioMed Research International*, 2014, 1–7.

[22] **KLeekayai T, Suntornsuk W**, Production and characterization of chitosan obtained from *Rhizopus oryzae* grown on potato chip processing waste, *World Journal of Microbiology and Biotechnology*, Vol. 27, 2011, 1145–1154

[23] **Suntornsuk W, Pochanavanich P, Suntornsuk L**, Fungal chitosan production on food processing by-products, *Process Biochemistry,* Vol. 37, 2002, 727–729

[24] **M. Kaya, I. Akata, T. Baran, A. Mentes**, *Food Biophysics*, Vol. 10, 2015, 162-168

The Second Edition of the International Congress of Applied chemistry and Environment
30th-31th October and 01st November 2020, Tunisia

ICACE 2020

Effect of geographic variation and extraction method on the chemical composition of *Borago officnalis* L. extracts

Imene Zribi [a], Ridha Ghali [b], Manef abderabba [a]

(a) Laboratoire Matériaux, Molécules et Applications (LMMA), Institut Préparatoire aux études Scientifiques et Techniques (IPEST) , Université de Carthage, Avenue 14 Janvier, Site archéologique de Carthage ,BP 51 ,2070 La Marsa, Tunisie
(b) Institut Supérieur de Biotechnologie, BiotechPôle, BP-66, 2020, Sidi Thabet, Ariana-Tunis - 2020 Tunis.

ABSTRACT

Aromatic plants are nowadays the basis of phototherapy and homeopathy and have more interest given to their chemical diversity and functional activities. One of these plants known for its virtues and medicinal uses is *Borago officinalis* L. The present work was aimed to analyse the methanolic and ethanolic extracts of *Borago Officinalis* L. collected from different geographic regions of Tunisia; using two various methods of extraction, by liquid chromatography coupled to mass spectrometry (LC/MS) method.
Yields varied considerably (from 7 to 22%). LC/MS analysis allowed to identify 11 phenolic compounds, revealing variations in the composition of the various extracts with a predominance for rosmarinic acid (0, 404± 0,037 – 7,272 ± 0,159 mg/ g MS).
The findings showed a remarkable difference and significant variations in quality and quantity of the secondary metabolites according to sampling region, organic solvent and extraction method.

KEYWORDS: *Borago officnalis* L., extracts, chemical composition, variations

1. INTRODUCTION

B. officinalis (*Borago officinalis* L.) is an annual plant species of the family of Boraginaceae that was first used as a salad and spice. Later, it became known for other properties [1].This plant grows on different types of soils [2].The oils from plant seeds have received considerable interest. In fact, investigations have improved the richness of borage seed oil in linoleic and gamma-linolenic acids which greatly help the prevention and treatment of various diseases mainly diabetes and cancer [3,4]. Many researches have also focused on the immunomodulatory effect of borage oil [5] and have shown its antispasmodic, bronchodilator, and cardiovascular effects [6].

In Tunisia, *B. officinalis* grows spontaneously in different bioclimatic zones and has a wide geographical distribution. Based on the foregoing, this investigation aims primarily the analysis of the geographical variations of the chemical composition of *B. officinalis* extracts collected from three different sites in Tunisia via liquid chromatography coupled to mass spectrometry (LC/MS) system in order to determine their quantitative and qualitative characteristics.

2. MATERIAL AND METHODS

Fresh flowering aerial parts of *B. officinalis* were collected at the full flowering stage during the same period (April 2016) from three different regions of Tunisia: Tunis, Bizerta, and Zaghouan. Each sample was air-dried at room temperature away from humidity as well as light [7]. All samples were authenticated by Pr. Mohamed Boussaid (Research Unit Phylogenetic Resources & Biotechnology, National University of Carthage).

Extracts preparation:

In order to optimize the bioactive compounds extraction, the aerial parts of *B. officinalis* were extracted by two different methods namely soxhlet extraction and cold maceration using two different solvent ethanol and methanol. After each extraction method, the crude extracts were weighted and kept in a dark flask until further experiment. The extraction yield for each extract was calculated

LC/MS analysis:

The phenolic compounds of the various extracts were determined using a Shimadzu Nexera LC system comprising a quaternary pump, an automatic sampler and a column associated with a triple quadruple mass spectrometer LC/MS-8030. Before analysis by LC/MS, the extracts were filtered. An intersil C18 column was used. The elution was carried out at a linear gradient and the injection volume was 5 μl.

The Second Edition of the International Congress of Applied chemistry and Environment
30th-31th October and 01st November 2020, Tunisia

ICACE 2020

Statistical analysis:

All results were expressed as means ± standard deviations and all measurements were done in triplicate. Statistical Analysis was carried out by one-way analysis of variance (ANOVA) and Duncan multiple range test using XLSTAT.

3. RESULTS AND DISCUSSIONS
3.1. Extraction yield

As described, the aerial part of *B. officinalis* was collected in three different localities in the northeast region of Tunisia. The organic extracts were prepared using two solvents; methanol and ethanol by two different extraction method; cold maceration and Soxhlet.

The extraction yields relative to the dry matter of the different extracts are expressed as shown in figure 1
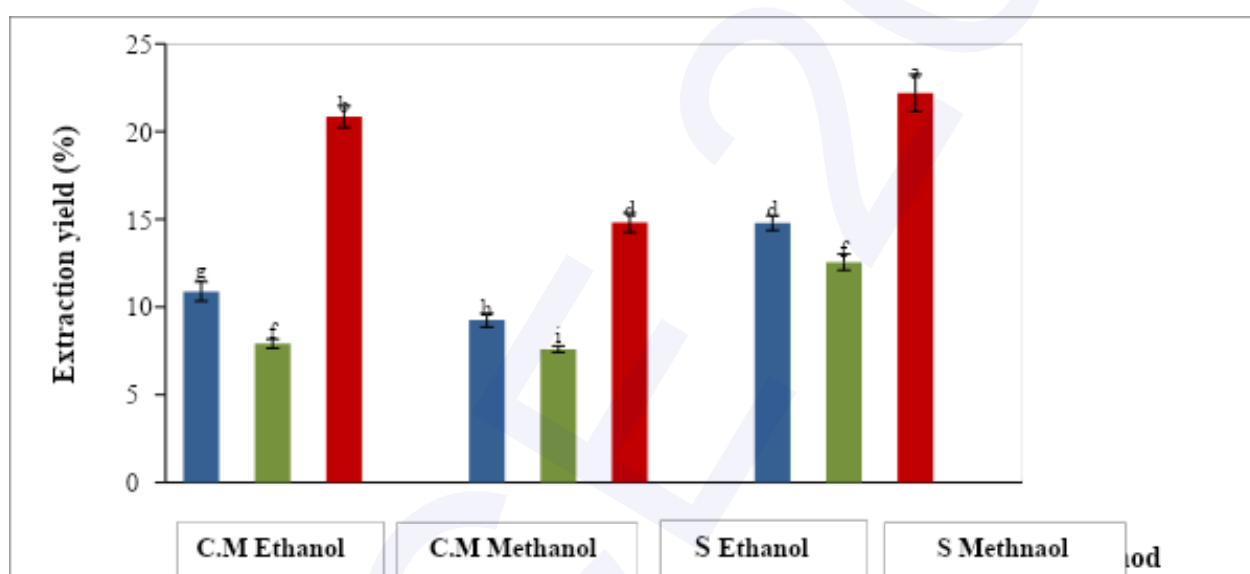
a-i: means within a column row with different letters were significantly different ($p<0.05$) ; CM : cold maceration ; S : soxhlet

Figure 1: Extraction yields of *B. officinalis* aerial parts

The yields of organic extracts vary significantly ($p < 0.05$) from 7.6 to 22.2 % depending on the geographic origin, the solvent and the extraction method used. These results are consistent with those of Yahyaoui et al. who demonstrated that the extraction yields vary considerably depending on solvents [8].

3.2. LC/MS results

Eight extracts of *B. officinalis* from the three regions prepared using two extraction methods and different solvents were analyzed by LC/MS. This method was used to quantify fourteen polyphenols in the plant extracts. The calibration curves were linear using concentrations ranging from 1 to 20mg/L. The identification of the compounds obtained was established by evaluating their retention times compared to those of the analytical standards.

The comparison of the concentration reveals that for all extracts, rosmarinic acid was the most abundant constituent. Its content varies from 0.404 ± 0.037 to 7.272 ± 0.159 mg/ g dw.

Figure 2 shows that all extracts from the Zaghouan region have a high concentration of romarinic acid regardless of the solvent and the extraction technique, with a maximum content for cold maceration in methanol. MMT and MMB extracts showed rosmarinic acid concentrations of 2.628 ± 0.036 and 2.461 ± 0.14 mg /g dw, respectively. The rosmarinic acid content of the SEB, SET and SEM extracts is low. Thus,

The Second Edition of the International Congress of Applied chemistry and Environment
30th-31th October and 01st November 2020, Tunisia

ICACE 2020

we can conclude that the methanol cold maceration method is the most suitable for the extraction of rosmarinic acid from medicinal plant.
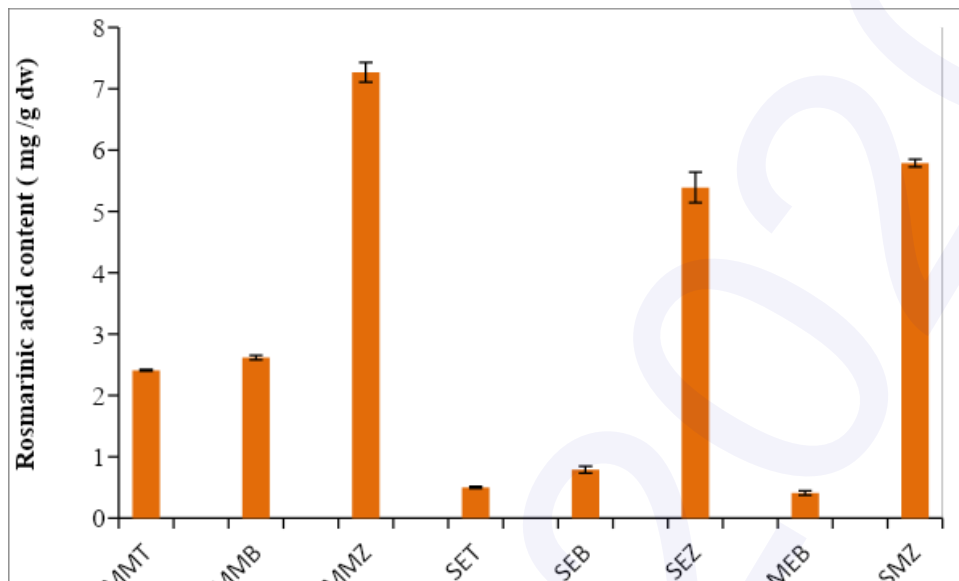
Figure 2: Rosmarinic acid content (mg/g dw)

Rosmarinic acid is known for its several biological activities such as antiviral, anti-bacterial and anti-inflammatory properties [9]. Several studies have proven its antioxidant power and justified its wide use in food industries [3].

Our results support the research of Ben Ghorbal et al. and Fan and Beta, who highlighted the variation in the phenolic profile of the extracts in dependence on the geographical origin of the plant [10, 11]. Moreover, Aichi-Yousif et al., confirmed the difference in the content of polyphenol extracts according to the solvent used [12]

Through these results, we can conclude that a large number of factors influence the extraction yield and the chemical composition of plant extracts, namely the extraction method, the solvent used, the geographic differentiation... [13]

4. CONCLUSION

The Present study describes the effect of extraction methods as well as the geographic sampling origin on the extraction yield and the chemical composition of *B. officinalis*. Remarkable variations are shown between the various extracts. The observed chemical variability may probably be related to environmental factors. The choice of the extraction method has also an important impact in determining the specific features.

REFERENCES

[1] **Branca, F. D. di O. e T.A.**, Trials related to the cultivation of wild species utilised in Sicily as vegetables. *Italus Hortus*, 2001.

[2] **Bermejo, J.E.H., León, J**., Neglected Crops: 1492 From a Different Perspective. in: FAO Plant Production and Protectionhttps://doi.org/10.1017/CBO9781107415324. 004.1994.

[3] **Asadi-Samani, M., Bahmani, M., Rafieian-Kopaei, M.**, The chemical composition, botanical characteristic and biological activities of *Borago officinalis*: a review. *Asian Pacific Journal of Tropical Medicine.* Vol. 7, 2014, 22–28.

[4] **Hamrouni, I.,Touati,S.,Marzouk,B**., Evolution des lipides au cours de la formation et de la maturation de la graine de bourrache (*Borago officinalis* L.). *Rivista Italiana Delle Sostanze Grasse*, 2002, 79–113.

[5] **Harbige, L.S., Layward, L., Morris-Downes, M.M., Dumonde, D.C., Amor, S.,** The protective effects of omega-6 fatty acids in experimental autoimmune encephalomyelitis (EAE) in relation to transforming

growth factor-beta 1(TGF-β1) upregulation and increased prostaglandin E2 (PGE2) production. *Clinical and Experimental Immunology*. Vol. 122, 2000, 445–452

[6] **Gilani, A.H., Bashir, S., Khan, Aullah,** Pharmacological basis for the use of *Borago officinalis* in gastrointestinal, respiratory and cardiovascular disorders. *Journal Ethnopharmacology.* 114, 2007, 393–399.

[7] **Li, T.S.C., Wardle, D.A.,** Effects of Root Drying Temperature and Moisture Content on the Levels of Active Ingredients in *Echinacea* Roots. *Journal of Herbs, Spices & Medicinal Plants*, 2005. https://doi.org/10.1300/j044v08n01_03

[8] **Yahyaoui, M., Ghazouani, N., Sifaoui, I., Abderrabba, M**., Comparison of the Effect of Various Extraction Methods on the Phytochemical Composition and Antioxidant Activity of *Thymelaea hirsuta* L. aerial parts in Tunisia. *Biosciences Biotechnology Research Asia,* 2017.

[9] **Petersen, M., Simmonds, M.S.J**., 2003. Rosmarinic acid. Phytochemistry.

[10] **Ben Ghorbal, A., Leventdurur, S., Agirman, B., Boyaci-Gunduz, C.P., Kelebek, H., Carsanba, E., Darici, M., Erten, H.,** Influence of geographic origin on agronomic traits and phenolic content of cv. Gemlik olive fruits. *Journal of Food Composition and Analysis,* 2018.

[11]**Fan, G., Beta, T.,** Discrimination of geographical origin of Napirira bean (*Phaseolus vulgaris* L.) based on phenolic profiles and antioxidant activity. *Journal of Food Composition and Analysis,* 2017.

[12] **Aichi-Yousfi, H., Meddeb, E., Rouissi, W., Hamrouni, L., Rouz, S., Rejeb, M.N., Ghrabi-Gammar, Z.,** Phenolic composition and antioxidant activity of aqueous and ethanolic leaf extracts of six Tunisian species of genus Capparis-Capparaceae. *Industrial Crops and Products*, 2016, https://doi.org/10.1016/j.indcrop.2016.07.051

[13] **D. Khilifi, R.M. Sghaier, S. Amouri, D. Laouini, M. Hamdi, J. Bouajila,** Composition and anti-oxidant, anti-cancer and anti-inflammatory activities of Artemisia herba-alba, *Ruta chalpensis* L. and *Peganum harmala* L. *Food and Chemical Toxicology,* 2013

Design of a new Carbonic Anhydrase inhibitors derived from 1,5-Benzodiazepines

Ismail Chiraz[a], Winum Jean Yves[b], Gharbi Rafik[a]

(a)   Research unit of Applied Chemistry and Environment, Faculty of Sciences of Monastir , Avenue of Environment 5019 Monastir
(b)   Institute of Biomolecules Max Mousseron, ENSCM, University of Montpellier,8 avenue of normal school 34296 Montpellier
E-mail: chiraz_ismaail@outlook.fr

ABSTRACT
Here we report the synthesis of new potential candidates as Carbonic Anhydrase inhibitors, derivatives from 1,5-benzodiazepines benzene sulfonamides. The synthetic route used was a copper catalyzed cycloaddition between propargylated 1,5-benzodiazepine-2-ones and benzene sulfonamide azides. All the synthesized targets have been characterized by ^{1}H/^{13}C NMR and HRMS.

KEYWORDS: 1,5-benzodiazepine-2-ones- Carbonic Anhydrase- Sulfonamide azides Click chemistry

1. INTRODUCTION

The development of 'privileged heterocyclic scaffolds' is a rapidly emerging subject in medicinal chemistry. [1] Benzodiazepines and their polycyclic derivatives are one of the most explored compound classes as privileged scaffolds in drug discovery. They are amongst therapeutic agents, which have widespread use in treatment of central nervous system disorders. It is well proven that the presence of two or more heterocyclic pharmacophores linked and/or fused within a same framework could contribute to provide a significant positive effect on the overall biological efficiency in the resulting poly-heterocycle [2]. Including 1,5-benzodiazepines moiety, considerable attention has been directed towards the synthesis of polycyclic 1,5-(BZD)s in particular (1,5-benzodiazepine-spacer arm -triazole unit) type. Moreover, sulfonamide derivatives have been well known as a potential candidate inhibitors of the carbonic anhydrase enzyme. Our strategy was the design of a new compound which links between benzodiazepines and benzene sulfonamides via Click Chemistry.

We start by preparing the different N-propargylated 1,5-benzodiazepin-2-ones, and different sulfonamides azides as useful key intermediates in the synthesis of molecular hybrids via an alkyne/azide Cu(I) catalyzed 1,3-dipolar cycloaddition reaction.

2. MATERIAL AND METHODS

Chemical reagents and solvents were purchased from commercial suppliers (Merck, Aldrich, and Fluka) and were used as received without further purification.
All the melting points were determined in open glass capillaries and are uncorrected. ^{1}H-NMR and ^{13}C-NMR spectra were recorded in DMSO [d6] and CDCl$_3$ on 'Brucker Avance 400 MHz' spectrophotometer with TMS as internal standard. HRMS was also used to characterize these compounds.
The reactions were monitored by thin-layer chromatography (TLC) on silica gel G plates in the solvent system Cyclohexane/Ethyl acetate mixture (6:4) and the spots were visualized with UV light.

3. RESULTS AND DISCUSSIONS

We started by the synthesis of the *N*-prop-2-yn-1,5-benzodiazpin-2-one as a dipolarophilic precursor, which thus passes through a deprotonation of intermediate 4-(2-hydroxyphenyl)-1,3-dihydro-1,5-benzodiazepin-2-ones **1** with Potassium hydroxide in tetrahydrofuran at 0 °C in the presence of propargyl bromide (scheme 1). Target **2** was obtained in 90% yield.

The Second Edition of the International Congress of Applied chemistry and Environment
30th-31th October and 01st November 2020, Tunisia

ICACE 2020
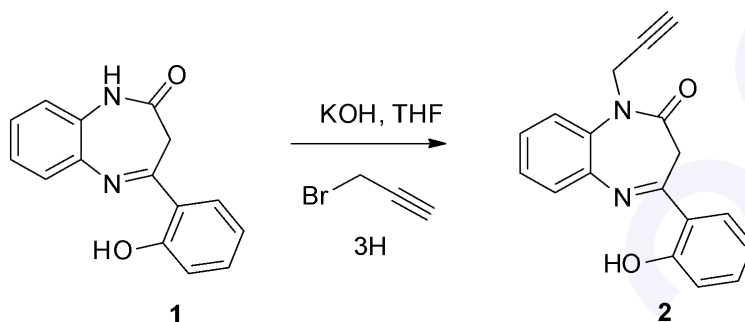
After preparing compound **2**, a series of benzene sulfonamide azides was prepared. The proper amino-benzene-sulfonamide (0.5 g, 1.0eq) was dissolved in a 2M HCl aqueous solution (5 mL). Then, NaNO2 (1.2 eq) was slowly added at 0°C and the reaction mixture was stirred at the same temperature for 0.5h. Thereafter NaN3 (1.5 eq) was added portion-wise and the mixture was stirred at r.t. for 0.5h. The obtained precipitate was filtered-off and washed with water to afford the corresponding azido-benzene-sulfonamides
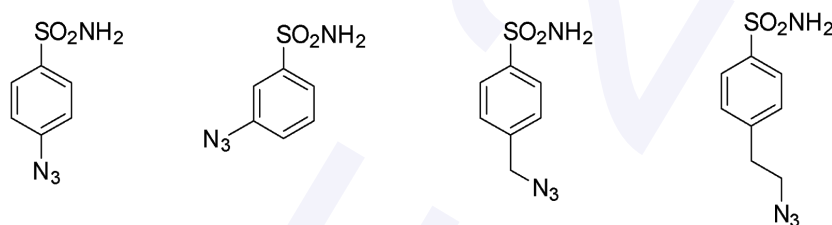
Once sulfonamides azides and propargylated 1,5-benzodiazepin-2-ones have been prepared as useful key intermediates, the last stage was the access of molecular hybrids **3(a-z)** via an alkyne/azide Cu(I) catalyzed 1,3-dipolar cycloaddition reaction. (scheme 2)
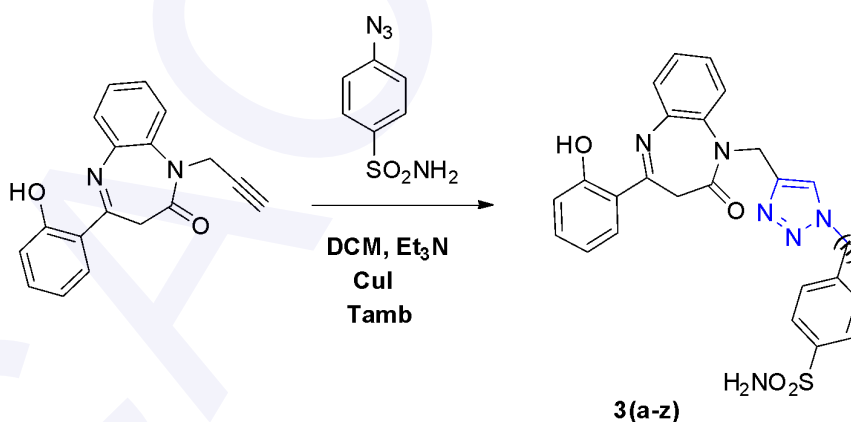
Scheme 2: Synthesis of molecular hybrids 2(a-z)

4. CONCLUSION

In conclusion, this work reports a novel synthetic access to readily conjugatable 1,5-benzodiazepinones benzene sulfonamides. Besides, optimization studies of subsequent *1,3*-dipolar cycloaddition reaction of benzodiazepines with benzene sulfonamides azides were carried out successfully, thus offering an effective strategy for the preparation of benzodiazepinone conjugates suitable for an array of aforementioned biological applications.

REFERENCES

[1] **S. Chander, C.R Tang, H. M. Al-Maqtari, J. Jamalis, A. Penta, T. Ben Hadda, H. M. Sirat, Y. T. Zheng**, Murugesan Sankaranarayanan, Synthesis and study of anti-HIV-1 RT activity of 5-benzoyl-4-methyl-1,3,4,5-tetrahydro-2H-1,5-benzodiazepin-2one derivatives, *Journal of Bioorganic Chemistry*, Vol. 72, 2017,74-79.

[2] **I. Filali, M. A. Belkacem, A. Ben Nejma, J. P. Souchard, H. Ben Jannet, J. Bouajila**, Synthesis, cytotoxic, anti-lipoxygenase and anti-acetylcholinesterase capacities of novel derivatives from harmine, *Journal of Enzyme Inhibition and Medicinal Chemistry*, 2016, 1475–6374.

Ecological Textiles
&
Para-textiles

The Second Edition of the International Congress of Applied chemistry and Environment
30th-31th October and 01st November 2020, Tunisia

ICACE 2020

Ecological dyeing process using aqueous residue from *Dittrichia graveolens* hydrodistillation

Nawres Gharred[a], **Noureddine Baaka**[a], **Sonia Dridi-Dhaouadi**[a,*]

(a) Research Unit Applied Chemistry and Environment 13ES63, Faculty of Sciences, Avenue de l'environnement 5019 Monastir –Tunisie.

* E-mail address : sonia.dridi@ipeim.u-monastir.tn

ABSTRACT

The release of aqueous residues generated by the extraction process of essential oils presents a real risk of environmental pollution. This work aims to reduce this risk by exploiting the aqueous residues of the *Dittrichia graveolens* plant in the dyeing of polyamide textile fibers. First,the aqueous residue was analyzed by evaluating the content of coloring species in terms of total polyphenols (237 mg $EqC.g^{-1}$) and flavonoids (91 $mg.EqAG.g^{-1}$). HPLC analysis allowed the identification of catechin and quercetin as two of the coloring molecules present in this aqueous residue. Second, the optimum dyeing conditions were evaluated by the surface response methodology at pH, temperature and duration of 3, 80°C and 90 min, respectively. Finally, the pollutant load of the aqueous residue was evaluated by oxidation test and the determination of the total polyphenols concentration before and after dyeing.

KEYWORDS: Hydrodistillation aqueous residue, flavonoids, HPLC analysis, dyeing optimization, pollutant load

1. INTRODUCTION

The textile dyeing and essential oil extraction industries are among the best performing industries in the Mediterranean basin [1] [2]. Although their fields of activity do not seem to be linked, these two types of industries have in common, in addition to their geographic proximity, their considerable volume of colored water discharges. Faced with this ecological awareness that characterizes the first half of the 21st century, scientific research has increasingly focused on the development of cleaner industrial processes. Thus, in the field of textile dyeing, researchers like Ben Ticha et al. have carried out major work to replace synthetic dyes toxic to the environment with natural dyes while obtaining excellent dyeing performance [3]. On the other hand, the only research work dedicated to ecological methods of extracting essential oils concerns the substitution of organic solvents with water under standard or supercritical conditions [4].

The idea behind this work is to reduce the environmental impact of the extraction process of essential oils at the same time as the dyeing process of textiles. This can be done by taking advantage of the aqueous residue from the hydrodistillation, rich in colored substances, to dye the textile fibers. In this work, the aqueous residue generated by the hydrodistillation process of the wild plant *Dittrichia graveolens (D. graveolens)* was used for the dyeing of polyamide fibers. First, a chemical characterization of the aqueous residue was evaluated. Secondly, the aqueous residue was valued as a dye bath for the polyamide fabric, the dyeing process was modeled and optimized thanks to Minitab 18 software using the response surface methodology (RSM). The color strength (K/S) and fastness parameters were determined for the optimum dyeing conditionsFinally, the environmental impact of the residual dye bath was studied by evaluating the contents of total polyphenols and flavonoids as well as the chemical oxygen demand (COD) before and after dyeing.

2. MATERIAL AND METHODS

2.1. Materials

The colored aqueous extract generated from the extraction of essential oil from the dried leaves and flowers of *Dittrichia graveolens* has been tested for dyeing a multifiber fabric. Knitted polyamide (jersey and weight of 302 g.m $^{-2}$) was used for the dyeing process. The dyeing process was carried out in a laboratory-dyeing machine (Ahiba Datacolor International, USA) at 60°C for 60 min at a liquid ratio of 40:1.

2.2. Characterization of the aqueous residue of D. graveolens hydrodistillation

The total polyphenols were estimated using the Folin-ciocalteu reagent according to the method of Mcdonald et al. [6]. On the other hand, the flavonoid contents were determined by the method described by Amel et al. [7]. The UV-visible spectrum of the aqueous extract was obtained using a Camspec M 108 spectrophotometer. The IR spectrum of coloring powder obtained after lyophilization of the aqueous *D.graveolens* extract is carried out by the Perkin Elmer FTIR infrared spectrometer. The HPLC spectra of the aqueous residue were performed using Agilent 1200 Series HPLC System. The analysis was carried out according to the following protocol [8].

2.3. Dyeing quality evaluation

The dyeing quality was evaluated using the color strength parameter (K/S) measured by SpectroFlash SF300 spectrophotometer (Datacolor International, USA) using D65 and 10° standard observer. Optimisation studies were conducted using response surface methodology (RSM) and Minitab 18 software (Version18, State College, PA, USA). Specific tests include color fastness to washing according to ISO 105-C06, colorfastness to rubbing ISO 105-X12 and colorfastness to light ISO 105-B02.

2.4. *Residual dye bath analysis*

The pollutant load of the aqueous residue was evaluated by oxidation test and the determination of the total polyphenols concentration before and after dyeing. The Chemical Oxygen Demand (COD) was determined according to standard methods described by Rice et al. [9]

3. RESULTS AND DISCUSSIONS

3.1. Characterization of the aqueous residue of D. graveolens hydrodistillation

The aqueous residue of the hydrodistillation of *D. graveolens*, characterized by a yellowish-brown color, has a concentration of total polyphenols and flavonoids of 237 mg.EqAG.g^{-1} and 91 mg.EqC.g^{-1}, respectively. The UV-visible and infrared spectra of the aqueous residue confirm the presence of flavonoids. FTIR, UV-vis spectrophotometry and HPLC analysis allowed the identification and evaluation of catechin (5.92 mg. g^{-1} of extract) and quercetin (4 mg. g^{-1} of extract) as two of the coloring molecules present in this aqueous residue.

3.2. Modelling and optimization of the dyeing process

The process of dyeing a polyamide fabric with the aqueous residue was optimized by the surface response methodology using the Minitab software. Thus, the optimum dyeing conditions were evaluated at pH, temperature and duration of 3, 80°C and 90 min, respectively, giving a maximum value of K / S color yield (equal to 7.5). The dyeing performance of this process was evaluated by measuring, under the previously determined optimum conditions, the fastness properties of rubbing, light and washing equal to 4, 3 and 4-5.

3.3. *Residual dye bath analysis*

The reduction in the pollutant load of the aqueous residue after its use as a dye bath has been evaluated at 10.3, 8.4, 11.6 and 15.6 % in terms of polyphenols, flavonoids, chemical oxygen demand (COD) and colour, respectively.

4. CONCLUSION

In the context of the recovery of aqueous residue from the hydrodistillation which the discharge presents a risk of environmental pollution, a study of their coloring power in the textile field was conducted. Thanks to their richness in flavonoids, the aqueous extract of *Dittrichia graveolens* revealed good dyeing results, especially with polyamide. HPLC analysis allowed us to detect quercetin and catechin two flavonoids present in our aqueous extract and which contribute to the coloring of textile fibers. The design of the response surface is proven to be effective and reliable to determine the optimal conditions for the dyeing process. The optimal dyeing parameters obtained were 3, 80°C and 90min for pH dye bath, temperature and duration dyeing respectively. On the other hand, The ecological dyeing process by hydrodistillation aqueous contributed to reduce the pollutant load generated by this effluent.

REFERENCES

[1] **Plan, M.A.**, Pollution prevention in the textile industry within the Mediterranean region, 2002.

[2] **Baser, K.H.C., Buchbauer, G.**, Sources of essential oils, Handbook of Essential Oils: Science, Technology, and Applications, Second Edition, 2015.

[3] **Ben Ticha, M., Haddar, W., Meksi, N., Guesmi, A., Mhenni, M.F.**, Improving dyeability of modified cotton fabrics by the natural aqueous extract from red cabbage using ultrasonic energy, *Carbohydrate Polymers*, Vol. 154, 2016, 287–295.

[4] **Bishr, M., El-Degwy, M., Abdel Hady, M., Amin, M., Salama, O.**, Supercritical fluid extraction of γ-Pyrones from Ammi visnaga L. fruits. Futur, *Journal of pharmaceutical Sciences*, Vol. 4, 2018,57–62.

[5] **Legube, B., Merlet, N., Brunet, R.**, L'analyse de l'eau, 9th ed. Dunod, Paris, 2009.

[6] **Acanthaceae, C.B.C., Adesegun, S.A., Fajana, A., Orabueze, C.I., Coker, H.A.B.**, Evaluation of Antioxidant Properties of *Phaulopsis fascisepala* C.B.Cl. (*Acanthaceae*), *Engineering, Construction and Architectural Management*, Vol. 6, 2009,227–231.

[7] **Bouzidi, A., Benzarti, A., Arem, A. El, Mahfoudhi, A., Hammami, S.,** Chemical composition , antioxidant and antimicrobial effects of Tunisian *Limoniastrum guyonianum Durieu* ex Boiss extracts, *Pakistan journal of pharmaceutical Sciences,* Vol. 29, 2016,1299-305.

[8] **Farías-Campomanes, A. M., Rostagno, M. A., Coaquira-Quispe, J. J., Meireles, M. A. A.,** Supercritical fluid extraction of polyphenols from lees: overall extraction curve, kinetic data and composition of the extracts, *Bioresources and Bioprocessing*, Vol. 2, 2015, 45.

[9]**Rice E. W., Baird R. B., and Eaton A. D.** 2017. "Standard Methods for the Examination of Water and Wastewater", 23rd ed., *Journal of Chemical Information and Modeling*.

Development and optimization of a new process to dye cotton with indigo carmine

Maha Abdelileh [a, b], **Manel Ben Ticha** [a, c], **Nizar Meksi** [a, b]

(a) University of Monastir, Faculty of Sciences of Monastir, Research Unity of Applied Chemistry and Environment, 5000Monastir, Tunisia.
(b) University of Monastir, National Engineering School of Monastir,Department of Textile, 5000 Monastir, Tunisia.
(c) University of Taif , University college of Turabah, Fashion design and fabric department, Taif , Kingdom of Saudi Arabia

E-mail: maha.abdelileh@gmail.com

ABSTRACT

The present paper investigates an ecological exhaust dyeing process of cotton with indigo carmine in which the conventional reduction step of indigo dyeing process is eliminated following the substitution of the insoluble indigo by the soluble indigo carmine. To improve the exhaust dyeing process, the dyeing step was carried on modified cotton with a cationic agent. The effect of the main operating conditions such as: the indigo carmine amount, the dyeing temperature, the dyeing duration and the alkali concentration on the quality of this dyeing were studied. The performances of the dyeing process were evaluated by measuring the color strength (K/S) of the coloured cotton. A surface design was employed for experimental design and optimization of results. It was found that the color strength obtained from this new process has improved compared to untreated cotton fibers.

KEYWORDS: Green process, indigo carmine, modified cotton.

1. INTRODUCTION

Indigo is currently one of the most consumed dyes in the textile sector, due to the popularity of blue jeans, which are dyed with indigo. Dyeing textile with indigo involves usually a reduction step in order to obtain their water- soluble form. So far, in most industrial dyeing processes indigo blue is converted to the colorless soluble leuco indigo form by a chemical reduction with sodium dithionite[2], which is considered toxic and hazardous to handle [1]. The use of this reducing agent is the cause of several technical and ecological problems. So, several approaches have been suggested to replace the harmful reducing agent with a more attractive alternative in order to achieve a clean indigo dyeing process. In this study, we propose to develop a new cleaner process for dyeing cotton in which indigo itself is replaced with indigo carmine. Indigo carmine is a dye of natural origin. It is a blue powder with a purplish luster, named indigo disulfonic acid; two sulfonate groups attached to the indigo molecule (see Figure1). The consequence of this chemical formula is the water solubility of the dye which makes the dyeing process easy, in the contrast to the vat dyeing process for indigo [3].
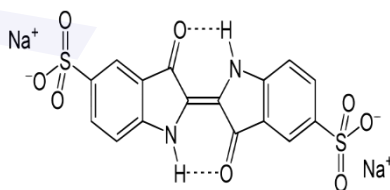
Figure 1: Chemical structure of indigo carmine.

Indigo carmine has only been used for dyeing of protein fibers such as wool and silk [4]. The dyeing process by indigo carmine creates beautiful and bright shades, which are different from those obtained by the traditional dyeing process of indigo [5]. Unfortunately this dye has no affinity for cotton as well as low fastness to light and washing. So it is necessary to develop a new process to accomplish a satisfactory dyeing quality.

The Second Edition of the International Congress of Applied chemistry and Environment
30th-31th October and 01st November 2020, Tunisia

ICACE 2020

The present work focuses on enhancing the dyeability of cotton to indigo carmine. The effects of the main experimental conditions (indigo carmine amount, dyeing temperature, dyeing duration, concentration of sodium carbonate) on the quality of this dyeing process were investigated. Besides, modelling and optimization of some experiments were investigated in order to improve the performances of this exhaust dyeing process.

2. MATERIAL AND METHODS
2.1. Chemicals and Materials used
Indigo carmine ($C_{16}H_8N_2Na_2S_2O_8$, Sigma-aldrich, Swizerland) is the dye used for dyeing cotton fabrics. Sodium carbonate (Na_2CO_3, Shamlab, Syria) is used during the dyeing process. Sera Fast GMX noted SRF (CPM, Tunisia) was used as a cationic agent.
Commercially bleached but unfinished cotton fabric supplied from SITEX, Tunisia was used with a density by area of $270 g.m^{-2}$.

2.2. Methods
2.2.1. The cationization process
The bleached cotton samples were modified using SRF cationic agent. The proposed method for this process was to treat cotton before dyeing by indigo carmine in a bath containing 6, 5% of SRF cationic agent, 0, 15g.L⁻¹ of sodium hydroxide for 42 min at 45°C. After that, treated samples were squeezed and dried at room temperature.

2.2.2. The dyeing process

The cationized fabrics were dyed at a liquor ratio of 1:50. The fabrics were introduced in a laboratory autoclave machine (Ahiba Datacolor international, USA), the temperature was raised at the rate of 4°C per minute to 100°C and the dyeing was continued for further 60 minutes at this temperature. After that, the dyed samples were cold rinsed with water, and finally dried at room temperature.

2.2.3. Testing of color strength (K/S)
The reflectance value of the dyed samples was measured at 620 nm on a spectroflash SF 300 spectrophotometer with data Master 2.3 software (Datacolor international, USA) , and the (K/S) value was calculated according to the following equation [6]

$$K/S = \frac{(1-R)^2}{2R} - \frac{(1-R0)^2}{2R0} \qquad (1)$$

2.2.4. Design of experiment (DOE)

A response surface methodology was used to study and optimize the effect of certain physico-chemical parameters on the dyeing quality. Using the software Minitab (version 14, State college, PA, USA), the run of experiments was designed by RSM for four factors and three levels.

3. RESULTS AND DISCUSSIONS
3.1. Factors affecting the dyeing process
3.1.1. Effect of indigo carmine amount
The effect of the concentration of indigo carmine amount on the color strength parameter (K/S) was evaluated, and the results are summarized in Figure 2(a). Based on this figure, it can be seen that the color strength increases as the concentration of indigo carmine increased till reaching 5% and above this concentration the dyeing parameter values were gradually decreased.

3.1.2. Effect of dyeing temperature

The exhaustion dyeing temperature for 1% of indigo carmine and 60 minutes of dyeing duration was varied from 20°C to 100°C and the evolution of the color strength was studied. The experimental results are reported in Figure 2(b). From this figure it can be observed that the best dyeing quality is obtained at a

temperature of 30°C and above this value a rapid decrease of the dyeing parameter takes place. This decrease is expected since indigo carmine just like indigo have a better affinity at lower temperatures [7].

3.1.3. Effect of the dyeing duration

During constant heat, the dyeing duration was varied between 5 and 28min and the evolution of the color strength was studied. The obtained results are reported in Figure 2(c). Based on this figure it can be seen that the highest color strength is observed at a period of 10 minutes. As time proceeds the   color strength decreases gradually. Therefore, there is no need to increase the dyeing time above 10 minutes.

3.1.4. Effect of sodium carbonate concentration

The effect of the alkalinity in the medium on the color strength was studied by varying the amount of sodium carbonate from 0 to $0.3g.L^{-1}$. Based on the results consigned in Figure 2(d), it can be noted that the color strength increases when the amount of alkali increases until $0.005g.L^{-1}$ and above this value the dyeing parameter decreases gradually. In fact the addition of a small amount of alkali improves the penetration of the dye in the fiber.
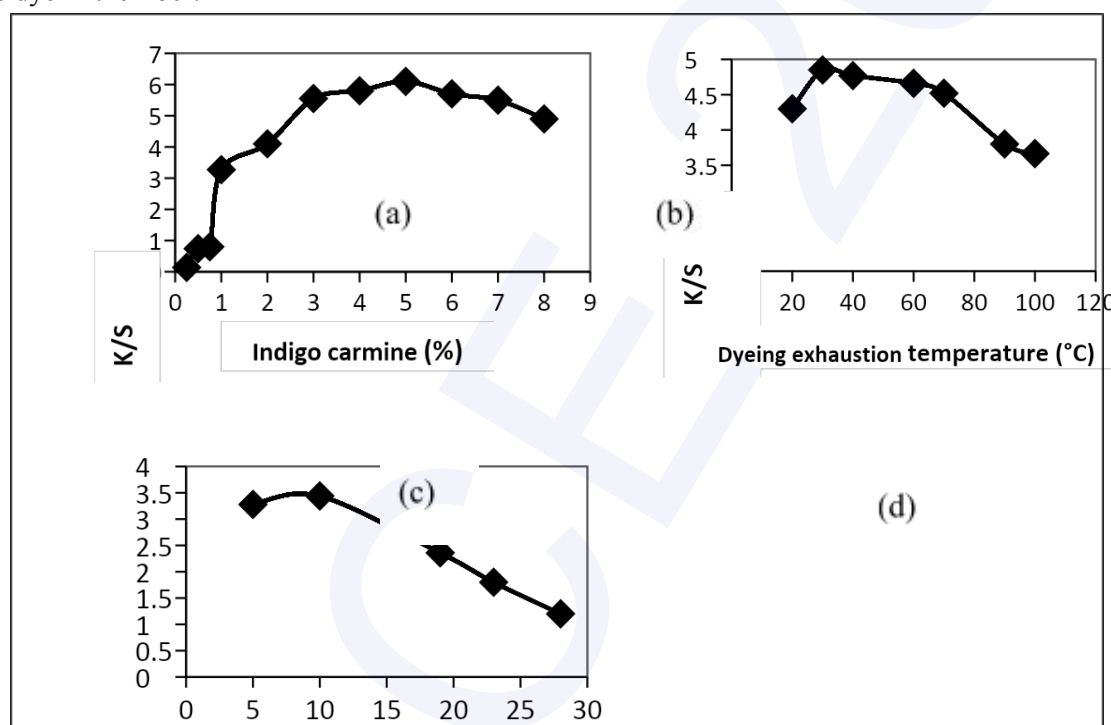
Figure 2. (a) Effect of indigo carmine amount, (b) effect of the dyeing exhaustion temperature, (c) Effect of the dyeing duration,(d)Effect of the Sodium carbonate concentration on the evolution of the color strength (K/S).

3.2. Modeling and Optimization of the dyeing process

3.2. 1. Response surface regression

The general behavior of some phenomena can be simulated by a mathematical equation, which represents the regressions models. The chosen parameters in this study were: the indigo carmine
amount, the dyeing temperature, the dyeing duration and the concentration of sodium carbonate. In this section, they will be called factors or variables presented in Table1. The analyzed result is the color strength parameter.

Table 1. Studied variables and their levels for a surface design

Variable	Symbol	Coded variable level		
		-1	0	1
Indigo carmin amount (%)	col(%)	2	5	7
Temperature (°C)	T (°C)	20	30	60
Sodium carbonate (g/L)	cs (g/L)	0	0,005	0,01
Duration (min)	t (min)	5	10	20

Modelling of the experimental plan leads to the following equation:

$$K/S = -4,49 + 1,498\,col(\%) + 0,2225\,T(°C) + 0,434\,t(min) + 306\,cs(g/L)$$
$$- 0,1688\,col(\%)*col(\%) - 0,002633\,T(°C)*T(°C) - 0,01694\,t(min)*t(min)$$
$$- 32519\,cs(g/L)*cs(g/L) + 0,00073\,col(\%)*T(°C) + 0,0111\,col(\%)*t(min)$$
$$+ 6,3\,col(\%)*cs(g/L) - 0,00201\,T(°C)*t(min) - 0,13\,T(°C)*cs(g/L)$$
$$+ 0,37\,t(min)*cs(g/L)\ \ with\ R² = 83,7\% \tag{2}$$

Where col(%) is the percentage of indigo carmine, T°(C) is the dyeing temperature, t(min) is the dyeing duration, cs(g/L) is the concentration of sodium carbonate and R^2 is the squared multiple correlation coefficient.

3.2.6. Response optimization

The optimum conditions of the dyeing process with indigo carmine after surface modification were predicted by the response optimizer tool of Minitab 14 software for maximized response. Response optimization indicates that optimum operating conditions are an indigo carmine amount of 5%, a dyeing temperature of 40°C, a dyeing time of 12.5 min and a sodium carbonate concentration of 0.005g.L^{-1}. In this case, the Minitab software gives a theoretical color strength of about 6.94. Dyeing experiments were carried out according to these experimental conditions and an experimental value of 6.9 was obtained. Following the comparison between the experimental value and the predicted value, it could be deduced that the developed model is suitable.

4. CONCLUSIONS

The purpose of this study is to develop an ecological dyeing process of cotton fibers by indigo carmine, leading to the best dyeing quality. The dyeing step was performed on modified cotton by a cationic agent. Finally, by modeling the experimental surface plan, it was found that optimal dyeing quality was obtained for an indigo carmine amount of 5%, a dyeing temperature of 40°C, a dyeing time of 13 min and a sodium carbonate concentration of 0.005g.L^{-1}.

REFERENCES

[1] **Bechtold, T., Turcanu, A.** Indirect electrochemical reduction in vat dyeing: greener chemistry replaces traditional processes, *Journal of Cleaner Production*, Vol 17, 1996, 1669-1679.

[2] **Schlüter, H.** Die vorteile der indanthren farbstoffe als kriterium für ihre segmentpezifische anwendung', *Textilveredlung,* 1990, 25, 218–221.

[3] **De Keijzer, M., Van Bommel, M.R., Keijzer, R.H., Knaller, R., Oberhumer, E.**, Indigo carmine: Understanding a problematic blue dye, *Studies in Conservation*, 2012, 57 87-95.

[4] **L.P. Donald, M.L. Gary, S.K. George,** Introduction to organic laboratory techniques: A Contemporary Approach .U.S.A.W.B Saunders , 1976.

[5] **S. Lowengard,** The creation of color in eighteenth-century Europe*,* Columbia University Press, USA, 2006.

[6] **Kubelka, P., Munck,F.,** Ein beitrag zur optik der farbanstriche, *Z. Technical Physics*, 12, 1931, 593-601.

[7] **JIWALAK, N.,** A study of the adsorption of indigo and indigo derivates onto silk, 2010, suranaree university of technology.

The Second Edition of the International Congress of Applied chemistry and Environment
30ᵗʰ-31ᵗʰ October and 01ˢᵗ November 2020, Tunisia

ICACE 2020

Fabric's thermal properties modification through the nanocomposite coating

Sawssen Ezzine[a], Khaled Abid[a] and Nèji Ladhari[a]

(a)   Textile Engineering Laboratory, University of Monastir, Ksar Hellal 5070, Tunisia
E-mail: sawssenezzine88@gmail.com

ABSTRACT

This paper explores a comparison of thermal properties of nanocoated polyester fabric for coatings synthesized with two different additives: Tunisian natural clay and titanium dioxide. They have respectively the advantages to be cheap and non-toxic. Then, they were added to two different resins, polyacrylate and polyurethane, widely used for numerous textile improvements such as permeability and brightness effects.

This study led us to say that both loads (clay and titanium dioxide) contributed to modifying the thermal properties of coated fabrics with respect to unloaded coated ones. Both loads bring a higher barrier to air and more hydrophobicity. And, the investigated thermal properties were air permeability (AP) and thermal conductivity (λ). They have been measured in controlled thermal and humidity conditions in a climatic chamber.

Finally, we conclude clay to be more effective than titanium dioxide.

KEYWORDS: Polyester fabric, nanoparticles, nanocomposite, coating, Thermal properties.

1. INTRODUCTION

Comfort is not a textile property: it is a human feeling, a condition of ease or well-being that is influenced by many factors including textile properties [1]. Comfort of clothing can be classified into three different categories: thermal comfort, tactile sensation and pressure sensation [2]. Thermal comfort is related to the way clothing buffers and dissipates metabolic heat and moisture [3], which depends on many textile properties, such as thermal conductivity, air permeability, thickness, fabric structure, finishing, etc.

Preliminary tests on a coated knitted polyester (PES) fabric which contains different types of nanoparticles are shown in this paper. A comparative evaluation with an uncoated PES fabric has been carried out.

The coating is one of the important techniques for adding value to textiles. Coating extends the range of the functional performance properties of textiles and the use of these techniques is increasing rapidly as the application for functional textiles become extensive. The coating technique imparts smart properties to fabrics. Having widespread applications across a range of technical textile sectors increases functionality and durability as well as value.

The polyester fabric was coated with nanoclay and TiO2 nanoparticles in a polymer resin, under ambient conditions, which has a very specific characteristic (sticky effect, anti tear… etc). This can explain the use of resin in the textile industry and even in many other domains such as food, aviation, aerospatial … etc.

2. MATERIAL AND METHODS

2.1. Material

Commercially undyed 100% polyester knitted fabric is used in this study. It was supplied by MonasTex Tunisia and its principal physical characteristics are fabric weight of 135g/m2 and fabric thickness of 0.74 mm.

It was scoured then with petroleum ether for 30 min to remove residues and then washed thoroughly with demineralized water and dried in a vacuum oven at room temperature for 12 hours. After being dried to a stable weight, the cleaned PET fabrics were stored in a desiccator for use.

The Tunisian natural clay was directly extracted from the soil in its raw state. It was then crushed and dried during 24 h in an oven (100 °C). This clay was then filtered through a fine sieve after eliminating impurities like little stones. The titanium dioxide was filtered according to the same procedure. We used these fillers to

The Second Edition of the International Congress of Applied chemistry and Environment
30th-31th October and 01st November 2020, Tunisia

ICACE
2020

manufacture the nanocoatings when they were added to commercial resins, polyacrylate (PAC) and polyurethane (PU). This requires a very good dispersion of particles in the matrix to avoiding agglomeration phenomena [4].

2.2. Methods

PES fabrics were characterized according to the following tests:

- Air permeability (AP) (ISO9237:1995); and
- Thermal conductivity

So the main parameters of the coating process which can affect the air permeability and the thermal conductivity are:

- Nanoparticles (nanoclay or titanium dioxide)
- Quantity of deposit nanoparticles (0%, 1%, 5% and 10%)
- Polymer resin (PU, PAC)

Experiments were carried out using a factorial design and the obtained results are analyzed using MINITAB 17 software.

3. RESULTS AND DISCUSSIONS

3.1. Air permeability

The air permeability is determined with the FX3300 device (TEXTEST, Switzerland) according to ISO 9237:1995.

It corresponds to an air flow passing perpendicularly through a fabric area of 20 cm² by measuring at a given pressure (100 Pa) its difference across the fabric test area over a given time.

Air permeability is a measure of how well air is able to flow through a fabric. It can be measured on either dry or damp fabrics.

The results were illustrated as shown in the next figure as the main effect plot for air permeability for the treated fabrics.
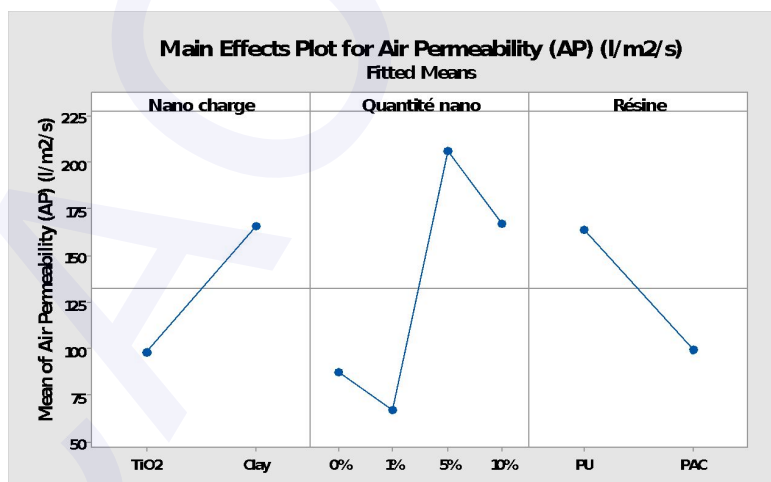
Figure 1: Main effects plot for air permeability of the coated fabric

A fabric which has good air permeability, however, does not necessarily have good moisture vapor permeability. Air permeability is likely to be lower in fabrics where the percentage or quantity of nanoparticles is 5 %.

So, the AP of coated fabric was smaller than that of uncoated fabric This suggests that treated fabrics were more porous, and more air is trapped into the fabric structure.

As a result, the air permeability of the knitted fabrics can decrease with an increased quantity of nanoparticles.

And a slight variation in this parameter will cause a significant effect on air permeability.

3.2. Thermal conductivity

Thermal conductivity is an intrinsic property of material that indicates its ability to conduct heat. NEOtim FP2C instrument was used to measure the thermal conductivity of fabric.

The results were illustrated as shown in the next figure as the main effect plot for thermal conductivity for the treated fabrics.
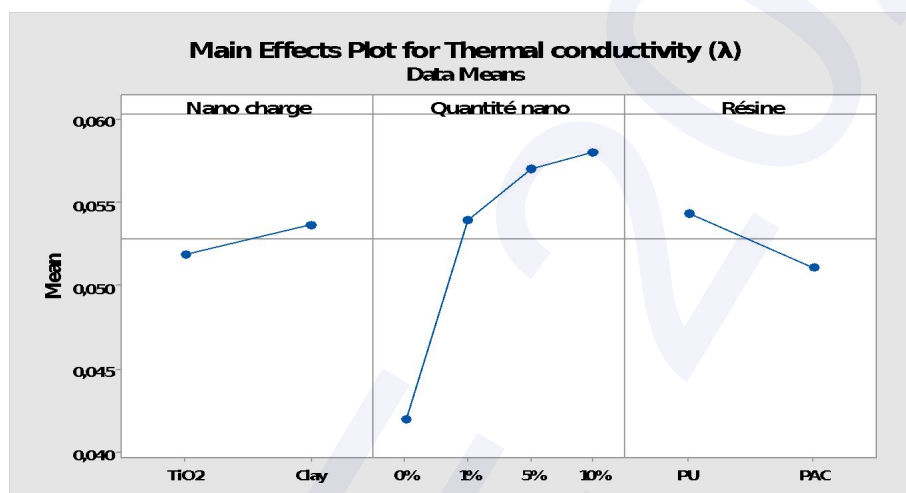
Figure 2: Main effects plot for the thermal conductivity of the coated fabric

It was revealed that parameters that affect the most thermal conductivity is the quantity of the nanoparticle added to resin.

4. CONCLUSION

The thermal characterization of knitted PES fabrics was carried out. The back-side of fabric contains different types of activated particles (nano clay and TiO2) trapped within the PES fibres.
The thermal properties in the dry state of fabrics are affected by their structure because of the trapped air within the fabrics. So, the air permeability of the fabric was linked with the types and orientation of the fibres in the fabric structure. There was a strong relationship between the thickness and the thermal conductivity of the fabric. The most important factor affecting the thermal conductivity was the thickness of the fabric.
It can be concluded that fabrics that have high air permeability values are preferred for comfortable uses.
And, the fabric samples were produced from polyester yarn, so the density of the fabrics helped us to understand the effect of the knit type and yarn count on the thermal properties of the fabrics, in conjunction with the weight and the thickness.

We can finally conclude that, in any case, with a low amount of clay or TiO2 particles added to the PAC and PU resins, the air barrier properties of the coated fabric are globally enhanced, which give them properties suitable for many technical applications [5].

REFERENCES

[1] **B.J. Collier and I. H.H. Epps,** *"Textile Testing and Analysis"*, Prentice-Hall, Englewood Cliffs, 1999.
[2] **Y. Li**, The Science of clothing comfort, *Textile Progress,* Vol. 31, N.1-2, 2001, 22-32.

[3] **P. Verdu, J.M Rego, J.Nieto and M. Blanes**, Comfort analysis of Woven/Polyester fabrics modified with a new elastic fiber, part 1 preliminary analysis of comfort and mechanical properties, *Textile Research. Journal,* Vol. 79, 2009, 14-23.

[4] **K. Abid, S. Dhouib, F. Sakli,** Modelling of Thermal Behaviour of a Fabric Coated With Nanocomposites, *Journal of Applied Sciences, Vol. 1*, 2010, 71–74

[5] **Sen, K.; Tech, M,** *In Handbook of Coated Textiles*, J. editor, Reeves Brothers, INC.; Kanpur, India, 2001, 141–161.

Capillary water absorption in a coated waterproof breathable double-sided knit

Imene GHEZAL[a,b], Ali MOUSSA[a,b], Imed BEN MARZOUG[a,c], Ahmida EL-ACHARI[d,e], Christine CAMPAGNE[d,e] and Faouzi SAKLI[a,c].

(a) Textile Engineering Laboratory, University of Monastir, 5070 Ksar-Hellal, Tunisia
(b) National Engineering School of Monastir, University of Monastir, 5019 Monastir, Tunisia
(c) Higher Institute of Technological Studies of Ksar-Hellal, 5070 Ksar-Hellal, Tunisia
(d) Université Lille Nord de France, 59000 Lille, France
(e) ENSAIT, GEMTEX, 2 Allée Louise et Victor Champier 59100 Roubaix, France
E-mail: elghezalimene@hotmail.com

ABSTRACT

This research aims to evaluate the wicking behaviour of a double-sided fabric before and after undergoing an ecological coating process. A cotton/ polyester knit was coated with a mixture of a fluorocarbon resin and an acrylic paste in order to enhance its hydrophobicity without restricting its breathability. The coating process does not require water use and does not generate wastewater. Since fabric breathability is associated with its moisture evacuation capability, weight of water absorbed by capillarity was measured before and after the coating treatment. It was found that the applied coat reduced significantly micro- and macro spaces. As a result, the weight of capillary absorbed water decreased along fabric's wale and course directions.

KEYWORDS: capillary rising, wicking, double-sided knit, ecological coat, capillary absorbed water.

1. INTRODUCTION

Breathability is a major factor when it comes to decide about the comfort level of an apparel [1, 2]. Physiological comfort depends on the ability of a fabric to evacuate transpiration either in its vapour form (insensible perspiration) or its liquid form (sensible perspiration also called sweat) [3, 4]. The ability of apparel to transport a liquid from its inner-side to its outer-side defines its ability to confer comfort to the wearer [4]. Capillarity phenomenon is responsible of water transport through a fabric and it is defined as the ability of liquids to be displaced from wettable capillaries to non wettable ones [Dynamic capillary rise]. Wicking can be defined as the spontaneous liquid flow resulting in a porous material. This flow is driven by capillary forces resulting from fabric surface wetting [5, 6].
In this research, the wicking behaviour of a double-sided cotton/ polyester knit was studied by measuring the capillary absorbed water weight. Tests were done before and after the coating treatment and according to wale and course directions.

2. MATERIAL AND METHODS

2.1. Coating process

A double-sided knit with a cotton inner-face and a polyester outer-face was coated with a mixture of a fluorocarbon resin and an acrylic paste by using the screen coating process. Quantities of fluorocarbon resin and acrylic paste are equal to 2.7% and 412 g.m^{-2}, respectively [7, 8]. Both products were supplied from CHIMITEX-Tunisia (Figure 1). The coat was applied to the polyester outer-face in order to enhance its hydrophobicity without restricting the breathability of the double-sided knit. The substrate was dried for 20 min at 90°C and reticulated at 150°C for 13.5 min.
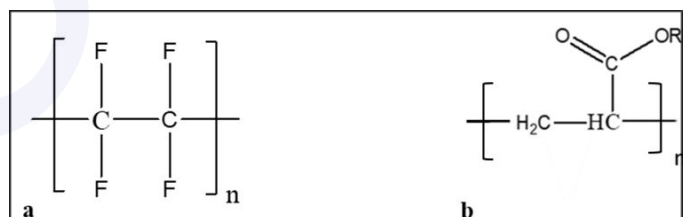
Figure 1: Chemical formulas (a) fluorocarbon polymer, (b) acrylic polymer

2.2. Determination of weight of capillary absorbed water

Textiles are hierarchical porous structures. Micro- and macro-spaces are defined as voids between fibers and yarns, respectively. Capillary forces drive a spontaneous liquid flow in the fabric porous structure. This phenomenon is called wicking [6]. The capillary pressure is given by Laplace equation (equation 1) [9, 10, 11]:

$$P_c = \frac{2\gamma \cos\theta}{r} \qquad (1)$$

Where P_c is the capillary pressure, γ is the liquid surface tension, θ is the contact angle between the tested sample and the used liquid, and r is the capillary radius.

Figure 2: Used GBX-3S Tensiometer and a suspended sample with its bottom end dipped in distilled water.

To determine the weight of water absorbed by capillary action, a GBX-3S Tensiometer was used (Figure 2). Samples of 6 cm × 3 cm were cut from the double-sided knit along wale and course directions and suspended in a way to form a meniscus when their bottom ends are driven down to reach the distilled water surface (surface tension = 72,8 mN.m-1 ; d= 1 g.cm-3). A weighing sensor associated to a balance system helps in determining the weight of water absorbed by the sample through capillary action.

The double sided fabric was tested before and after the coating treatment and according to wale and course directions. Test duration is equal to 600 s. Tests were repeated three times. For each test, the experimental data of gain and absorbed water by capillary rise as function of time were represented. Difference between the gain and weight value read on the top balance corresponds to the meniscus weight. Capillary absorption coefficient C can be determined by using equation (2) [10, 11].

$$C = \frac{m\,(mg)}{A\,(mm^2)} \qquad (2)$$

Where m (mg) is the absorbed water through capillary action and A (mm²) is sample section.

Considering that sample section is negligible, the curve C = f (t) is equivalent to the curve m = f (t) where C (mg.mm^{-2}) is the water capillary absorption coefficient, m (mg) is the weight of capillary absorbed water, and t (s) is test time.

3. RESULTS AND DISCUSSIONS

Figure 3 shows gain and weight of water absorbed by capillarity of experimental double sided-fabric wicking according to wale direction as function of time before and after the coating treatment.

The used knit is considered as a hierarchical porous structure. Capillaries are the result of voids between fibres and yarns. After meniscus formation and bottom sample wetting, the liquid fulfil micro-capillaries (inter-fibre space) and then macro-capillaries (inter-yarn space) also called small reservoirs. Capillary water rise is vertical than water propagates perpendicular to the test direction. After a determined test time the pressure difference between micro- and macro-capillaries is equal to zero and a capillary equilibrium height is achieved.

It can be noticed that after the coating process, values of gain and water weight absorbed by capillarity decreased significantly. In fact, capillary rise is the result of macro- and micro capillary rises. Since

The Second Edition of the International Congress of Applied chemistry and Environment
30th-31th October and 01st November 2020, Tunisia

ICACE 2020

inter-fibre and inter-yarn spaces were fulfilled with the coat paste, the fabric porosity decreased which affected the sizes and distributions of capillaries in the tested knit. As a result, gain and weight of water absorbed by capillarity decreased significantly.
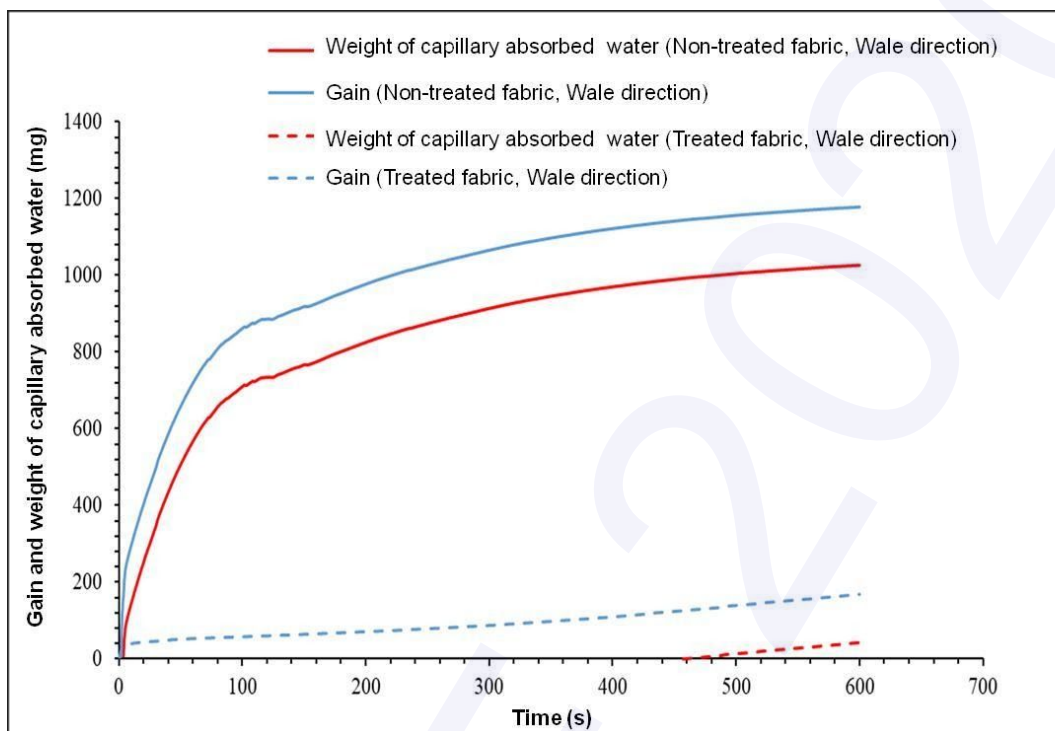

Figure 3: Gain and weight of capillary absorbed water as function of time for the double-sided knit before and after the coating treatment.

Same results were obtained for coated and uncoated samples when tests were done according to course direction.
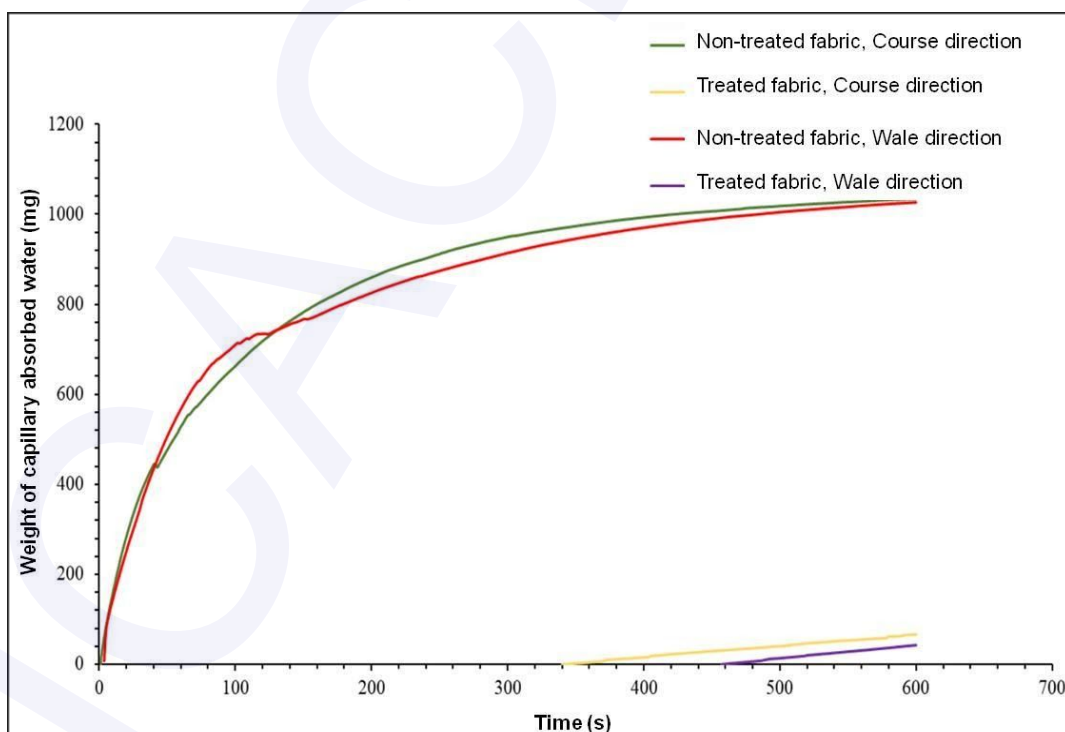

Figure 4: Weight of capillary absorbed water as function of time for the double-sided knit before and after the coating treatment.

Figure 4 shows weight of capillary absorbed water of the double sided-fabric according to wale and course directions as function of time, before and after the coating treatment.

The speed value of capillary rise for the non-treated fabric obtained according to course direction is slightly higher than the value obtained according to wale direction. This can be explained by the fact that liquid weight absorbed by capillarity and capillary action wicking time are influenced by the fabric geometric capillary distribution [6]. The slight difference in inter-yarn and inter-fibre spaces leads to a higher weight of capillary absorbed water according to course direction.

Higher values of water weight and speed rise were obtained before the coating treatment. Wetting causes capillary forces. In a capillary system, wicking is the result of spontaneous wetting [6]. After the coating treatment, fabric wettability decreased significantly which caused a decrease in capillary rise kinetic. The water weight absorbed through capillary phenomena remains equal to zero even after 340 s and 457 s test time when tests were done according to course and wale directions, respectively.

For coated samples, the water weight value obtained according to course direction is slightly higher than the one obtained when tests were done according to wale direction. This is the result of both capillaries size and distribution in the knit according to both directions. Also scarping direction during the coating treatment may be the cause of the obtained results (scarping was done according to wale direction).

4. CONCLUSION

The wicking behaviour of a coated double-sided fabric, before and after a coating treatment, was analyzed by measuring the weight of water absorbed by capillarity. It was found that the uncoated fabric has a higher wicking behaviour before the coating treatment. After coating, the surface free energy of the fabric decreased significantly which made its wetting difficult. Added to that, the coat paste fulfilled micro- and macro capillaries. Both cited reasons made difficult the absorption of water by capillarity action.

REFERENCES

[1] **A. Mukhopadhyay, V. K. Midha**, A review on designing the waterproof breathable fabrics Part I: Fundamental principles and designing aspect of breathable fabrics, *Journal of Industrial Textiles*, Vol.37, No.3, 2008, 225-262.

[2] **A. Boughattas, S. Benltoufa, F. Fayala**, Moisture management properties of double face DENIM fabrics, *International Journal of Applied Research on Textile*, Special Issue, 2019, 38-43.

[3] **M. Azeem, A. Boughattas, J. Wiener, A. Havelka**, Mechanism of liquid water transport in fabrics, A review, *Fibres and Textiles*, Vol.4, 2017, 58-65.

[4] **T. S. Smith**, *The physiology of health; or, An exposition to the physical and mental constitution of man with a view to the promotion of human longevity and happiness*, Forgotten Books, London, 458.

[5] **A. Chatterjee, P. Singh**, Studies on wicking behaviour of polyester fabric, *Journal of Textiles*, 2014, 14.

[6] **R. Fangueiro, A. Filgueiras, F. Soutinho X. Meidi**, Wicking behaviour and drying capability of functional knitted fabrics, *Textile Research Journal*, Vol.80, No.15, 2010, 1522-1530.

[7] **I. Ghezal, A. Moussa, I. Ben Marzoug, A. El Achari, C. Campagne, F. Sakli**, Evaluating the mechanical properties of waterproof breathable fabric produced by a coating process, *Clothing and Textiles Research Journal*, Vol.37, No.4, 2019, 235-248.

[8] **I. Ghezal, A. Moussa, I. Ben Marzoug, A. El Achari, C. Campagne, F. Sakli**, Development of an ecological coating process for textile hydrophobicity enhancement, *International Congress of Applied Chemistry and Environment*, Sousse, Tunisia, 2018.

[9] **B. Das, A. Das, V. K. Kothari, R. Fanguiero, M. Araijo**, Moisture transmission through textiles Part I: Process involved in moisture transmission and the factors at play, *AUTEX Research Journal*, Vol.7, No.2, 2007, 100-110.

[10] **A. E. Fanaei**, Thesis: Caractérisation expérimentale des écoulements capillaries dans les renforts fibreux à double échelle de porosité, *Monreal University,* Canada.

[11] **H. Gidik**, Thesis: Réalisation d'un fluxmètre thermique à gradient tangentiel de température à paroi auxiliaire textile intégrant des fils thermoélectriques : Application à la mesure des transferts thermiques et hydriques, *Université des sciences et technologies de Lille 1,* France.

Ecological and clean process for dyeing advanced bicomponent polyesters filaments (PET/PTT)

Marwa SOUISSI[a,b], Mounir ZAAG[c], Nizar MEKSI[a,b], Hatem DHAOUADI[a]

(a) University of Monastir, Faculty of Sciences of Monastir, Research Unit of Applied Chemistry and Environment, 5019 Monastir, Tunisia
(b) University of Monastir, National Engineering School of Monastir, 5019 Monastir, Tunisia
(C) Société Industrielle des Textiles (SITEX), 5070 Ksar-Hellal, Tunisia.

Email: souissi.marwa20@yahoo.com

ABSTRACT:

Despite the various efforts of researchers, dyeing polyesters still present several problems which should be resolved. Indeed, manufacturers prefer dyeing polyester under pressure at temperatures close to 130°C to have less toxic textile effluents at the end of the dyeing and to present a textile product which is not dangerous for the health of the consumer. This paper is devoted to study the possibility of replacing toxic carriers with biological ones. Three kinds of biological carriers (Ortho-vanilin, Para-vanilin and Coumarin) are used to dye innovative bicomponent filaments knitted fabric with CI Disperse Yellow 211. Dyeing performances of biological carriers were compared to traditional ones such as dichlorobenzene, benzylbenzoate, phenylphenol, and a commercial Livster BF carrier. This study confirms that biological carriers can be a potential cure to replace the toxic ones and to have at the same a good color yield.

KEYWORDS: Dyeing, Bicomponent filaments, Biological carrier, Toxic.

1. INTRODUCTION

Nowadays, textile industry is looking for new alternatives and tends to use more efficient, innovative and ecological methods while guaranteeing quality and competitiveness. For several years, great effort has been devoted to adapting textile chemistry using natural, biological and environmentally friendly products [1,2]. For this reason, several research studies have focused on replacing toxic products for the environment with others that are less harmful, even natural and biologic [3,4]. Recently, considerable attention has been paid to innovative bicomponent polyester filaments composed of polyethylene terephthalate (PET) and polytrimethylene terephthalate (PTT). The two polymers making up the yarn are extruded from the same spinneret, adjacent and arranged side by side [5,6].

Despite the efforts made by researchers to improve the quality of polyesters which is used more and more until reaching in 2009 an overall production equal to 31.9 million tonnes; around 45% of world fiber production [3].The dyeing of polyesters always presents problems because until now industries prefer to dye the polyesters at high temperatures around 135 °C instead of using exhaustion process at 100 °C with the use of auxiliary products called carriers. The most popular carriers are butyl benzoate, methylnaphthalene, dichlorobenzene, diphenyl and o-phenylphenol. They make it possible to dye even deep shades at boiling point with greater speed. These carriers are used for dyeing PET fibers in order to improve adsorption and accelerate diffusion of disperse dyes into the fiber at low temperature and pressure conditions. Nevertheless, most of carriers are toxic for humans and aquatic organisms [7]. During dyeing and rinsing, a large amount of carriers is released into wastewater, but a part of them remains entrapped in the fiber [8] and is likely to be emitted into air during drying and thermofixation. In this context, biological carriers are of great interest and their uses would be interesting in the dyeing of polyesters. However, natural carriers such as natural vanillin and coumarin are very expensive and they have been replaced by synthesized ones [9]. In addition, these naturals substances are known for their antioxidant activity [10], their antimicrobial and anti-mutagenic effects [11]. In this article, two types of vanillin will be evaluated: Para and Ortho-vanillin and coumarin are presented in Figure 1.

In order to remedy all these problems, this research paper demonstrates the feasibility of dyeing bicomponent polyesters filaments using exhaustion process, thus replacing commercial toxic carriers by others more ecological which respect the nature.

2. MATERIAL AND METHODS

2.1. Textile support

Textile samples used during this study are jersey fabrics knitted with 100% bicomponent filaments (60%PET/40%PTT) purchased from Invista Company (United States). Fabrics were made using circular knitting machine type TRICOLAB gauge 12 (Sodemat, France).

2.2. Dyeing procedure

Dyeing process of knitted fabrics with CI Disperse Yellow 211 is shown in Figure 1. In fact, for each dyeing, 1.2% disperse dye are added after 15 min. The liquor-to-fiber ratio is equal to 10:1. Mcilvaine Buffer solution containing disodium phosphate (Na_2HPO_4) and citric acid ($C_6H_8O_7$) is used to ensure that the pH was stable throughout the dyeing process. In this study, three toxic carriers (Livster BF, o-phenylphenol and benzylbenzoate) and three kinds of biological carriers (o-vanilin, p-vanilin and coumarin) were used and evaluated.
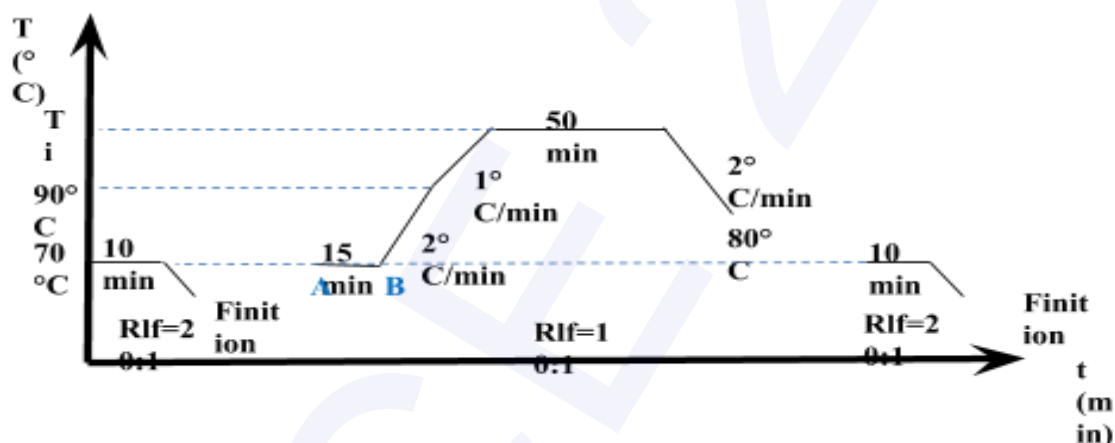
Figure 1: Dyeing process.

2.3. Dye bath exhaustion

At the end of the dyeing, the extent of the dye bath exhaustion $E(\%)$ was determined by measuring, using the Spectrophotometer Libra S6, the absorbance of the residual dyebath at λ_{max} = 452 nm. The dye bath exhaustion $E(\%)$ is then given by the following equation:

$$E\ (\%) = \frac{Abs_0 - Abs_{res}}{Abs_0} \times 100 \qquad (1)$$

where Abs_0 and Abs_{res} are the absorbance values of the initial and the residual dyebaths, respectively.

2.4. Measurement of color

Colors of dyed samples were measured using a spectrophotometer Spectraflash 600 Plus (Datacolor), under the following conditions: illuminant D65 and 10° standard observer. For this, each measured sample were presented at several levels of thickness (four layers) for maximum opacity.

3. RESULTS AND DISCUSSIONS

A series of dyeing of bicomponent filaments was carried out using 1.2% of CI Disperse Yellow 211 (dyeing process in Figure 1). The concentration of each used carrier was varied (ranging from 0 up to 0.16 mol/L) in order to evaluate their performances. Obtained values of dye bath exhaustions are shown in Figure 2. Results prove that the use of toxic carriers improves the dye bath exhaustion until added concentration of 0.6 mol/L. Beyond this concentration, dye bath exhaustion decreases. This decrease, probably due to a degradation of the dye molecules, is accompanied by a loss of elasticity and softness of dyed samples.

The Second Edition of the International Congress of Applied chemistry and Environment
30th-31th October and 01st November 2020, Tunisia

ICACE 2020
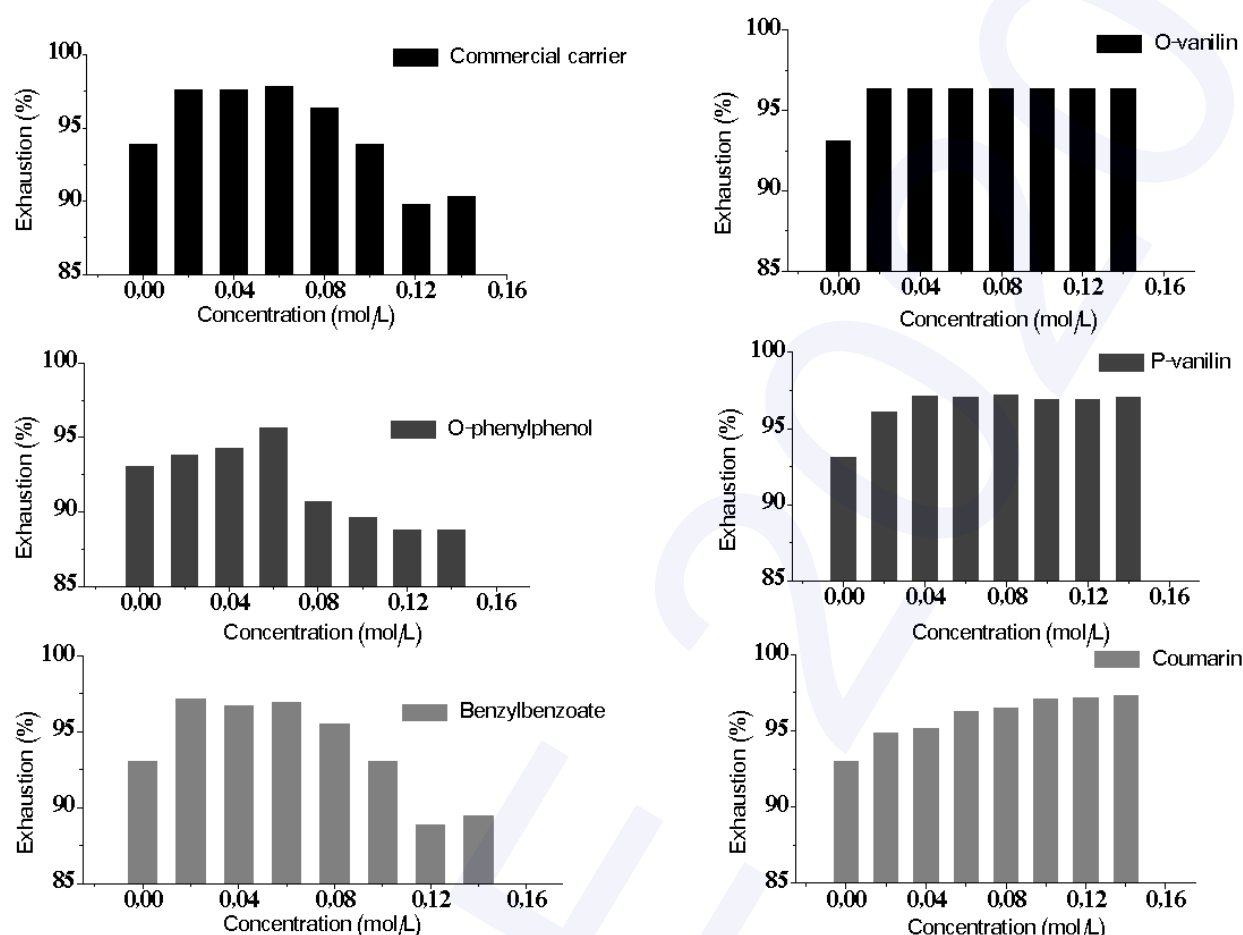
Figure 2: Effect of toxic and biological carriers' concentrations on dye bath exhaustions.

In the case of biological carriers, the obtained values of dye bath exhaustion are slightly better than those reached by toxic ones. Moreover, a concentration values equal to 0.02 mol/L of p-vanilin and o-vanilin are found sufficient to obtain an excellent color yield. More importantly, the excess of molecules in the dye bath did not cause degradation in the used molecular dye and dyed filaments retain their good mechanical and chemical properties.

Table 1 summarized obtained values of dye bath exhaustions and colors of samples dyed using different dyeing processes. Results showed that dyeing process at 100 °C with the use of o-vanilin as biological carrier offers good dyeing performances (dye bath exhaustion = 96.07% and K/S = 23.16) better than those obtained at 130 °C (without carrier).

Table1: Dye bath exhaustions, color strength and color coordinates of samples dyed using different dyeing processes.

Dyeing process	Dye bath Exhaustion (%)	K/S	L^*	a^*	b^*
At 100 °C (without carrier)	93.24	18.74	75.44	10.40	47.34
At 100 °C (with 0.02 mol/L of o-vanilin as carrier)	96.07	23.16	74.31	10.21	46.88
At 130 °C (without carrier)	94.68	23	75.04	9.64	47.94

4. Conclusion

The study presented in this paper proved the possibility to use biological products, namely vanillin and coumarin, as substituting of toxic carriers used for dyeing of bicomponent polyester filaments with disperse dyes. Obtained results showed that the dye bath exhaustion values using o-vanillin, p-vanillin and coumarin

are better than those obtained by toxic carriers. In addition, it is found that dyeing process at 100 °C using biological carriers is more effective and economic than dyeing at 130 °C.

References

[1] Souissi M, Guesmi A, Moussa A, Valorization of natural dye extracted from date palm pits (Phoenix dactylifera) for dyeing of cotton fabric. Part 2: Optimization of dyeing process and improvement of colorfastness with biological mordants, *Journal of Cleaner Production*, Vol. 204, 2018, 1143-1153.

[2] Montoneri E, Boffa V, Savarino P, Tambone F, Adani F, Micheletti L, Gianotti C, Chiono R, Use of biosurfactants from urban wastes compost in textile dyeing and soil remediation, *Waste Management* , Vol.29, 2008, 383-389.

[3] Ozturk E, Yetis U, Dilek F B, Demirer G N,A chemical substitution study for a wet processing textile mill in Turkey. *Journal of Clean Production*, Vol.17, 2009, 239-247.

[4] Hansonn S, Molander, L, Ruden C, The substitution principle, *Regulatory Toxicology and Pharmacology* , Vol. 59, 2011, 454-460.

[5] Jin L, Fumei W, Bugao X, Factors affecting crimp configuration of PTT/PET bi-component filaments, *Textile Research Journal,* Vol.81, No.5, 2010, 538-544.

[6] Fumei W, Fei G, Bugao X, Elastic Strain of PTT/PET Self-Crimping Fibers. *Journal of Engineered Fibers and Fabrics,* Vol.8, No.2, 2013, 50-55.

[7] Tavanaie, Polypropylene/poly (butylene terephthalate) melt spun alloy fibers dyeable with carrier-free exhaust dyeing as an environmentally friendlier process. *Journal of Cleaner Production,*Vol.18, 2010, 1866-1871.

[8] Shenai VA, Toxicity of polyester dyeing carriers. *Textile Dyer and Printer*, Vol. 31, 1998, 11-16.

[9] McShan D, Heuristic search for metabolic engineering: de novo synthesis of vanillin. *Computers & Chemical Engineering*, Vol.29, 2005, 499-507.

[10] Tai A, Sawano T, Yazama F, Ito H, Evaluation of antioxidant activity of vanillin by using multiple antioxidant assays. *Biochimica et Biophysica Acta (BBA)-General Subjects*, Vol.1810, 2011, 170-177.

[11] Walton N J, Mayer M J, Narbad A, Vanilin. *Phytochemistry*,Vol.63, 2003, 505-515.

The Second Edition of the International Congress of Applied chemistry and Environment
30th-31th October and 01st November 2020, Tunisia

ICACE 2020

A new natural color indicator extracted from *Carissa macrocarpa* fruit

Imene Ghezal [a, b], Ibtissem Moussa [b, c], Faouzi Sakli [a, d]

(a) Textile Engineering Laboratory, University of Monastir, 5070 Ksar-Hellal, Tunisia
(b) National Engineering School of Monastir, University of Monastir, 5019 Monastir, Tunisia
(c) Research Unit of Applied Chemistry and Environment, Faculty of Sciences, University of Monastir, Monastir, Tunisia
(d) Higher Institute of Technological Studies of Ksar-Hellal, 5070 Ksar-Hellal, Tunisia

E-mail : elghezalimene@hotmail.com

ABSTRACT :

In this research, a natural color indicator was extracted from *Carissa macrocarpa* fruit. For this purpose, a microwave-assisted extraction was used. Two extraction methods were elaborated. The first one was by using water as a solvent. The second one was done with 70% ethanol/ 30% water solution. Both extraction processes were realized in a microwave power equal to 500 watts and an extraction time of four minutes. To evaluate the efficiency of the used extraction processes, anthocyanins concentration was calculated. They were equal to 28.3 mg/100 mL and 5.8 mg/100 mL, respectively for ethanol/water and water solvents. Based on these results, the ethanol/ water solvent was found to be five time more efficacious than water solvent in anthocyanins extraction.
The pH of anthocyanins extract solution was also varied from 1.0 to 10.0 and solution color variations were noticed in different pH.

KEYWORDS: Natural color indicator, *Carissa macrocarpa* fruit, Anthocyanins, Microwave-assisted extraction.

INTRODUCTION

Some synthetic dyes and chemicals used in their synthesis were found to be toxic. Modern researches focus on eco-friendly natural dyes that are not hazardous to health and environment [1,2,3]. A natural dye is a colorant extracted from insect, animal, vegetable, or mineral sources [4]. Based on its chemical structure, a natural dye can belong to indigoids, naphtoquinones, anthroquinoids, ketones, inines, polymethines, flavanols, flavanones, flavones, and chlorophyls [5]. Some pH sensitive dyes can be used as pH indicators [6]. An exemple of natural plants colorants are anthocyanins. They are glycosides formed of the anthocyanidin aglycone and glycosically bonded mono- or oligosaccharidic units [7]. Anthocyanins are soluble in water and are known to be easily extracted [8]. Their extracts have antidiabetic, antibiotic, antioxidant, and chemoprotective activities which make them beneficial to our health [9]. The chemical structure of anthocyanins is presented in Figure 1 [10].

There are many sources for anthocyanins such us red berries, raspberries, and cherries [9]. In this research, a new source of anthocyanins was introduced. The extraction of anthocyanins from the fruit of *Carissa macrocarpa* also known as Natal plum or num-num was done by using alcoholic and aqueous solvents. *Carissa macrocarpa is* a plant from the *Apocynaceae* family. The plant fruit is ovoid and fleshy. Its length is about 15 mm. When mature, its color turns to red [11, 12].
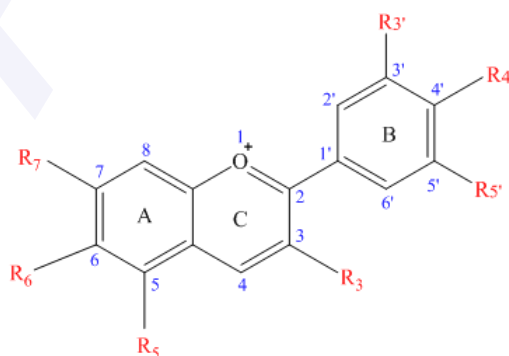
Figure 1. Basic anthocyanins structure [10]

Traditional extraction methods consume huge quantities of water, lot of time, and energy. They also generate huge amount of waste [13]. In recent years, more ecological techniques arose in order to ameliorate colorant yield, decrease extraction time, consumed energy, and solvent consumption [13].

For natural color extraction, a widely used method is the microwave-assisted extraction. Researchers found that this technique is eco-friendly and leads to an increase in the colorant yield [14].

In this research, the extraction of anthocyanins was done by using a microwave-assisted extraction method. Concentration of anthocyanins was determined. The pH of the extract was then varied in order to visualize anthocyanins solution color change.

1. MATERIAL AND METHODS

2.1. Preparation of anthocyanins extracts

Two solvents were used to extract anthocyanins from Natal plum fruit (Figure 2). The first solvent was water. The second one was a mixture of 70% ethanol (96%) and 30% water. In a chopper (Moulinex), 10 g of fruit were mixed with 100 mL of solvent. The solution was maintained in a microwave reactor for 4 min at 500 watts. Fruit extracts namely E_W and $E_{E/W}$, respectively for water and ethanol/water solvents were filtered with a filter paper.

Figure 2: *Carissa macrocarpa* (a) Plant and (b) Fruit

2.2. UV-vis spectroscopy of *Carissa macrocarpa* fruit

UV-vis spactra of Carissa macrocarpa fruit extracts were analyzed by using a DR 6000 UV-vis spectrophotometer (Figure 3) in the range of 300-700 nm. Fruit extracts with pH values from 1.0 to 10.0 were measured in the range 400-700 nm.

Figure 2 : DR 6000 UV-vis spectrophotometer

2.4. Total anthocyanins concentration

In order to determine the total anthocyanins concentration in the prepared extracts E_W and $E_{E/W}$, the pH difference method was used [15].

Determined volumes of NaOH and HCl were added to extract solutions in order to obtain pH values equal to 1.0 and 4.5. Extracts' absorbances were measured at the extract maximum absorption wavelength (535 and 510 nm for ethanol water and water solvents extracts, respectively) and at 700 nm. By using equations (1) and (2), anthocyanins concentrations were calculated and expressed as mg cyanidin-3-glucoside per 100 mL extract.

$$Anthocyanins\ concentration = \frac{\Delta A \,.\, M_W \,.FD.1000}{\varepsilon \,.L} \qquad (1)$$

$$\Delta A = (A_{\lambda\ vis\ max} - A_{700})\ \text{PH=1,0} - (A_{\lambda\ vis\ max} - A_{700})\ \text{PH=4,5} \qquad (2)$$

Where ΔA is the difference between absorbances at λ_{max} and 700 nm, M_W is the molecular mass of cyanidin-3-glucoside (449.2 g/mol), FD is the dilution factor, ε is the molar extinction coefficient for cyanidin-3-

glucoside ($26900\ cm^{-1}.M^{-1}$), L is the optical path (cm), and 1000 is the conversion factor from grams to milligrams.

2. RESULTS AND DISCUSSIONS

2.1 Characterization of aqueous and alcoholic extracts of *Carissa macrocarpa* fruit

The pH values of Natal plum extracts were equal to 3.12 and 3.86 for E_w and $E_{E/w}$, respectively. Appearances of both extracts are shown in Figure 4. Solutions are colored and translucent. The color of the aqueous extract is salmon. The alcoholic extract presents deeper and more violaceous color than the aqueous one.

Figure 4 shows also the UV-visible spectrums of aqueous and alcoholic extracts. The highest absorption wavelengths were obtained at 510 and 535 nm for aqueous and alcoholic, respectively. The difference in obtained wavelengths is the result of different anthocyanins types in both extracts.

When calculating the anthocyanins concentrations in aqueous and alcoholic extracts, values were equal to 5.8 mg/100 mL and to 28.3 mg/100 mL, respectively. So it can be deduced that ethanol/water solvent present a higher efficiency than aqueous solvent for extracting anthocyanins from Natal plum fruit.
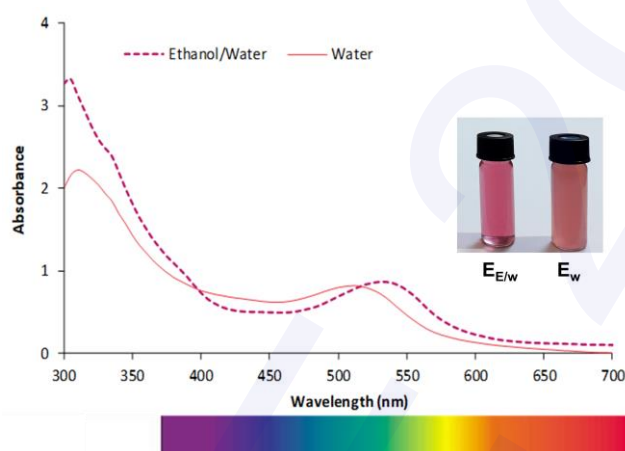
Figure 4: Visual appearance and UV-Visible spectrum of aqueous and alcoholic anthocyanins extracts of Natal plum fruit.

3.2. UV-vis spectra of Natal plum fruit alcoholic extract in various pH ranges

pH effect on the light absorbency of the Natal plum fruit alcoholic extract was analyzed by varying the solution pH from 1.0 to 10. Acidic conditions give anthocyanins red color. As well as pH increases, anthocyanins color changes from salmon to pink to plum to fade blue to green.

Figure 5: (a) Color variations, (b) UV-vis spectra of alcoholic anthocyanins extracts.

The Second Edition of the International Congress of Applied chemistry and Environment
30th-31th October and 01st November 2020, Tunisia

ICACE 2020

From Figure 5(a), it can be noticed that the alcoholic extract color varied from salmon (pH value equal to 1.0) to green (pH value equal to 10.0). It was also noticed that an increase in the pH value from 1.0 to 6.0 leads to a decrease in the solution absorbance (Figure 5(b)). Extract solution color changed from pink (pH value equal to 2.0) to plum (pH value equal to 5.0) and turned to fade blue when the pH value was equal to 8.0. When pH value was varied from 8.0 to 10.0, the color of the extract tended to change from fade blue to green. When the pH values of the alcoholic extract were lower than 6.0, the wavelength corresponding to the maximum absorption pick was obtained at 535 nm. When it was higher than 6.0, the maximum absorbance pick shifted to 585 nm. Bathochromic and hypochromic shifts come as a result of extract pH variation.

CONCLUSION

In this research, a new natural color was extracted from *Carissa macrocarpa* fruit by using two solvent types; water and a mixture of ethanol and water (70% ethanol and 30% water). The alcoholic extract was found to be five times richer in anthocyanins than the aqueous one.

When varying solution pH, the *Carissa macrocarpa* extract color varied from salmon to fade green which make it appropriate to be used as a color indicator.

REFERENCES

[1] **N. Meksi, W. Haddar, N. Bakka, M. Mejri, and M. F. Mhenni**, Eco-friendly Dyeing of Modified Cotton Fabrics Using Olive dyes Extracted from Olive Mill Wastewater: Focus on Dyeing Quantities and Environmental Performances, *International Journal of Applied Research on Textile*,2018, Vol.6, No.1, 46-64.

[2] **A. Guesmi, N. Ben Hamadi, N. Ladhari, and F. Sakli**, Dyeing Properties and Colour Fastness of Wool Dyed with Indicaxanthin Natural Dye, *Industrial Crops and Products*, 2012, Vol.37, No.1, 493-499.

[3] **A. Guesmi, N. Ben Hamadi, N. Ladhari, and F. Sakli**, Sonicator Dyeing of Modified Acrylic Fabrics with Indicaxanthin Natural Dye, *Industrial Crops and Products*, 2013, Vol.42, 63-69.

[4] **B. H. Patel**, *Handbook of Textile and Industrial Dyeing*, Woodhead Publishing Limited, Oxford, 2011, 680.

[5] **B. Glover,** Doing what comes naturally in the dyehouse, *Journal of the Society of Dyers and Colourists*, 2008, Vol.114, No.1, 4–7.

[6] I. Choi, J. Y. Lee, M. Lacroix, J. Han, Intelligent pH indicator film composed of agar/potato starch and anthocyanin extracts from purple sweet potato, *Food Chemistry*, 2017, Vol. 218, 122-128.

[7] **M.L. Blackhall, R. Berry, N. W. Davies, and J. T. Walls**, Optimized extraction of anthocyanins from Reid Fruits' Prunus avium 'Lapins' cherries, *Food Chemistry*, 2018, Vol.256, No.8 , 280–285.

[8] **Y. S. Musso, P.R. Salgado, and A.N. Mauri**, Smart gelatin films prepared using red cabbage (Brassica oleracea L.) extracts as solvent, *Food Hydrocolloids*, 2019, Vol.89,674–681.

[9] **M.L. Blackhall, R. Berry, N.W. Davies, and J.T. Walls**, Optimized extraction of anthocyanins from Reid Fruits' Prunus avium 'Lapins' cherries, *Food Chemistry*, 2018, Vol.256, No.8 , 280–285.

[10] H. E. Khoo, A. Azlan, S. T. Tang, and S. M. Lim, Anthocyanidins and anthocyanins: colored pigments as food, pharmaceutical ingredients, and the potential health benefits, *Food and Nutrition Research*, 2017, Vol. 61, No. 12.
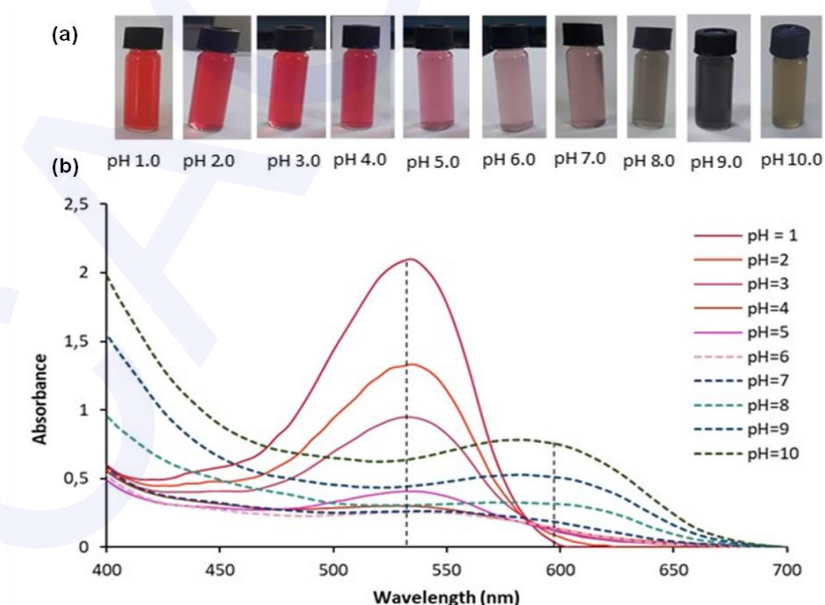
[11] **R. Moodley, N. Koorbanally, and S. B. Jonnalagadda**, Elemental composition and fatty acid profile of the edible fruits of Amatungula (Carissa macrocarpa) and impact of soil quality on chemical characteristics, *Analytica Chimica Acta*, 2012, Vol.730, No.6, 33–41.

[12] **A. M. Allahverdiyev, M. Bagirova, S. Yaman, R. Cakir Koc, E. S. Abamor, S.C. Ates, S. Y. Bayadar, S. Elcicek, and O.N. Ozel**, Chapter 17- Development of New Antiherpetic Drugs Based on Plant Compounds , Fighting Multidrug Resistance with Herbal Extracts, Essential oils and their Components, 2013, 245-259.

[13] **W. Liu, C. Yang, C. Zhou, Z. Wen, and X. Dong**, An improved microwave-assisted extraction of anthocyanins from purple sweet potato in favor of subsequent comprehensive utilization of pomace, *Food and Bioproducts Processing*, 2019, Vol.115, No.5, 1–9.

[14] **R. M. Hassan, A. F. Zulrushdi, A. M. Yusoff, N. Kawasaki, and N. A. Hassan**, Comparisons between Conventional and Microwave-Assisted Extraction of Natural Colorant From Mesocarp and Exocarp of Cocus Nucifera. *Journal of Materials Science and Engineering B.*, 2015, Vol.5, No.4, 152-158.

[15] **T. Fuleki and F.J. Francis**, Quantitative methods for anthocyanins, *Journal of food science*, 1968, Vol.33, No.1, 78-89.

The Second Edition of the International Congress of Applied chemistry and Environment
30th-31th October and 01st November 2020, Tunisia

ICACE 2020

Accelerated weathering of recycled nonwovens used as sustainable agrotextiles

Houcine Abidi [a], **Sohel Rana** [b], **Walid Chaouch** [a], **Bechir Azouz** [a], **Mohamed Ben Hassen** [c, a], **Raul Fangueiro** [d]

(a) *Laboratory of Textile Engineering, Higher Institute of Technological Studies, University of Monastir, Hadj Ali Soua, BP 68, Ksar-Hellal 5070, Tunisia*
(b) *Department of Chemical Sciences, School of Applied Sciences, University of Huddersfield, Huddersfield HD1 3DH, UK*
(c) *Department of Industrial Engineering, College of Engineer, Taibah University, 344 Madina zip code 41411, Saudi Arabia*
(d) *Centre for Textile Science and Technology (2C2T), University of Minho, Guimarães, Portugal*

* *E-mail address :* houcine.abidi@gmail.com

ABSTRACT

The removal of agricultural residual plastic films is nowadays a big concern for all environmentalists. Several ecological alternatives were developed for more sustainable products and cleaner production. In this work, the effect of 3 months of exposure under accelerated weathering conditions (UV light, moisture and heat) on the properties of two textile recycled nonwovens used as a sustainable alternative to plastic mulching films, was investigated. Results showed that thermostability and mechanical properties of the clothing textile waste felt (TWF) and cotton waste nonwoven (CWNW) decreased after accelerated weathering. The chemical variation of the composition of CWNW and TWF as well as the degradation rate of natural and synthetic fibers due to the photolysis and hydrolysis caused by accelerated weathering conditions were studied following the FTIR spectroscopy and the fibrous composition variation of the blended TWF structure.

KEYWORDS: accelerated weathering, textile waste, sustainable, mulching, recycling

1. INTRODUCTION

Textile fibers, since their discovery, were mainly used for clothing applications. But with the technological development, these materials became more used in a wide variety of technical applications (Automotive and aeronautics , medical and hygiene applications, protection and defense, civil and agricultural engineering…) and their use keeps growing continuously [1]. In the agricultural field, the use of technical textiles showed a promising development which led to the birth of new textile-based materials called Agrotextiles [2].

The agrotextiles are mainly made from raw materials to ensure good mechanical properties and high weathering resistance. However, with the development of recycling technologies, the use of recycled materials in agrotextiles manufacturing started to emerge for environmental reasons as well as economical interest [3]. In this work, the evaluation of agrotextiles issued from textile waste recycling industry (mono fiber and blended structures) was investigated because of the lack of researches regarding the textile wastes products valorized in agricultural applications. In the textile industry, the end-of-life products could be landfilled, incinerated or recycled. The recycled textiles are mainly used in automotive stuffing, furniture padding, dampening and thermal insulations materials in construction applications [4].

In the agricultural field, the use of recycled textiles as a sustainable geotextile to substitute plastic ones covering the soil to avoid erosion or to control weeds growth was studied. A comparative study between the mechanical properties and the degradation rate of cotton waste film versus the current polyethylene films used for mulching applications were conducted by Jun Luo et al. The variation of agrotextiles properties during the time of use were studied in several research works. The degradation of agrotextiles under outdoor natural weathering conditions [5] or/and laboratory accelerated weathering conditions were investigated [6]. The influence of exposure time to UV light and water spray on the chemical changes and mechanical properties of biodegradable agrotextiles based on natural fibers such as wool were investigated in different works or synthetic ones like polyethylene films.

2. MATERIAL AND METHODS

The Second Edition of the International Congress of Applied chemistry and Environment
30th-31th October and 01st November 2020, Tunisia

ICACE 2020

2.1. Two textile structures were used for this study:

A cotton nonwoven with a density of 200 g/m² and a thickness of 2 mm and a felt composed from a blend of textile fibers with a density of 500 g/m² and 700 g/m² and a thickness of 7 and 10 mm respectively. The consolidation of the felts was done by a needling machine equipped with crown barb needles. A total of 1500 needles/m along 2.5 m working width with a stroke frequency of 350 strokes/min and a penetration needle depth reaching 3 mm were used for the consolidation. Regarding the cotton nonwoven, the structures were strengthened with a needling machine with a stroke frequency of 150 strokes/min and a penetration needle depth 1 mm.

2.2. Accelerated weathering tests

The samples were placed in a QUV accelerated weathering tester (QUV/Spray, Q-Lab) according to ASTM D4355 about Deterioration of Geotextiles by exposure to Light, Moisture and Heat. The samples (10 x 8 cm2) were exposed to alternating cycles of UV light and moisture under elevated temperature to simulate outdoor conditions of sunlight, dew and rain. In this study, each 24-hour weathering cycle consists of 12 hours of UV light (UVA 340 lamp with an irradiance equal to 76 W/m²/nm) at 50ºC and 12 hours of water condensation at 40ºC.

2.3. Tensile strength testing

The dynamometric tests were performed using a Dynamometer HOUNSFIELD H10KSMachine. The samples were subjected to the tensile tests at a constant speed of 25 mm/min, a load range of 50N, an extension range of 50 mm and a gauge length equal to 25 mm.

2.4. Dynamic mechanical analysis

The analysis was performed using a Hitachi 7100 with Dual Cantilever as a measurement mode. The heating rate was fixed at 3ºC/min with a temperature range from 30ºC until 150ºC.

2.5. Differential scanning spectrometry

DSC analysis was performed in a DSC METTLER TOLEDO with a temperature range from 0ºC until 500ºC in nitrogen atmosphere (80 mL/min) and under a constant heating of 10ºC/min. The weight of the sample should be between 5 and 10 mg. The mean values of 3 replicates were used.

2.6. Thermogravimetric Analysis

TGA analyses were performed in a STA Hitachi 7200 with a temperature range from 30ºC until 600ºC in nitrogen atmosphere (200 mL /min) and under a constant heating of 10ºC/min.

2. RESULTS AND DISCUSSIONS

3.1. Tensile strength testing

After 3 months of exposure to artificial weathering conditions of UV light, humidity and heat, the tensile properties of textile waste nonwovens were investigated. The results of tensile strength are shown in Figure 1. The accelerated weathering conditions decreased the mechanical properties of mulching structures with different rates especially after the first month of exposure in both machine direction (warp) and cross direction (weft). In the machine direction, the degradation was higher for the cotton based structure compared to blended structures since the degradation rate of natural fibers is higher than synthetic ones. The CWNW lost more than 65% of tensile strength after the 1st month and more than 85% after 3 months. The TWF showed more resistance to accelerated weathering conditions and lost around 50% of tensile strength after 3 months. The CWNW showed higher tensile values compared to TWF because its structure was reinforced with yarns along the machine direction. After the 1st month, the decrease of tensile strength values was lower, and a plateau was observed for TWF tensile curves.

The Second Edition of the International Congress of Applied chemistry and Environment
30th-31th October and 01st November 2020, Tunisia

ICACE
2020
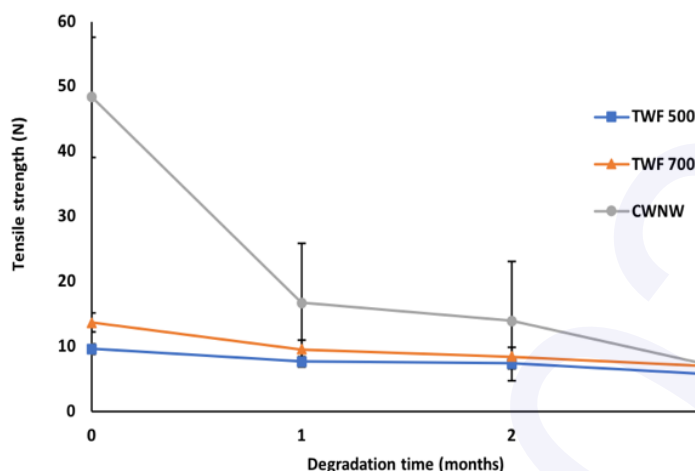
Figure 1: Tensile strength versus the degradation time under accelerated weathering

3.2. Dynamic mechanical analysis (DMA)

The DMA data revealed that the UV radiation, moisture vapor and heat effect decreased the mechanical properties of CWNW and TWF with a higher rate for the former. During the accelerated weathering, the repeated cycles altering UV light and moisture under high temperature degraded the fibers and decreased the mechanical performances of the samples. The absorption of moisture due to the water vaporization wetted the sample and caused the fibers swelling. The second half of the weathering cycle dried the sample and the moisture desorption resulted in fibers contraction. This altering swelling-contraction degraded gradually the fiber and thus the textile structure. The cleavage of chemical bonds and the degradation of the fibrous networks under the action of UV, humidity and heat during the exposure time in the accelerated weathering machine induced a variation in storage modulus E' and damping factor Tan δ. The glass transition temperature was identified from the Tan δ curves showed in Figure 15. The Tg values of weathered TWF decreased with incremental degradation time because of the chain scission of polymers due to photochemical degradation. The combined actions of UV light, moisture and heat decreased the molecular weight of the polymers and then decreased the glass transition temperature of TWF.
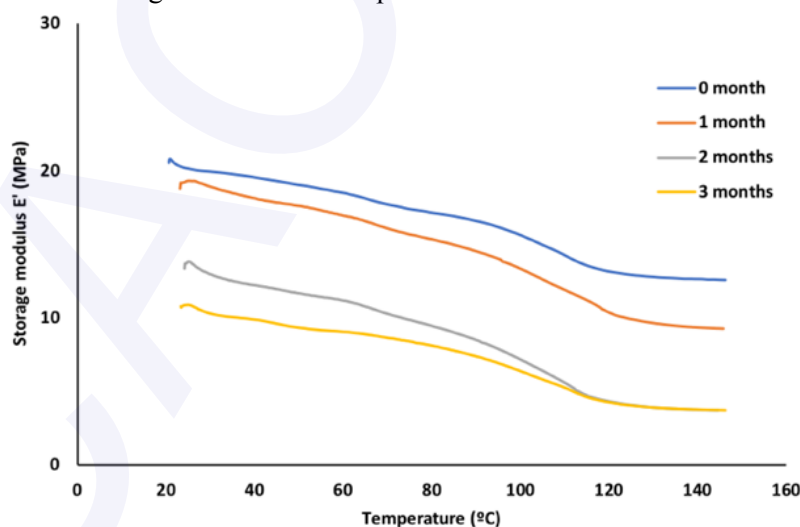
Figure 2: Effect of exposure time to accelerated weathering conditions on storage modulus E' for TWF

3.3. Differential scanning spectrometry (DSC)

The influence of the accelerated weathering conditions of UV light, humidity and heat on the thermal parameters of textile waste structures were revealed by the differential scanning calorimetry DSC. The Tg (glass transition temperature), Tc (crystallization temperature), Tm and Td (respectively melting temperature and decomposition temperature) and the corresponding enthalpies ΔHc (crystallization enthalpy), ΔHm and ΔHd (respectively melting temperature and decomposing enthalpy) were followed during 3 months of exposure time. Results are shown in Table 4. For both structures, the DSC thermograms showed an endothermic peak under 100ºC corresponding to the water desorption. The peak intensity is proportional to the amount of water present in the samples. The endotherm corresponding to the glass transition temperature could be overshadowed by the endotherm resulting from the moisture removal. The simulated weathering conditions induced a decrease of Tg for the TWF during the exposure time reflecting t e decrease in molecular weight and the degradation of macromolecular chains under UV, moisture and heat. The decrease in Tg for the TWF was higher after the first month indicating that the accelerated weathering enhanced the degradation and resulted in a structural reorganization during the exposure time.
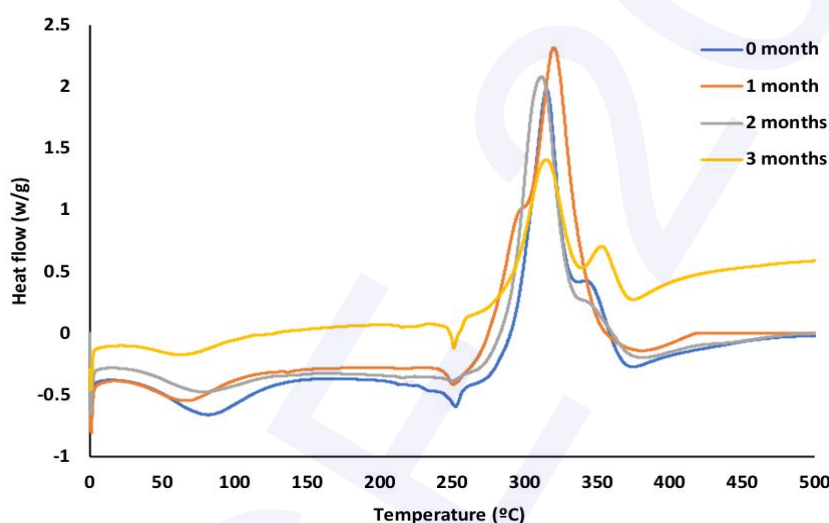
Figure 3: Effect of exposure time to accelerated weathering on the thermal parameters of the TWF revealed by DSC thermograms

3.4. Thermogravimetric analysis (TGA)

The exposure to UV light, moisture and heat decreased the thermal stability of TWF and CWNW. The more the samples are weathered the higher is the degradation rate. The TG curves showed a multi-step decomposition for both samples. The thermal degradation for CWNW exposed to simulated weathering conditions is higher than TWF since the latter contains less natural fibers which degrade faster than synthetic ones. The weight loss increased with the exposure time for TWF and CWNW. After 3 months, the CWNW was completely decomposed at 410ºC as shown in Figure 10 contrary to TWF which showed more resistance to artificial weathering and the final residue was more than 30% at 600ºC after the same exposure time as shown in Figure 4.
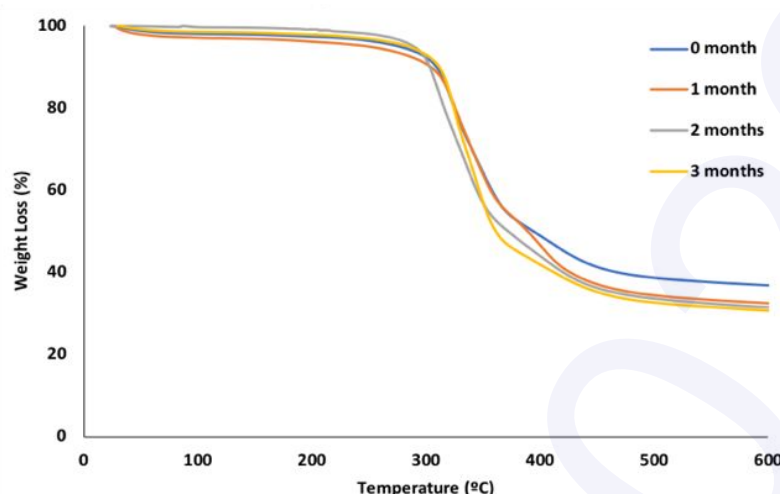
Figure 4: Effect of exposure time to accelerated weathering on the thermogravimetric analysis (TGA) for TWF

3. CONCLUSION

The effect of accelerated weathering conditions on the mechanical and thermal properties of clothing textile waste and cotton spinning waste nonwovens was investigated. The evolution of these properties was studied during 3 months of exposure in a QUV machine. The objective of the study was to understand the mechanism of degradation of TWF and CWNW under the effect of UV light, moisture and heat. The results showed that the accelerated weathering of mulching structures decreased their weight as well as their mechanical properties. The two samples showed a decrease in tensile strength and elongation at break during all the exposure time. The fibrous composition variation of the blended TWF structure gave an idea about the degradation of both natural and synthetic fibers under accelerated weathering and confirmed the faster rate for natural ones. The thermal parameters revealed by DSC analysis and TGA results showed that the accelerated weathering conditions enhanced the thermal degradation of both structures. The exposure under UV light, moisture and heat decreased the thermal stability of TWF and CWNW and the degradation rate is higher for the more weathered samples. The mechanical properties revealed by DMA decreased also and the structures are more brittle, and their mechanical resistance is lower after accelerated weathering.

REFERENCES

[1] **Pritchard M,** *Handbook of Technical Textiles,* 2000

[2] **Palamutcu S,** *Technical Textiles for Agricultural Applications*, 2017

[3] **Leon A.L,** Efficient technical solution for recycling textile materials by manufacturing nonwoven geotextiles, IOP Conference Series Materials Sciences, 2016

[4] **Roznev A,** Recycling in textiles, 2008, HAMK University of Applied Sciences, 22.

[5] **Dierickx W**, Natural weathering of textiles used in agricultural applications, 2004, *Geotext. Geomembranes,* Vol 22, 255–272.

[6] **Gibbs D,** Durability of Polyester Geotextiles Subjected to Australian Outdoor and Accelerated Weathering Durability of Polyester Geotextiles Subjected to Australian Outdoor, 2016

POSTER

COMMUNICATIONS

Treatment of industrial discharge and environmental impacts

The Second Edition of the International Congress of Applied chemistry and Environment
30th-31th October and 01st November 2020, Tunisia

ICACE 2020

Evaluation of intense African dust events and contribution
to PM10 concentration in Tunisia.

Houda Chtioui[*]**, Karim Bouchlaghem, and Mohamed Hichem Gazzah**

Université de Monastir, Faculté des Sciences de Monastir, Laboratoire de Recherche de physique Quantique et Statistique, LR18ES18, Av. de l'Environnement 5000 Monastir, Tunisie;
* *chtiouihouda1974@yahoo.com*
* *bouchlaghemkarim@yahoo.fr*
*hichem.gazzah@fsm.rnu.tn

ABSTRACT :

This study focuses both qualitatively and quantitatively on the assessment of the contribution of the Saharan dust events to the PM10 concentration in Tunisia. We Apply a current method following EC guidelines for the demonstration and subtraction of PM10 excess attributable to natural sources under the Directive 2008/50/EC. The maps and Backtrajectories used in this study have revealed coherence between the African Saharan origins, the dust transport and the intrusion during the intense Saharan dust event.

The calculation of the Saharan dust contribution to the daily PM10 concentration in the considered stations has been obtained in several steps. First, we have determined the daily PM10 concentration measured in each station during the events as well as the regional Background (RB). We have quantified the contribution of Saharan dust (CDij) to PM10 concentration in an ith site During a jth event day by the subtraction of the calculated regional background (RBij) from PM10ij measured daily concentration. This study shows a frequent exceedance of the average daily value of the PM10 concentration. For instance, a value of 1190 μg/m³ is measured in Gabes. This value is reduced to 160 μg / m³ after subtracting the contribution of Saharan dust. These contributions can reach 88% of the daily PM10 measured values. After the elimination of Saharan dust contribution, the daily PM10 concentration has remained higher compared to the limit value.

KEYWORDS : Pm10, Regional Background Concentration, Saharan Dust, Ec Guidelines, Mediterranean.

The Second Edition of the International Congress of Applied chemistry and Environment
30th-31th October and 01st November 2020, Tunisia

ICACE 2020

Preparation of photo catalyst based on Co-ZnO and its application in the photo degradation of dye Rhodamine 6G

Ait Ben Hammou Nabil, Khalef El Hossein, Bouchenafa-saib Naima

Physical chemistry of the interfaces of materials applied to the environment. Technology faculty, Blida 1 University, Soumaa road BP270 Blida, Algeria

aitbenhamounabil@yahoo.fr

ABSTRACT

Water treatment of recalcitrant organic pollutants such as dyes, pharmaceuticals and pesticides remains a major challenge which is ineffective by conventional methods. Heterogeneous photocatalysis has emerged in recent years, and It appears that zinc oxide is the most studied semiconductor in photocalysis applications. With a wide band gap (3.3 eV), ZnO can absorb UV light with the wavelength equal or less than 385 nm. However , it is desirable ZnO should absorb visible light and elevate the photocatalytic activity. For that, it is necessary that the band gap of ZnO has to be narrowed or split into several sub-gaps. In the present work, we have synthesises pure ZnO and cobalt doped ZnO nanoparticles by Co-precipitation method. The photoactivity of the catalysts prepared, assessed through photocatalytic degradation kinetics of Rhodamin 6G, Only one irradiation domain was used, namely near visible (400 nm). The samples were analyzed using a SHIMADZU UV-vis spectrophotometer. During these tests, the temperature was kept constant. The results shows that the photocatalytic degradation of the dye in the visible light in the presence of Co-ZnO is more advanced in comparison with the ZnO undoped. The increase in the activity is mainly attributed to red-shift (wavelength larger) in the absorption spectrum due to doping, the band gap of ZnO doped is passed at 2.8 eV. An XRD analysis of the photocatalysts showed the formation of the wurtzite structure phases of the nanoparticles of pure ZnO and doped ZnO. Obtained results allow us to demonstrates a facile single-step route for synthesis of cobalt doped ZnO nanoparticles with showing high visible light photocatalytic activity compared to ZnO, the doping may be considered a breakthrough in large-scale utilization of heterogeneous photo catalysis via visible light for the water and environmental decontamination.

KEYWORDS: Cobalt-doped zinc oxide 1, Visible photocatalyst 2, wurtzite 3, Doping 4.

Binary adsorption of nickel and lead onto clayey organic soil

Mohamed ABDELWAHEB[a];Hatem DHAOUADI[a], Sonia DRIDI-DHAOUADI[a]

[a] University of Monastir, Faculty of Sciences of Monastir, Research Unity of Applied Chemistry and Environment-5000 Monastir, TUNISIA

ABSTRACT

The use of treated wastewater for agricultural soils irrigation is an alternative to the lack of water that affects Tunisia. However, treatment plants rarely takes into account the elimination of heavy metals such as lead and nickel which are very toxic to the environment and especially to surface and groundwater. The competition between those two metal cations is always present, it is thus interesting to make their study together in order to quantify their adsorption capacities compared without competition. The soil used is clayey soil at first and then a soil containing 2.7% of humic acid was prepared by adsorption-desorption experiences of humic acid in clayey soil. The work objectives is to quantify the risk of groundwater pollution in the nickel and lead adsorption with humic acid and in competition mode. The retention isotherms on all cases and the extended Langmuir, Langmuir modified and competitive, extended Freundlich, Redlich Peterson unmodified, Redlich Peterson modified and competitive, extended Sips multi-compounds models were applied. All experimental isotherms have been successfully adjusted using Redlich Peterson modified and competitive (R^2=0.96) expression for the different soil. The amounts of nickel and lead retained by the clayey soil, for an initial pollutant concentration equal to 1 mmol/L, were evaluated at 0.007 and 0.009 mmol /g respectively and with humic acid were evaluated at 0.01mmol/g for both of pollutants. This amount is 0.02 and 0.008 mmol/g for the lead and nickel and 0.006 and 0.008 mmol/g in the same clayey soil with and without humic acid but both of heavy metals are present in the solution.

At least, the nickel presents the greatest risk to contaminate the groundwater in all cases but the humic acid is a good barrier to prevent the water underground of these contaminations.

KEYWORDS: heavy metals, humic acid, competition, soils, adsorption isotherm

Thermochemical calculations to follow the reactions of thermal decomposition of Phosphogypsum

Saloua JEMJAMI

Laboratory of Applied and Environnemental Chemistry
Faculty Of Sciences and Thechniques– BP 577,Km 3, Route de CASA, SETTAT - MOROCCO
University Hassan premier. BP 26000, SETTAT MOROCCO
Email : j.saloua.1@gmail.com / saloua.jemjami@uhp.ac.ma

ABSTRACT

During the last decades, the thermodynamic methods and calculations found several applications in the analysis of the various processes, and the follow-up or the creation of new technologies. The types of application of thermochemical calculations can be summarized as follows:

- Development of the new high-temperature technological processes;
- Optimization of chemical processes, including synthesis of refractory materials and materials of microelectronics;
- Examination of stability of materials at high temperatures and in various middle;
- Investigation of the chemical processes occurring in power-generating facilities, including the nuclear plants;
- Optimization of raw materials use in waste management;
- Study of the emissions of burning products and industrial gases emitted into the atmosphere;
- Development of the processes preventing environmental pollution;
- Investigation of the processes of mineral genesis, formation of planets and stars atmosphere, as well as other geo- and astro-chemical processes.

In this work, we use the thermochemical calculations based on the minimization of the free enthalpy to follow reactions of thermal decomposition of phosphogypsum. The phosphogypsum is one of the most significant industrial solid wastes from the phosphorus chemical industry. It's obtained by the production of phosphoric acid from natural phosphate rock according to the following reaction:

$$Ca_3 (PO_4)_2 + 3 H_2SO_4 + 6 H_2O \ \square\ 2 H_3PO_4 + 3 (CaSO_4.2H_2O) \text{ (phosphogypsum)}.$$

The purpose of our project is to carry out fundamental studies with a view to recovering phosphogypsum by a thermal process. We are used the HSC CHEMISTRY DATABASE to following:

- $\square$ The Thermal decomposition of $CaSO_4$.
- $\square$ The Thermal decomposition of $CaSO_4$ in the presence of a gas mixture CO_2/CO.
- $\square$ The Thermal decomposition of $CaSO_4$ in the presence of a gas mixture CO_2/CO with the addition of Fe_2O_3.

KEYWORDS: thermochemical, thermal, decomposition, phosphogypsum.

Effect of acid treatment and pore size of clay in the CO_2 adsorption capacity

Nesrine Chouikhi [a], Sabrine Besghaier [a], Juan Antonio Cecilia [b], Mohamed Chlendi [a], Enrique Rodriguez Castellon [b] and Mohamed Bagane[a]

(a) *Laboratory of Applied Thermodynamics,* National Engineering School of Gabes, *Rue Omar Ibn Elkhattab, Gabès, 6029, Tunisie, Gabes 6029, Tunisia*

(b) *Departamento de Química Inorgánica, Cristalografía y Mineralogía, Facultad de Ciencias, 29071 Málaga, Spain*

E-mail:chouikhi.nesrine@gmail.com

ABSTRACT

Clays are very important industrial minerals; they have been in use as raw materials for the adsorption of CO_2. The aim of this work is to improve the adsorption capacity of clay by making modification in their structure and to study the effect of pore size in the textural properties and the CO_2 adsorption capacity. A natural clay preparation was made by purifying the crude clay to remove the impurities. Tow values of clay's pore size were studied 40 and 60 μm. An alteration of the natural clay's structure was carried out through its acid activation by sulfuric acid at 35% concentration by mass.The textural properties of the obtained clays were characterized by BET. Finally, a significant increase in the CO_2 adsorption capacity has been shown after activation treatment.

KEYWORDS : clay, CO_2 adsorption, capacity, activation, pore size

The Second Edition of the International Congress of Applied chemistry and Environment
30th-31th October and 01st November 2020, Tunisia

ICACE 2020

Improvement of mineral clay properties with an acid treatment

Sabrine Besghaier [a*], **Nesrine Chouikhi** [a], **Juan Antonio Cecilia** [b], **Mohamed Chlendi** [a], **Enrique Rodriguez Castellon** [b] **and Mohamed Bagane** [a]

(a) University of Gabes, National Engineering School of Gabes, Laboratory of Applied Thermodynamics, Rue Omar Ibn Elkhattab, Gabès, 6029, Tunisie, Gabes 6029, Tunisia.
(b) Universidad de Málaga, Departamento de Química Inorgánica, Cristalografía y Mineralogía, Facultad de Ciencias, 29071 Málaga, Spain
E-mail:sabrine.besghaierr@gmail.com

ABSTRACT:

Clays have been treated and modified by several methods to improve their physicochemical properties. The sulfuric acid treatment is one of the most used methods due to its simple protocol and the low cost of sulfuric acid.

The aim of this work is to present the properties of the studied clay before and after the acid treatment based on some characterization techniques such as Measurement of Specific Surface (BET Method), Mineralogical Analysis (XRD), Infrared Spectroscopy Analysis (FTIR-IR) and a thermogravimetric analysis (ATG).

KEYWORDS: Minerals clays, activation, sulfuric acid

The Second Edition of the International Congress of Applied chemistry and Environment
30th-31th October and 01st November 2020, Tunisia

ICACE 2020

Effects of C/N Ratio on Carbon and Nitrogen removals
in a Hybrid Biological Reactor

Hela Machat[a,b], **Nicolas Roche**[c], **Hatem Dhaouadi**[b]

(a)   Institut Supérieur Agronomique de Chott-Mariem, 4042 Sousse, Tunisia
(b)   Université de Monastir, Faculté des Sciences, Département de Chimie, UR13ES63-Chimie Appliquée et Environnement, Bvd de l'Environnement, 5000 Monastir, Tunisia
(c)   Aix Marseille Univ, CNRS, IRD, INRA, Coll France, CEREGE, BP 80, 13545 Aix-en-Provence, France

machat.hela@gmail.com

ABSTRACT

The objective of this study was to evaluate the effects of C/N ratio on the biological removal of carbon and nitrogen using an Integrated Fixed-film Activated Sludge (IFAS) reactor for nearly half a year. The results showed that the efficiency of organic matter removal was greater than 90% regardless of the value of the C/N ratio. Nitrogen removal was affected by the C/N ratio. Indeed, at a C/N ratio equal to 10, nitrogen removal efficiency was maximum with an average removal of 96.54%, 86.1% for ammonium and total nitrogen, respectively. Under this condition, the nitrification and denitrification rates were very important. Conversely, with a C/N ratio of 4, removal rate dropped significantly. Indeed, the average ammonium and total nitrogen removal were 82% and 53%, respectively.

KEYWORDS: C/N ratio, Integrated fixed-film activated sludge, nitrification, denitrification

.

The Second Edition of the International Congress of Applied chemistry and Environment
30th-31th October and 01st November 2020, Tunisia

ICACE
2020

Gas Hydrate Formation Process for Capture of CO_2 from Natural Gas: Experimental and Modelling Study of the Effect of New Kinetic Promotors

Said Samer[a, b], Saheb Maghsoodloo Babakhani[c], Mohamed Belloum[a] and Jean-Michel Herri[c]

(a)   Laboratory of Materials Chemistry and the Living (LCMVAR), University of Batna 1, 05000 Batna, Algeria
(b)   Health and Safety Institute (HSI), University of Batna 2, Fesdis, 05078 Batna, Algeria
(c)   Mines Saint-Etienne, 42023 Saint-Etienne, France

ABSTRACT

The gas hydrate crystallization process has recently risen as a novel and promising technology for reducing greenhouse effect and obtaining clean energy resources. However, the low hydrate formation rate, low gas selectivity and low gas storage capacity have been proved as the major bottlenecks for its successful application. Using nanoparticles as promotor is a novel technique for the enhancement of gas hydrate formation process. In this article, a batch reactor was used to investigate the effects of Cu and CuO nanoparticles on the enhancement separation of CO_2 from natural gas by means of gas hydrates. The natural gas stream was represented by a mixture of CO_2-CH_4. In the experimental setup, nanofluids of Cu and CuO with particle weight percentages ranging from 0.1 to 0.3 wt % were respectively prepared, CO_2-CH_4 gas mixture was injected in the reactor containing pure water and different prepared nanofluids. The pressure and temperature were maintained at 4.0 MPa and 274.15 K, while the magnetic stirrer speed was set at 350 rpm. The obtained results showed that the nanoparticles of Cu, at the beginning of the process and up to a certain maximum concentration, can enhanced the gas dissolution (up to 24%), improve the gas consumption by crystallization up to 23%, improve the gas capture selectivity up to 29% but these effect becomes negative at the end of process, while the nanoparticles of CuO can improve the gas dissolution up to 40%, increase the gas consumption by crystallization up to 50% and no positive effect was observed on the capture selectivity.

KEYWORDS

Separation, gas hydrates, nanoparticles, kinetic promotor, CO_2.

The Second Edition of the International Congress of Applied chemistry and Environment
30th-31th October and 01st November 2020, Tunisia

ICACE 2020

Experimental investigation of a novel tow stage ESP associated with unipolar charger used for ATEX filtration

Kherbouche Fouad[a] , Berdadi bendaha mourad[b]

(a)   LSTE Laboratory, Université Mustapha STAMBOULI de Mascara, BP 305 mascara-29000
(b)   Université Abdelhamid Ibn BadisMostaganem, Avenue HamadouHossine, Mostaganem 27000

E-mail : kherbouche.fouad@univ-mascara.dz / kherbouche.fouad@gmail.com

ABSTRACT:

Gas explosion is one of the most serious problems in the operation of the electrostatic precipitators (ESPs) which are applied to clean polluted gases, specifically the explosive atmosphere. To reduce the electrostatics hazards we performed in this investigation a novel two stages electrostatic precipitator using a monopolar charger (needle to ring configuration) positioned outside of the main gas flow (10 L/m) in order to ensure the separation from the direct interaction with the polluted gas (ATEX). In order to enhance the collision between the ions and the pollution an external electric field is imposed between the monopolar charger and the grounded electrode also the second stage is added to enhance the collection efficiency. This laboratory scale ESP was studied experimentally for submicron's incense particles with a mean diameter of 0.3 µm. The number of charges per particle has been measured by an electric low-pressure impactor (ELPI) at real time. The particle charging and collection efficiency characteristics of incense particles were quantitatively investigated under different applied negative DC voltage. The ratio of the submicron-sized aerosols was significantly increased with the increase of applied voltage, the collection efficiency reached 99 % under -30kV-DC.

KEYWORDS:MIE, Two stages ESP, Monopolar charger, Collection efficiency, Corona discharge.

The Second Edition of the International Congress of Applied chemistry and Environment
30th-31th October and 01st November 2020, Tunisia

ICACE 2020

Characterizations and valorization of olive mill wastewater by adsorption onto activated carbon.

Bekri Imene [A], Taleb Safia[b], Taleb Zoubida [B], Belfedal Abdelkader[a]

(a) Laboratory of Physical Chemistry of Macromolecules and Biological Interfaces, University of Mascara, Algeria

(b) Laboratory of Materials & Catalysis, University of Sidibel-Abbes

E-mail: imene.bekri@univ-mascara.dz

ABSTRACT :

In the Mediterranean countries, olive oil production is considered as an important economic activity among agro-industrial production, at the same time, the discharge of wastewater from oil mills (OMWW) and the solid effluents (pits) of the olive are often discharged into nature, without any prior treatment. The result is a negative impact on the environment . OMWW and olive stones are collected in a local olive oil mill. Activated carbon is obtained by a physical activation process. This was first characterized by Fourier Transform Infrared Spectroscopy (FTIR). OMWW is also characterized by metric pH, chlorides, sodium, potassium, calcium, conductivity, chemical oxygen demand (COD), turbidity, volatile matter and ash, dry matter, moisture content, suspended solids, floating matter, fat and FTIR spectroscopy. Our results show that OMWW is an extremely polluting acidic effluent. This pollution results from the presence of mineral organic matter. By FTIR spectrophotometer, the OMWW shows many vibration bands, the most interesting being the O-H band indicating the presence of polyphenol compounds. The adsorption rates of the OMWW are 57.4%, 27.5% and 35.85%, after a contact time of 120 min, 105 min and 120 min, for CA NO 3/10, CA NO 4/10 and CA NO 5/10 respectively. The pH after adsorption increases and is found to be equal to the neutral pH. The results of this study illustrate a retention of the liquid effluent (OMWW) by activated carbons with waste from the olive food industry.

Keywords: OMWW, activated carbon, adsorption, kinetics adsorption, FTIR.

Study of acetone flux adsorbed by activated carbon AC35

Noujoud Benkahla[a*], Foued Mhiri[b]

(a)   *Laboratory of Thermal and Energy Systems Studies (LESTE), LR99ES31,Faculty of Sciences of Monastir, 5000 Monastir, Tunisia.*
(b)   *Laboratory of Thermal and Energy Systems Studies (LESTE), LR99ES31, Preparatory Institute for Engineering Studies of Monastir, , Monastir, Tunisia.*

noujoud1369@hotmail.com

ABSTRACT

Air pollution, mainly caused by anthropogenic activities or by natural disasters, resulted in numerous global consequences for environmental level, such as acid rain, depletion of the ozone layer, and increased greenhouse effects. Also this kind of pollution has detrimental effects on the human health and nature too leading to many serious troubles such as anemia, kidney disease, nervous disorders and even can lead to death.

Among the different methods of eliminating pollution present in the solid, liquid or gaseous phases. Mention may be made of membrane filtration, chemical precipitation, ion exchange and adsorption. In recent years, adsorption techniques for air treatment have become more popular in terms of their effectiveness in removing pollutants by porous materials. Activated carbon is by far the most widely used porous material in environmental technology because of the ease with which it allows the removal of organic and inorganic compounds from aqueous and gaseous effluents.

In this context, we have proposed a mathematical model based on the flow of the quantity of matter through a closed surface.

The experimental study of the flow of the amount of acetone adsorbed by a spherical grain of activated carbon AC 35 is in perfect agreement with the adsorption process: adsorption by micropores followed to adsorption by mesopores and then that of macropores and the lateral surface of the grains of activated carbon AC35.

Each isotherm of the flow as a function of the pore radius has an inflection point. Mathematically, this type of curve is described by two equations. One corresponds to adsorption in micropores and mesopores $[r_0 < r \leq r_2]$ and the other corresponds to adsorption by macropores and the lateral surface of the activated carbon grain AC 35 $[r_2 \leq r]$.

There is a good agreement between the mathematical result and the experiment; this implies that, mathematically, the three regions found experimentally on the curve of the flux as a function of the pores radius are reduced to two: adsorption in the micropores and the mesopores (filling volume), multilayer adsorption in macropores and on the lateral surface. These results justify the existence of the two most commonly used models, Dubinin-Astakov (in the case of microporous filling) and BET (in the case of multilayer adsorption).

KEYWORDS: Adsorption, activated carbon AC 35, Acetone, Flow, Interaction potential

Adsorption of lead(II) ions onto activated carbon prepared from prickly pear seeds (after extraction essential oil)

Rimene Dhahri [a,b], Asma Bouzidi[a,c,] Younes Moussaoui[b,d]

(a)   Materials, Environment and Energy Laboratory (UR14ES26), Faculty of Sciences of Gafsa, University of Gafsa, Tunisia.
(b)   Faculty of Sciences of Gafsa, University of Gafsa, Tunisia.
(c)   National Engineering school of Gafsa, University of Gafsa, Tunisia.
(d)   Organic Chemistry Laboratory (LR17ES08), Faculty of Sciences of Sfax, University of Sfax, Tunisia.
E-mail: dhahririmene@gmail.com

ABSTRACT

This study investigates the adsorption capacity of natural and low-cost activated carbon prepared form prickly pear seeds (after extraction essential oil) for the removal of lead (II) ions from aqueous solution.
Batch adsorption experiments were carried out to evaluate the effect of process parameters: solution pH, adsorbent dosage, contact time, initial metal ion concentration of Pb(II) ions removal.
The experimental results indicate that the process is very rapid and the adsorption capacities increased with an increase in the adsorbent dosage. Maximum adsorption occurred at higher pH between 8 and 10. Adsorption kinetics follows the pseudo-second order model instead of pseudo-first-order model, and fits the Langmuir model with $R^2 = 0.985$ suggesting that the adsorption is a monolayer phenomenon. Moreover, the maximum sorption capacities obtained with Langmuir isotherm model are 102 mg/g, which probably occurs on energetically homogeneous sites.

KEYWORDS: Activated carbon, prickly pear seeds, Phosphoric acid, Lead (II).

The Second Edition of the International Congress of Applied chemistry and Environment
30th-31th October and 01st November 2020, Tunisia

ICACE
2020

Comparison of the degradability of three reactive dyes by fenton process

Nour El Houda Slama, Ghazza Masmoudi, Hatem Dhaouadi

Research unit of applied chemistry & environment (URCAE), Faculty of Sciences of Monastir,

Address; Tunisia, Monastir, Avenue of the environment, 5019

E-mail: nhslama@gmail.com

ABSTRACT:

Textile industry is considered as a serious threat to the environment due to the complexity and diversity of the used dyes and chemical additives. The advanced oxidation process is a promising technology for complex wastewater treatment since they are conducted by the production of the highest strong oxidant (OH$\cdot$) which reacts in a non-selective way with all organic groupements until their mineralization. In this study, infrared (IR) spectroscopy was used to identify the functional groups present in the studied reactive dyes (Dark blue, reactive red 293, reactive yellow 145). Fenton reagent (Fe^{2+}/H_2O_2) was then used to oxidize the reactive dyes separately and mixed. The effect of molar ratio [dye]:[Fe^{2+}]:[H_2O_2] on the degradation of these dyes was studied at pH = 3 and normal laboratory atmosphere and temperature. The degradation of dyes was more than 90 % in less than 20 min fenton treatment.

KEYWORDS: Reactive textile dyes, infrared spectroscopy, fenton process, degradation.

Sustainable processes and clean technologies

New CeO_2-TiO_2, WO_3-TiO_2 and WO_3-CeO_2-TiO_2 meso-structured aerogel catalysts for the low temperature NO-SCR by NH_3 in excess O_2

Jihene Arfaoui[a], Abdelhamid Ghorbel[a], Carolina Petitto[b], Gerard Delahay[b]

(a) *Université Tunis El Manar, Laboratoire de Chimie des Matériaux et Catalyse, Département de Chimie, Faculté des Sciences de Tunis, Campus Universitaire Farhat Hached d'El Manar, 2092, Tunis, Tunisia.*
(b) *Institut Charles Gerhardt Montpellier, CNRS/ENSCM/UM, Matériaux Avancés pour la Catalyse et la Santé, 240 avenue du Professeur Emile Jeanbrau, Montpellier, France*

* Corresponding author: E-mail address: jihenar@yahoo.fr

ABSTRACT

Nitrogen oxides (NO_x), emitted from the combustion of fuels in stationary and mobile processes, are among the main atmospheric pollutants that causes a variety of harmful environmental and human heath effects. In order to meet the stringent environmental regulations, research in the field of NO_x abatement has grown significantly in the past two decades. Up to now, the selective catalytic reduction using NH_3 (NH_3-SCR) as reductant is still the most powerful method for NO_x removing from stationary source and V_2O_5-TiO_2 promoted with WO_3 or MoO_3 is reconized as the most commonly used catalyst for this process.

In this work, a new CeO_2-TiO_2, WO_3-TiO_2 and WO_3-CeO_2-TiO_2 meso-structured aerogel catalysts were successfully prepared by the one-step sol gel method associated with the supercritical drying process for the low temperature NO-SCR by NH_3 reaction. The physicochemical properties of the samples, calcined at 500 °C, have been examined by XRD, N_2 adsorption-desorption, H_2-TPR and NH_3-TPD. The results reveal that all the obtained aerogel catalysts are highly crystallized solids developing essentially the diffraction peaks of TiO_2 anatase phase. They are classified as mesoporous materials with a high surface area (70 $<S_{BET}<$106 m^2/g) and large porosity ($0.27<V_{PT}< 0.46$ cm^3/g). It was also shown that the addition of Ce and/or W influences differently the total acidity and the reducibility of aerogel catalysts and clearly affect their activity in the SCR of NO by NH_3 which follow this order: TiO_2 $<WO_3$-TiO_2 < CeO_2-TiO_2< WO_3-CeO_2-TiO_2. This result indicates that cerium species are more active in the low temperature SCR-NO than tungsten ones (NO conversions obtained at 300 °C using CeO_2-TiO_2 and WO_3-TiO_2 are 75 % and 0 %, respectively). On the other hand, it can be suggested that the interaction between Ce and W species play a key role in improving the reactivity of WO_3-CeO_2-TiO_2 catalyst in the SCR of NO, particularly at low temperatures. Interestingly, the NO conversion reaches 85 % at 300 °C and exceed 90 % between 320 and 420 °C over this new aerogel catalyst.

KEYWORDS: Aerogel catalysts, CeO_2, WO_3, TiO_2, Low temperature SCR-NO.

The Second Edition of the International Congress of Applied chemistry and Environment
30th-31th October and 01st November 2020, Tunisia

ICACE 2020

Electrochemical study of a material on a modified electrode

Rakhrour Waffa[a], Selloum Djame [a], Benalia Mokhtar[b]

(a)University of Kasdi Merbah Ouargla

(b)University of Ammar Theliji Laghouat

(a)   email wrakhrour@gmail.com

(b)   email selloumdjamel@gmail.com

(c)   email benalia_mokhtar@yahoo.fr

ABSTRACT

The aim of this work was to present the electrodeposition of metals (Cu, Sn) and the electropolymerization of monomer (aniline) on a semiconductor which is silicon (Si) to increase its electrical conductivity. This electroplating was done using two different electrochemical methods (Cyclic Voltametry and Chronoamperometry) by varying several conditions (concentration, pH and scanning speed). Finally, we characterized our samples by impedance. This study was carried out using a Voltalab PGZ 301 device.

KEYWORLDS: electropolymerization, electrodeposition, modified electrodes, photovoltaic cells.

The Second Edition of the International Congress of Applied chemistry and Environment
30th-31th October and 01st November 2020, Tunisia

ICACE 2020

Preparation of catalysts based on iron oxyhydroxides and zirconium and their application for the degradation of 4-nitrophenol by a heterogeneous Fenton-like process.

Hafsa Loumi[a, b], Faiza Zermane[a,B], Benamar Cheknane[a,B], Naima Bouchenafa[a], Omar Bouras[b]

(a) *Laboratoire de Chimie Physique des Interfaces des Matériaux Appliquées à l'Environnement, Département de Génie des Procédés, Université Blida 1, BP 270, 09000 Blida, Algérie*

(b) *Laboratoire Eau Environnement et Développement Durable ; Département de Génie des Procédés Université Blida 1, BP 270, 09000 Blida, Algérie*

Corresponding author's: hafsaloumi7@gmail.com

ABSTRACT

The present study consists to prepare a series of catalytic grains based on iron oxyhydroxides and zirconium as a precursor. The prepared catalysts are for degradation of the organic pollutant 4-nitrophenol in the presence of H_2O_2 in aqueous media under normal conditions of temperature and pressure. After the preparation by co-precipitation of the several samples of catalysis at different rations supports, different techniques are used to characterize these materials. The crystallinity of the catalytic grains was examined by XRD technique. For morphology, microstructure and surface composition, SEM is used. The catalytic activity of these sample grains has been tested for the oxidation of 4-nitrophenol in the liquid phase. Catalytic tests reveal that the catalytic activity (conversion rates) of the different samples is of about 92.74% with a diameter between 0.4mm<d<1mm after four hours of contact times with The best catalytic grains are those based on $H_{75}Zr_{25}Fe$. In addition, the catalytic activity of the various catalysts is higher in neutral media than in acidic and basic media.

KEYWORDS: Oxyhydroxides, Zirconium, catalyst, Oxidation; 4-nitrophenol.

.

The Second Edition of the International Congress of Applied chemistry and Environment
30th-31th October and 01st November 2020, Tunisia

ICACE 2020

Study of copper based heteropolysalts in the effeciency of synthesis of

5-ethoxycarbonyl-4-phenyl-6-methyl-3,4-dihydropyridin-2(1H)-one

Khiar Chahinaz[a], Mazari Tassadit [a,b]

(a)   Laboratoire de chimie appliqué et du génie chimique (LCAGC), Faculté de chimie, Université Mouloud Mammerie Tizi-Ouzou UMMT),
15000 Tizi-Ouzou, Algérie
(b)   Laboratoire de Chimie du Gaz Naturel, Faculté de Chimie, Université des Sciences et de la Technologie Houari Boumediéne, USTHB,
E-mail:chanez-kh@hotmail.fr

ABSTRACT

The efficiency of various heteropoly compounds as well-known solid acids is investigated for the three-component condensation reaction of an aldehyde, b-ketoester and urea to afford the dihydropyrimidinones (DHPM). Compared to the classical Biginelli reaction conditions, this new method consistently has the advantage of excellent yields and short reaction time[1].In the other hand dihydropyrimidinone (DHPM) have a very important pharmacological properties, such as antiproliferative, antiviral, antitumor, anti-inflammatory, antibacterial, and antitubercular activity [2].

The objective of this study is the use of Kegginheteropolyacid (HPAs) noted $H_3PMo_{12}O_{40}$ and its ammonium salts$H_{3-2x}Cu_xPMo_{12}O_{40}and(NH_4)_{3-2x}Cu_xPMo_{12}O_{40}$ in Biginellicyclocondensation reaction using: benzaldehyde, acetoacetate and urea with ratio (2:2:3) [3]. After synthesis, the prepared catalysts were characterized by: BET surface area, X- ray diffraction, Infra-red spectroscopy and DHPM by FT-IR, ^{1}H and ^{13}C NMR.

The reaction results show that $H_3PMo_{12}O_{40}$ is the best catalyst in our reaction conditions with an excellent yield around 94% which can be explained by significantly higher Brønsted acidity compared to that of traditional mineral catalysts [4]. On the other hand other excellent yields have been obtained in the presence of $Cu_{0.25}H_{2,50}PMo_{12}O_{40}$and $(NH_4)_{3,00}Cu_{0,00}PMo_{12}O_{40}$ 76% and 60% respectively.

In conclusion, using HPAs in Biginelli process can offer high yields of DHPMs, mild reaction conditions, simple experimental procedure and product isolation and recyclability of materials without considerable loss in its activity. Then the protocol should be complementary to the existing methods. It leads not only to economical automation but also to reduces hazardous pollution to achieve environmentally friendly processes which can enter in the field of green chemistry.

KEYWORDS:heteropoly salts, copper, Biginelli reaction, green chemistry.

REFERENCES

[1] **R. Fazaeli, S. Tangestani Nejad, H. Aliyan , M. Moghadam**, **Applied Catalysis A: General**, Vol. 309, 2006, 44–51
[2] **S. Suresh, S. Jagir Arkivoc.** Vol. 66, 2012, 133.
[3] **C. Khiar, T. Mazari. L. Bennini, M. Halouane, M.J. Benito Gonzalez, S. Menad, S. Tezkratt, C. Rabia,** *Green processing and synthesis,* Vol. 6, 2017, 533.
[4] **P.M.Sanjeev, S.G. Gavisiddapa,** Catalysis Communications, Vol. 8, 2007, 279.

The Second Edition of the International Congress of Applied chemistry and Environment
30th-31th October and 01st November 2020, Tunisia

ICACE 2020

Zn based phosphomolybdates salts as an environmentally substitutes to HNO_3 use in the adipic acid production

Dahbia.Amitouche[a,b], Tassadit.Mazari[a,b], Sihem.Mouanni[b], Catherine Roch Marchal[c], Chérifa Rabia[b]

(a)   Laboratoire de Génie chimie et de Chimie Appliquée (LCGA). UMMTO, Tizi Ouzou 15000, Algérie
(b)   Laboratoire de Chimie du Gaz Naturel, Faculté de Chimie, USTHB, BP32, EI-Alia, 16111Bab-Ezzouar, Algérie
(c) ILV-UMR 8180 CNRS, Bâtiment Lavoisier, Université de Versailles-St Quentin-en-Yvelines
78035 Versailles Cedex, France

ABSTRACT:

Zinc-based phosphomolybdates salts of Keggin structure with formula of $H_{3-2x}Zn_xPMo_{12}O_{40}$ and $(NH_4)_{3-2x}Zn_xPMo_{12}O_{40}$ (x:0-1.5) have been prepared, characterized by several physicochemical analysis and tested in the adipic acid (AA) synthesis from the oxidation of cyclohexanone in soft conditions without solvent or phase transfer agent. H_2O_2 (30%) has been used as green oxidant. The catalytic process of the oxidation was examined in situ by multinuclear NMR (^{31}P, ^{95}Mo, ^{17}O). A correlative UV-Visible kinetic study was carried out in parallel. At the end of the reaction, the identification of the products and by-products was accomplished using ^1H, ^{13}C, ^1H-^1H (Cosy) NMR and MS spectroscopies. The obtained results showed the efficiency of this new alternative with about 57% of AA yield in these environmentally conditions.

KEY WORDS: Catalysis; Polyoxometallates, H_2O_2 green oxidant,Adipic acid, Cyclohexanone Oxidation.

The Second Edition of the International Congress of Applied chemistry and Environment
30th-31th October and 01st November 2020, Tunisia

ICACE 2020

New catalytic systems for an eco-friendly coumarins production according to Pechmann condensation protocol

Leila.Bennini[a,b], Tassadit.Mazari[a,d], Chahinez.Khiar[a],Malika Makhloufi[b], Catherine.Marchal.Roch[c], Chérifa Rabia[d]

(a) Laboratoire de Génie chimie et de Chimie Appliquée (LCGA). UMMTO, Tizi Ouzou 15000, Algérie
(b) Laboratoire de Physico-Chimie des Matériaux, LPCM, UMMTO,Tizi Ouzou ,15000, Algérie
(c) 1LV-UMR 8180 CNRS, Bâtiment Lavoisier, UniversitedeVersailles-St Quentin-en-Yvelines 78035 Versailles Cedex, France
(d) Laboratoire de Chimie du Gaz Naturel, Faculté de Chimie, USTHB, BP32, EI-Alia, 16111Bab-Ezzouar, Algérie.

ABSTRACT:
Keggin polyoxometalates (POMs) materials have been widely studied in organic reactions because of their multi-functionality (acid and redox properties), simplicity of synthesis, environmental character and the possibility of their reuse.

In the present work, we report an efficient and green method for the synthesis of coumarins via the Pechmann condensation protocol catalyzed for the first time by $H_{3-2x}FeyPMo_{12}O_{40}$under solvent-free conditions.

After synthesis and characterization of the POMs systems, the reaction conditions were optimized. The effect of several reaction parameters on the yield of coumarins was studied such as: temperature and reaction time, reagent ratio, catalyst composition and weight, reduction and hydration level of the POMs and others.

Compared to classical Pechmann reaction conditions, the present method has the advantage to give very good yields (71-87%) with a short reaction time (30min) and a low temperature (80°C), without the use of solvent or other auxiliary.

In the end, the "green" or environmental aspect of this study was highlighted by the realization of the reaction heptagrams and tetragrams according to Xavier Battaille's model.

 KEY WORDS: Coumarin, POMs, Green Chemistry, Catalysis, Pechmann

The Second Edition of the International Congress of Applied chemistry and Environment
30th-31th October and 01st November 2020, Tunisia

ICACE 2020

Controlled release study of a water-soluble drug from microspheres as drug carriers

Boumediene Fatima Zohra[a], **Faiza Debab**[a] , **Meryem Mouffok**[2], ,**Haouaria Merine**[a]

(a) Physical and Organic Macromolecular Chemistry Laboratory (LCOPM), Faculty of Exact Sciences, Djillali Liabes University of Sidi Bel-Abbes, Algeria.
(b) Department of Chemistry, Faculty of Materials Sciences, Ibn Khaldoun University of Tiaret, Algeria.

ABSTRACT:
The aim of the present study is the preparation of 2-aminobenzothiazole-loaded microspheres based on cellulose derivatives for controlled and prolonged release. Micro-encapsulation by simple emulsion (O/W) solvent evaporation method was carried out to prepare these formulations using two cellulose derivatives as matrices: ethylcellulose (EC) and cellulose acetate butyrate (CAB). The optimization of the experimental parameters such as the polymer/solvent ratio, the matrix type, stirring speed and the number of blades was studied to get high encapsulation efficiency of drug. The effect of the selected parameters on microsphere characteristics, as well as the release rate was investigated. SEM images show that obtained microparticles are spherical in shape. The effective entrapment of 2-amino-benzothiazole (2-ABZT) in the microspheres was confirmed by FTIR spectroscopy and XRD diffraction. The encapsulation efficiency was improved when the polymer concentration increased reaching 89%. We have obtained microspheres in the range of 61-278 µm with EC by varying process conditions and closed to 113µmwith CAB. The *in vitro*release kinetics of the cation of 2-ABZT were established at 37°C in simulated gastric medium pH 1.2 and the obtained data were analyzed according to Fick's law. The results showed that the surface morphology and the encapsulation efficiency of the microspheres depended strongly on the polymer/solvent ratio and the release rate can be controlled by adjusting the process conditions.

KEYWORDS: Microencapsulation;Solvent Evaporation Method; Process Parameters; Drug Release;

.

The Second Edition of the International Congress of Applied chemistry and Environment
30th-31th October and 01st November 2020, Tunisia

ICACE 2020

Fluorescence quantum yield of natural dye extracted from tunisien plant

Nourhéne Slama[a], **Manel Ben Ticha**[a,b], **Badreddine Smiri**[c], **Ritha Mghaieth**[c], **Hatem Dhaouadi**[a]

(a) Research Unit of Applied Chemistry and Environment, Faculty of Sciences of Monastir, 5000 Monastir, Tunisia.

(b) National School of Engineers of Monastir, 5000 Monastir, Tunisia, 5019 *Monastir, Tunisia.*

(c) *Laboratory of Micro-Optoelectrics and Nanostructures,Faculty of Sciences of Monastir, 5000 Monastir, Tunisia.*

ABSTRACT

In this study, we managed to extract a natural dye from the bark of *Juglans regia L*. The extraction technique was assisted by microwave at a concentration of 5g / L, a power of 850W, a pH equal to 5 and an extraction time equal to 4 min. Following the application of the dye extract on an acrylic textile support, it was discovered that our dye has a fluorescent appearance. Afterwards, the evaluation of the dye quality was carried out by the measurement of the dye coloring force (K / S) and by measuring the intensity of PL of acrylic fabrics dyed in the microwave at a power equal to 350W and a duration of 3min with the extract already prepared. After studying the effect of certain factors (pH, power, concentration and duration of dyeing) on the dyeing process, Subsequently we optimized this process thanks to the Surface Response Method.

The evaluation of the results was based on the measurement of the intensity of PL and the measurement of the K / S color strength of the dyed textile substrates with these extracts.

As a result of the strength control method, good washing fastness, acceptable friction and light fastness have been noted. This allows us to deduce that our optimal extract is a promising source of natural dye. The antioxidant activity of the extract was also measured with DPPH method. The results showed that the phenolic antioxidants from the extract exhibited very strong radical scavenging effect and antioxidant power.

KEYWORDS: extraction, microwave, natural dyes, optimisation, fluorescent.

.

Green synthesis of α-aminophosphonates from α-amino acids esters under microwave irradiations

Sara Boughaba[a], Zineb Aouf,[a] Nour-Eddine Aouf[a]

(a)   Laboratory of Applied Organic Chemistry, Bioorganic Chemistry Group, Department of Chemistry, Faculty of Sciences, Badji Mokhtar-Annaba University, Box 12, 23000 Annaba, Algeria.

E-mail : saraboughaba92@yahoo.fr

ABSTRACT

Recently, the α-aminophosphonates have received considerable attention in organic and medicinal chemistry because of their structural resemblance with α-amino acids. They are used as antitumor agents, antivirals, anti-inflammatory and antibiotics. As a result, a number of procedures have been developed for their synthesis. However, many of these methods suffer from some disadvantages such as long reaction times, environmental pollution caused by utilization of organic solvents and expensive catalyst.
Microwave irradiations offers a cleaner and easier pathway compared to conventional methods, it has several advantages such as high temperature homogeneity, instantaneous and rapid heating, allowing the progress of reactions without solvent with a maximal efficiency.

In this context, an efficient and eco-friendly protocol has been described for the synthesis of α-aminophosphonates via one pot reaction between amino acids esters, various aromatic aldehydes and triethylphosphite under microwave irradiations and solvent-free conditions, the corresponding α-aminophosphonates were formed in good yields. This method offers advantages such as simplicity workup with the green aspects by avoiding expensive catalysts and toxic solvents, good yields, short reaction times.
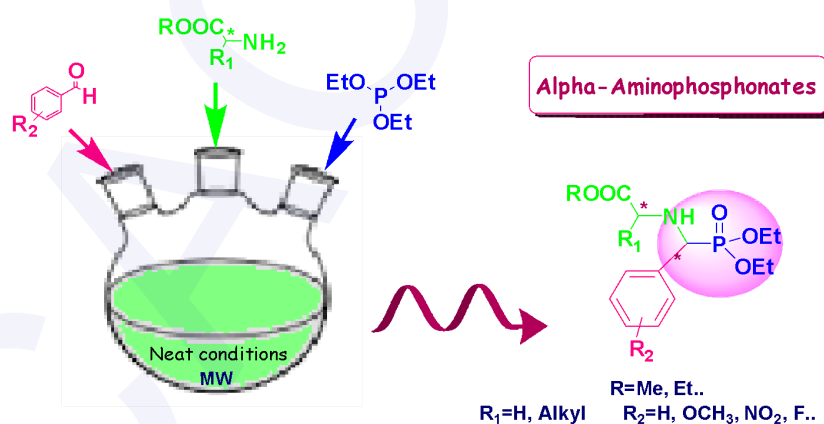
KEYWORDS: green Chemistry, amino acids esters, α-aminophosphonates, microwave irradiations.

The Second Edition of the International Congress of Applied chemistry and Environment
30th-31th October and 01st November 2020, Tunisia

ICACE 2020

Effects of microorganisms on materials and the environment

Hannachi Mohamed Tahar[a, b], Bradji Mohamed[a, b]

(a) Laboratory of environment, University Larbi Tébessi-Tébessa,12000, Algeria,
(b) Laboratory, University Larbi Tébessi-Tébessa,12000, Algeria,

E-mail: Mohamedtah334@gmail.com

ABSTRACT

The microorganisms have been identified like one vector of the dissemination of the metallic pollutants in soils and promote the degradation of most of the materials in their natural environment, including metallic materials. The experiences of simultaneous transfer of metals and bacterial colloids showed an affinity more important of metals for the bio-colloidal fraction than for the porous environment coming with an acceleration of their transfer until an advanced factor. Thesis processes can be ominous or quoted its industrial heart the economic stake ace heart the pollution of soils heart conditions geo-chemical of the middle and one speaks of the environment and health.

KEYWORDS: Bacteria, Biofilm, Corrosion, Degradation, Sulphato Reducing (BSR).

.

Viscosity of Imidazolium-based Ionic Liquids at Different Temperatures: Cation and Anion Effects

Affaf Djihed Boualem [a,], **Ali Mustapha Benkouider** [a,], **Ahmed Yahiaoui** [a,], **Aicha Hachemaoui** [a]

Laboratory, Laboratoire de la chimie ORGANIQUE, macromoleculaire et matériaux fonctionnels-

University of Mustapha Stambouli of Mascara Algeria

E-mail: affaf04blm@gmail.com

ABSTRACT:

According to the common definition, ionic liquids (ILs) are organic salts where the metling temperature is low then 100 ºC. ILs are a prospective replacements for organic solvents in sustainable processes of chemical industry [1] and electrochemistry [2].

Group contribution methods for the estimation of liquid viscosity usually use some variation of temperature dependence proposed by de Guzman known as the Andrade type equation
Based on experimental viscosity data collected from the literature and using temperature data obtained from a predictive method previously mentioned and proposed by the authors, a higher order group contribution is proposed to predict viscosity of imidazolium based ILs including tetrafluoroborate (BF_4), hexafluorophosphate(PF_6), chloride (Cl), bis(trifluoromethanesulfonyl)amide (Tf_2N) anions covering wide ranges of temperatures 273.15 K to 438.15 K and viscosity 0.0159 Pa.S to 2.7 Pa.S.
A good agreement was shown between the calculated viscosities and experimental literature data.
For about 6000 data points of 400 ILs studied the average deviation and a square correlation coefficient (R^2) were 3.02%, 0.82 respectively. The database used to build the new model is semi-randomly divided into the training set (80% of the whole dataset) and the test set (20% of the whole dataset). Training dataset was used during training process of model while the test dataset is used to test the predictive capability and reliability of the developed model The group contribution method developed here can be used to calculate the viscosity of new ionic liquids in wide ranges of temperatures at atmospheric pressure and, as data for new groups of cations and anions became available.

KEYWORDS: Ionic Liquid, Anion, Cation, Viscosity.

References:

[1] **Plechkova, N.; Seddon, K.** Applications of ionic liquids in the chemical industry. *Chemical Society Reviews*, Vol.37, 2008, 123–150.
[2] **Armand, M.; Endres, E.; MacFarlan, D.; Ohno, H.; Scrosati, B.** Ionic-liquid materials for the electrochemical challenges of the future. *Nature Materials,* Vol. 8, 2009, 621–629.

The Second Edition of the International Congress of Applied chemistry and Environment
30th-31th October and 01st November 2020, Tunisia

ICACE 2020

Green sustainable process for the synthesis of daiazaphospholidines

Bouchareb Fouzia[a, b], Diaf Ilhem[b], Berredjem Malika[a], Aouf Nour-eddine[a]

(a)   Laboratory of Applied Organic Chemistry, Synthesis of Biomolecules and Molecular Modelling Group, Sciences Faculty, Chemistry Department, Badji-Mokhtar - Annaba University, Box 12, 23000 Annaba, Algeria.
(b) Chemistry Department. Sciences & Technologie Faculty, Chadli Bendjedid - EL Tarf University, Box: 73, El Tarf 36000 Algeria.

E-mail:boucharebfouzia@yahoo.fr

ABSTRACT

The traditional notion of yield is no longer sufficient to assess the efficiency of chemical processes. Trying to implement lucrative chemistry requires introducing new concepts that aim to reduce or eliminate the source of hazardous substances, the use of renewable raw materials, and greater energy efficiency of products. With the awareness of the environmental impact of human activities and the emergence of the concept of sustainable development, chemists strive to put principles into practice by developing methods aimed at minimizing chance during syntheses, and have control over reactivity in order to avoid the production of undesirable compounds and thus limit the quantities of waste. This turnaround finds its origin in Green Chemistry.

The objective of this work is in this contribution; our group consists in favoring solvents which are less harmful to health and the environment. Better yet, use water as a solvent and also promote selective catalytic systems.

In this work, we thought it would be interesting to develop an original method by using ultrasound for the condensation of bis phosphoramidate and dibromoethane in order to prepare new Diazaphospholidines in one step.

KEYWORDS: Green Chemistry, Ultrasound, Diazaphospholidines, Phosphoramidates, phenyl phosphonic dichloride.

Management and valorization of bio-ressources and industrial waste

Co –composting of date palm wastes and poultry manure

Fathia Madi[a] ,Ridha Hachicha[a] ,Mansour Haddad[b]

(a)Laboratory of Enzymatic Engineering and Microbiology, National Engineering School of Sfax,B.P.1173-3038 ,Sfax,Tunisia
(b) Laboratory of Arid Lands and Oasiann Cropping. Arid Regions Institute of Gabes-Tunisia
Email :madifathia@hotmail.fr

ABSTARCT

The date palm Phoenix dactylifera generates massive quantities of wastes such as leaves and rachis which constitute a source of pollution and a refuge for insects, in parallel in arid regions the problems of deterioration in soil fertility and organic matter deficiency are so expressed. Composting seems to be a very promising ecological and biological method for the valorization of palm wastes and the production of a soil amendment. This work deals with the co-composting of palm waste with poultry manure with a well-defined proportion. Thus, during this process, which lasted 170 days, a physico-chemical parameters (temperature, pH, electrical conductivity, organic matter, total organic carbon, total nitrogen) and biological parameters (respirometric test , germination test) are studied. The produced compost was applied for barley cultivation and its effectiveness was evaluated by biometric parameters (aerial seedling height, stem diameter) of barley plant in comparison with soil (control) and a compost of palm waste and goat manure. The results of physico-chemical and biological analysis showed a decrease in organic matter and C/N ratio during composting processes from 83.15% to 49.77% and from 34.35% to 13.95% respectively. The compost obtained has a germination rate of 85.7% reflecting its non-phytotoxicity. Moreover the values recorded for biometric parameters of barely plant shows that the produced compost is an efficient amendment for soil.

KEYWORDS: palm date wastes, poultry manure, valorization, compost, barely plant

Optimization of preparation conditions of prickly pear seed cake derived activated carbon using experimental design approach and its application for Cadmium removal

Rimene Dhahri [a,b], Asma Bouzidi[a,c,] Younes Moussaoui[b,d]

(a)   Materials, Environment and Energy Laboratory (UR14ES26), Faculty of Sciences of Gafsa, University of Gafsa, Tunisia.
(b)   Faculty of Sciences of Gafsa, University of Gafsa, Tunisia.
(c)   National Engineering school of Gafsa, University of Gafsa, Tunisia.
(d)   Organic Chemistry Laboratory (LR17ES08), Faculty of Sciences of Sfax, University of Sfax, Tunisia.
E-mail: dhahririmene@gmail.com

ABSTRACT

This study evaluates the use of prickly pear seed cake, a by-product of prickly pear seed oil extraction, as a new precursor for producing activated carbon by phosphoric acid activation, and their ability for Lead removal from aqueous solution. Factors influencing the activation process, such as carbonization temperature (A), activation temperature (B), activation time (C) and impregnation ratio (D), were studied. Moreover, a full factorial experimental design at two levels (2^4) was developed to reduce the number of experiments and reach optimal preparation conditions for the removal of Lead ions from aqueous solutions. Design Expert 11.1.2.0 Trial software was used for generating the statistical experimental design and analyzing the observed data.

According to the ANOVA, the most significant effects for the adsorption of lead, were impregnation ratio (B), activation time (D) and the interaction between them (BD) (Eq. (1)).

$$Pb = +106.63+17.01 \times B -7.74 \times D -5.67 \times BD \qquad (1)$$

Therefore, the adsorption of lead capacity increased with an increase in the impregnation ratio and decreased with decreasing of activation time.

Thus, the interaction between them (BD) presented a negative impact on the adsorption of lead response.

At a carbonization temperature of 600°C, a mass activation ratio of 2:1 (gH_3PO_4/g_{carbon}), an activation temperature of 400°C, and an activation time of 1 h, the optimal response corresponded to the maximum adsorption of Pb (II) 158.40 mg/g by the obtained activated carbon. The correlation between the theoretical and experimental response calculated by the model showed that the experimental data were in agreement with the data predicted by the model.

KEYWORDS: Activated carbon, prickly pear seeds, experimental design, Lead (II).

Valorization of prickly pear seed waste as precursor for the production of activated carbons

Nourhen Hsini[a], Hatem Dhaouadi[a], Niklas Hedin[b], Sonia Dridi-Dhaouadi[a,c]

(a) Research Unity of Applied Chemistry and Environment, University of Monastir, Faculty of Sciences of Monastir, 5000 Monastir, TUNISIA.

(b) Department of Materials and Environmental Chemistry-Arrhenius Laboratory, Stockholm University, SE-106 91 Stockholm Sweden.

(c) University of Monastir, Preparatory Institute for Engineering Studies, -5000 Monastir, TUNISIA.

E-mail: hcini.nourhen2016@gmail.com

ABSTRACT

New activated carbons were prepared by H_3PO_4 activation of prickly pear seed (PPS) waste collected from the Tunisian agro-food industry. Conditions for the synthesis of the activated carbons such as the impregnation ratio ImRa (0.5–2), dwell temperature (400–800 °C) and time (30–60 min) were optimized using experimental design and response surface modeling (RSM). The methylene bleu essay (MB), iodine number (I_2) and the BET surface area (S_{BET}) were measured and used as design responses. With respect to these responses, PAC400 (555 $m^2.g^{-1}$) and PAC800 (1270 $m^2.g^{-1}$) were the optimized activated carbons, which were achieved with ImRa of 1.5 and activation time of 60 min at temperatures of 400–800°C. These activated carbons were characterized with physicochemical methods including pHpzc, Boehm titration, scanning electron microscopy, Infra-Red spectroscopy, Raman spectroscopy and N_2 and CO_2 adsorption/desorption analyses.

This work shows that the low cost PPS waste could be efficiently valorized for the production of activated carbons with high porosity.

KEYWORDS: prickly pear seed waste, activated carbons, H_3PO_4 activation

.

Functional morphology, physico-chemical and thermal investigations of *Opuntia* (Cactaceae)

Faten Mannai[a], Younes Moussaoui[b, c]

(a) Material, Environment and Energy Laboratory (UR14ES26), Faculty of Science of Gafsa, Tunisia
(b) Organic Chemistry Laboratory (LR17ES08), Faculty of Sciences of Sfax, Tunisia
(c) Faculty of Sciences of Gafsa, University of Gafsa, Tunisia
E-mail: mannai_faten@yahoo.com

ABSTRACT

The present study has been carried out to understand more fully the structural, chemical and thermal effects of *Opuntia*(Cactaceae) cladodes and to help in evaluating other potential uses of this byproduct. The functional anatomy studies of fresh Opuntia cladode wereevaluated by light microscopy. The obtained micrographs show that fresh cladode formed by a thick hard skin, central core and multilayers of cells with heavily thickened cells containing green plastids, mucilage and calcium oxalates. The chemical evaluation of dried cladode (DC) was studied and results show the high content of polysaccharides; it has been conceder as renewble and suitable source of polysaccharides. The crystallinity and calcium compounds of DC were analyzed by X-ray diffraction. Thermal resistance of DC was controlled by thermogravimetric analyses under nitrogen and oxidative atmospheres. The obtained XRD results show that DC having an importante critalline region and diffrents natural calcium based-crystals. TGA results prove thatDChaving an enhanced thermal resistance under nitrogen atmosphere.

KEYWORDS: Opuntia, renewable, polysaccharides, calcium oxalates.

.

Identification and valorization of natural substances

The Second Edition of the International Congress of Applied chemistry and Environment
30th-31th October and 01st November 2020, Tunisia

ICACE 2020

Extraction and analysis of phenolic acids belonging to derivatives of hydroxybenzoic acids and hydroxycinnamic acids by PLS-IRTF-ATR in plant extracts

Nachida Bensemmane[a]*, Naima Bouzidi[a], Yasmina Daghbouche[a], Mohamed El Hattab[a]

(a)*University Blida 1, Laboratory of Natural Products Chemistry and of Biomolecules, Faculty of science*
P.O. Box 270 - Blida, Algeria

*Email: joey200@hotmail.fr

ABSTRACT

Our study contributes to the realization and development of a PLS-FTIR-ATR multicomponent calibration method for the quantification and simultaneous determination of phenolic derivatives in plant extracts by PLS-FTIR.

Hydroxybenzoic and hydroxycinnamic acids are present in almost all spices. In addition, their role as natural antioxidants is of interest for the prevention and treatment of cancer, inflammatory and cardiovascular diseases.

To verify the effect of the component of the multivariate calibration matrix on the determination of phenolic acids in plants, a strategy was considered to build the calibration models namely; three hydroxybenzoic derivatives (salicylic acid, p-hydroxybenzoic acid and vanillic acid) were used at two levels of concentration. This study will make it possible to correctly choose the component of the matrix that can represent the class of phenolic acids. Various optimization parameters were studied during the modeling: the optimization ranges, the option of spectral pretreatment, the spectral regions and the ranks of the model. We also performed quantification and simultaneous determination of phenolic acid compounds in plant extracts namely; oregano, star anise, cinnamon of China, composed of p-coumaric acid, p-hydroxybenzoic acid and *trans*-cinnamic acid respectively, by PLS-IRTF-ATR using different models optimized by internal calibration.

The results of the calibration revealed that the PLS-IRTF-ATR models of the two matrices considered were adequate for the simultaneous determination of phenolic acids by providing analytical errors RMSECV and RMSEE less than 0.1 with good coefficients of determination, respectively, of $R^2 > 99.52$ and $R^2 > 99.71$. The results of the PLS-IRTF-ATR internal calibration of the plant extracts show that all the models are validated by taking into consideration the concentration range of each standard established during the calibration.

KEYWORDS: Multi-component calibration, PLS-IRTF-ATR, phenolic acids, plant extracts, hydroxybenzoic and hydroxycinnamic acid derivatives.

The Second Edition of the International Congress of Applied chemistry and Environment
30th-31th October and 01st November 2020, Tunisia

ICACE 2020

Investigation of green corrosion inhibitor based on *Aloe vera (L.) Burm*. F. for the protection of bronze B66 in 3% NaCl

Bouchra Benzidia[a], Najat Hajjaji[a], Abdellah Srhiri[b]

(a)   *Laboratory of Materials, electrochemistry and Environment (LMEE), Department of Chemistry,Faculty of Science, Ibn Tofail University, BP 133, 14000, Kenitra, Morocco.*
(b)   *Servichim Sarl, 101 Rue Maamoura, n. 10 Kenitra, Morocco.*
E-mail: n_hajjaji@yahoo.fr

ABSTRACT:
The objective of this work is the development of a new green inhibitor extracted from *Aloe vera* (L.) *Burm*. F. (syn. *Aloe barbadensis* Mill.) for the corrosion inhibition of bronze B66 in a neutral chloride environment (3% NaCl). The tannins extract was obtained from the green rind of *Aloe vera* by maceration process method. The major compound of the TAV is linolenic acid (16.59%). The study of the tannins extract from *Aloe vera* (TAV) was carried out by coupling gravimetric and electrochemical (stationary and transitory) methods, namely the plot of the polarization curves and electrochemical impedance diagrams. Surface analysis of bronze samples was performed using an SEM (scanning electron microscope) coupled to EDS (energy dispersive X-ray spectroscopy), which helped to highlight the protective effect of the TAV studied. The experimental results obtained allowed to note that the inhibition efficiency reaches 89% at 150 ppm of TAV in 3% NaCl. This inhibitor acts by modifying the mechanism of the processes involved at the interface Bronze 3% NaCl.

KEYWORDS: *Aloe vera*, Bronze B66, Corrosion inhibition, TAV, 3% NaCl.

Effect of extraction technique on phenolic compounds and antioxidant properties of green hull *Pistacia vera L.*

Manel Elakremi[a,c,*], **Leyre Sillero**[b], **Lazher Ayed**[d], **Jalel Labidi**[b], **Younes Moussaoui**[a,c]

(a)   Organic Chemistry Laboratory (LR17ES08), Faculty of Sciences of Sfax, University of Sfax, Tunisia.
(b)   Department of Chemical and Environmental Engineering, Biorefinery Processes Research Group, University of the Basque Country, Spain
(c)   Faculty of Sciences of Gafsa, University of Gafsa, Tunisia.
(d)   National School of Engineers of Gafsa, University of Gafsa, Tunisia.
*Email: manel.elakremi@yahoo.com

ABSTRACT

Pistacia vera L. (pistachio) belongs to the Anacardiaceae family. The production of pistachio in Tunisia generates a large amount of potentially valuable wastes such as green hull. The biomass from plants constitute an important source of biologically active secondary metabolites such as phenolic derivatives, flavonoids and terpenes... The isolation of new potentially bioactive natural products may reduce the use of synthetics molecules in food, pharmaceutical and fragrance industries. The aim of this work was to extract bioactive molecules from *Pistacia vera* geen hull using two techniques of extraction (maceration and ultrasound Bath). The influence of these methods on the extraction yiels was evaluated. The extracts of hull were analyzed in order to determine their total phenolic contents (TPC), total flavonoids content (TFC) as well as their antioxidant activity using DPPH˙ free radical scavenging assay, reducing antioxidant power by FRAP and Trolox Equivalent Antioxidant Capacity (TEAC) using ABTS. The GC-MS and FTIR analysis of the green hull extracts exhibited numerous compounds. The results showed that the ultrasound assisted extraction exhibited the highest yield and the best antioxidant activities.

KEYWORDS: Green hull extracts, phenolic derivatives, antioxidant activities, GC-MS.

.

Valorization of industrial waste from the lime peel - *citrus aurantifolia* - from the Blida region (Algeria) by extracting essential oils

Boudjit Djamila[a], Elhadi Djamel[b] , Announ Mohamed[a]

(a)   *Laboratoire Matériaux et Environnement; Faculté de Technologie, Université de Médéa,* Ain D'Heb, 26001 Médéa, -Algérie
(b)   *Laboratoire d'analyse fonctionnelle des procédés chimiques ; Département De Génie Des Procédés, Faculté De Technologie, Université De Blida,* BP 270 route de Soumâa Blida -Algérie*.*
ndboudjit@gmail.com

ABSTRACT

The use of *citrus peel* is a problem that periodically arouses the interest of industrialists, but it seems that the enthusiasm of researchers is rarely followed by achievements.

The increased demand for essential oils in the food industry, perfumery and pharmacy sector highlights a need to optimize current production processes. As with all industrial processes having to deal with this problem, their improvement is geared towards an increase in the extraction yield, and in the quality of the products obtained.

This study is part of a research program that aims to develop solid waste from industrial units producing juices by extracting essential oils from the peel of lime - *citrus aurantifolia*.

The lime peels - *citrus aurantifolia* were dried in an Excalibur type dehydrator at 35 ° C for 35 hours. After drying, they are cut, crushed and sieved. The sieving provides 7 samples of lime powder with different particle sizes. An 8th sample, called a control, is made from pieces of fresh bark. The extraction of essential oil from these 8 samples is carried out in the laboratory, by microwave assisted hydro-distillation (HDMO) (Clevenger type device mounted on microwave).

When the particles are less than 300 μm in diameter, the yield of essential oil increases proportionally to the particle size, going from 5.04% to 21.84%. Beyond 300 μm in diameter, the efficiency of HE is inversely proportional to the size of the particles and it goes from 21.84% to 2.52%. On the other hand, the results obtained by measuring the physicochemical properties of the essential oils of the lime peel, show that the size of the particles has no influence on the quality of the essential oils extracted.

KEYWORDS: *Citrus*; Lime -*citrus aurantifolia*; Essential oil; Hydrodistillation; Granulometry.

The Second Edition of the International Congress of Applied chemistry and Environment
30th-31th October and 01st November 2020, Tunisia

ICACE 2020

Antioxidant power and bioactive effect of (*Rosmarinus officinalis* L.) obtained with non-conventional extraction methods

Nedra Dhouibi[a], Concetta Maria Messina[b,c], Rosaria Arena[b,c], Simona Manuguerra[b,c], Maria Morghese[b,c], Hatem Dhaouadi[a]

(a)   *Université de Monastir, Faculté des Sciences, Département de Chimie, UR13ES63-Chimie Appliquée et Environnement, Bvd de l'Environnement, 5000 Monastir, Tunisie*
(b)   *Università degli Studi di Palermo, Dipartimento di Scienze della Terra e del Mare DiSTeM, Laboratorio di Biochimica Marina ed Ecotossicologia, Via G. Barlotta 4, 91100 Trapani, Italy*
(c)   *Consorzio Universitario della Provincia di Trapani, Istituto di Biologia marina, Via G. Barlotta 4, 91100*
E-mail: nedra.dhouibi@yahoo

ABSTRACT

Rosemary (*Rosmarinus officinalis* L.) is a xeromorphic plant belonging to the family of Lamiaceae. It grows spontaneously on mountains, cliffs and stony places, near the sea, particularly in the Mediterranean basin and is widespread in Africa, Europe and Asia. This aromatic plant is consumed since antiquity and sought for its antioxidant and biological virtues. The high level of phenolic compounds justifies its remarkable antioxidant capacity. The predominant antioxidants are phenolic diterpenes (carnosol, rosmanol, rosmadiol, methyl carnosate), phenolic acids (carnosic acid, rosmarinic acid and hydroxycinnamic acid) and flavonoids. In this study, we investigated the antioxidant properties of four extracts of Tunisian rosemary obtained with non-conventional extraction techniques (i.e. sonication and supercritical extraction) under different operating conditions. The antioxidant abilities were assessed through *in vitro* assays including total phenolic content (TPC), free radical scavenging and ferric ion reducing power assays. TPC of the four rosemary extracts has been evaluated, the best amount of phenolic compounds 85.27 mg GAE/g extract was recorded in ultrasonic extract (UE), the DPPH scavenging test was determined and UE exhibited the lowest $IC_{50} = 0.14$ mg/mL. Similiar to the previous antioxidant test, the lowest $EC_{50} = 0.94$ mg/mL was also registered for UE. As the UE presented the best antioxidant abilities in vitro, it was selected for the test of antioxidant activity in HS68 human skin fibroblast cell line. The evaluation of antioxidant activity of ultrasonic extract in these cells has been carried out with 0.16 µg/mL after the induction of oxidative stress with hydrogen peroxide. The results determined by the MTT test showed a strong protective effect against ROS similar to that of natural (GA) and synthetic (NAC) antioxidants for the cells pretreated with rosemary UE.

KEYWORDS: Rosemary, antioxidant, sonication, supercritical extraction.

.

The Second Edition of the International Congress of Applied chemistry and Environment
30th-31th October and 01st November 2020, Tunisia

ICACE 2020

Phytochemical study of *Dittrchia graveolens* essential oil and biological evaluation

Nawres Gharred[a], **Nadir Bettache**[b], **Alain Morere**[b], **Chantal Menut**[b], **Sonia Dridi-Dhaouadi***[,a]

(a) Research Unit of Applied Chemistry and environment 13ES63, Faculty of Sciences, Avenue de l'environnement, 5019 Monastir –Tunisie.
(b) Glyco anad Nano Vectors for Therapeutic Targeting Team, IBMM, Faculty of pharmacy, 15 Avenue Charles Flahault, PO Box 14491, 34093 Montpellier, France
* E-mail address : sonia.dridi@ipeim.u-monastir.tn

ABSTRACT

The objective of this work was to determine the chemical composition of the essential oil extracted by hydrodistillation from tunisian *Dittrichia graveolens* plant and evaluate its antioxidant and cytotoxic effects. Thirty-five compounds of the *Dittrichia graveolens* essential oil were identified by GC/MS. The main of these compounds are sesquiterpenes and monoterpenes with yields of 32,63 and 39,03% respectively. The volatile extract was evaluated for its antioxidant effect by the DPPH and ORAC tests which revealed a good capacity to inhibit the decrease of fluorescein fluorescence (20 mg EGA/g of extract) but a weak anti-radical effect. On the other hand, the essential oil was tested for its cytotoxic effects against an hepatocellular carcinoma cell line HepG-2 which revealed a significant toxicity, reaching an IC_{50} equal to 0,15 mg/mL.

KEYWORDS: *Dittrichia graveolens*, essential oil, GC/MS, antioxidant effect, cytotoxic effect

.

The Second Edition of the International Congress of Applied chemistry and Environment
30th-31th October and 01st November 2020, Tunisia

ICACE 2020

Chemical composition and antiviral activity of essential oils
from *Osmunda regalis*

Sihem Bouazzi[a] , Habib Jmii[b] , Ridha El Mokni[c,d,e] , Khaled Faidi[a], Danilo Falconieri[f], Alessandra Piras[f], Hela Jaïdane[b], Silvia Porcedda[f], Saoussen Hammami[a,⋆]

(a) *Research Unit of Applied Chemistry and Environment (UR13ES63), University of Monastir, Faculty of Sciences of Monastir, Tunisia*
(b) *Laboratory of Transmissible Diseases LR99ES27, Faculty of Pharmacy, University of Monastir, Avenue Avicenne, 5000 Monastir, Tunisia*
(c) *Department of Life Sciences, Laboratory of Botany and Plant Ecology, Faculty of Sciences of Bizerta, Jarzouna-7021, Bizerta, University of Carthage, Tunisia*
(d) *Department Pharmaceutical Sciences "A", Laboratory of Botany, Cryptogamy and Plant Biology, Faculty of Pharmacy of Monastir, BP 207, Avenue Avicenna-5000, University of Monastir, Tunisia*
(e) *Department of Silvo-Pastoral Resources, Laboratory of Silvo-Pastoral Resources, Silvo-Pastoral Institute of Tabarka, BP. 345, Tabarka 8110, University of Jendouba, Tunisia*
(f) *Department of Chemical and Geological Science, University of Cagliari, Cittadella Universitaria di Monserrato,, Italy*
Bouazzi-sihem@hotmail.com

ABSTRACT

As a medicinal plant *Osmunda regalis* is endowed of a great source of active ingredients useful to treat some diseases and could be considered of a highly efficient remedy. The chemical composition of the essential oil obtained by hydrodistillation of *O. regalis* aerial parts was characterized for the first time by gas chromatography equipped with flame ionization detector and gas chromatography coupled to mass spectrometry. The main compounds were identified as: hexahydrofarnesyl acetone, 2,4-di-tbutylphenol and phytol. Furthermore, *O. regalis* essential oil was evaluated in vitro for its antiviral activity against Coxsackievirus B4 (CV-B4) on the basis of MTT assay. Thus, the volatile oil, being non-toxic against the tested cell line, exhibited a relevant anti-Coxsckievirus B4 activity (IC_{50} =2.24 ± 0.99) μg/mL. The obtained results suggest that *O. regalis* may constitute a source of potential antiviral agents.

KEYWORDS: *Osmunda regalis*, Essential oil, MTT assay Antiviral activity.

.

The Second Edition of the International Congress of Applied chemistry and Environment
30th-31th October and 01st November 2020, Tunisia

ICACE 2020

.

Green synthesis and characterization of colored clays:
cosmetic applications.

Safa Gamoudi[a,b]**, Amira Amraoui**[a]**, Ezzeddine Srasra**[a]

(a)   Laboratory of Composite Materials and Clay minerals National Center for Research in MaterialsSciences, Borjcedria, Tunisia
(b)   Preparatory Institute for Engineering Studies of Bizerte, Carthage university.
Corresponding author: safagamoudi@gmailcom

ABSTRACT

On the basis of a previous detailed characterization of the Tunisian clay for pharmaceutical and cosmetic applications [1], this Tunisian clay was used to prepare natural colored clays by solid-state reaction. The structural properties, photo- and thermal stability of the resulting samples were characterized by X-ray diffraction (XRD), Fourier transform infrared spectroscopy (FTIR), Differential scanning calorimetry analysis (DSC) and UV-visible spectroscopy. The XRD results of colored clays obtained using solid-state reaction indicated a slight difference and decreased intensity in basal spacing when compared to values obtained from purified clay. FTIR analysis confirmed changes in functional groups and surface properties of purified clay. The bands characteristic of C=O stretching vibrations of ketones, aldehydes, lactones or carboxyl groups and aliphatic C—H stretching vibrations in an aromatic methoxyl group, in methyl and methylene were shown in the spectrum of colored samples. These clays could be broadly used in the cosmetic applications.

KEYWORDS: Green synthesis, clay, flower, cosmetic application.

[1] Gamoudi S. and Srasra E., Characterization of Tunisian clay suitable for pharmaceutical and cosmetic applications, *Applied Clay Sciences*,Vol. 146, 2017, 162-166

TThe Second Edition of the International Congress of Applied chemistry and Environment
30th-31th October and 01st November 2020, Tunisia

ICACE
2020

Chemical composition and insecticidal activity of *Clinopodium nepeta* subsp. *nepeta* essential oil

Haïfa Debbabi[a], Ridha El Mokni[b,c,d], Ikbal Chaieb[e], Filippo Maggi[f], Giovanni Caprioli[f] and Saoussen Hammami[a]

(a) Research Unit 13ES63, Applied Chemistry and Environment, Monastir University, Faculty of Sciences of Monastir, Monastir 5000, University of Monastir, Tunisia
(b) Department of Life Sciences, Laboratory of Botany and Plant Ecology, Faculty of Sciences of Bizerta, Jarzouna-7021, Bizerta, University of Carthage, Tunisia
(c) Department Pharmaceutical Sciences "A", Laboratory of Botany, Cryptogamy and Plant Biology, Faculty of Pharmacy of Monastir, BP 207, Avenue Avicenna-5000, University of Monastir, Tunisia
(d) Department of Silvo-Pastoral Resources, Laboratory of Silvo-Pastoral Resources, Silvo-Pastoral Institute of Tabarka, BP. 345, Tabarka 8110, University of Jendouba, Tunisia
(e) University of Sousse, Regional Centre of Research on Horticulture and Organic Agriculture, 57, Chott Mariem, TN-4042 Sousse, Tunisia
Dipartimento di Scienze Chimiche, School of Pharmacy, University of Camerino, Camerino, Italy

ABSTRACT

The control of stored product insect pests depends mostly on the utilization of synthetic pesticides. Nevertheless, the application of these pesticides leads to many problems such as the development of insect resistance, environmental contaminations and adverse effects on human health. Plant derived substances, in particular essential oils, have been the subject of increasing attention in their safe and eco-friendly application to crops. The aim of this study is to investigate the biological effects of *Clinopodium nepeta* subsp. *nepeta* volatile extracts against *Tribolium confusum*. The essential oil from the aerial parts was obtained by hydrodistillation in a Clevenger type apparatus, its chemical composition was analyzed using gas chromatography and mass spectrometry techniques. The toxicity and the repellent activity were evaluated against *T. confusum*. Thus we demonstrated that the oxygenated monoterpenes-rich essential oil exhibited significant repellent properties.

KEYWORDS: *Clinopodium nepeta* subsp. *nepeta*, Essential oil composition, Insecticidal activity.

The Second Edition of the International Congress of Applied chemistry and Environment
30th-31th October and 01st November 2020, Tunisia

ICACE 2020

Composition and insecticide potential against *Tribolium confusum* of the essential oil extracted from wild carrot (*Daucus carota* subsp. *maritimus*)

Siwar Majdoub[a], Ridha El Mokni[b,c,d], Ikbal Chaieb[e], Alessandra Piras[f], Silvia Porcedda[f] and Saoussen Hammami[a]

(a) Research Unit 13ES63, Applied Chemistry and Environment, Monastir University, Faculty of Sciences of Monastir, Monastir 5000, University of Monastir, Tunisia

(b) Department of Life Sciences, Laboratory of Botany and Plant Ecology, Faculty of Sciences of Bizerta, Jarzouna-7021, Bizerta, University of Carthage, Tunisia

(c) Department Pharmaceutical Sciences "A", Laboratory of Botany, Cryptogamy and Plant Biology, Faculty of Pharmacy of Monastir, BP 207, Avenue Avicenna-5000, University of Monastir, Tunisia

(d) Department of Silvo-Pastoral Resources, Laboratory of Silvo-Pastoral Resources, Silvo-Pastoral Institute of Tabarka, BP. 345, Tabarka 8110, University of Jendouba, Tunisia

(e) University of Sousse, Regional Centre of Research on Horticulture and Organic Agriculture, 57, Chott Mariem, TN-4042 Sousse, Tunisia

(f) Department of Chemical and Geological Science, University of Cagliari, Cittadella Universitaria di Monserrato, S.P. Monserrato-Sestu km 0,700, 09042 Monserrato, Italy

E-mail address: majdoubsiwar17@yahoo.fr

ABSTRACT

Currently, natural products and essential oils have emerged as an excellent alternative to synthetic insecticides as a means to contribute to insect pests management. For this reason, the essential oil extracted from the Tunisian wild carrot *Daucus carota* subsp. *maritimus*, was investigated for its chemical profile, its toxicity and repellency effects against *Tribolium confusum* adults. Qualitative and quantitative analyses of the chemical composition on the basis of gas chromatography and mass spectrometry techniques (GC/FID and GC/MS) revealed the presence of 25 organic volatiles representing 96.1% of the whole constituents. Elemicin and geranyl acetate have been identified as the major aroma. Regarding the repellency assay, results demonstrated that *D. carota* L. subsp. *maritimus* essential oil displayed significant repellent properties.

KEYWORDS: *Daucus carota* subsp. *maritimus*, Essential oil, Chemical composition, Insecticidal activity, *Tribolium confusum*.

The Second Edition of the International Congress of Applied chemistry and Environment
30th-31th October and 01st November 2020, Tunisia

ICACE 2020

Micromorphological investigation and spectrophotometric analysis of the rosmarinic acid extracted from raw material of rosmarin (*Rosmarinus Officinalis L.*) growing in Tunisia and Russia

Louati Habib[a], Serebryanaya Fatima[a], El Mokni Ridha[b]

(a) Medical and pharmaceutical Institute of Pyatigorsk, Russia
f.k.serebryanaya@pmedpharm.ru
(b) UNIVERSITY OF MONASTIR, Faculty of Chemist's shop of Monastir, TUNISIA

ABSTRACT
The purpose of our study was to develop a qualitative and quantitative determination of hydroxycinnamic acids like rosmarinic acid which has left grass of *Rosmarinus officinalis* coming from Tunisia. The analysis by TLC was accomplished in a system of solvents formed by formic acid, acetone anhydride and chloride of methylene (with the following volumes: 8.5: 25: 85).
The identification of phenolic derivatives was accomplished in light UV (365 nm) according to the specific fluorescence of the cafeinic acid and some rosmarinic acid (blue fluorescence). The spectrophotometry analysis was used to quantify the quantity of hydroxycinnamic acids in terms of rosmarinic acid. The content of the hydroxycinnamic acids was about 5.88 ± 0.25 %. Micromorphological studies allowed to discern the following diagnostic indications: the breath shortness of the stem and of the leaf, formed by staked multicellular hair, was well developed. The leaf type is dorzoventral. It is a hypostomatic, stomatal and diacytic apparatus.

KEYWORDS: *Rosmarinus officinalis L.*, phytochemical analysis, rosmarinic acid chromatography, spectrophotometry, micromorphological studies

Ecological Textiles
&
Para-textiles

Effect of Parameter of Pumice Stone Washing on the Bagging Properties of Denim Garments

Ben Fraj Abir[a], **Gazzah Mouna**[a], **Boubaker Jaouachi**[a]

(a)   Textile Engineering Laboratory (LGTEX), ISET Ksar Hellal
E-mail: abir1991_benfraj@yahoo.fr

ABSTRACT

Fabric Bagging is a type of three dimensional plastic deformations that occurs in knees and elbows. The aim of this work is to evaluate the effect of stone wash treatments parameter (washing temperature, amount of stone and time) on the bagging properties of denim fabrics. Garments were washed using pumice stone of 100%, 150%, 200% owg (On the weight of garments) for 30, 45, 60 minutes in 30, 45, 60°C temperature.

The results show that all these parameters have an effect on the bagging phenomenon. In fact, for the residual bagging height, we found that the amount of pumice has the greatest effect, then the time factor and finally the temperature. For the quantity of stone, we find that the residual bagging height increases up to 150% then it decreases. While for the time factor, we find that the residual bagging height increases until reaching the maximum at 60 min. For temperature, the residual bagging height increases from 30 ° C to 45 ° C then it begins to decrease. It can be concluded that it's preferable to work at 60°C for 30 min with 100% of quantity of pumice to have the minimum of residual bagging height.

KEYWORDS: Denim, Bagging, amount of stone, time, washing temperature.

Microwave-assisted extraction and dyeing of bicomponent polyesters filaments with fluorescent natural dye

Marwa Souissi[a,b], Mounir Zaag[c], Nizar Meksi[a,b], Hatem Dhaouadi[a]

(a) University of Monastir, Faculty of Sciences of Monastir, Research Unit of Applied Chemistry and Environment, 5019 Monastir, Tunisia
(b) University of Monastir, National Engineering School of Monastir, 5019 Monastir, Tunisia
(c) Société Industrielle des Textiles (SITEX), 5070 Ksar-Hellal, Tunisia

E-mail: souissi.marwa20@yahoo.com

ABSTRACT:

Bicomponent polyesters filaments are known for their excellent resiliency, softness, chemical stability, and high extensibility which make them particularly suitable for various applications. This paper is devoted to study the dyeing of these advanced polyesters filaments with extracted natural dye using microwave assisted. The effect of dyeing parameters (power of microwave, dyeing duration and dye concentration) on dyeing performances (color strength, CIELab coordinates and photoluminescence) was then investigated. Experiments were carried out using full factorial experimental design to be able to analyze the main effects of each parameter, to detect interactions between these parameters and to deduce optimum conditions for dyeing process. The fastness properties of dyed samples were also evaluated. Obtained results indicate interesting washing and rubbing fastness in the range of 4-5.

KEYWORDS: bicomponent filaments; natural dye; microwave assisted; photoluminescence.

Sustainable dyeing of wool fabric using kermes oak as source of natural colorant

Noureddine Baaka[a], Adel Mahfoudhi[a]

(a)   Research Unit Applied Chemistry & Environment (UR13ES63). University of Monastir. Faculty of Sciences of Monastir. 5000 Monastir. Tunisia

* E-mail address : nouri.baaka@gmail.com

ABSTRACT

The present study was concerned with the extraction of natural colorant from kermes oak (*Quercus coccifera* L.) fruits and the application of the extracted dye on wool fibers in the presence and absence of various mordants. The effect of dyeing time and dye bath temperature were investigated.

The effect of mordant type with different mordanting methods on dyeing quality was also examined. Four salt metals were used in this study; ferrous sulphate, stannous chloride, alum, and copper sulphate. The effect of these mordants on color of dyed wool samples was investigated in terms of CIELab (L*, a*, b*) and K/S values. Light, washing and rubbing fastness of dyed samples were evaluated according to ISO standards. The obtained shades for the control samples were brown; while the mordanted samples a wide range of light to dark brownish colors with a significant enhancement in color strength values.

The results indicated that mordanting gave deep shades and enhanced fastness properties.

KEYWORDS: *Quercus coccifera* L.; Salt mordants; Wool; Meta-mordanting; Fastness properties.

Rheological study of ecological printing pastes on the quality of printed cotton fabrics

Amel Ben Fadhel[a], Wafa Haddar[a], Wafa Miled[b], Nizar Meksi[a]

(a) Université de Monastir, Unité de Recherche en Chimie Appliquée & Environnement, Faculté des Sciences de Monastir, 5000 Monastir, Tunisie.

(b) Laboratoire de génie textile, Université de Monastir - ISET Ksar Hellal, Département de génie textile, 5070, Ksar Hellal, Monastir, Tunisie.

Email:benfadhelamal19891@gmail.com

ABSTRACT

The present work aims to study the characterization of the shear rheology of a 100% bio-sourced printing paste.The effect of the dye concentration (varied from 0.5 to 4g/100g of printing paste weight), urea amount (varied from 2.5 to 15g/100g)by using aluminum and ferrous salts as mordentson the rheological properties was investigated.The amount of dye and urea were varied depending on the thickener agent and the water respectively. Printing performances were appreciated by measuring the integral of the color strength (K/S) and fastness to washing, rubbing and light. Results showed that in the presence of the ferrous salt, the cellulosic thickener agent allowed the highest viscosity with 0.5g/100g of dyestuff powder in the printing paste (equal to 844.0.137 mPa.s^{-1}) and with 15g/100g of urea in the printing paste (equal to 1407.333 mPa.s^{-1}). In addition, this study revealed that when the dye amount increases, the viscosity decreases for any type of mordant studied. On the other hand, the shear viscosity increases with the increase of urea.All results showed also that the use of bio-sourced compounds in optimized conditions allowed the formation of a consistent paste that can be used in standard printing process.

KEYWORDS: ecological printing pastes, bio-sourced compounds, shear rheology, viscosity, cotton fabrics.

.

The Second Edition of the International Congress of Applied chemistry and Environment
30th-31th October and 01st November 2020, Tunisia

ICACE
2020

Relation between Mechanical properties of pvc synthetic leather and calcium carbonate

Mouna Stambouli[a] , Slah Msahli[a] , Sondes Gargoubi[b] ,Walid Chaouch[a] , Riadh Zouari[a,] Aweb Baccar[c]

(a)   Textile Engineering Laboratory of ISET Ksar Hlel,University of Monastir, Tunisia
(b)   Textile Engineering laboratory of ISET KSAR HLEL ,University of Monastir, Tunisia, Chimitex Plus, Sousse, Tunisia
(c)   PLASTISS: industry of synthetic leather situated in Sayada ,Monastir
E-mail:mounastambouli@gmail.com

ABSTRACT

As a part of improving the manufacturing process of PVC synthetic leather in PLASTISS industry (industry of synthetic leather situated in Sayada, Monastir). This study examines the effect of calcium carbonate on the mechanical properties of PVC synthetic leather especially on the break strength, elongation at break and tears resistance. The result confirms that the break strength, the elongation at break and the tear resistance are greatly increased with the increasing of the concentration of calcium carbonate regardless of its origin.

Calcium carbonate can give rise to large improvement in mechanical properties of PVC synthetic leather.

KEYWORDS: Synthetic leather, PVC, Calcium carbonate, particle size. PLASTISS

.